Exploring Iminium
Ion Catalysis.

Timothy J K Gibbs

A Thesis Submitted for the
Degree of Doctor of Philosophy

at

Cardiff University

2008

UMI Number: U585077

UMI

Dissertation Publishing

ProQuest

Abstract

This thesis is composed of two central themes of research; *Chapters* **2-6** describe efforts to understand and increase the activity of iminium ion catalysts. *Chapters* **7-9** are free-standing investigations exploring concepts and observations that were encountered through the course of the research.

Chapter **1** briefly introduces iminium ion catalysis before discussing the experimental and theoretical techniques that are routinely applied to investigate reaction mechanism. The discussion of techniques is divided into three sections; structural, kinetic and theoretical methods. This is followed by a passage that highlights the reported techniques that have been applied to understand mechanisms of iminium ion catalysed processes.

Chapter **2** highlights the work previously conducted within the group developing catalysts for the iminium ion catalysed Diels-Alder reaction and describes a SAR study designed to understand the relationship between the α-effect and β-EWG components of catalysts to aid future catalyst design. The study found that the components work independently. *Chapter* **3** describes a further SAR study conducted to provide evidence for the role of the β-EWG in increasing catalyst activity. The important conclusions drawn were that β-EWG was not acting as a proton shuttle as previously hypothesised and that EWG's that do not contain a carbonyl group could be exploited to increase the activity of a catalyst.

Chapter **4** describes investigations into mechanistic aspects of the catalytic cycle for the iminium ion catalysed Diels-Alder reaction. The isolation of key iminium ion intermediate allowed for structural studies and kinetic investigations of the individual steps of the catalytic cycle. The Diels-Alder cycloaddition was found to be the RDS and the physical reasons for this were understood. The hypothesis was formed that a lowering in the LUMO energy of the dienophile by including a strong β-EWG into the catalyst would accelerate the overall catalytic cycle.

Chapter **5** describes the application of our findings to the design and synthesis of more active catalysts based around the scaffold of MacMillans imidazolidinone catalyst. The inclusion of an additional β-EWG within the catalyst scaffold provided unprecedented levels of activity supporting our hypothesis. The development and evaluation of a predictive theoretical tool for catalytic activity is also discussed.

Chapter **6** shows the preliminary development of piperazinones as catalyst for the iminium ion catalysed Diels-Alder reaction of aldehydes and ketones. *Chapter* **7** describes our efforts to develop a chiral dynamic resolution procedure for the iminium ion catalysed Michael addition reaction of nitroalkanes to α,β-unsaturated ketones.

Chapter **8** reports the development of a one-pot monocarboxymethylation procedure for primary amines and diamines using glyoxylic acid under mild conditions. *Chapter* **9** describes the first aminocatalytic method for the preparation of non-natural and natural bis-indolyl alkanes.

Acknowledgements

Table of contents

Chapter 2: Investigations to Determine the Role of the β-EWG within Secondary Amine Catalysts Based Around the α-Effect

Chapter 3: Investigations to Discover the Function of the β-Electron Withdrawing Group

Chapter 4: Studies to Determine the Mechanism of the Organocatalysed Diels-Alder Reaction

Chapter 5: Design and Synthesis of More Active Catalysts for the Organocatalysed Diels-Alder Reaction

Chapter 6: Development of a Novel Catalytic Architecture for the Secondary Amine Catalysed Diels-Alder Reaction of Eneones

Abbreviations

A	Arrhenius parameter
Ac	acetyl
APcI	atmospheric pressure chemical ionisation
Ar	aromatic
atm.	atmosphere(s)
Bn	benzyl
Boc	*tert*-butoxycarbonyl
b.pt.	boiling point
br	broad
Bu	butyl
cat.	catalyst
Cbz	benzyloxycarbonyl
column chromatography	flash column chromatography
Cy	cyclohexane
d	day(s)
d	doublet
DCA	dichloroacetic acid
DFT	density functional theory
DMF	dimethylformamide
DMSO	dimethyl sulfoxide
DNPH	2,4-dinitrophenylhydrazine
E_a	activation energy
Et	ethyl
ES	electrospray
ESR	electron spin resonance
ether	diethyl ether
EWG	electron withdrawing group
e.e.	enantiomeric excess

equiv. (eq.)	equivalent(s)
GC	gas chromatography
GCMS	gas chromatography mass spectroscopy
GLC	gas-liquid chromatography
h	hour(s)
HF	Hartree-Fock
HOMO	highest occupied molecular orbital
HPLC	high performance liquid chromatography
HRMS	high resolution mass spectrometry
i	iso
IR	infra red
k	rate constant
k	kilo
KIE	kinetic isotope effect
LA	Lewis acid
PE	petroleum ether 40–60 °C
Lit.	literature
LUMO	lowest unoccupied molecular orbital
M	molar
m	mass
m	multiplet
Me	methyl
min.	minute(s)
MM	molecular mechanics
mmol	millimole(s)
MO	molecular orbital
mol	mole(s)
mp	melting point
MHz	megahertz
MS	mass spectrometry
MsOH	methane sulphonic acid

Ms	mesyl
NBS	*N*-bromosuccinimide
n	*normal*
n.d	not determined
NMR	nuclear magnetic resonance
NOESY	nuclear Overhauser enhancement spectroscopy
No	Number
p	*para*
p	pentet
PES	potential energy surface
Ph	phenyl
pK_a	acid dissociation constant
PMP	*p*-methoxyphenyl
Pr	propyl
q	quartet
quant.	quantitative
R	gas constant
RDS	rate determining step
rt	room temperature
s	singlet
SAR	structure-activity relationship
sept.	septet
sol^n.	solution
T	temperature
t	tertiary
t	triplet
TCA	Trichloroacetic acid
TEMPO	2,2,6,6-tetramethylpiperidine-1-oxyl
tert	tertiary
TFA	trifluoroacetic acid
TfOH	triflic acid

THF	tetrahydrofuran
TLC	thin layer chromatography
p-TSA	*para*-toluene sulfonic acid
UV	ultra-violet
vol.	volume(s)
vs.	versus
w/v	weight/volume
w/w	weight/weight
z	charge
Å	Angstroms
Δ	heat
σ	sigma
*	chiral

Chapter 1: Introduction: Techniques Available for the Elucidation of Reaction Mechanism and their Application to Iminium ion Catalysis

1.1 Introduction

1.1.1 Asymmetric Catalysis within Synthetic Chemistry

The concept of asymmetric catalysis is arguably the most appealing in synthetic chemistry as it allows for the preparation of valuable chiral products with substoichiometric quantities of catalysts. Asymmetric catalysis has distinct advantages over resolution and chiral pool methods by minimising waste and providing a broad substrate scope. The area receives significant attention in a wide range of chemical research disciplines and continues to grow as a concept and a science.

1.1.2 Organocatalysis

Organocatalysis can be defined as 'the acceleration of chemical reactions with a substoichiometric amount of organic compound which does not contain a metal atom'.[1] Asymmetric organocatalysis was first practised in the 1970's[2] using proline but it was only at the start of this decade that the potential of the field was realised and exploited. The growth and expansion of the area is illustrated by analysis of the annual publications within the discipline over the last ten years (*Figure 1.1*).
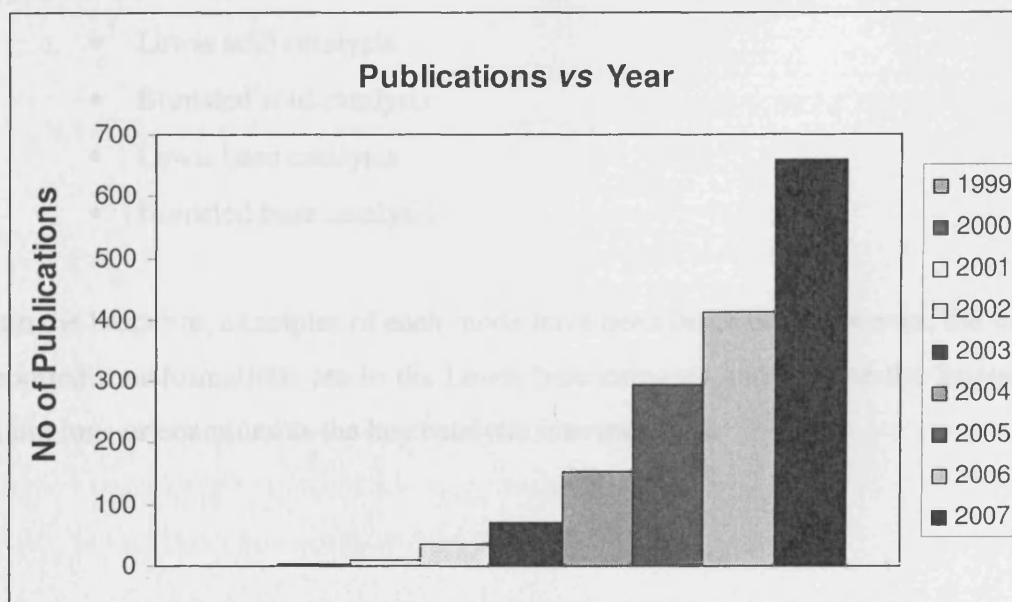
(*Figure 1.1*) Number of publications *vs* year based on a SciFinder search using 'Organocatalysis' as the key word.

1.1.3 Organocatalysis within Asymmetric Catalysis

Of the efficient catalytic asymmetric reactions known, the majority involves an organometallic species. These metal catalysed reactions are widely used within chemical research but do not figure so prominently in industrial processes due to the expenses of scale. Therefore, development of less sensitive and less toxic methods is of interest in all aspects of synthetic chemistry. The future for development of efficient, robust, non-toxic and environmentally benign systems is far brighter for the field of organocatalysis.

Organocatalysis is an attractive alternative to metal catalysed processes and frequently provides superior levels of enantioenrichment. The field of organocatalysis has produced a remarkable number of efficient systems in its short history.[1] Organocatalysis is still very much in its infancy and therefore should not currently be viewed as an alternative to metal based catalysis but as a complimentary tool to be used in conjunction with existing methods to realise synthetic targets.

1.1.4 Classification of Organocatalysts

Organocatalytic processes can be classified according to the mode of action of the catalyst;[3]

- Lewis acid catalysis
- Brønsted acid catalysis
- Lewis base catalysis
- Brønsted base catalysis

Within the literature, examples of each mode have been described. However, the majority of reported transformations are in the Lewis base category and involve the formation of iminium ions or enamines as the key catalytic intermediates.

1.1.5 Enamine Catalysis

Enamine catalysis represents the most successful branch of organocatalysis to date. Conceptually, enamine catalysis can be thought of as an alternative method for the generation of enolates that has numerous practical advantages over traditional methods. Enamine catalysis is a Lewis base method as the lone pair of the enamine raises the energy of the HOMO of the nucleophile increasing the associated nucleophilicity.

Enamine catalysis has been applied to many reactions that would normally involve the generation of an enolate. Catalysed reactions include the aldol,[4] Robinson annulation,[5] Mannich,[6] α-amination,[7] α–aminooxylation,[8] conjugate addition,[9] [4+2] cycloaddition,[10] [2+2] cycloaddition[11] and the Mortia-Baylis-Hillman reaction,[12] among others. The general enamine catalytic cycle for proline is shown below (scheme 1.1).
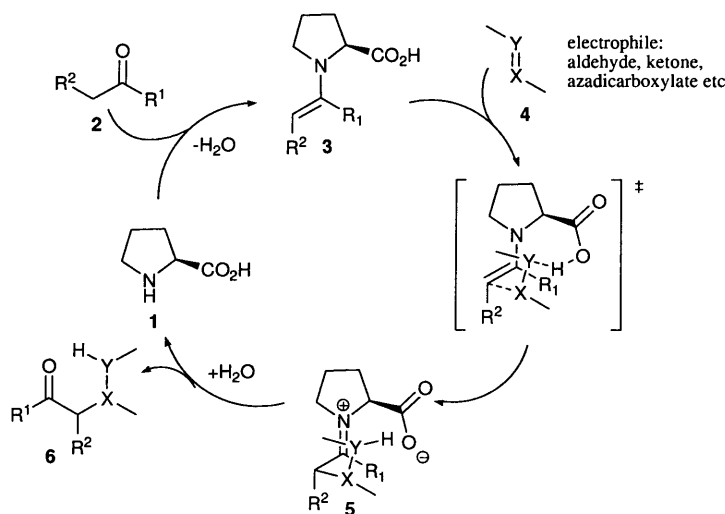
(Scheme 1.1)

Condensation of the amine catalyst (**1**) and a carbonyl (**2**) gives an iminium ion which is rapidly converted to the nucleophilic enamine species **3**. The enamine is sufficiently reactive to attack electrophile **4** which generates an iminium ion **5**. Subsequent hydrolysis releases the reaction product **6** along with the amine catalyst **1** to continue the catalytic cycle.

1.1.6 Iminium ion catalysis

Conceptually, iminium ions can be thought of as being analogous to Lewis acid activated α,β-unsaturated carbonyl compounds and they posses similar π-electronics (*Scheme 1.2*). Iminium ions increase activity by accepting electron density from the C=C of the parent α,β-unsaturated carbonyl compound and thus lower the energy of the LUMO (the π* of the iminium ion derived from the parent carbonyl compound) which decreases the energy difference for interaction with the HOMO of the reaction partner resulting in a lower energy transition state and hence rate acceleration.
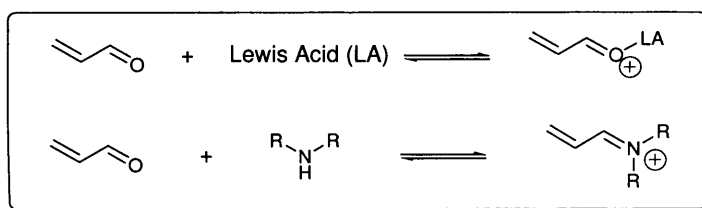
(Scheme 1.2)

The use of iminium ion technology has distinct practical advantages over the majority of Lewis acid catalysed reactions. The iminium ion catalysed reactions are inherently tolerant to air and moisture and are often conducted at ambient temperature. The area of iminium ion catalysis has been extensively reviewed.[13] To date this methodology has been used in a number of asymmetric organic transformations including Diels-Alder[14] and [3+2] dipolar cycloadditions,[15] Michael[16] and conjugate[17] additions, conjugate reductions,[18] ene reactions,[19] cyclopropanations,[20] aziridinations[21] and epoxidations.[22]

Structurally, the favoured catalysts for iminium ion accelerated processes are based around pyrrolidine (e.g. **11**) or imidazolidinone scaffolds (e.g. **7-10**), using the high nucleophilicity of the nitrogen lone pair generated by ring strain. The use of a co-acid is necessary to accelerate formation and hydrolysis of the reactive iminium ions, allowing for greater efficiency in the overall process.
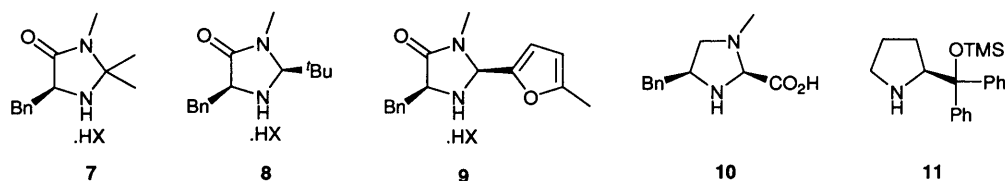
(Figure 1.2) Popular catalysts for iminium ion catalysed transformations.

1.2 Methods of Determining Reaction Mechanism

1.2.1 Mechanism

Reactions are often written as simple transformations involving the conversion of one molecule to another. In actual fact, discreet intermediates are often involved. The study of mechanism is to understand the structural, thermodynamic and chemical relationships between each of the individual species that are formed in a reaction sequence.

Although the methods available to study mechanism have been categorised and discussed individually in this thesis, a single method provides insufficient evidence to confirm a proposed mechanism (although a single valid experiment is sufficient to discount a proposed mechanism). Therefore, numerous methods are often employed to provide sufficient evidence to support a mechanistic proposal.

1.2.2 The Philosophical Background to Physical Organic Chemistry[24]

Before discussion of the toolkit available to elucidate mechanism it is worth highlighting the philosophical constraints that an experimentalist must operate under. Detailed discussion can be found in historic and philosophical texts.[23] The principle concept is that it is not possible to prove the mechanism of a reaction. It is, however, possible to disprove a mechanism by providing evidence to the contrary. Therefore, the acceptance of mechanism is based around strong supporting evidence in the absence of conflicting evidence.

A mechanism is to all extents and purposes a product of the human mind and therefore to ensure that a proposed pathway is reasonable there are some minimum requirements that a proposed mechanism should posses before consideration.[24] The proposed mechanism should be:-

- Consistent with all of the available experimental data and should not be in direct conflict with any data (provided there is not strong independent evidence which devalues the contradicting evidence). Neutrality can be accepted on certain issues.

- Testable by experimental means that would provide evidence to the contrary if not successful.

- Where possible, free of *ad hoc* modifications to explain inconsistencies with experimental observations.

In the event that numerous mechanistic proposals are consistent with minimum requirements, and equally consistent with available experimental data, then favour is given to the simplest.

1.2.3 The Toolkit

Currently, chemists have a plethora of techniques at their disposal to gain insight into the mechanics of a reaction. These methods can be categorised into three main groups; structural, thermodynamic and theoretical. The following passage will provide a brief overview of the techniques that are often employed to provide evidence for mechanistic pathways.

1.2.4 Structural Methods

Structural studies are the simplest and often the most definitive method for providing evidence for a mechanistic pathway. These studies take the form of isolating and characterising reaction products and/or intermediates using physical methods such as spectroscopy and crystallography. The structure of reaction products often contain information which can be used to infer the reactants and intermediates that preceded them.

There are many techniques available that relate spectroscopic properties to physical structure. Such techniques include, infra-red spectroscopy (IR), ultra-violet spectroscopy (UV), fluorescence spectroscopy, ESR spectroscopy, mass spectrometry, NMR spectroscopy, atomic spectroscopy and X-ray crystallography.

1.2.4.1 Product Studies

The detection of chirality within a product can provide valuable information regarding the symmetry of the preceding intermediates or transition states,[25] however, the absolute configuration of the products must first be determined. This is frequently achieved by sophisticated spectroscopic methods or X-ray crystallography. A classic application of chirality study is the nucleophilic substitution reactions on aliphatic carbons achieved in the 19th century.[26] Modern chirality studies can take a number of forms from racemisation or exchange studies to sophisticated mechanistic tools such as the Tolbert analysis[27] and concepts such as the Skell hypothesis[28] which have been used to investigate the mechanisms of many reactions.[29]

The use of isotopic labelling has also emerged as a powerful tool in mechanistic determination.[30] Isotopes possess the same chemical properties but differ in their physical properties, for example, molecular weight and NMR activity. This provides a convenient tool to monitor the final positions of labelled atoms within reaction products. A classic example of isotopic labelling is the hydrolysis of esters.[31] The use of ^{18}O labelled water can provide evidence as to whether acyl (13) or alkyl (14) bond cleavage occured in ester

hydrolysis reaction (*Scheme 1.3*). Labelling experiments however, can be applied to more complex systems, for example, the ozonolysis of olefins.[32]
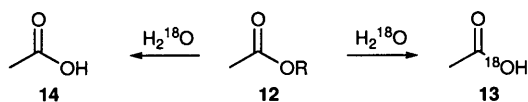
(*Scheme 1.3*)

Mechanistic information can also be provided by variation of the reaction conditions. Common variables include reaction time and temperature. This method, however, must be validated as altering the conditions may lead to an alteration of the mechanism. A reduction in reaction temperature can often allow for the detection and isolation of intermediates. Additionally, lengthening reaction times of reversible reactions encourages the formation of greater quantities of the thermodynamic product.

1.2.4.2 Intermediate Studies

Product studies can be of limited use as it is possible that many intermediates could lead to a given product. Therefore, it is desirable to isolate or directly detect intermediate species within a reaction sequence. Intermediates can often be detected with routine analysis such as GC-MS or NMR techniques under normal chemical conditions. However, this is not always possible and therefore numerous methods have been developed to detect and characterise intermediate species.

Low temperature techniques are often employed to increase the lifetime of transient species. An example of such a technique is matrix isolation infra-red spectroscopy where intermediates are trapped using a solid argon matrix.[33] Intermediate compounds such as benzyne **16** and cylclobutadiene **15** have been characterised by this method (*Figure 1.3*).

(Figure 1.3)

9

Chemical trapping of intermediates is also possible where a reagent is introduced that is designed to react with an intermediate to yield a distinct product. A classic example is that of TEMPO **17**, which is routinely used to selectively trap carbon centred radicals **18** (*Scheme 1.5*).[34] Conjugated dienes have also been used successfully to trap benzyne intermediates **16** [35] which have only been physically detected through matrix isolation.[36]
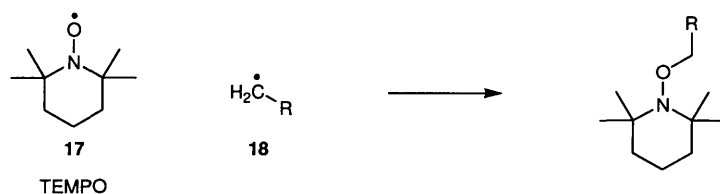
(*Scheme* 1.5)

Many sophisticated spectroscopic techniques have also emerged for direct detection of intermediates. NMR, ESR, mass spectrometry and laser techniques can all be employed. NMR has been used to detect and characterise carbonium ions in superacid media[37] and techniques developed such as spin-saturation transfer[38] while ESR has proved a reliable method for the detection of radical intermediates.[39] The unique properties of laser radiation have lead to the development of spectroscopy on a picosecond timescale for the detection of short lived intermediates.[40]

1.2.5 Kinetic Methods

Once the species that are involved in a mechanistic pathway have been identified it is often desirable to conduct studies to understand the relationships of the individual components. This provides information that will subsequently lead to a fundamental understanding of the transformation.

1.2.5.1 Rates of Reaction

Measurement of the rate of a chemical transformation is of fundamental importance. The reaction order for a proposed mechanism can be predicted. Experimental determination of the order of reaction provides strong evidence to support or discount a mechanism. It is noteworthy however, that many proposed mechanisms may be predicted to have the same reaction order. Rate measurements can be achieved by numerous methods that can quantitatively relate the concentration of a compound with time. UV and NMR are frequently used to monitor kinetics although numerous other techniques based on IR, fluorescence and calorimetry, amongst others, have been employed.

With the advent of modern instrumentation and techniques, the kinetics of reactions of the scale of 10^{-12} s can be determined. For reactions of the order 10^{-1}-10^{-3} s stopped flow methods are commonly applied.[41] For reactions of the scale of 10^{-6}-10^{-12} s the use of pulses of electricity, sound or light (lasers are needed for the fastest reaction) are used to perturb systems from equilibrium and then the restoration of equilibrium is observed.[41]

The use of isotopes in kinetic measurements can yield valuable mechanistic data. Primary and secondary Kinetic Isotope Effects (KIE) have been exploited by mechanistic chemists. The physical origin for KIE is complex when constructed properly and is covered elegantly by Carpenter.[42] Primary KIE's involve the cleavage of the isotope containing bond before or in the rate determining step whereas secondary KIE's involves cleavage of a bond α or β to the isotopic atom. Primary KIE's can be successfully observed using a range of isotopic atoms while secondary KIE are of a much smaller magnitude and therefore only observable for X-H/D bonds.

The observation of a primary KIE provides evidence for participation of a bond breaking before or during the rate determining step of the reaction. The method has been applied successfully to rationalise the mechanism of many reactions.

The use of the Hammett equation is another method that allows the electronic nature of the transition state to be probed. Examination of the relationship of the electronic nature of substituents and the respective rate can provide evidence to support or eliminate mechanistic proposals.[43]

1.2.5.2 Activation Parameters

There are three equations that describe the temperature dependence of a reaction. The Arrhenius equation is the most simplistic model and allows for measurement of activation energy E_a along with a pre-exponential factor A.

$$k = Ae^{-\frac{E_a}{RT}}$$

Transition state theory (Eyring equation) relates the rate constant k to enthalpy of activation $\Delta H^{\ddagger}$ and the entropy of activation $\Delta S^{\ddagger}$.

$$k = \frac{k\,T}{h} e^{\frac{\Delta S^{\ddagger}}{R}} e^{-\frac{\Delta H^{\ddagger}}{RT}}$$

Finally, collision theory is constructed from a detailed collision model Z a steric factor p and a Boltzmann energy term $-E^*/RT$. Collision theory is effective at predicting rate constants of simplistic reactions in the gas phase but is quite arbitrary for larger molecules and reactions in solution.

$$k = pZe^{-\frac{E^*}{RT}} \qquad Z = d_{AB}^2 \sqrt{\frac{8\pi kT}{m_A m_B}}\,(m_A + m_B)$$

Using these equations it is possible to extract activation parameters provided that rate constants are measured at a range of temperatures. Methods such as Benson additives[44]

and computational chemistry can provide good estimates of activation parameters for proposed mechanisms and become powerful tools when combined with experimental data for supporting or eliminating mechanistic proposals.

1.2.6 Theoretical Methods[45]

Chemists have always used theory to develop models to aid the understanding of chemical reactivity. In recent years there has been an explosion in computing technology and power. This affordable and accessible technology has allowed chemists to model more complex systems. Modern theoretical studies can contain tens of thousands of calculations which require computing ability that was not available until very recently.

Theoretical chemistry needs further development before it can be treated as a definitive tool for predicting and explaining reaction mechanism. However, theoretical chemistry is an extremely influential method when used in conjunction with physical experiment. Numerous theoretical models have emerged each with its merits and faults. An overview of the techniques frequently used is given below

1.2.6.1 Molecular Mechanics (MM)

Molecular Mechanics Force Field (MMFF)[46] is the most simplistic theoretical model, requiring relatively small amounts of resources and providing cheap and rapid calculations, which are ideal for studying large systems such a proteins. Highly accurate MMFF models have been developed through careful parameterisation.[47] MMFF is purely mechanical and therefore does not account for electron interactions and inadequately describes systems dominated by these effects. An example of a MMFF is MM2. The MM2 force field can be superficially described as:[45]

- Purely mechanical model (no electrons included)
- Can provide bond lengths accurate to 0.01 A
- Can provide bond angles within a few degrees
- Conformational energies to 1 kcal mol^{-1} with careful parameterisation
- Vibrational frequencies accurate to 20-30 cm^{-1}

1.2.6.2 Self Consistent Field Theory (SCF)

The majority of theoretical techniques are based around SCF. The techniques involve the construction of a wavefunction in which a term describing the electron correlation is included. The varying expense and accuracy of these techniques is proportional to the manner in which electron interaction is considered. The simplest SCF treatments are semi-empirical methods[48] that discard certain electron correlations in the wave function and subsequently introduce experimental or higher theoretical data. As with MMFF, semi-empirical methods rely on careful parameterisation for accuracy. A popular semi-empirical method is the Austin Model 1 (AM1). Some interesting features of AM1 are highlighted below:[45]

- Direct calculation of valence electrons only
- Non-classical compounds considered to be less stable
- Faster calculations than higher SCF or DFT methods
- Sterically crowded and hyper coordinate compounds appear too unstable
- Rotational barriers often underestimated
- Four membered rings appear too stable
- Calculated activation barriers often too high
- For pericyclic reactions biradicaloid mechanisms favoured

In the Hartree-Fock (HF)[49] model the influence that an electron feels is treated as the average field of all other electrons. This average treatment fails to account for specific electron repulsion and can lead to shorter bond lengths and higher total energies (E_{HF}) than true energies, it also poorly describes highly delocalised systems. Common features of HF are:[45]

- Good accuracy for bond lengths and angles for standard organic molecules
- Conformational energies accurate to 1-2 kcal mol^{-1}
- Vibrational frequencies systematically 10-12% too high for most covalent bonds
- Zero point vibrational energies inaccurate by ~1-2 kcal mol^{-1}
- Protonation/deprotonation energies in gas phase inaccurate by ~10 kcal mol^{-1}

- Atomisation/homolytic bond-breaking reactions inaccurate by 25-40 kcal mol^{-1}

In the instances when HF theory is inappropriate, e.g. when investigating aromaticity, polarisation or delocalisation, then use of higher level theories is needed that correlate electron-electron interactions. There are many different treatments of electron correlation from those just above HF to complex detailed theories. The high level SCF methods are considered to be the benchmark for theoretical calculations. The electron-correlation theories can be described as being:[45]

- Straightforward to interpret complete electronic description
- Highly accurate rivalling experiment for small organic molecules
- Very time consuming and therefore expensive
- Strongly basis set dependent
- Straightforward to improve systematically

1.2.6.4 Density Functional Theory DFT

DFT uses an electron density functional (e.g. B3LYP)[50] to replace the many body electronic wavefunction used in methods based on HF. This treatment requires less computation time but is of similar accuracy, greatly reducing cost. In principle, DFT is an exact quantum mechanical method, providing that the true functional is known. However, a degree of arbitrariness is involved when choosing functional combinations and therefore validation of the results is often necessary. Another consequence of this is that systematic improvement is difficult. DFT methods often display the following features:[45]

- Straightforward interpretation of results
- Large molecular systems can be examined
- Little basis set dependence
- Variable accuracy, validation often necessary
- Systematic improvements not possible

1.2.6.5 Selection of Theoretical Method

The selection of a theoretical method for the study of a system is normally governed by economic and time constraints. Ordinarily, lower levels of theory are applied to basic structural optimisations of normal organic molecules. High levels of theory are generally applied to compounds or transition state modelling where structure specific interactions of electrons are important. The size of a molecule or the complexity of a system also governs the level of theory that can be used. Practicality dictates that only small molecules can be treated with the highest levels of theory, whereas huge protein molecules are frequently modelled with MMFF. It is for this reason that simplified structures are often used for theoretical calculations.

1.3 Mechanistic Studies of Iminium Ion Catalysed Processes

The primary objective of the majority of investigators in the field of organocatalysis has been the discovery of novel organocatalytic asymmetric reactions rather than development of existing methods. This approach is understandable given the vast potential of the field and its relative youth. A consequence of this is that mechanistic aspects of the reactions have been generally overlooked. The following section will highlighted the mechanistic studies that have been conducted within the field of iminium ion catalysis.

1.3.1 Structural Studies

The majority of publications in the field of iminium ion catalysis describe asymmetric transformations. Consequently, there is a mass of structural information through enantioenriched reaction products determined by crystallography and sophisticated NMR studies. The information obtained by determining the absolute configuration of reaction products has lead to numerous proposed transition state models and mechanisms with little supporting evidence. Transition state models based purely on structural information have been proposed for the enantioselective organocatalytic Diels-Alder,[51] [2+2],[52] [4+3],[53] [3+2] dipolar cycloadditions,[54] Michael additions,[55] hydrogenation,[56] epoxidation,[57] ene,[58] Baylis-Hillman[59] reactions along with numerous organocatalytic

17

cascade processes.[60] The reports that support mechanistic proposals based on structural studies with computational or thermodynamic studies are discussed under these headings.

The study of non-linear behaviour has been applied successfully within the field of enamine catalysis to reveal mechanistic insights. Non linear studies involving iminium ions have proved less successful. Hanessian conducted nonlinear studies for the Michael addition of nitroalkanes to cyclic enones using *L*-proline as the catalyst and piperazine derivatives as additives.[61] A nonlinear effect was observed for the reaction using *trans*-2,5-dimethylpiperazine as an additive. Clear mechanistic conclusions could not be drawn as the system was complex, similar behaviour has, however, been reported for metal ligand based systems.[62]

1.3.2 Kinetic Studies

There are few reports of thermodynamic mechanistic investigations within the literature of iminium ion catalysis.

The most complete mechanistic investigation came form the group of Ogilvie who employed a combination of structural, kinetic and computational techniques to probe the mechanism of the organocatalysed Diels-Alder reaction with an asymmetric hydrazide catalyst **21** (*Scheme 1.6*). Ogilvie used ^{1}H NMR studies to detect and then observe the individual species in the catalytic cycle as the reaction proceeded.[63] The kinetic evidence provided clearly indicated that the rate determining step of the catalytic cycle was the Diels-Alder cycloaddition reaction. It was also concluded that the hydrolysis step was rapid as the Diels-Alder cycloaddition iminium ion adducts **23** were not observed in significant quantities.

(Scheme 1.6)
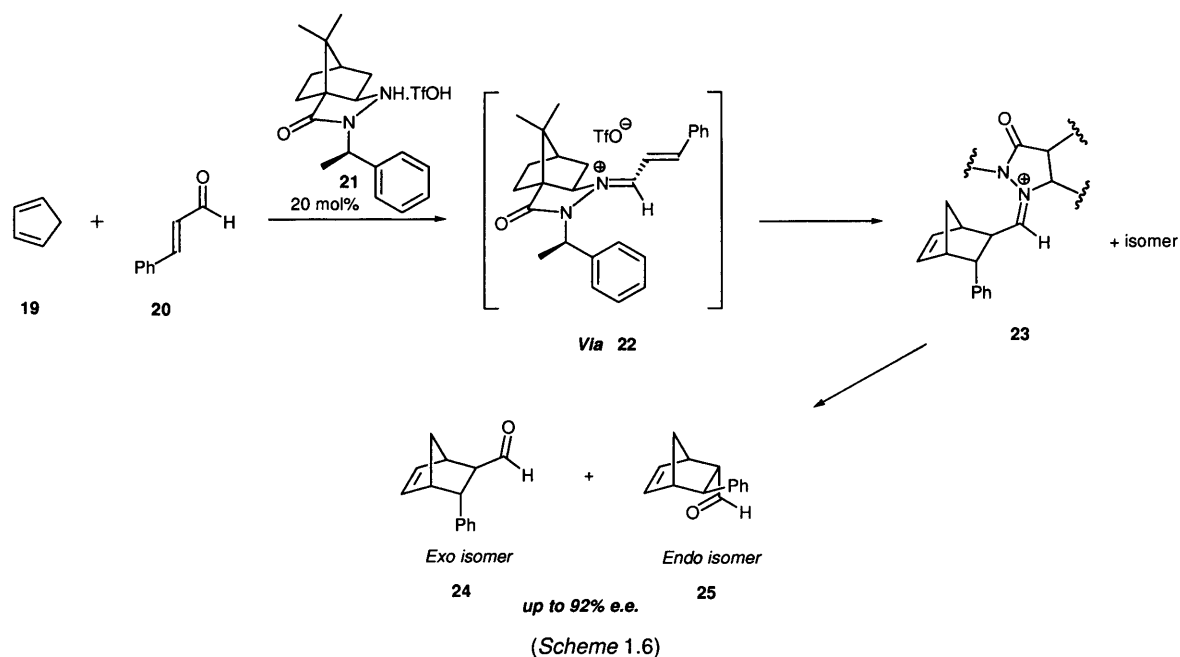
Ogilvie subsequently isolated and crystallised the iminium ion intermediate **22** and combined this with PM3 semi-empirical computational studies to rationalise the favoured reactive conformation in solution.[64]

MacMillan undertook kinetic studies using ^{1}H and ^{15}N NMR to explain the efficiency of [(nosylimino)iodo] benzene **30** as an in situ source of iodosobenzene **27** as an alternative to oligomeric iodosobenzene in an organocatalytic asymmetric epoxidation reaction.[65]

(Scheme 1.7)
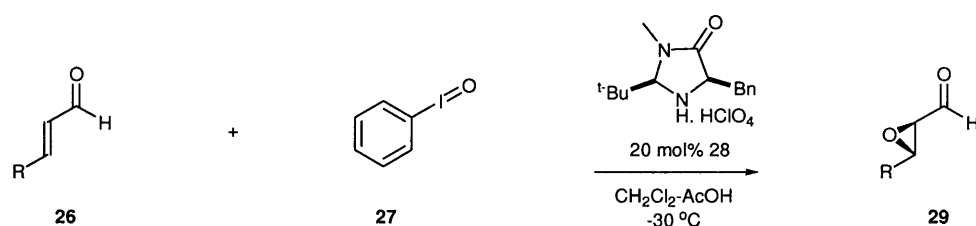
MacMillan used ^{1}H NMR studies to determine the rate of formation of **27** from **30** and from oligomeric iodosobenzene. The experiments clearly indicated that **27** formed much faster from oligomeric iodosobenzene (*ca* 35% after 1h) and remained at a constant level for 6 h. The active oxidant **27** formed at a much slower rate from **30** steadily increasing to 15% conversion after 6 h.

30   **27**

(*Scheme* 1.8)
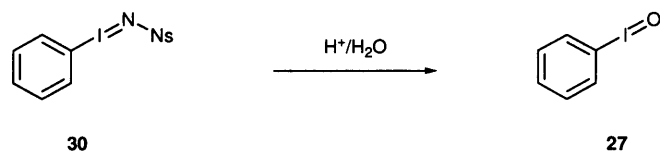
Subsequent ^{15}N NMR experiments demonstrated that compound **27** degenerated the reaction catalyst **28** resulting in compounds **31**, **32** and **33** when oligomeric iodosobenzene was used as the source of oxidant **27**. However, when **30** was used as the oxidant precursor only decomposition product **32** was observed in comparatively minor concentrations.

28   **27**   **31**   **32**   **33**

(*Scheme* 1.9)
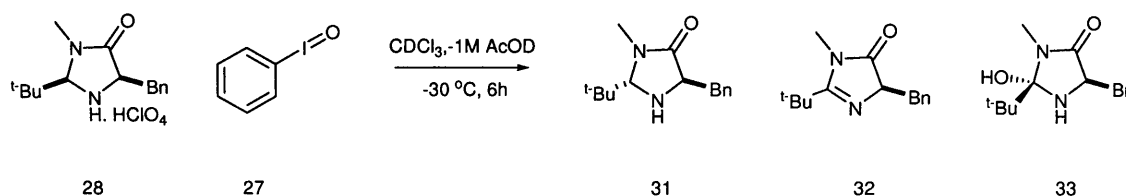
The work provided evidence that elegantly explained the increased reaction efficiency and levels of asymmetric induction observed when using **30** as the source of stoichiometric oxidant which was described as an 'internal syringe pump effect'. The results of this study demonstrated that the use of routine analytical tools can provide powerful evidence to rationalise experimental observations.

In a report on an asymmetric epoxidation reaction Córdova concluded that the reaction was possibly first order in respect to the pyrrolidine based catalyst **11** for catalyst loadings up to 10 mol%.[66]

26   **29**

(*Scheme 1.10*)
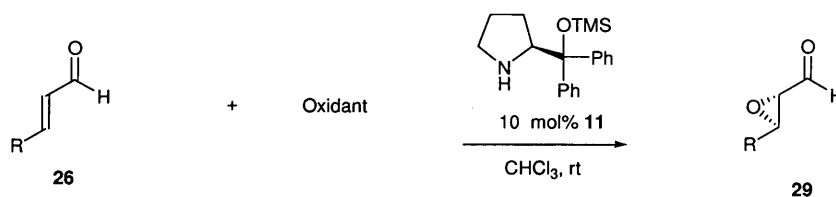
The reasons for his investigations are not entirely clear as the initial rates would be expected to be pseudo first-order in this process, independent of the true reaction order.

The rate constants are also plotted in unusual units and no information is published as to how the kinetic information was obtained.

1.3.3 Computational Studies

Theoretical studies represent the largest portion of mechanistic studies undertaken within the field of iminium ion catalysts. The primary role of these studies is to provide support and further refinement to existing proposals based on structural studies.

The level of theory and detail of the studies vary dramatically from simple low level molecular modelling which supports proposed intermediates to full theoretical papers calculating the relative energies of the species in the catalytic cycle concerned.

1.3.3.1 Molecular Mechanics Studies

The simplest molecular model employed for molecular modelling (CS Chem3D Pro™ 4.0) was used by Karlson to provide relative energies of the reactive conformations of iminium ion intermediates in an asymmetric 1,3-dipolar cycloaddition reaction of nitrone **35** with α,β-unsaturated aldehyde **34** (*Scheme 1.11*).[67] Unsurprisingly, the application of the simplistic model to a complex reaction involving charged species led to ambiguous conclusions being drawn.
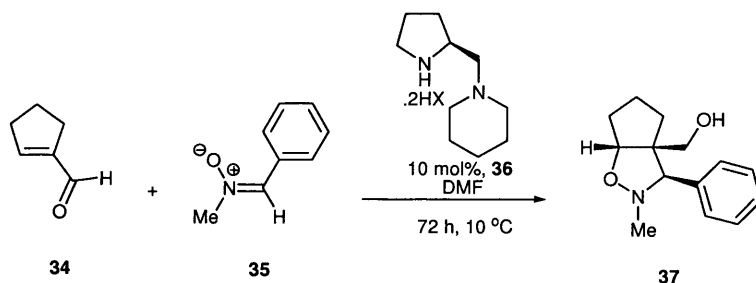
(Scheme 1.11)

The group of MacMillan have employed Monte Carlo (MC) simulations using the MM3 force field[68] to rationalise the sense of asymmetric induction for a number of their imidazolidinone based catalysts **7, 8** and **9**.

21
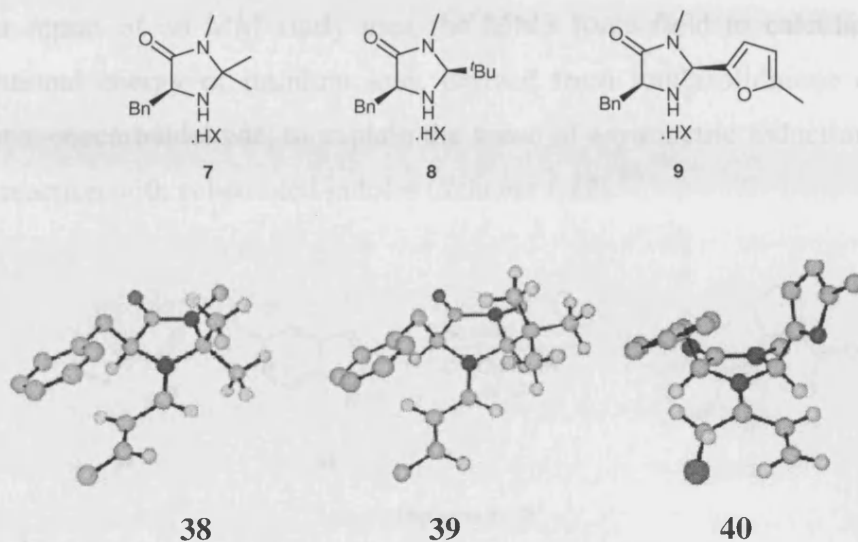
The calculated structures are in agreement with the sense of asymetric induction observed in the reaction products. The conformation of iminium ion **38** has been used to rationalise the asymmetric Diels-Alder reaction,[69] 1,3-dipolar cycloaddition[70] and Michael addition of pyrrole[71] with α,β-unsaturated aldehydes. The conformation of iminium ion **39** has been used to rationalise the asymmetric Mukaiyama-Michael,[72] Michael addition of indole[73] and conjugate reduction reactions.[74] Finally, the conformation of iminium ion **40** has been applied to explain the asymmetric induction of the Diels-Alder reaction with α,β-unsaturated ketones.[75] Subsequent to these reports higher level DFT calculations indicate that the structure of **38** may not be entirely correct (*Figure 1.4*).[76] The correction however, does not, in this case, affect the sense of asymmetric induction and therefore is of limited importance. However, this does serve as a potent reminder that critical analysis of the considered choice of theoretical method is important.
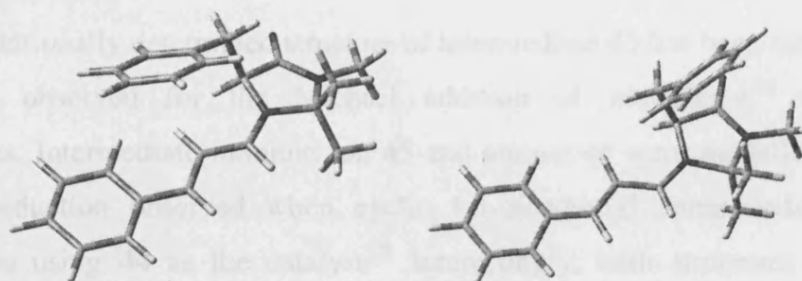
(*Figure 1.4*) Left: MacMillan's calculated lowest energy conformation; Right: Calculated conformation reported by Houk.

A further report of an MM study uses the MM3 force field to calculate the relative conformational energy of iminium ions, derived from imidazolidinone catalyst **9** and cyclopent-1-enecarbaldehyde, to explain the sense of asymmetric induction in a Michael addition reaction with substituted indoles (*Scheme 1.12*).[77]

(Scheme 1.12)

1.3.3.2 Semi Empirical Studies

Semi-empirical calculations have also been used to model iminium ion catalysed processes. The group of Jørgensen employed PM3 semi-empirical calculations to discover the minimum energy conformation of the iminium ion intermediate of the imidazoline based catalysts **10** and **44** to rationalise the asymmetry observed in a series of Michael additions to α,β-unsaturated ketones.

The computationally determined structure of intermediate **43** has been used to explain the asymmetry observed for the Michael addition of nitroalkane[16] and malonate[78] nucleophiles. Intermediate iminium ion **45** and aminal **46** were modelled to explain the sense of induction observed when cyclic 1,3-dicarbonyl compounds were used as nucleophiles using **44** as the catalyst.[79] Interestingly, both structures **45** and **46** are proposed as possible reactive intermediates. Furthermore, calculations indicated that the energy of the LUMO of **46** is activated when compared to the parent ketone.

Disappointingly, no further investigations to attempt to identify the actual catalytic species have been reported.

Nevalainen and co-workers also used PM3 calculations to provide supporting evidence for the favoured *E*-geometry of an iminium ion intermediate to rationalise the observed sense of asymmetric induction in an organocatalysed 1,3-dipolar cycloaddition reaction.[80]

The most detailed semi-empirical study using AM1 of iminium ion catalysed processes investigates the Diels-Alder reaction with protonated ammonia as a catalyst.[81] The study investigated various reaction pathways indicating that cycloaddition across the C=C bond was most favourable energetically.
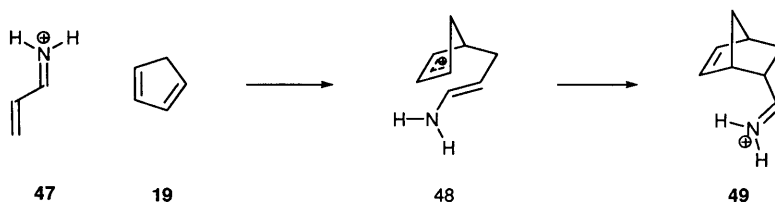
(Scheme 1.13)

The study also found that the cycloaddition was a step-wise process, firstly forming an intermediate cation **48** followed by ring closure (*Scheme 1.13*). However, higher level calculations of reactive Diels-Alder systems have been conducted suggesting that the Diels-Alder cycloaddition although asynchronous is concerted.[82] This demonstrates the pitfalls of theoretical chemistry when little thought is given to experimental evidence and oversimplified models are employed.

1.3.3.3 DFT Studies

DFT studies are the most detailed and frequently applied of the methods in the theoretical literature on iminium ion catalysis. The DFT studies reported are either detailed theoretical studies or are provided as supporting evidence for proposed transition states and intermediates.

The group of Houk have made several theoretical contributions to the field of organocatalysis.[83] Detailed DFT (B3LYP) studies of MacMillan's asymmetric Diels-

Alder reaction[84] and asymmetric Michael addition[85] have been published. The calculated conformational energies of the corresponding reactive iminium ion intermediates and transition-states are obtained and applied to statistically predict the level of asymmetry observed. The studies correlate with experimental evidence and are therefore useful in mechanistic interpretation. Comprehensive and detailed studies such as these represent the bench mark for theoretical investigations within the field to date.

Subsequently, Uggerund published a detailed study validating the use of DFT for investigation of nucleophilic addition reactions to α,β-unsaturated carbonyl compounds.[86] The study involved comparison of high level *ab initio* calculations to the faster and cheaper DFT calculations. The study found that DFT (B3LYP) performed well and also revealed an unexpected intermediate **53** for the iminium ion catalysed Michael addition of nitromethane (*Scheme 1.14*).
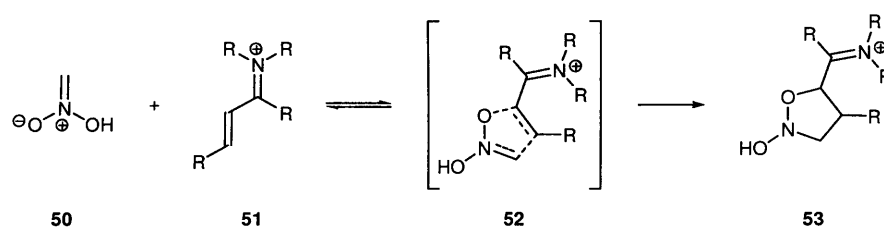
(*Scheme 1.14*)

The study also found that protonated acrolein is more activated to nucleophilic attack than the corresponding iminium ion **51**. This study highlights how detailed theoretical studies can provide interesting predictions which can be explored experimentally.

A DFT (B3LYP) study conducted by Platts examined the performance of numerous catalysts in key stages of the iminium ion catalysed Diels-Alder reaction.[87] An energy profile for iminium ion formation was determined and the relative energies associated with a series of catalysts were calculated. The study found that the introduction of an α-heteroatom and β-electron withdrawing group into acyclic catalysts lowered the activation barrier of iminium ion formation. The energy of the cycloaddition step was also measured and found to have a lower activation barrier than for iminium ion formation. The inclusion of an α-heteroatom and a β-electron withdrawing group within

the catalyst is known to accelerate the reaction when compared to standard catalysts and therefore it was suggested that the rate determining step may be iminium ion formation.[88]

Recently, Jørgensen has applied DFT (B3LYP) calculations rather than semi-empirical PM3 calculations to aid mechanistic understanding. The calculations were used to compare structural optimisations of reaction intermediates. The calculations identified the energetically favoured species to explain the observed asymmetry in the respective products for the Michael addition of a range of N-containing heterocycles[89] and a domino Michael-aldol-S_N2 reaction (Scheme 1.15).[90] The computational results were consistent with the sense of asymmetric induction in both cases.
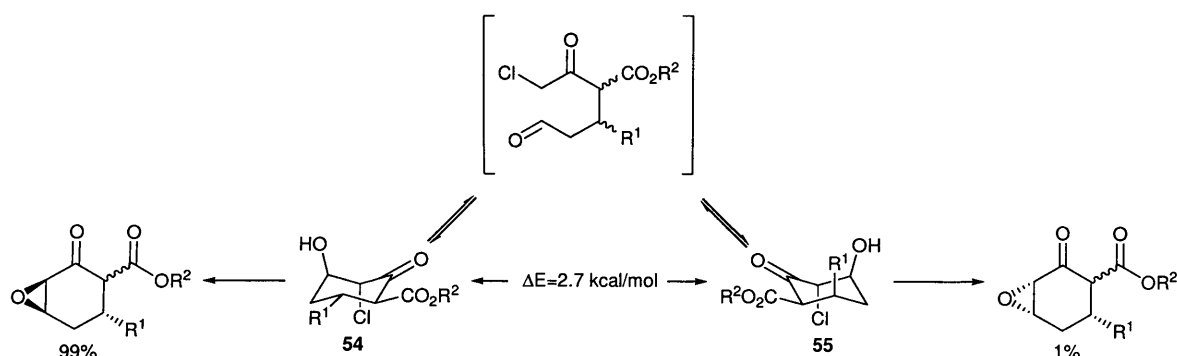
(Scheme 1.15)

The computations indicated that the formation of **54** in the ring forming intramolecular-aldol reaction was considerably more stable than **55** providing an explanation of the excellent levels of asymmetry observed (Scheme 1.15).

Córdova has used DFT to calculate possible theoretical transition-states and intermediates for an iminium ion catalysed hydrophosphination reaction to explain the observed enantioselectivity (Scheme 1.16).[91]
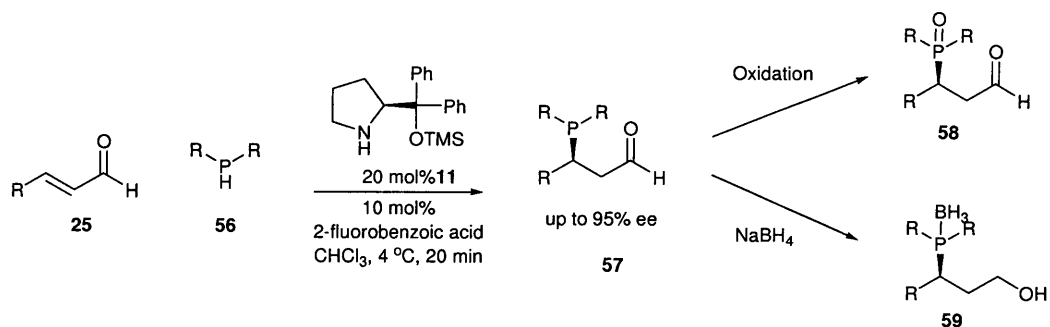
(Scheme 1.16)

The computations supported the hypothesis that the *E*-iminium ion was lower in energy than the *Z*-isomer, rationalising the observed asymmetry in intermediate **57**. Compound **57** was however, not isolable and therefore was further elaborated *in situ* by oxidation to phosphine oxide **58** or treatment with $NaBH_4$ to give the alcohol **59**.

1.4 Conclusions

The potential for the discovery of novel asymmetric reactions or sequences within the field of iminium ion catalysis is vast. It is for this reason that the majority of leading researchers within the field pursue this goal. The discovery of novel methodology is of course important, however, there is a culture within the field that seeks only to display novel reactions or applications rather than to gain a thorough understanding of the reactions and their scope. Furthermore, there are several reasons why the organocatalytic methodology is not practical for widespread chemical manufacture at a large scale, notably, catalyst inefficiency and narrow substrate scope.

Within the field of iminium ion catalysis little effort has been deployed to understand the exact mode of action of the catalysts in the reactions. Frequently, groups postulate a transition-state based on structural studies of the reaction product and then use simple molecular modelling to provide supporting evidence. While in the majority of cases the transition states proposed seem perfectly viable, it is of extreme importance for future synthetic development that physical experiments are also conducted to validate the theory and provide a better mechanistic understanding.

The most thorough mechanistic study to date was conducted by Ogilvie who used a combination of techniques including qualitative kinetic measurements, structural studies and computational studies to gain a mechanistic insight. However, Oglivie's catalyst is considerably less efficient than others reported for the Diels-Alder reaction. Supporting theoretical studies investigated the mode of asymmetric induction rather than attempting to understand the low activity of the catalyst. From a developmental point of view the catalyst scaffold induces near perfect levels of asymmetry in the product therefore there is little room for improvement, whereas there is a significant potential to increase activity

when compared to similar catalysts. This preoccupation with asymmetry is mirrored across the field of organocatalysis.

Kinetic and thermodynamic studies are the least represented of the mechanistic tools that have been used to investigate iminium ion catalysed processes, however, it is this class of study that will allow for a fundamental understanding of the catalytic processes. Development of more efficient catalysts to address the issues of low activity will be accelerated once sufficient mechanistic evidence is available to allow for rational design.

The lack of detailed mechanistic evidence for iminium ion catalysed processes is primarily a consequence of the infancy of the subject, encouraged by the fact that much kudos and consequently funding is given to large synthetic groups with high publication rates. Almost all the sub-disciplines of organocatalysis are fiercely competitive which might lead to a lack of mechanistic information being communicated and certainly promotes the culture of rapid publication and short-term investigations. With time, the field will mature and longer-term detailed studies will become more evident within the literature. Currently, the potential for detailed mechanistic investigations of organocatalytic transformations appears bright and exciting. It was these factors coupled with our curiosity, which provided the impetus for the investigations carried out within this thesis.

Chapter 2: Investigations to Determine the Role of the β-EWG within Secondary Amine Catalysts Based Around the α-Effect

2.1 Introduction

2.1.1 The Aim of the Research

The overall goal of the research began as an attempt to develop novel, highly active catalysts for a range of asymmetric iminium ion catalysed processes.

2.1.2 Previous Work Within the Group

Work began within the group in an attempt to make more active catalysts for iminum ion catalysed transformations.[92] Catalysts reported within the literature were of moderate activity presenting a developmental opportunity. The investigation began with the choice of the iminium ion catalysed Diels-Alder reaction as a tool to systematically improve catalyst design. The generalised catalytic cycle of this transformation is shown below (*Figure 2.1*).
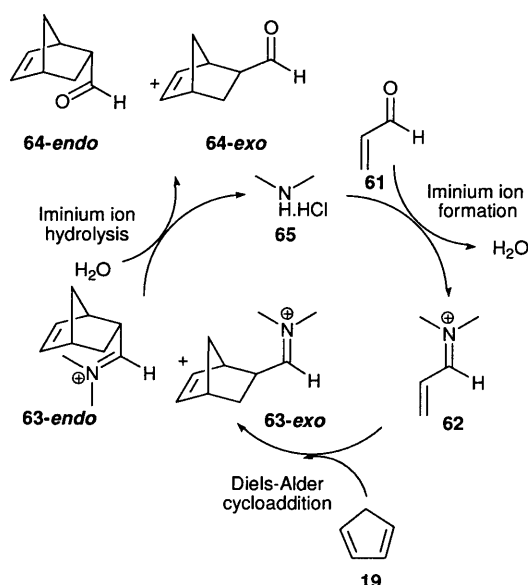
(Figure 2.1)

The proposed catalytic cycle has three major components. The initial step is iminium ion formation, in which the secondary amine salt **65** condenses with the α,β-unsaturated aldehyde **61** to yield the activated iminium ion **62**. The iminium ion then undergoes a cycloaddition reaction with a diene such as cyclopentadiene **19** to yield the Diels-Alder iminium ion adduct **63**. The cycle is complete when a molecule of water hydrolyses **63** to

30

yield the product of the reaction **64** and regenerate the amine **65** which can continue the catalytic cycle.

From the initial observation that all the effective catalysts reported in the literature contained a nucleophilic amine bound within a five-membered ring it was rationalised that the nucleophilicity of the amine was crucial to catalytic activity and that iminium ion formation was likely to be the rate determining step.[93] Therefore, the group sought to find ways to increase the nucleophilicity of the amine and thus increase the catalytic activity. Work began to prepare a series of catalysts utilising the α-effect to achieve this increased activity.

2.1.3 The α-effect

The α–effect can be defined as the increased nucleophilicity of a heteroatom by an adjacent heteroatom bearing a lone pair of electrons. The specific origin of this effect is not fully understood although many suggestions have been put forward. The two that are most widely accepted are:

- The interaction of the adjacent lone pairs leads to an increase in the energy of the HOMO of the nucleophile accelerating orbital controlled reactions.[94]

- The extra lone pair of electrons stabilises the transition state (stabilisation is substrate specific).[95]

Although a complete theoretical understanding of the α-effect remains elusive, it is the α–heteroatom's ability to increase reactivity that is of interest to the synthetic chemist and of which there can be no dispute.[96]

In order to allow direct comparison of a specific catalyst's activity the Diels-Alder cycloaddition between cinnamaldehyde **20** and cyclopentadiene **19** was used as a standard transformation.
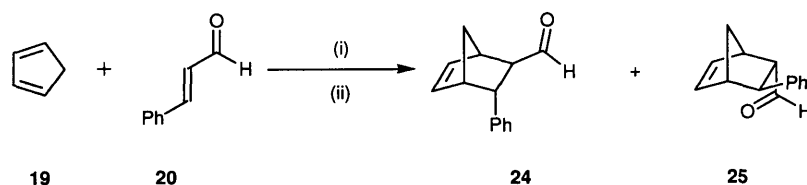
(i) Catalyst (10 mol%), MeOH, 25 °C. (ii) TFA, CHCl₃, H₂O

(Scheme 2.1)

The catalysts that were initially investigated to determine if the α-effect would accelerate the iminium ion catalysed Diels-Alder reaction were dimethylamine hydrochloride **65** as the standard, *N,N'*-dimethylhydrazine dihydrochloride **66**, *N,N'*-diphenylhydrazine dihydrochloride **67** and *N,O*-dimethylhydroxylamine hydrochloride **68**. On obtaining proof of principle more detailed studies would be warranted (*Figure 2.2*).
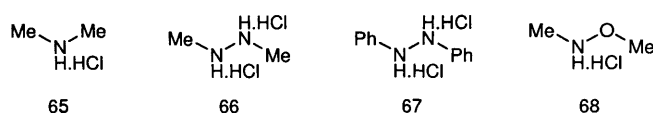
(Figure 2.2)

In the absence of catalyst and in the presence of 10 mol% triethylamine hydrochloride the reaction of cinnamaldehyde **20** and cyclopentadiene **19** gave a 7% conversion after a 48 h period with predominance of the kinetically favoured *endo*-isomer **25**. With dimethylamine hydrochloride **65**, at a 10 mol% loading, 22% conversion was observed with approximately 2:1 ratio of *exo* **24** to *endo* **25** isomer (the observation of this ratio is diagnostic of an iminium ion catalysed reaction). *N,N'*-Dimethylhydrazine hydrochloride **66** and *N,N'*-diphenylhydrazine hydrochloride **67** both demonstrated increased reactivity relative to the standard dimethylamine hydrochloride catalyst **65** (48%, 72 h and 33%, 48 h, respectively). However, *N,O*-dimethylhydroxylamine hydrochloride **68** displayed a greater increase providing a 65 % conversion under identical conditions. The results of this experiment clearly indicated that the α-effect could be used as a tool to increase reactivity in iminium ion catalysis.
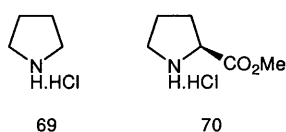
(Figure 2.3)

During this work another interesting observation was made when examining cyclic catalysts. Proline methyl ester hydrochloride **70** demonstrated superior activity to pyrrolidine hydrochloride **69** as a catalyst for the standard Diels-Alder reaction, suggesting that inclusion of a carbonyl group β– to the reactive nitrogen could increase activity. With these results to hand the next stage was to develop catalysts based around the α-effect to rival and compete with the reported cyclic catalysts in terms of efficiency.
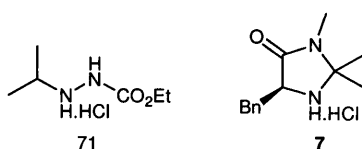
(Figure 2.4)

The benchmark catalyst for this transformation is MacMillans catalyst **7** which facilitates a quantitative conversion for the standard Diels-Alder reaction after an 8 h period with excellent levels of asymmetric induction ≥90% e.e.[14] The group began research to develop catalysts that could provide a more efficient catalyst than **7**. The first step in the right direction was synthesis of catalyst **71** (*Figure 2.4*) which was prepared in two steps from commercially available ethyl carbazate and acetone. Catalyst **71** took the reaction between cinnamaldehyde **20** and cyclopentadiene **19** under the standard conditions to 93% after 48 h.

The success of these experiments led to a comprehensive structure activity relationship (SAR) study based around five variables of the newly developed catalytic architecture (*Figure 2.5*).[97]
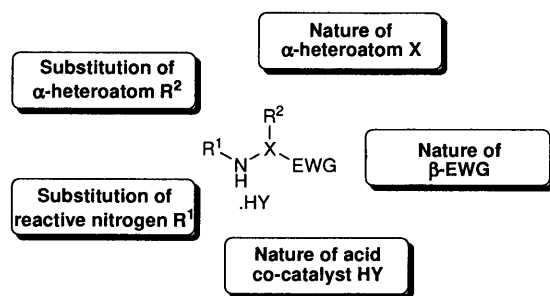
(Figure 2.5)

The SAR resulted in numerous catalysts being prepared which allowed for many comparisons to be drawn, however, only the structural features important for activity will be highlighted. The SAR can be summarised with the following statements:

- The optimal α-heteroatom X is nitrogen.

- The optimal co-acid is HCl.

- The optimal substitution α- to the reactive nitrogen is secondary (R^1).

- Optimal EWG is ethyl carbamate.

- Optimal substitution on the α-heteroatom X is tertiary (R^2).

- Most active catalyst scaffold was based around a six- membered ring.

- Catalysts based around five membered rings were ineffective.

Catalysts **72** and **73** were the optimal catalysts prepared for the cyclic and acyclic series respectively (*Figure 2.6*).
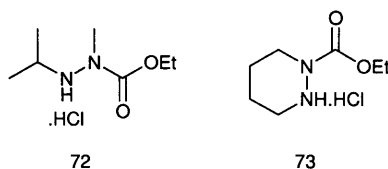
(Figure 2.6)

Catalyst **72** and **73** accelerated the standard Diels-Alder reaction to 86% and 89% conversion respectively after a 3 hour period at 10 mol% loading.

The SAR study succeeded in producing more active catalysts than those reported in the literature for the Diels-Alder reaction. It was also observed that the β-EWG held a vital role in facilitating increased activity. However, it was not clearly apparent how the EWG increased the catalyst activity in the transformation. We therefore sought to make a series of catalysts that could generate information as to role of the EWG to aid our understanding of the α–effect catalysts.

34

2.2 Results and Discussion

2.2.1 Separating the α–effect and the β-EWG

The initial investigation sought to increase the reactivity of the catalysts by introduction of the α–effect, however, this was only achieved by incorporation of a β–EWG, the role of which was not understood.

The first question that was addressd was whether the EWG was directly affecting the α-heteroatom responsible for increasing the nucleophilicity of reactive nitrogen or was the effect independent? To provide an answer to this question we sought to include both structural features into a series of catalysts in a manner that would allow us to probe the role of the respective structural features. The structures **74, 75, 76** and **77** were proposed to achieve our aim.
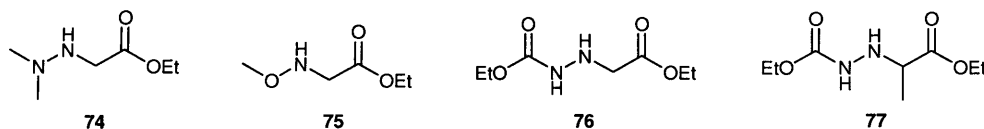
(Figure 2.7)

The targets were chosen to allow direct comparison of structurally similar catalysts in the acyclic series. These targets also had the advantage that the synthesis was anticipated to be straightforward. Catalyst **74** allowed for separation of the α-effect facilitated by a nitrogen atom remote from the β-EWG while catalyst **75** was prepared as the oxygen analogue of catalyst **74**. Catalyst **76** allowed us to observe the effect of including an additional β-EWG on catalyst activity. Catalyst **77** was targeted as previous synthetic studies indicated that the increase in substitution α- to the reactive nitrogen should further increase activity.
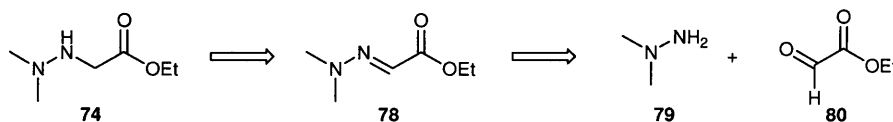
(Scheme 2.2)

Synthesis of catalyst **74** was envisaged from condensation of *N,N*-dimethylhydrazine **79** with ethylglyoxylate **80** to afford the hydrazal **78** which could be subsequently selectively reduced to achieve the target **74** (*Scheme 2.2*). The other catalysts **75-77** were envisaged using similar methodology.

2.2.2 Synthesis of Catalysts

The synthesis of **74** proved to be difficult with many attempts needed to finally achieve the target compound in 5% overall yield (*Scheme 2.3*). The initial condensation of the hydrazine **79** with ethyl glyoxylate **80** was efficient, although the imine intermediate was not rigorously purified. Considerable problems arose on reduction of the imine. Many methods were employed unsuccessfully including hydrogenation, reduction with sodium triacetoxyborohydride and sodium borohydride. Initially, sodium cyanoborohydride was unsuccessful, but finally granted access to the reduced catalyst **74** by increasing the number of equivalents of hydride to three and decreasing the pH of the reaction.
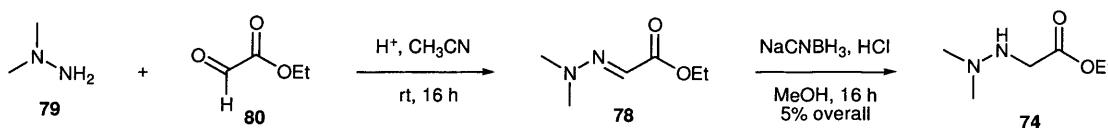
(Scheme 2.3)

The reaction proceeded with low conversion determined by ^{1}H NMR (*ca* 20%) but the amount of compound obtained after purification was significantly lower than the conversion. A likely explanation for this is that the compound **74** has a low boiling point and therefore significant quantities were lost on concentration of the fractions after column chromatography. Despite this frustrating observation we were able to access sufficient quantities of **74** in order to examine its activity as an iminium ion catalyst.

Catalysts **75, 76**, and **77** were synthesised in poor to average overall yields by a reductive animation procedure.

36

83a X = NH, R^1 = Me$_2$, R =H
83b X = O, R^1 = Me, R = H
83c X = NH, R^1 = CO$_2$Et, R =H
83d X = NH, R ^{1}= CO$_2$Et, R =Me

82a R = H
82b R = Me

74 2%
75 5%
76 25%
77 35%
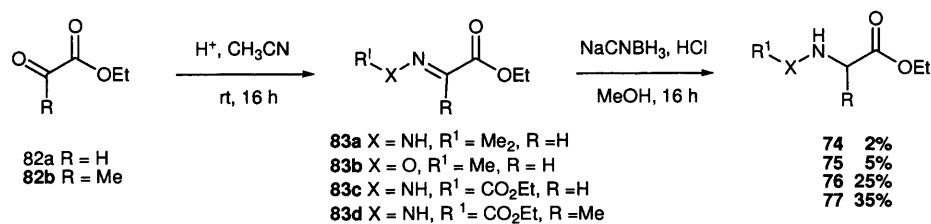
(Scheme 2.4)

2.2.3 The Standard Procedure for Analysing Catalyst Efficiency

To allow for direct comparison with previous work in the group a standard set of conditions was applied for the Diels-Alder cycloaddition *(Scheme 2.5)*.

(i) Amine catalyst.HCl (10 mol%), MeOH, 25 °C, 24 h (ii) TFA, CHCl$_3$, H$_2$O, rt, 16 h
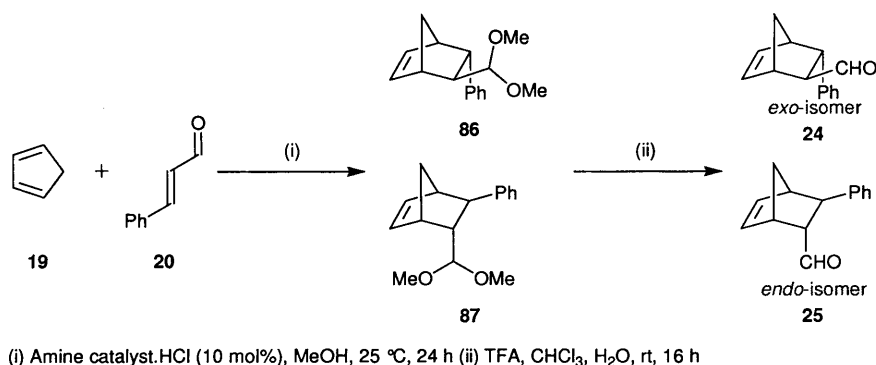
(Scheme 2.5)

The reaction was preformed in a set sequence. Initially 10 mol% of catalyst was placed in methanol (2 mL). To this was added the cinnamaldehyde **20** (1 eq) and the reaction mixture allowed to stir for 2 minutes at 25 °C before addition of cyclopentadiene **19** (2.5 eq). The reaction was promptly sealed and allowed to stir for a specific time. The starting time of the reaction was taken as the addition of cyclopentadiene **19**. Upon completion of the reaction time the mixture was diluted with dichloromethane and reduced *in vacuo* to remove the cyclopentadiene **19** and hence terminate the reaction. Hydrolysis of the methyl acetals **86** and **87** was achieved by stirring in a TFA, water and chloroform mixture overnight. Neutralisation of the acidic solution followed by extraction gave the crude product for analysis. Further purification was possible with column chromatography but was not routinely conducted.

The conversion of the reaction was analysed using the crude product. This was possible as there were discreet and distinct peaks in the ^{1}H NMR spectrum which allowed for comparison of the ratio of product and starting material through integration. It had been shown that the signals corresponding to the *exo*-**24** and *endo*-**25** isomers appeared at δ 9.85 and δ 9.53 respectively with cinnamaldehyde **20** at δ 9.64 (*Figure* 2.8).[98]
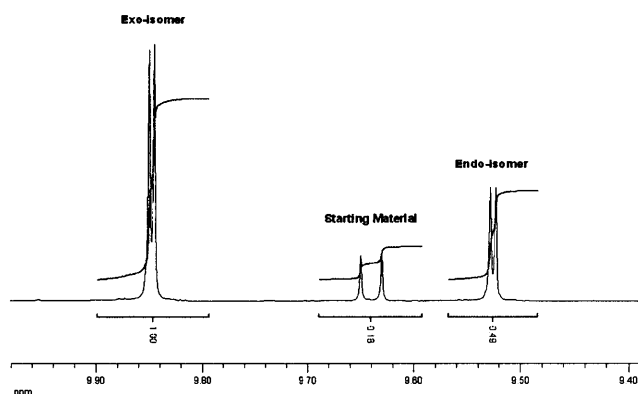
(Figure 2.8) ^{1}H NMR spectrum of the region used to calculate conversion and *exo:endo* ratios for catalytic runs.

This method had previously been validated by comparison of the isolated yield of the experiment with those predicted from the conversion (determined by the method outlined above) being within experimental error (1-2% yield).[99] There was no evidence of side reactions other than dimerisation of cyclopentadiene **19** which occured in a small and comparable extent in all catalytic runs independent of catalyst.

2.2.4 Performance of Catalysts

Catalysts were submitted to standard reaction conditions to gauge their respective activities (*Tables 2.1 and 2.2*).
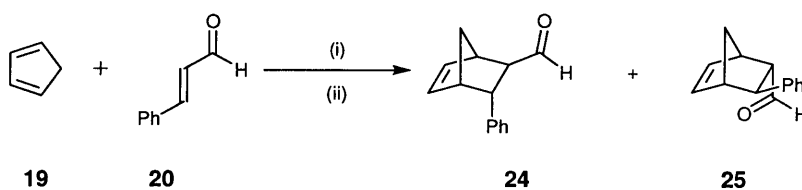
(i) Catalyst (10 mol%), MeOH, 25 °C. (ii) TFA, CHCl$_3$, H$_2$O

(Scheme 2.6)

38

Entry	Catalyst[a]	Structure	Conversion %[b]	exo:endo
1	74.HCl		4	n.d.
2	75.HCl		62	66:34
3	76.HCl		65	65:35
4	77.HCl		94	67:33
5	85.HCl		94	65:35

(a) Reactions were carried out at 25 °C for 6 hours with 10 mol% catalyst in methanol.

(b) Conversion determined by ^{1}H NMR of crude reaction mixtures.

(c) *exo/endo* ratios determined by ^{1}H NMR of crude reaction mixtures.

(Table 2.1)

Entry	Catalyst[a]	Structure	Conversion %[b]	exo:endo
1	74.HCl		16	64:36
2	75.HCl		83	66:34
3	76.HCl		88	65:35
4	77.HCl		94	67:33
5	85.HCl		94	65:35

(a) Reactions were carried out at 25 °C for 24 hours with 10 mol% catalyst in methanol.

(b) Conversion determined by ^{1}H NMR of crude reaction mixtures.

(c) *exo/endo* ratios determined by ^{1}H NMR of crude reaction mixtures.
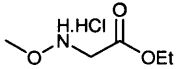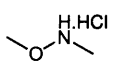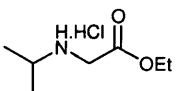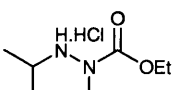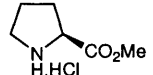
(Table 2.2)

Hydrazine **74.**HCl proved to be a disappointing catalyst for the reaction especially when compared with catalyst **75.**HCl. Catalyst **74** was difficult to synthesise with doubts over its stability. However, when the results from 6 h and 24 h are compared it suggests that the amount of compound catalysing the reaction remains constant as the conversion after 24 h (16%) is four times the magnitude of the conversion after 6 h (4%) which is expected in the early part of the kinetics for a first order process. A possible explanation in hindsight could be the formation of the dihydrochloride salt **88** which would severely alter the magnitude of the α–effect as the lone pair believed to be responsible for increased nucleophilicity would be protonated and hence **88** would no longer posses the α–effect. Due to the difficulties associated in the preparation of catalyst **74** investigations into whether this was the case were not conducted.

(Figure 2.9)

Catalyst **75** provided the most interesting results of those examined as it took the standard reaction to 62 and 83 % conversion after 6 h and 24 h respectively. When catalyst **75.HCl** was compared to catalysts **68, 72** and **70** interesting conclusions could be drawn (*Table 2.3*).

Entry	Catalyst[a]	Structure	Conversion %[b]	exo:endo
1	**75**.HCl		62	66:64
2	**68**		<5	n.d.
3	**89**		<5	64:36
4	**72**		98	65:35
5	**69**		<5	n.d.
6	**70**		62	70:30

(a) Reactions were carried out at 25 °C for 24 hours with 10 mol% catalyst in methanol.

(b) Conversion determined by ^{1}H NMR of crude reaction mixtures.

(c) exo/endo ratios determined by ^{1}H NMR of crude reaction mixtures.

(Table 2.3)

Catalysts **68** and **89** both contain less nucleophilic nitrogens and gave conversions less than <5% after 6 h. Catalyst **75**.HCl contains a nucleophilic nitrogen as well as β–EWG and is reasonably active (*Table 2.3, entry 1*). Catalyst **72** (*Table 2.3, entry 4*) is considerably more active than **75** but this can easily be attributed to superior structural features determined form the results of the previously conducted SAR study; namely the α-heteroatom is nitrogen along with secondary substitution α- to the reactive nitrogen. Comparing this result with that of proline methyl ester hydrochloride **70** (*Table 2.3, entry 6*) and pyrrolidine hydrochloride **69** (*Table 2.3, entry 5*) it can be concluded that in order to have an active catalyst a nucleophilic nitrogen is required (achieved either by incorporation into a five membered ring or by utilising the α-effect) along with a β–carbonyl based EWG. Importantly, these functionalities may be separated to obtain high activity.

Interestingly, incorporation of an additional EWG as in catalyst **76** (*Table 2.2, entry 3*) increases the conversion only slightly. With consideration of the structural differences

41

and previous SAR studies the catalysts can be thought of as having similar activity. This suggests that only a single β-EWG is necessary for efficient catalysis. The activities observed for catalysts **77** and **85** are consistent with the results of previous investigations.[99]

An explanation that would be consistent with the results obtained might be that the carbonyl in the β-position could be acting as a proton shuttle, aiding in the protonation and deprotonation of the various intermediates **81a** and **81b** involved in formation (and/or hydrolysis of iminium ion **84** (*Scheme 2.7*). If indeed it is these types of processes that are kinetically significant, then acceleration by a proton shuttling effect would increase the overall rate of iminium ion formation and hence the catalytic cycle, providing that iminium ion formation was the RDS.
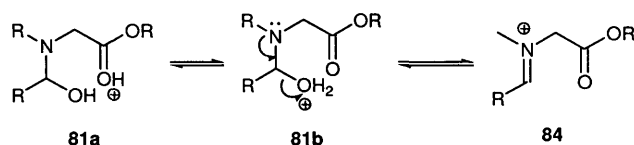
(Scheme 2.7)

This model is consistent with the fact that the α–heteroatom and the β-EWG can be separated spatially and with no loss of catalyst activity, and also the fact that a second β-EWG leads to no further gain in activity.

2.3 Conclusions

This study, along with previous investigations highlighted the need for both a nucleophilic nitrogen and a carbonyl based β-EWG within the catalyst architecture for high activity. The study also demonstrated that the two effects appeared to operate independently and therefore could be separated to allow for more structurally diverse catalysts to be designed. However, it was still unclear as to what was the mode of action of the β-EWG, despite the fact that synergy with the α-effect could be eliminated.

Chapter 3: Investigations to Discover the Function of the β-Electron Withdrawing Group

3.1 Aim of the Investigation

The aim of this study was to synthesise a number of novel catalysts, based around the acyclic catalyst architecture developed previously within the group, to probe the optimal electronic properties for the β-carbonyl electron withdrawing group to increase catalyst activity. Appropriate electron withdrawing/donating groups were introduced to allow for a Hammett plot to be obtained.

3.2 Introduction

The results of previous experiments lead us to hypothesise that the β-EWG was acting as a proton shuttle in iminium ion formation and thus increasing the efficiency of iminium ion formation and hydrolysis, accelerating the catalytic cycle. We sought to provide evidence for this mode of action and attempted to tune the electronics of the β-EWG to provide more active catalysts, while providing information to aid future rational design of chiral catalysts.

To provide supporting evidence for our hypothesis we designed an SAR study in which variation of the electron density centred on the carbonyl might provide more active catalysts and further our understanding. Considered choice of the catalyst scaffold to be modified would allow us to construct Hammett plots by relating the *pseudo* first order rate constants of the overall catalytic cycle to the Hammett parameters of the substituents.

3.2.1 Catalyst Design

The catalyst scaffolds chosen for elaboration were **90** and **91**. The reasons for this were three fold: Firstly, the catalysts had moderate activity over a 6 h period (76% and 58% conversion respectively) which would allow for any alteration in activity to be easily observed. Secondly, synthesis of the catalysts was envisaged to be short and straightforward. Finally, electronically perturbing substituents placed on the benzoyl EWG groups allow for Hammett analysis to be conducted.
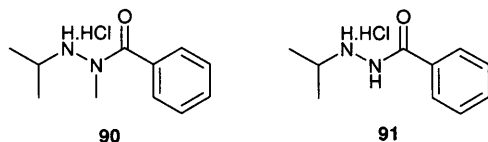
(Figure 3.1)

The catalysts chosen as targets were designed to include a range of stronger and milder β-EWG relative to the standard catalysts **90** and **91**. We also targeted catalysts that could not be used in a Hammett plot but would allow qualitative conclusions to be drawn about the nature of the β-EWG.
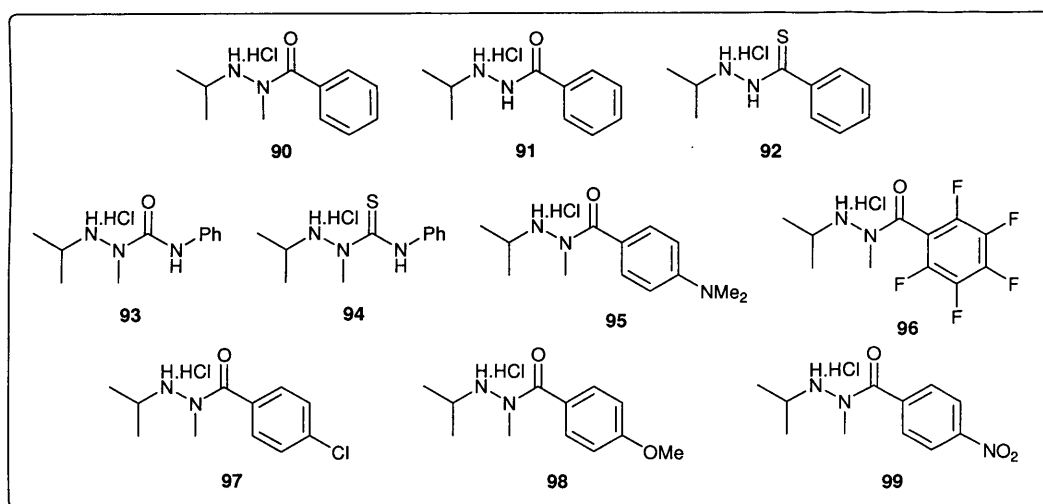
(Figure 3.2)

Catalysts **90** and **95-99** were targets for the Hammett analysis. Catalysts **92** and **94** were designed to replace the oxygen of the carbonyl with a sulphur atom to explore the effect on catalyst activity. Catalyst **93** was chosen to investigate the effect of a strong electron donating group on activity.

3.3 Results and Discussion

3.3.1 Synthesis

Synthesis began with formation of hydrazone **100** from the condensation of acetone and *N*-methylhydrazine **101** (70%) followed by coupling with the corresponding acid chloride to yield the catalyst precursor which was subsequently reduced to yield the target catalysts in yields of 13-73% from **100**.
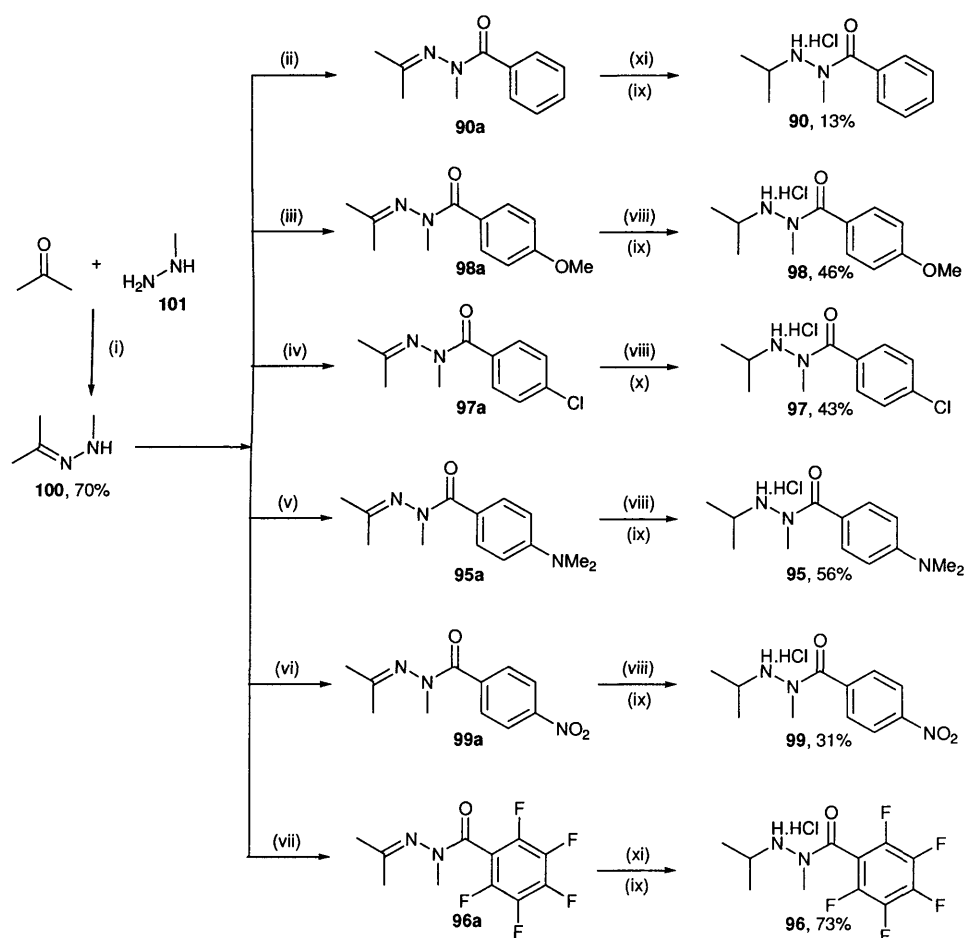
(i) KOH, <35 °C, (ii) PhCHO, CH_2Cl_2, rt,16 h, (iii) 4-OMe-C_6H_4CHO, CH_2Cl_2, rt, 16 h, (iv) 4-Cl-C_6H_4CHO, CH_2Cl_2, rt, 16 h, (v) 4-NMe_2-C_6H_4CHO, CH_2Cl_2, rt, 16 h, (vi) 4-NO_2-PhCHO, CH_2Cl_2, rt, 16 h, (vii) C_6F_5CHO, CH_2Cl_2, rt, 16 h, (viii) 3 eq $NaCNBH_3$, 2N HCl, MeOH, rt, 16 h, (ix) 5 eq HCl in ether, (x) HCl salt formed in reaction vessel with HCl in MeOH, (xi) H_2, PtO_2, EtOH, 16 h

(*Scheme 3.1*)

Compound **93** was synthesised in an analogous manner coupling the hydrazone **100** and phenyl isocyanate followed by reduction to yield the free base of the catalyst (*Scheme 3.2*). Synthesis of **94** was attempted, however, difficulties were encountered in the purification with minor but detectible impurities present. No further studies were performed with catalyst **94**.

100   **93, 79%**

(i) CH_2Cl_2, rt, 16 h, (ii) $NaCNBH_3$, 2N HCl, MeOH, 16 h, (iii) 5 eq HCl in MeOH
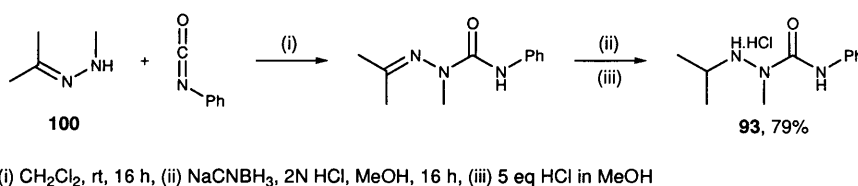
(*Scheme 3.2*)

Catalyst **91** was synthesised from commercially available benzoic hydrazide **102** and acetone to yield hydrazide **103** followed by a reduction and salt formation to give **91** (*Scheme 3.3*).[100]

102   **103, 86%**   **91, 82%**

(i) CH_3CN, rt, 16 h, (ii) H_2, PtO_2, EtOH, 16 h, (iii) 5eq HCl in ether
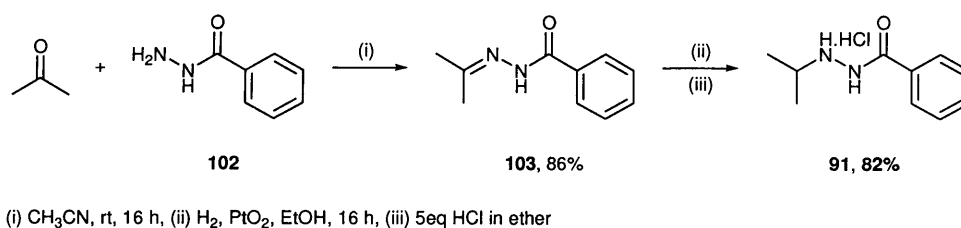
(*Scheme 3.3*)

Catalyst **92** was synthesised from compound **103** using Lawesson's reagent to convert the carbonyl to the corresponding thio carbonyl. The product was reduced and the salt formed to yield the catalyst **92** (*Scheme 3.4*).

103   **104, 55%**   **92, 49%**

(i) Lawesson's reagent, CH_3Ph, Δ, N_2, 16 h, (ii) $NaCNBH_3$, 2M HCl, MeOH, 16h, (iii) 5 eq HCl in ether
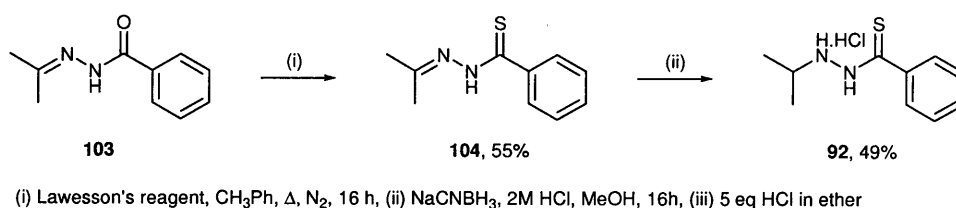
(*Scheme 3.4*)

The salts of all the catalysts (except **97**) were formed on adding 5 equivalents of HCl in methanol to the free base. The salt of **97** was generated *in situ* for the catalytic run by adding a single equivalent of HCl in MeOH of known concentration. This method was validated by comparing the performance of the free base of catalyst **91,** forming the salt *in situ,* with that of the preformed HCl salt. The results were found to be within experimental error (*ca* 3%) confirming the validity of this method. This was necessary to allow for direct comparison with experiments previously conducted.

3.3.2 Catalyst Performance

Once the catalysts were prepared they were examined in the standard Diels-Alder reaction between cinnamaldehyde **20** and cyclopentadiene **19** for 6 h.
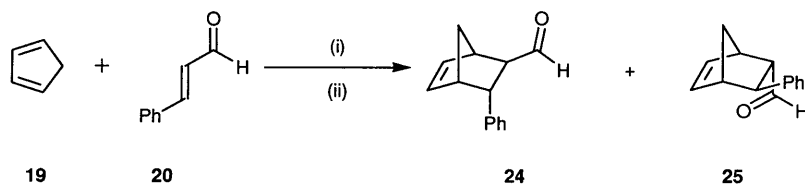
(i) Catalyst (10 mol%), MeOH, 25 °C. (ii) TFA, CHCl₃, H₂O

(*Scheme 3.5*)

Entry	Catalyst[a]	Structure	Conversion %[b]	*exo:endo*
1	**90**		76	67:33
2	**91**		58	62:38
3	**92**		<5	n.d.
4	**93**		25	69:31
5	**95**		75	65:35
6	**96**		61	72:28
7	**97**		52	62:38
8	**98**		77	69:31
9	**99**		77	56:35

(a) Reactions were carried out at 25 °C for 6 hours with 10 mol% catalyst in methanol.

(b) Conversion determined by ^{1}H NMR of crude reaction mixture.

(c) *exo/endo* ratios determined by ^{1}H NMR of crude reaction mixture.

(*Table 3.1*)

The results of this study yielded some interesting but overall disappointing results. The catalyst with the lowest activity was **92** (*entry 3*, <5%). The reaction appeared extremely sluggish, especially when compared to the equivalent catalyst **91** (*entry 2*, 58%), such

that after a 6 h period insufficient product was formed to enable measurement of an *exo:endo* ratio. It is noteworthy, however, that the ^{1}H NMR spectrum of the reaction mixture indicated that some other process may have occurred as it appeared uncharacteristically complex and untidy. Whether or not the catalyst was just poor or had reacted in a different manner was not defined, however, it can be concluded that thiocarbamate EWG's were not effective within the catalyst scaffold for this transformation.

The introduction of a urea based EWG in catalyst **93** had a detrimental effect on catalyst activity (*entry* 4, 25%) when compared to standard catalyst **90** (*entry* 1, 76%). The urea group was chosen for the high electron density that would be present on the carbonyl from donation of the lone pairs of the nitrogens. It was concluded that this effect was possibly too strong for optimal catalyst activity.
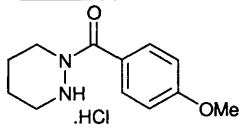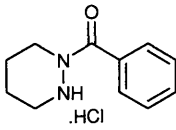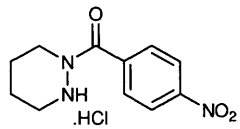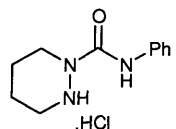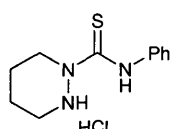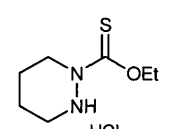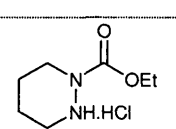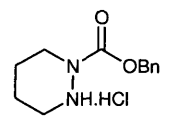
The catalysts designed to have lower electron density on the carbonyl of the EWG displayed a mixture of results. Catalyst **97** (*entry* 7, 52%) gave the lowest conversion followed by **96** (*entry* 6, 61%). Catalyst **99** (*entry* 9, 77%) displayed similar activity to the standard **90** (*entry* 1, 76%). It is clear from these results that apart from commenting on individual catalysts there was no apparent relationship between electron density on the carbonyl oxygen and catalyst activity.

The catalysts designed to have greater electron density on the carbonyl also provided inconclusive results. Catalysts **95** (*entry* 5, 75%) and **98** (*entry* 8, 77%) both gave conversions that were within experimental error of the standard catalyst **90** (*entry* 1, 76%) and therefore it can be concluded that these subtle changes in the electron density had no significant effect on reactivity.

Originally, the catalysts were designed to construct a Hammett analysis to yield information of the electronic environment of the key transition-state in the overall catalytic cycle. However, it is clear from the results (*Table 3.1*) that there was no

relationship between catalyst activity and electron withdrawing ability, therefore, a Hammett analysis was not conducted.

In parallel to this work on acyclic catalysts another group member conducted a similar study based on a cyclic catalyst scaffold (*Table 3.2*).[99]

Entry	Catalyst[a]	Structure	Time h	Conversion %[b]	*exo:endo*[c]
1	**105**		6	67	66:34
2	**106**		6	59	64:36
3	**107**		6	32	62:38
4	**108**		6	17	50:50
5	**109**		6	15	32:68
6	**110**		6	35	69:31
7	**73**		6	99	68:32
8	**111**		6	94	68:32

(a) Reactions were carried out at 25 °C for 24 hours with 10 mol% catalyst in methanol.

(b) Conversion determined by ^{1}H NMR of crude reaction mixtures.

(c) *exo/endo* ratios determined by ^{1}H NMR of crude reaction mixtures.
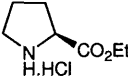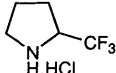
(*Table 3.2*)

The results obtained for the cyclic series were in good agreement with the acyclic series. Catalysts based on thiocarbamates **110** (*entry 6,* 35%) and urea derivatives **109** (*entry 5,* 15%) and **108** (*entry 4,* 17%) performed badly compared to standard catalyst **106** (*entry 2,* 59%). However, a small but significant increase was observed for the slightly electron donating *p*-methoxyphenyl catalyst **105** (*entry 1,* 67%) relative to standard catalyst **106** (*entry 2,* 59%). The catalyst containing a *p*-nitro EWG displayed reduced activity compared to standard catalyst **106** (*entry 3,* 32%).

The number of catalyst synthesised suitable for Hammett analysis was insufficient although the limited results looked promising. It is noteworthy, however, that none of the catalysts prepared had comparable activity to the previously synthesised benchmark catalyst **73** (*entry 1,* 99%). The study managed to discount numerous structural features for future design but provided little information that could be applied to enhance catalyst activity.

3.3.3 The Role of the Electron Withdrawing Group EWG

An important question that needed to be addressed to aid our understanding was whether the β-EWG must be carbonyl based to be effective. Therefore, we sought a commercially available catalyst that contained a nucleophilic nitrogen but also a strong β-EWG that could not act as a proton shuttle. Trifluoromethyl pyrrolidine (**112**) was selected as it would allow direct comparison with pyrrolidine hydrochloride (**69**) and proline methyl ester hydrochloride (**70**). The trifluoromethyl group is a very strong EWG but the fluorine atoms should not act as a proton shuttle. Catalyst **112** was converted to the HCl salt **112.HCl** and examined in the standard Diels-Alder reaction.

Entry	Catalyst[a]	Structure	Conversion %[b]	*exo:endo*[c]
1	**69**	N H.HCl	<5	n.d
2	**70**	N H.HCl CO₂Et	62	70:30
3	**112.HCl**	N H.HCl CF₃	93	68:32

(a) Reactions were carried out at 25 °C for 24 hours with 10 mol% catalyst in methanol.

(b) Conversion determined by ^{1}H NMR of crude reaction mixtures.

(c) *exo/endo* ratios determined by ^{1}H NMR of crude reaction mixtures.

(Table 3.3)

Catalyst **112.HCl** (93%, 6 h) was surprisingly active, especially given the fact that it had a simple structure compared to the more elaborate catalysts that we had prepared of similar activity. This result suggested that the β-EWG was acting on a purely inductive basis as it was difficult to envisage any other mode of action. We therefore concluded that ability of the β-EWG to act as a proton shuttle could also be excluded as an important feature in catalyst design.

The significant conclusion was that our understanding of the role of the β-EWG was inadequate. The underlying reason for this was that we had a poor understanding of the relationship of the individual steps of the catalytic cycle. This lack of knowledge made it extremely difficult to arrive at credible conclusions because our deductions to date were based largely on qualitative experiments.

3.4. Conclusions

Our attempts to prepare more active catalyst for the iminium ion catalysed Diels-Alder reaction by altering the electron density of the carbonyl group failed. Each of the novel catalysts prepared were of lower activity to catalysts previously prepared within the group. The catalysts prepared were designed to probe the electronic requirements of the carbonyl based β-EWG, however, due to the spread of results obtained, this was not possible. The effectiveness of trifluoromethyl pyrrolidine hydrochloride **112.HCl** as a catalyst suggested that the β-EWG was not exclusively acting as a proton shuttle as previously hypothesised. It was also concluded that detailed investigations into the mechanism of the catalytic cycle should be conducted to achieve a better appreciation of the relationships of catalyst architecture and activity.

Chapter 4: Studies to Determine the Mechanism of the Organocatalysed Diels-Alder Reaction

4.1 The Aim of the Research

The purpose of this investigation was to establish the kinetically important features within the catalytic cycle by measurement of the rate constants and activation energies associated with each step. We also sought to extract any additional information that would aid us in the rational design of secondary amine catalysts for the Diels-Alder reaction.

4.2 Introduction

Having spent much effort within the group developing and testing catalysts for the Diels-Alder reaction between cinnamaldehyde **20** and cyclopentadiene **19** it was evident that our conclusions were philosophically weak due to our inherent ignorance of the physical parameters of the catalytic cycle.
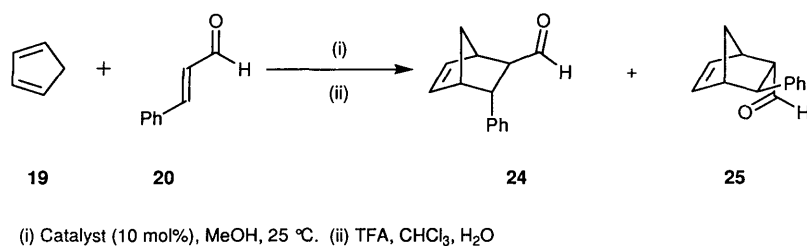
(i) Catalyst (10 mol%), MeOH, 25 °C. (ii) TFA, CHCl$_3$, H$_2$O

(Scheme 4.1)

To aid in the interpretation and also development of catalysts we sought to discover the relative rates and activation energies associated with the individual steps of the catalytic cycle. Previous attempts to understand the mechanism had been undertaken within the group and a range of techniques had been applied to gain an insight.[99] These attempts failed to provide any quantitative evidence for the mechanism but provided a solid platform from which to expand the research.

The previous work was thwarted by the inability to isolate iminium ions to allow for independent study of the individual steps of the reaction. To further this research we targeted the isolation of the iminium ion intermediate as the key task to unlock the kinetics of the reaction.

Concurrent with our investigations Ogilive published similar work based on the kinetic observation of his asymmetric α-effect catalyst **24**. The study comprised of monitoring the entire catalytic cycle by ^{1}H NMR and observing the relative quantities of the various intermediates against time. From the data obtained it was possible to identify the rate determining step which was highlighted as the Diels-Alder cycloaddition. However, as quantitative kinetic measurements were not conducted, no explanation could be given to explain the observation. From our preliminary studies we could postulate that the RDS was the Diels-Alder cycloaddition step form the observation that it was sluggish relative to the other steps in the catalytic cycle. Furthermore, Ogilive's catalyst, although asymmetric was not very active and the reactions were conducted in nitromethane and therefore, could have very different kinetics to the systems that were of interest to us. The publication, although elegant, failed to provide any of the explanations that we sought to further our understanding of the catalytic cycle. Therefore, we continued with our studies with a hope to satisfy our curiosity.

4.2.1 The Concept
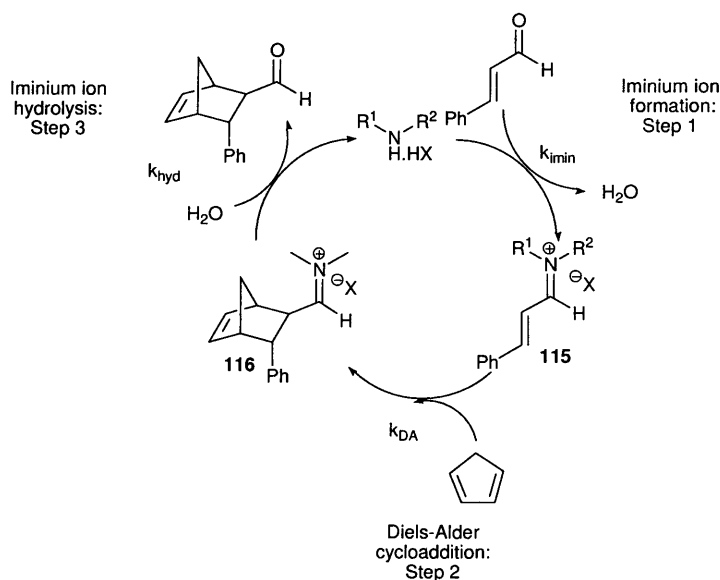
(Figure 4.1)

The isolation or favourable equilibrium in solution of an intermediate iminium ion **115** would allow for the determination of the kinetics for the formation of the iminium ion if a suitable physical technique could be found (*Scheme 4.2*).
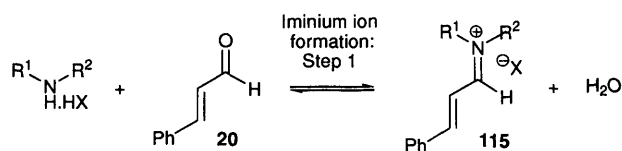
(Scheme 4.2)

The isolation of **115** would also allow for a subsequent independent reaction with cyclopentadiene **19** to form Diels-Alder iminium ion adduct **116** (and its *endo*-isomer). Under anhydrous conditions the isolation of compound **116** should also be possible (*Scheme 4.3*).
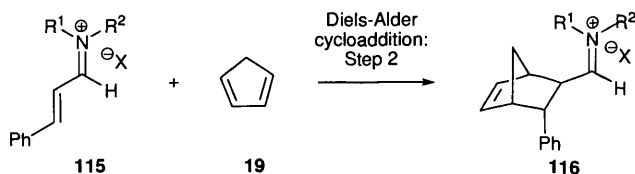
(Scheme 4.3)

The isolation of Diels-Alder iminium adduct **116** would also allow for the independent study of step 3 on addition of water (*Scheme 4.4*).
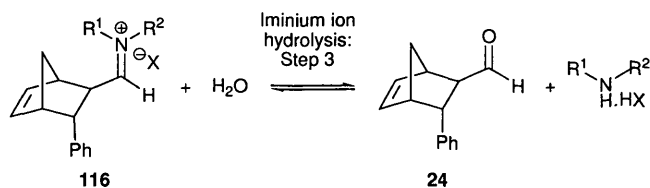
(Scheme 4.4)

The combination of the three steps would allow us to build up a picture of the entire catalytic cycle to aid in our understanding and the quest for more active catalysts.

4.3 Results and Discussion

4.3.1 Isolation of Iminium Ions

Previous attempts to isolate iminium ions as their HCl salts had proved unfruitful, indicating that modification of the system was necessary to achieve our aims. We therefore sought a catalyst-dienophile-co-acid combination that would provide a stable iminium ion (*Figure 4.2*).
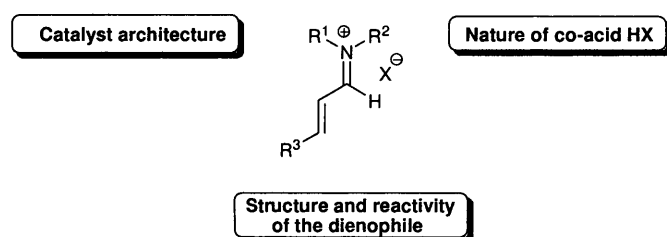
(Figure 4.2)

We began our search by identifying catalysts that would, from our experience, provide a practical and useful system for kinetic evaluation. We rationalised that we should select an active catalyst that we had previously studied on the bench, as the relative order of kinetics for each step might be different for less active catalysts (it was of course the active catalysts that interested us most). Also, the collection of data would be more rapid with an efficient system. The catalysts selected were trifluoromethyl pyrrolidine **112**, MacMillan's imidazolidinone **7** and the most active catalyst developed by the group to date **73** (*Figure 4.3*).
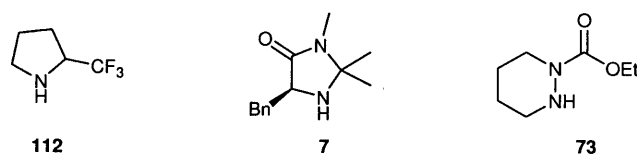
(Figure 4.3)

Our intention was to use either cinnamaldehyde **20** or its derivatives **117-121** as our dieneophile to ensure that our model system was as similar as possible to the system we had used for our SAR studies (*Figure 4.4*).
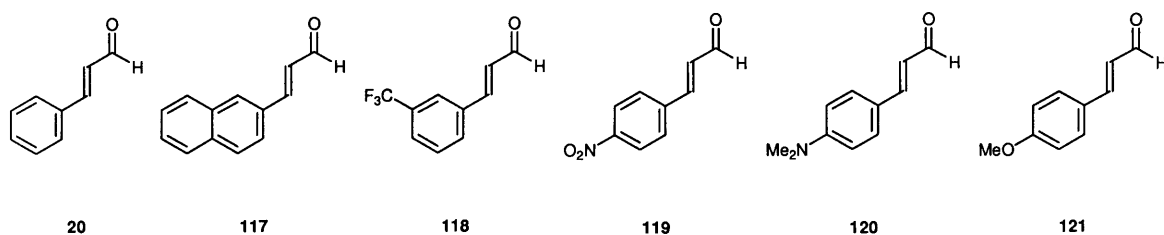
(Figure 4.4)

Compounds **117** and **118** were chosen as substrates for use with fluorescence spectroscopy as they are known fluorophores. **117** and **118** were synthesised *via* a literature Heck reaction.[101] The remaining aldehydes **119-121** were commercially available.

It was clear that the one aspect of our system that needed addressing was the co-acid as numerous attempts to isolate the iminium chloride salts had failed. This was believed to be due to their instability towards hydrolysis. We therefore sought a co-acid that might have a stabilising effect on the resulting iminium ion. To achieve this we selected a number of weakly coordinating anions highlighted as good candidates in a review of non-coordinating anions.[102] We selected hexafluorophosphoric acid HPF_6, tetrafluoroboronic acid HBF_4 and fluoroantimonic acid $HSbF_6$. Pleasingly, on reaction of one equivalent of cinnamaldehyde **20**, trifluoromethyl pyrrolidine **112** and aqueous HPF_6 in methanol at room temperature we obtained the iminium ion **122** in 82% yield as a geometrically pure bench stable compound.
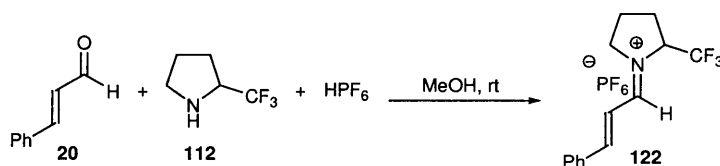
(Scheme 4.5)

This initial success allowed us to synthesise a range of iminium ions based on catalysts **112** and **7** with a variety of cinnamaldehyde derivatives and co-acids. These iminium ions were primarily characterised by HRMS and occasionally X-ray diffraction as in solution the majority of iminium ions were clearly in equilibrium with the starting materials making spectroscopic analysis difficult. Full analysis was conducted for the iminium ion **122** which was important to the study.

HPF_6 quickly emerged as the optimal co-acid for the isolable iminium ions although HBF_4 and $HSbF_6$ did yield iminium ions, but they appeared to be less stable than those derived from HPF_6. Catalyst **112** gave the most stable iminium ions isolated and therefore was selected for subsequent kinetic studies.

4.3.2 Structural Studies

Having synthesised numerous examples of stable iminium ions we attempted to grow crystals suitable for X-ray analysis. The iminium ions for which X-ray structures were determined are shown below (*Figure 4.5*).

(Figure 4.5)
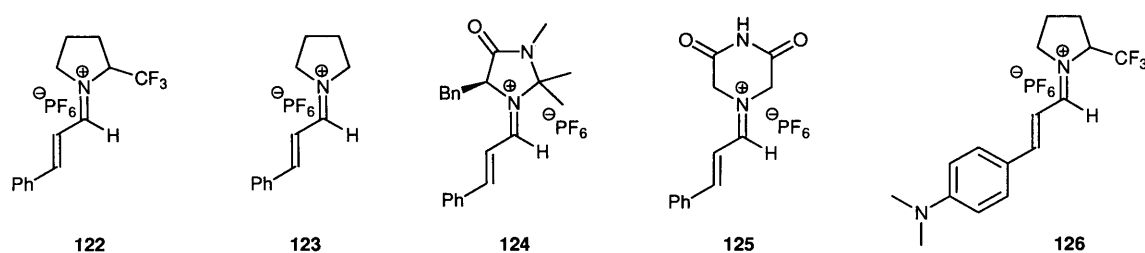
It was hoped that a comparison of structural features of the isolated iminium ions and their relative activity would structuaral information that could be related to the electronic of the π-system. A selection of these structures are shown below (*Figure 4.6*). These X-ray structures clearly show that the *E*-geometry is favoured for iminium ions **124** and **122** and that in all iminium ions the π-system is planar indicating good conjugation. The X-ray structures also provided structural information about the catalyst conformation in the iminium ion providing a more accurate model from which to design asymmetric catalysts. We have used the approach to investigate a novel class of secondary amines to be developed as asymmetric catalyst for iminium ion catalysed processes (*see Chapter 6*).
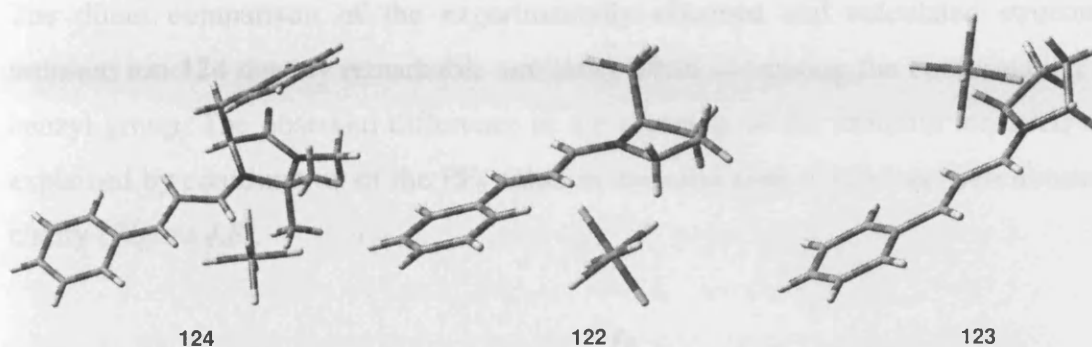
*(Figure 4.6) From left to right: X-ray structures of **124**, **122** and **123***

The isolation of the MacMillan derived iminium ion **124** allowed comparison of the solid-state structure with the two published calculated structures (MacMillan **124a**[103] and Houk **124b**[104]) and a calculated structure obtained during complementary theoretical studies conducted by Platts and Evans in Cardiff.[105] The structure reported by Houk was remarkably similar to the structure obtained from Evans's calculations and thus only the Evans structure of the two is shown (**124b**).
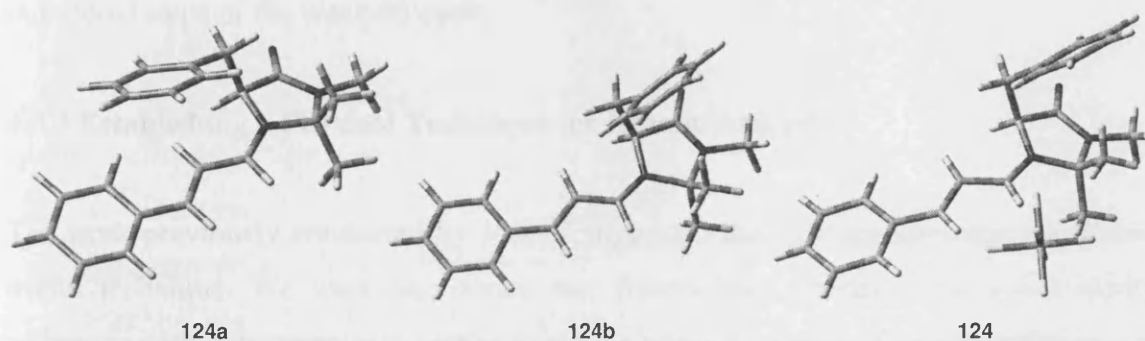
(Figure 4.7) From left to right: MacMillan's calculated structure **124a**, Evans calculated structure **124b** and X-ray structure **124**.

This evidence suggests that the structure proposed by MacMillan using low level MM3 calculations in which π–π stacking localises the benzyl arm over the iminium ion is incorrect in the solid-state. The most likely structure is the benzyl arm residing over the centre of the imidazolidinone ring of the catalyst **124** (*Figure 4.7*). However, the argument is academic as the mode of asymmetric induction is consistent for both conformations.

The direct comparison of the experimentally obtained and calculated structures of iminium ion **124** display remarkable similarity when comparing the conformation of the benzyl group. The observed difference in the planarity of the iminium ion itself can be explained by coordination of the PF_6 anion in the solid state which has been removed for clarity (*Figure 4.8*).
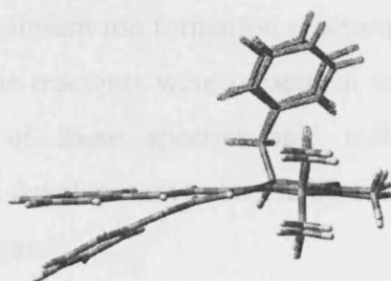
(Figure 4.8) Displaying the X-Ray **124** and the Evans calculated structures **124b** overlaid.

Having established that isolation of iminium ions was possible and fairly general for cyclic secondary amines with cinnamaldehyde derivatives and HPF_6, we sought to identify the technique that would be most useful for determining the kinetics of the individual steps of the catalytic cycle.

4.3.3 Establishing a Physical Technique for Kinetic Analysis

The work previously conducted by Jones[99] suggested that UV spectroscopy would be a useful technique. We were also aware that fluorescence spectroscopy was a similar technique with departmental expertise to aid the physical studies. To explore this avenue we synthesised reported cinnamaldehyde derivatives **117** and **118** with fluorescent tags by a Heck reaction between the aryl halide and acrolein ethyl acetal followed by acetal hydrolysis. Subsequently we formed the corresponding iminium ions using HPF_6 and trifluoromethyl pyrrolidine **112**.

It was clear from preliminary experiments that low concentrations were needed for UV and fluorescence spectroscopy which favoured the starting materials **20** and **112.HPF₆** in the equilibrium of step 1 (*Scheme 4.6*). The reason for this was that on dilution of the solution containing iminium ion **122** the relative amount of water present was drastically increased using bench solvents. This amount of water essentially made the hydrolysis reaction *pseudo* 1st order and hence independent of the concentration of the iminium ion, where as the forward iminium ion formation reaction was still a concentration dependant 2nd order reaction as the reactants were present in equimolar amounts. This observation highlighted that use of these spectroscopic techniques would require significant experimental effort and development to be useful, and therefore, we investigated NMR as an experimental technique.
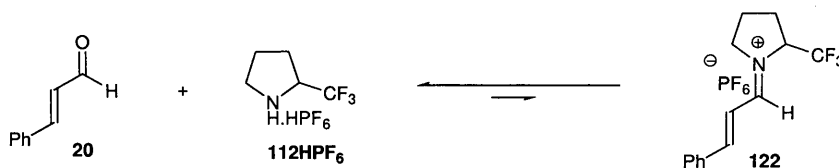
(Scheme 4.6)

Jones had previously discounted ^{1}H NMR as a useful technique as it appeared that the majority of the reaction had taken place before the first physical measurement could be made at approximately 7 minutes after mixing. We rationalised however, that reducing the concentration would decrease the actual rate of reaction and allow for physical measurements to be conducted. Furthermore, technical consultation indicated that methods were available for more rapid measurement of data points. Knowing this, qualitative experiments were conducted which clearly indicated that ^{1}H NMR would be a useful tool for the measurement of kinetics of iminium ion formation and of the subsequent Diels-Alder cycloaddition. The conditions and experimental details used are discussed in the following section.

4.3.4 Choice of Solvent for Study

The solvents of choice for the iminium ion catalysed Diels-Alder reaction for the majority of active catalysts are MeOH or MeOH/H$_2$O mixtures. However, mechanistic studies involving these solvents would be complex as the aldehydes in the reaction would be in equilibrium with their corresponding methyl acetals causing complications (*Scheme 4.7*).
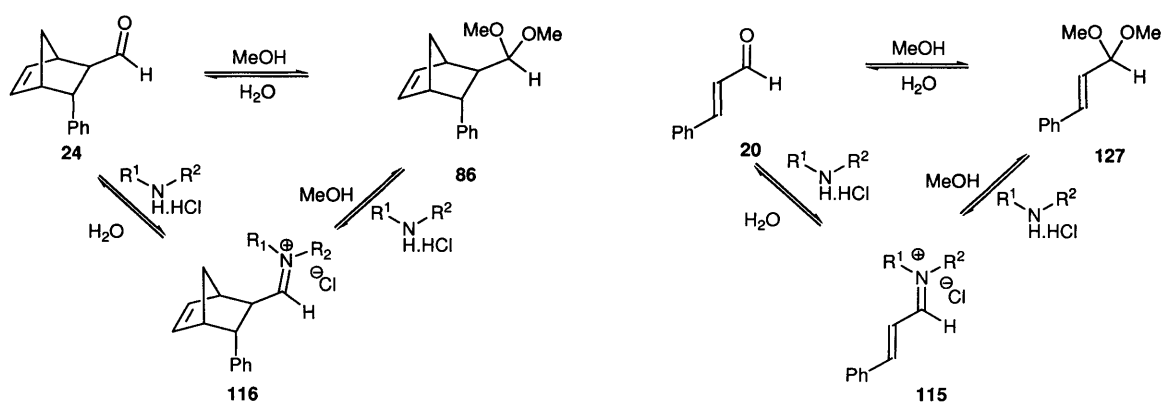
(Scheme 4.7)

If the reaction were to be conducted in MeOH then it would add extra equilibria to the catalytic cycle and thus create an additional level of complexity (*Scheme 4.7*). To circumvent this problem we sought a solvent that would maintain reactivity but would not react with the aldehydes and iminium ions in the reaction. The solvent would also have to be available in its deuterated form to be of use in NMR studies. Conducting a solvent screen revealed CH$_3$CN as the optimal reaction medium as it facilitated the fastest reaction for a non-alcoholic solvent.[106] Subsequently, it was found that the iminium ion of our model system **122** was only soluble in CH$_3$CN reinforcing our choice of solvent.

4.3.5 Validation of Model System

The components of our model system differ from those we would use to conduct the reaction on the bench. Therefore it was important to validate our model system by performing a bench reaction and then compare observations with the optimal system.

Comparison of the HPF$_6$ and HCl counter co-acids in methanol was not possible as the use of HPF$_6$ co-acid caused precipitation of the iminium ion **122** in the reaction vessel thus removing the active component from the catalytic cycle. We therefore conducted a reaction on the bench with HPF$_6$ in acetonitrile which gave 56% conversion in 6 h compared to HCl in methanol 93% in 6 h. Considering that we had moved form the optimal solvent and co-acid the drop in reactivity was expected.

No significant by-products were observed in the ^{1}H NMR of the crude reaction mixture consistent with the standard reactions. This evidence suggested that alteration of the co-acid affects the rate of the reaction but did not effect the mechanics of the reaction. Therefore, conclusions drawn from study of the model system should be applicable to the optimal bench system.

4.3.6 Iminium Ion Formation Step 1

We used the distinct ^{1}H NMR signal of the cinnamaldehyde **20** at 9.65 ppm and the iminum ion **122** at 8.64 ppm to allow us to monitor the progress of the reaction (*Figure 4.9*). Using the integrations of the peaks we could quantitatively determine the conversion of the reaction. The conversion was then related to concentration at any data point as the initial concentrations were known. This allowed us to extract the second order rate constant k_{imin} from a plot of 1/[A] vs t (*Appendix*) (where [A] is the concentration of the cinnamaldehyde) (*Appendix*).
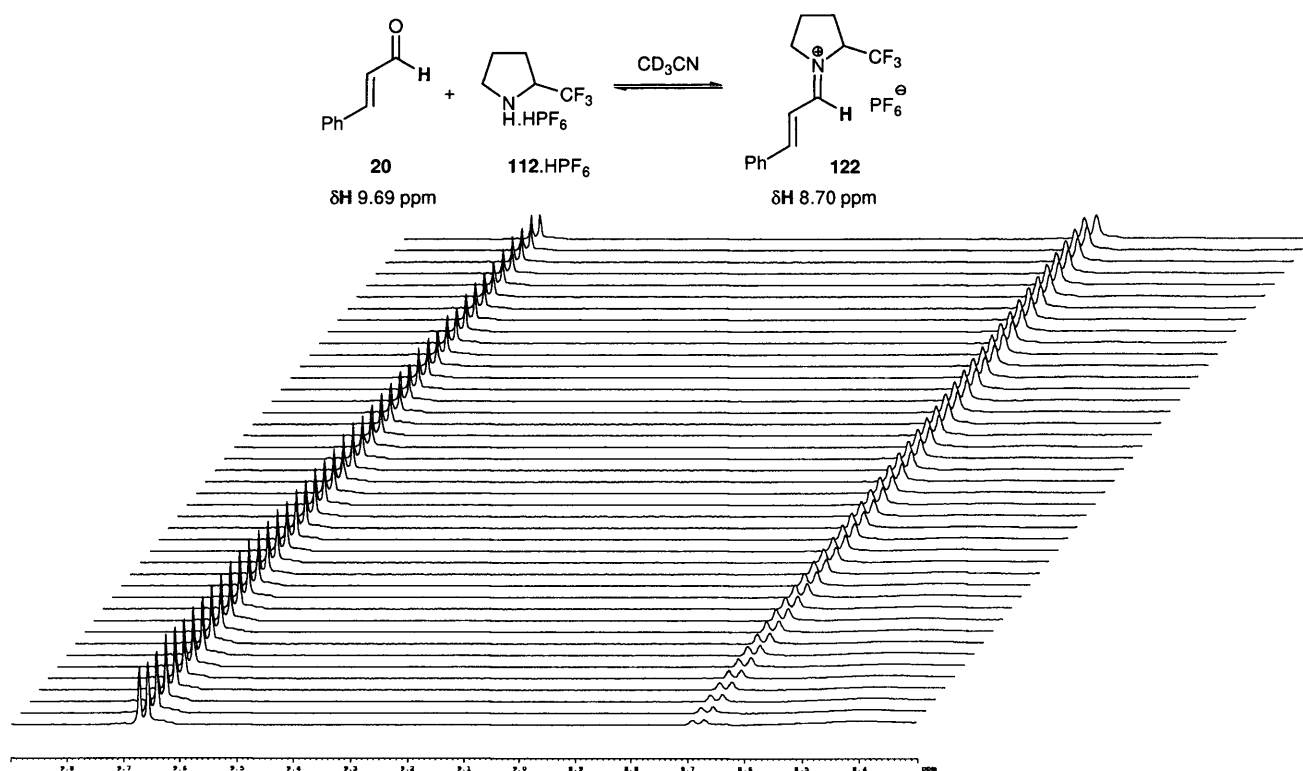
(Figure 4.9)

We measured the rate constants at 293, 298 and 303K (in duplicate) to allow the construction of an Arrhenius plot and hence determination of the activation energy. The rate constant was found to be $2.65 \pm 0.35 \times 10^{-3}$ dm^3 mol^{-1} s^{-1} at 293K.
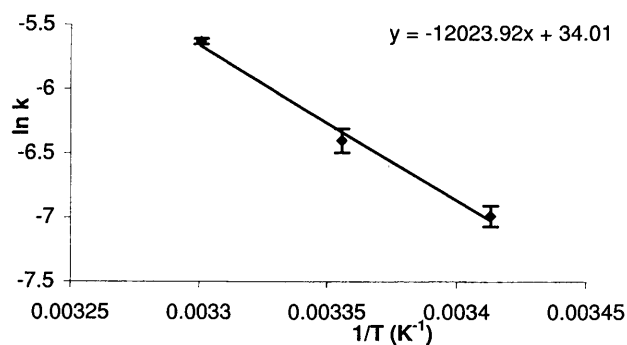
(Figure 4.10)

Measuring the rate constants at different temperatures allowed us to plot $\ln k_{imin}$ vs $1/T$ to obtain the E_a for step 1 at 100.0 ± 7.9 kJ mol^{-1} with an associated Arrhenius parameter A

67

of 6.694 $\times 10^{15}$ s^{-1}. The error on the intercept for the linear fit is $\pm$ 3.17 leading t a

uncertainty of $\pm$ $e^{3.17}$ (*Figure 4.8*). (*For experimental data see Appendix*)

4.3.7 Diels -Alder Cycloaddition Step 2

The Bruker 500MHz NMR machine was also employed for similar measurements of the Diels-Alder cycloaddition step. Ideally, we wanted to study steps **2** and **3** separately, however, this was not possible using our model system as the ^{1}H NMR signals of the Diels-Alder iminium ion adducts **130** and **131** overlapped with those of the iminium ion **122** at 8.64 ppm. Furthermore, the Diels-Alder iminium adducts **130** and **131** were observed to convert to side products corresponding to new unidentified broad peaks in the NMR signal at 9.21 and 9.33 ppm (*Scheme 4.8*). The reaction to these new unidentified peaks was not reversible by addition of 2 equivalents of water over a period of an hour (*see Appendix*).
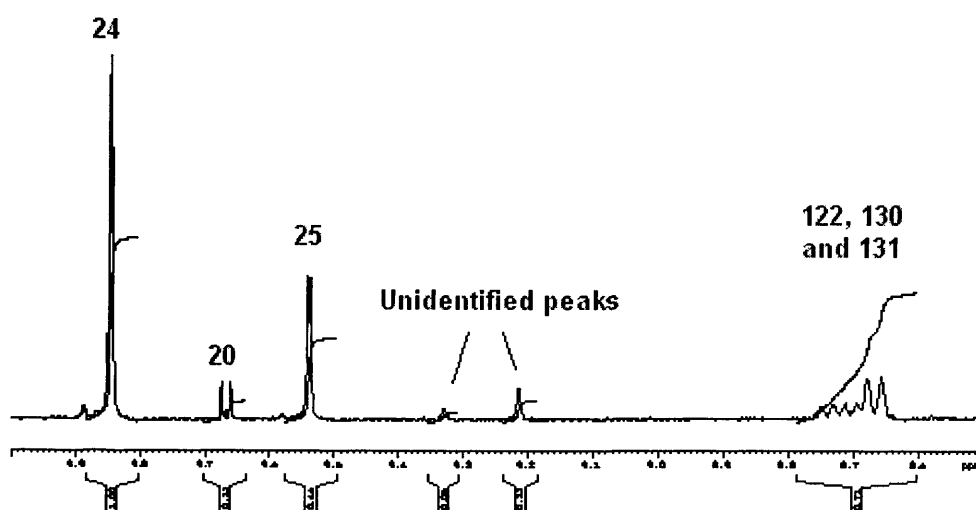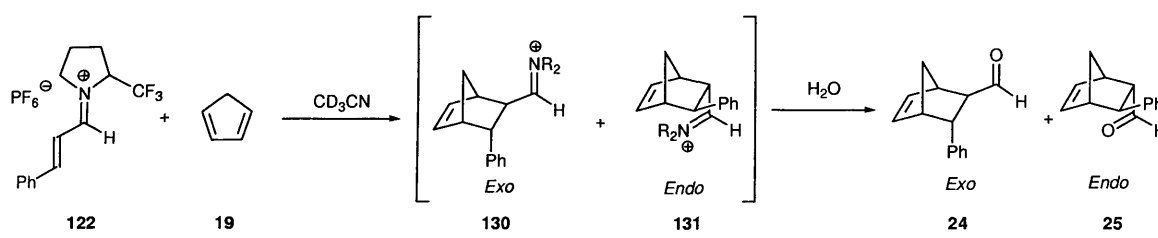
(Scheme 4.8)

We had strong evidence that the hydrolysis of the Diels-Alder iminium ion adducts **130** and **131** was extremely rapid relative to the Diels-Alder cycloaddition: When 2 equivalents of water were added to a CH_3CN solution of **122** followed by addition of **19**, the only observable peaks in the ^1H NMR were the Diels-Alder adducts **24** and **25** (Figure *4.11*). No indication of the intermediate iminium ions **130** and **131** could be detected. The absence of the unidentified peaks at 9.21 and 9.33 ppm in any of the reactions carried out in the presence of water in an NMR tube and on the bench suggested that there was never a sufficent amount of Diels-Alder iminium adduct formed in solution to facilitate this side reaction that was readily observed in absence of water. Furthermore, in the actual bench reactions MeOH or $MeOH/H_2O$ (19:1) are used as solvents so there are huge excesses of methanol and water present to hydrolyse the Diels-Alder iminium adducts **130** and **131** greatly reducing the kinetic significance of this step.

With 2 equivalents of water the reaction that we were effectively observing was the conversion of iminium ion **122** at (8.64 ppm) to the Diels-Alder products **24** and **25** (9.84 and 9.53 ppm respectively).
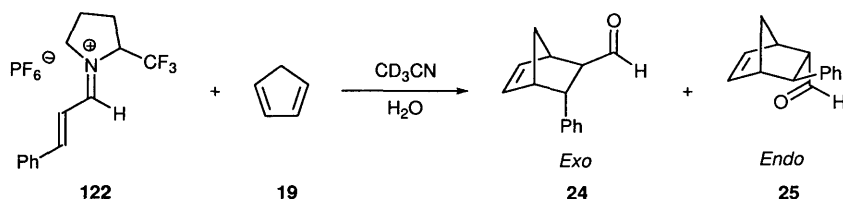
(Scheme 4.9)

Confident that the rate of hydrolysis was rapid compared to the cycloaddition we can state that our $k_{obs} = k_{DA}$. We then went on to measure the rate constants at a series of temperatures to allow us to calculate the Arrhenius parameter A and activation energy E_a.
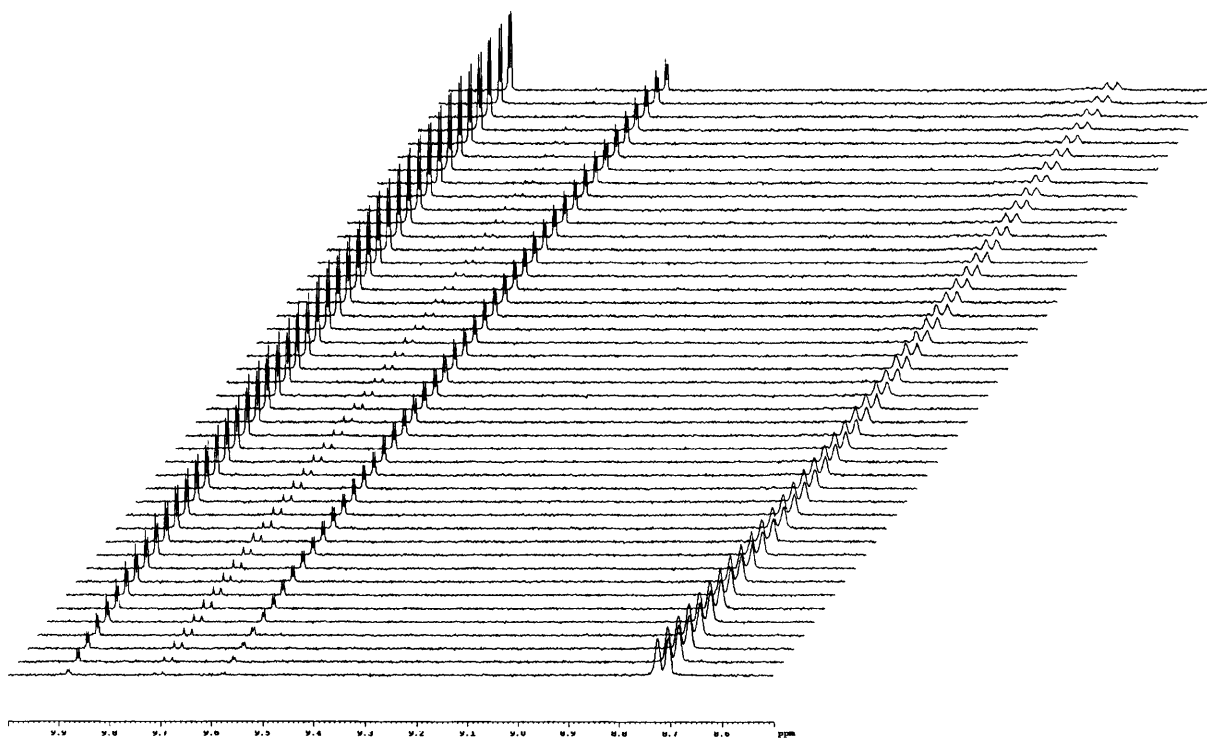
(Figure 4.11)

To allow for practical measurement 2.5 equivalents of cyclopentadiene were used as this accelerated the reaction to allow observation of the important portion of the kinetics within a one hour period. This treatment complicated the mathematics slightly but was easily manageable (*see Appendix*).
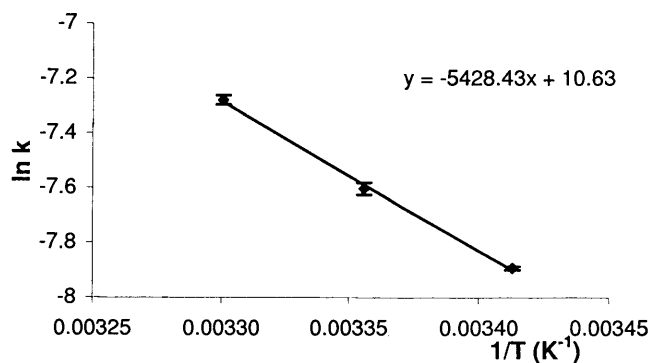
(Figure 4.12)

The second order rate constant of the Diels-Alder transformation was determined at 293, 298 and 303 K. The rate constant k_{DA} was found to be $3.74 \pm 0.02 \times 10^{-4} dm^3 \ mol^{-1} \ s^{-1}$ at 293K. The E_a for the Diels-Alder cycloaddition was found to be $E_a = 45.1 \pm 1.7 \ kJ \ mol^{-1}$

with an associated Arrhenius parameter value of 4.14 x 10^4 s^{-1} with an uncertainity of $\pm\ e^{0.17}$ (*Figure 4.12*).

4.3.8 Comparison to Theoretical Data

To compliment the experimental work Evans and Platts performed theoretical calculations to determine the activation energy of the individual steps of the catalytic cycle.[107] A comparison of the experimentally determined and calculated values for the E_a are shown below (*Table 4.2*).

Step	Experimental E_a (kJ mol^{-1})	Theoretical E_a (kJ mol^{-1})
Iminium ion formation 1	100.0 ± 7.9	96.9
Diels-Alder cycloaddition 2	45.1±1.7	62.3
Diels-Alder Iminium ion adduct hydrolysis 3	n.d.	73

(*Table 4.2*)

The theoretical data was found to be in reasonable agreement with the experimentally determined values. This experimental validation of the theoretical model was interesting as it provided the possibility of developing a predictive tool for catalyst activity.

4.3.9 Interpretation of Kinetic Data

By comparing the physical data for the steps of the catalytic cycle, we concluded that the Diels-Alder cycloaddition was the rate determining step of the catalytic cycle as it had a smaller rate constant than iminium ion formation. It can also be concluded that the Diels-Alder cycloaddition had the lower activation energy of the two steps measured.

The physical parameter that was most interesting for the development of more active catalysts was the magnitude and consequence of the Arrhenius parameter A. The A value contains qualitative information as to the nature of the transition state and is commonly

thought of as the number of collisions that take place per second, independent of the energy of the colliding molecules. This A value is then multiplied with the Boltzmann term containing the activation energy and temperature. Therefore, the magnitude of rate constant k at a constant T depends on A and E_a.
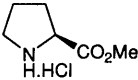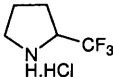
$$k = Ae^{-\frac{E_a}{RT}}$$

Iminium ion formation is a bimolecular reaction which requires two atoms to approach each other in the correct geometry for reaction. In this case it will be related to the Bürgi-Dunitz angle of $109°$. The probability of this collision is relatively high and is reflected in the A value of 6.694×10^{15} s^{-1} with a uncertainty of $\pm e^{3.17}$. The thermal Diels-Alder cycloaddition however, is a concerted process and therefore requires four atoms to collide in the correct geometry for reaction. The probability of this is far smaller as a consequence of the ordered transition state necessary for a pericyclic reaction which is clearly reflected in the magnitude of the A value of 4.14×10^4 s^{-1} with a uncertainty of $\pm e^{0.17}$.

It can be concluded that the Diels-Alder cycloaddition is the rate determining step due to the highly ordered concerted transition state that defines the reaction. The small magnitude of A is effectively constant for this pericyclic process and consistent with reported A values for uncatalysed Diels-Alder reactions.[108] Manipulation of the reactive system to achieve a higher value of A would be extremely difficult. Therefore, in order to increase the magnitude of the rate constant k_{DA} a lowering in the energy of the LUMO of the iminium ion should be targeted to decrease the magnitude of E_a which, according to our findings will accelerate the overall reaction.

This conclusion can be used to explain the need for a β-EWG in active catalysts. The β-EWG further reduces the energy of the LUMO of the iminium ion thus making it more active. Explanation of the reactivity of catalysts based on the pyrrolidine scaffold is also possible. We demonstrated that pyrrolidine hydrochloride **69** forms iminium ions (for X-ray data see Appendix) but is extremely sluggish in catalysing the Diels-Alder reaction (<5% 6 h, *Table 4.3 entry 1*). Proline methyl ester hydrochloride **70** is a significantly

more active catalyst containing a moderate EWG which is reflected in our catalytic observations (62%, 6 h, *entry 2*). Activity is increased further when a strong β-EWG is present such as trifluoromethylpyrrolidine hydrochloride**112.HCl** (93%, 6 h).

Entry	Catalyst[a]	Structure	Conversion %[b]	*exo:endo*[c]
1	**69**		<5	n.d
2	**70**	CO₂Me	62	70:30
3	**112.HCl**	CF₃	93	68:32

(a) Reactions were carried out at 25 °C for 6 hours with 10 mol% catalyst in methanol.

(b) Conversion determined by ^{1}H NMR of crude reaction mixture.

(c) *exo/endo* ratios determined by ^{1}H NMR of crude reaction mixture.

(*Table 4.3*)

4.3.10 Diels Alder Reaction with Cinnamaldehyde Derivatives

We had now hypothesised that the energy of the LUMO was responsible for overall activity. To allow us to test this for our system we wanted to examine a range of cinnamaldehyde derivatives (**20 119-121**) which would vary the electron density located in the LUMO of the dienophile and hence change the energy associated with it.
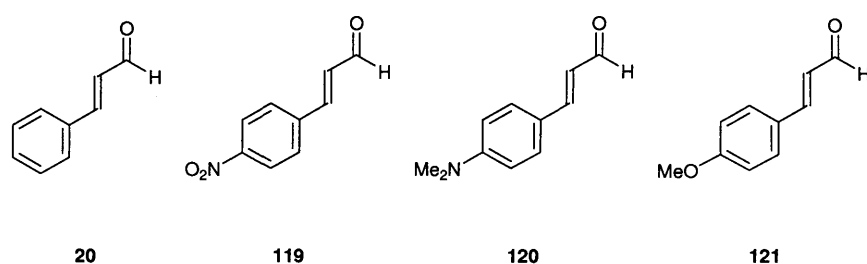
The aldehydes were submitted to the standard Diels-Alder reaction with cyclopentadiene and catalyst **7** in MeOH for 6 h (*Scheme 4.9*).
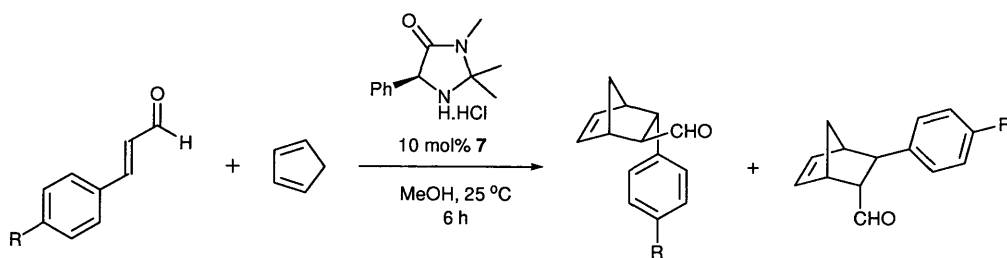
(Scheme 4.9)

Entry	Aldehyde[a]	Conversion %[a]	endo/exo
1	**20**	86	57:43
2	**119**	97	58:42
3	**120**	55	60:40
4	**121**	0	n.d

(a) Reactions were carried out at 25 °C for 6 hours with 10 mol% catalyst
in methanol.(b) Conversion determined by ^{1}H NMR of crude reaction mixture.
(Table 4.3)

Electron deficient aldehyde **119** (*Table 4.3 entry 2*) preformed best with 97% conversion followed by cinnamaldehyde **20** (*entry 1*) at 86% conversion. Electron rich aldehyde **121** (*entry 3*) gave 55% conversion while aldehyde **120** (*entry 4*) failed to react.

The usefulness of this study is limited, as the order of reactivity could have been predicted beforehand from frontier orbital arguments[109] and the electronics of the aldehyde will also effect iminium ion formation as there is a distinct difference in the electrophilicity of the respective carbonyl groups. However, what is significant is that with a strong electron donating group on the aldehyde **120** no reaction occured. This electron donating effect should also make the carbonyl less electrophilic and should decrease the rate of iminium ion formation. However, we were able to isolate compound **128** at ambient temperature from methanol (confirmed by HRMS). We were also able to crystallise iminium ion **129** derived from catalyst **112**. Catalyst **112** is of similar activity to catalyst **7** suggesting that iminium ion formation for catalyst with similar activity is not a significant step in the overall catalytic cycle for this substrate.
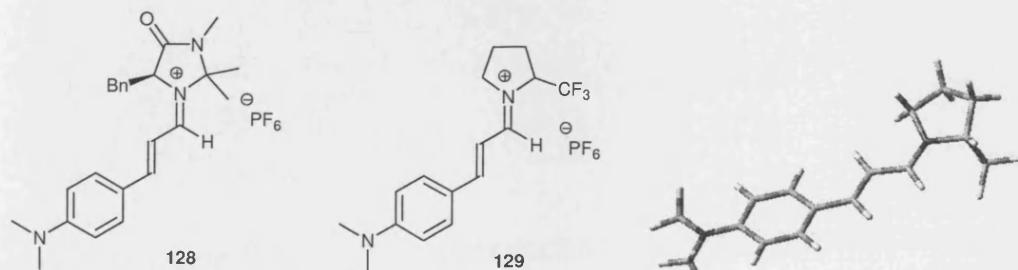
(Figure 4.13)

4.3 Conclusions

Isolation of the key iminium ion **122** allowed us to obtain kinetic data of the components of the catalytic cycle. From this data we can concluded that the Diels-Alder cycloaddition was the RDS of the catalytic cycle for our model system. The magnitude of the rate constant k_{DA} is governed by the associated *A* value. The small magnitude of the *A* value is a consequence of the highly ordered transition state of the concerted Diels-Alder reaction. Iminium ion formation was found to have an activation energy of 100 kJ mol^{-1} consistent with the theoretically calculated value. The hydrolysis of the Diels-Alder iminium adducts was found to be extremely rapid and not observable on the ^{1}H NMR timescale.

The conclusions drawn allowed us to rationalise the role of the β-EWG acting to lower the energy of the LUMO of the reactive iminium ion. The results could now be incorporated in the design of novel catalysts suggesting that increased electron withdrawing ability of the β-EWG should afford increased activity.

Chapter 5: Design and Synthesis of More Active Catalysts for the Organocatalysed Diels-Alder Reaction

5.1 The Aim of the Research

The aim of these synthetic investigations was to prepare a more active variant of MacMillans imidazolidinone catalyst **7** by incorporating an additional β-EWG. Upon synthesis, catalytic testing would be conducted to establish whether the information gained from our mechanistic studies could be successfully applied to increase catalyst activity.

5.2 Introduction

MacMillans imidazolidinone catalyst **7** has been extremely successful and efficiently catalyses a wide range of transformations.[110] Furthermore, other catalysts developed within MacMillans group based around a similar architecture catalyse an even wider number of transformations. However, widespread industrial use of the methodology has not occurred principally due to the high catalyst loadings that are necessary which can prove unworkable in large-scale synthesis. Increasing the reactivity of these catalysts while maintaining the asymmetric induction reported would therefore be more attractive to industry and academia alike.
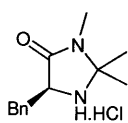
7

Having identified the Diels-Alder cycloaddition as the RDS of the catalytic cycle and acknowledged the physical reasons for the magnitude of the rate constant, we targeted a lowering in the energy of the LUMO of the iminium ion to increase the rate of the cycloaddition and therefore the overall catalytic cycle. In order to achieve this LUMO energy lowering effect we rationalised that inclusion of an additional β-EWG in the scaffold of catalyst **7** could lead to increased reactivity.

The proposed, and widely accepted argument to explain the asymmetry observed in the asymmetric Diels-Alder reaction catalysed by **7** is that subtle differences in the steric requirements for the *E*-isomer **132** and *Z*-isomer **133** of the iminium ion lead to the exclusive formation of the *E*-isomer. This can be visualised when the two isomers of the iminium ion are drawn with the benzyl group away form the π-system (as the evidence from our solid-state studies suggest might be the true conformation (Chapter 4). The iminium ion in the *Z*-conformation (**133**) has an additional steric interaction with the geminal dimethyl group of the catalyst. This steric interaction is absent in the *E*-conformation(**132**) and therefore it is favoured energetically (*Figure 5.1*).

E-Isomer **132**   Z-Isomer **133**
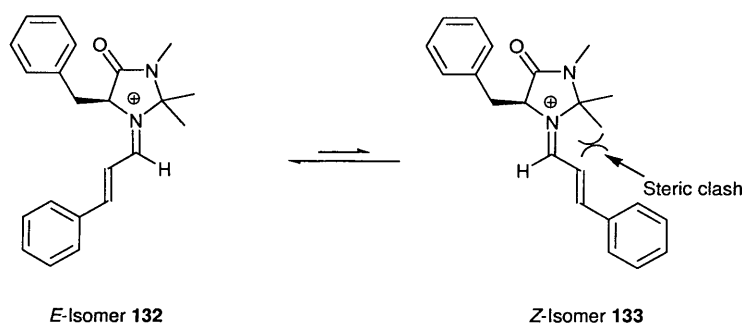
(Figure 5.1)

To ensure that this mode of asymmetry is maintained within our modified catalysts, it was imperative that we maintained this structural feature by designing catalysts with similar spatial coordinates.

79

5.3 Results and Discussion

5.3.1 Computationally Aided Catalyst Design

Initially, based on experience within the group, we selected a number of catalyst targets **134-137** that we believed would demonstrate increased activity (*Figure 5.2*).

134	135	136	137
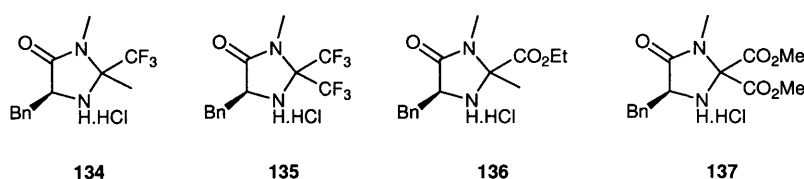
(Figure 5.2)

Catalyst **134** and **135** contained the trifluoromethyl functionality as the β-EWG which we had identified as a good candidate to increase activity. Compounds **136** and **137** were identified as good candidates form SAR studies prior to the mechanistic investigation.

Having hypothesised that it was the LUMO energy lowering ability of a catalyst that was important for activity (provided the active nitrogen was sufficiently nucleophilic) we saw the opportunity to use basic computational modelling to establish whether there was a correlation between the energy of the LUMO and catalyst activity.
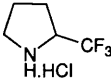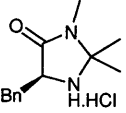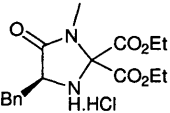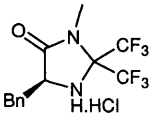
To achieve this we conducted Hartree-Fock (HF) geometry optimisations on the *E*-isomers of the iminium ions of the catalysts **134-137** with acrolein and then subsequently introduced a phenyl group into the plane of the iminium to represent cinamaldehyde. We then re-optimised the geometry using HF and it was from this final optimisation that we then extracted the energy of the LUMO corresponding to the π-system of the iminium ion. The values obtained could not be treated as absolute values. Instead it was the relative values that allowed direct comparison between activity determined experimentally and the calculated values of the LUMO energy. This form of calculation was also performed on iminium ion **122** and a pictorial representation of the results obtained in these investigations is shown in (*Figure 5.2*).
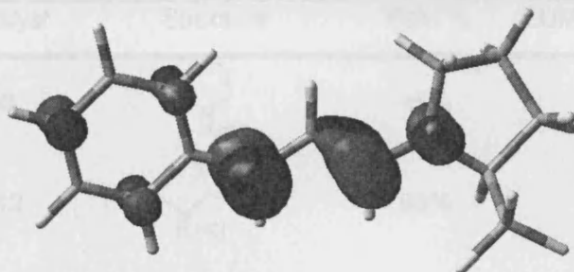
(Figure 5.2)

The results of these calculations had to be treated with some caution as it was known that HF is an inaccurate method for delocalised systems, such as the π–system of the iminium ion. This is due to the approximations made about electron correlation in the construction of the HF theory. These inaccuracies should be largely consistent for molecule of a similar structural class. HF does, however, have the advantage that it allows rapid and simple calculation of the LUMO energy which allows many catalysts to be screened in a short period of time. Higher levels of theory might provide more accurate calculations but the time and financial costs involved would be far greater.

A correlation was found between activity and LUMO energy for a catalyst of similar structural class. The correlation did not extend between structural classes. The example that illustrates this best is comparison of pyrrolidine hydrochloride **69** and trifluoromethyl pyrrolidine hydrochloride **112**.HCl. Pyrrolidine hydrochloride **69** is a poor catalyst (<5%, 6 h) although we have good evidence it formed iminium ions (X-ray). This suggested that the iminium ion was not sufficiently activated to facilitate a rapid Diels-Alder cycloaddition reaction. The pyrrolidine derived iminium ion had a calculated LUMO energy of -2.50 eV (*Table 5.1, entry 1*) Trifluoromethyl pyrrolidine derived iminium ion **122** however, was a considerably more active catalyst (93%, 6 h) and contained a β-EWG that lowered the energy of the LUMO. The calculated value obtained for **122** is -2.78 eV (*Table 5.1, entry 2*).

Entry	Catalyst	Structure	Yield %	LUMO energy eV
1	**69**		<5%	-2.50
2	**112**		93%	-2.78
3	**7**		80%	-2.72
4	**137**		n.d.	-2.72
5	**135**		n.d.	-3.24

(Table 5.1)

Knowing that the simplistic model that we had developed had some credibility we calculated the LUMO energy of the iminium ions of our proposed catalysts **137** and **135** which were -2.72 and -3.24 eV, respectively. The value obtained for the LUMO energy of the iminium ion of catalyst **135** was extremely interesting as, according to our hypothesis, it should be extremely active. We therefore devoted considerable attention to its preparation.

5.3.2 Catalyst Synthesis

Our initial attempt to synthesise the compounds **134-137** was analogous to the method described by MacMillan to prepare catalyst **7**.[111] The procedure involved reacting the precursor **138** and the corresponding carbonyl compound in methanol at reflux for 16 h with 10 mol% p-TSA as the catalyst.

The reaction of trifluoroacetone **139** with **138** led to the imine **140**. To encourage ring closure further attempts were conducted at higher temperatures but this led to occurrence of side reactions and decomposition.
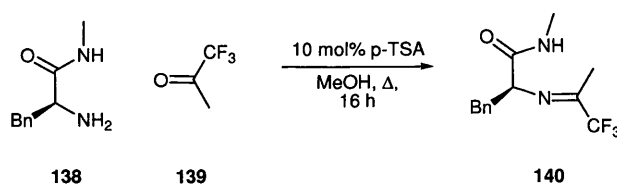
(Scheme 5.1)

The reaction of hexafluororacetone trihydrate **141** with **138** also proved unsuccessful with the initial mass of starting material recovered. This observation suggested that the hexafluoroacetone trihydrate was a poor electrophile. We therefore consulted the literature and found examples where the hexafluoroacetone was first dehydrated and bubbled through a reaction solution as a gas facilitating rapid and efficient condensation reactions.[112]
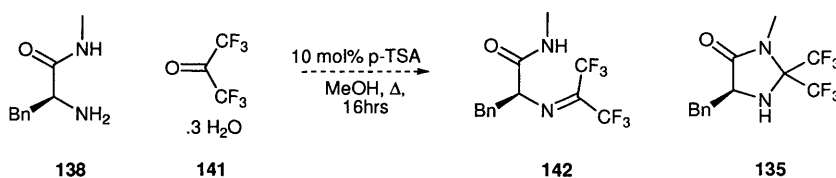
(Scheme 5.2)

Initially, we bubbled gaseous hexafluoroacaetone through methanol at room temperature containing **138** and *p*-TSA but recovered only starting materials upon work up. Following literature precedent we selected DMSO as a solvent for the reaction as it had been successfully utilised in similar reactions.[113] Attempts at room temperature yielded only starting materials. Conscious that temperature was important for successful reaction we repeated the reaction in DMSO at the elevated temperature of 80 °C. In the analysis of the resulting mixture we observed a molecular ion at the correct mass for the imine **142** or the desired catalyst **135**, however, the ¹H NMR clearly indicated that the isolated spots were not pure and further purification proved unsuccessful. Time restrictions ended our pursuit of this catalyst.
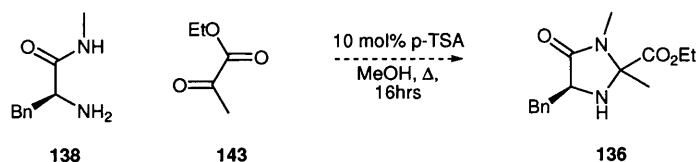
(Scheme 5.3)

The reaction of ethyl pyruvate **143** and **138** lead to a complex mixture of products from which no compound resembling **136** could be isolated. It was difficult to ascertain the fate of the starting materials. Further failed attempts, combined with the work previously conducted by Jones[99] led us to abandon **136** as a target.

The reaction of diethyl oxomalonate **144** with **138** led to similar results (*Scheme 5.4*).
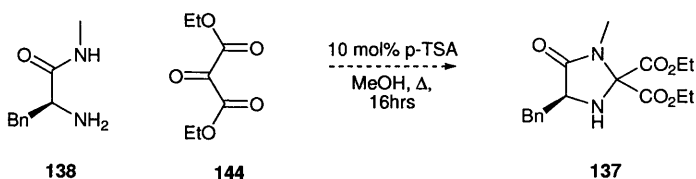
(Scheme 5.4)

5.3.3 Catalyst Redesign

Having failed in successfully synthesising the catalysts **134**, **135**, **136**, and **137** we set about attempting to introduce an alternative EWG into the MacMillan scaffold in an attempt to obtain proof of concept. This would allow us to establish if such modified catalysts would have greater activity. If proof of concept was obtained then significant synthetic effort would be justified in pursuit of our initial targets.

Analysing the catalysts reported by MacMillan we saw the opportunity to modify catalyst **145** by introducing benzaldehyde derivatives containing stronger EWGs (catalysts **146** and **147**). We also believed that the additional EWG introduced in catalyst **148** would provide a rate enhancement (*Figure 5.3*).
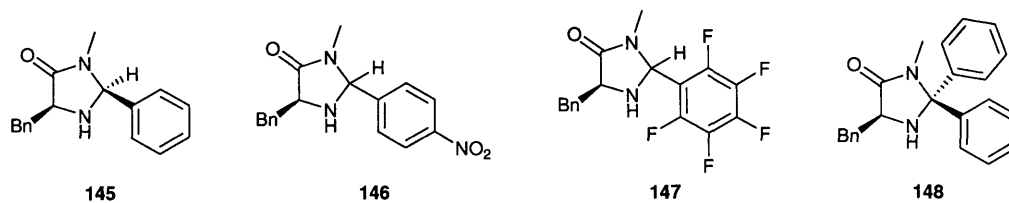
(Figure 5.3)

Mindful of the difficulties encountered with the synthesis of these types of compound we also selected other EWGs to hopefully increase the likelihood of a successful synthesis (*Figure 5.4*).
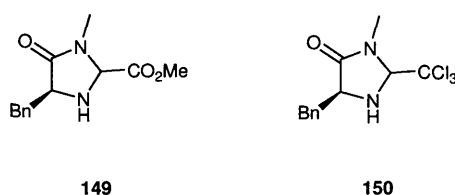
(Figure 5.4)

The attempts at the synthesis of **148** failed, more than likely due to the crowded nature of the ketone. The synthesis of **147** using the conditions of MacMillan led to a complex mixture of compounds from which the product could not be identified.

Reacting *p*-nitrobenzaldeyde **151** with **138** at 80 °C in MeOH yielded the corresponding imine **152**. To assist in the cyclisation of the amide onto the imine we added HCl in ether as a strong acid to form the corresponding iminium ion **153** (*Scheme 5.5*). This strategy proved unsuccessful, as the only compounds observed were the imine **152** and the initial starting aldehyde **151**.
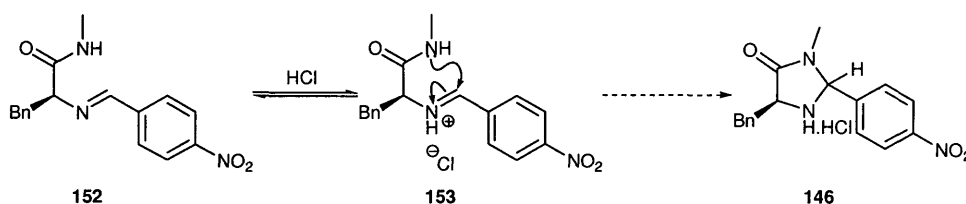
(Scheme 5.5)

Therefore, we attempted to form an iminium ion using protecting group strategies. We prepared the Boc **154**, Cbz **155** and Bn **156** protected MacMillan precursors (*Figure 5.5*). Reaction of **154** and **155** with a variety of aldehydes led to no reaction in MeOH at 80 °C and at elevated temperatures. The most plausible explanation for this is that the reduction in nucleophilicity of the protected nitrogen prevented formation of the iminium ion in both cases.

154 **155** **156**
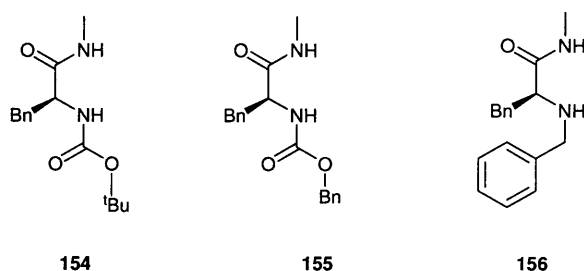
(Figure 5.5)

The benzyl protected catalyst **156** however, was still nucleophilic and on reaction with *p*-nitrobenzaldehyde **151** and glyoxylic acid **255** led to protected catalysts **157** (15%) and **158** (17%) respectively.

157 **158**
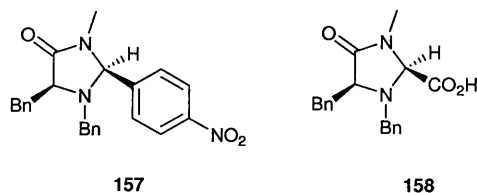
(Figure 5.6)

To convert **157** to **146** we performed a reduction using 10% Pd/C under an atmosphere of H₂ (*Scheme 5.6*). The benzyl protecting group was removed but we also reduced the nitro group to the aniline to give compound **159** (as might have been expected) thus replacing our desired EWG with and an electron donating group.

$$H_2, 10\% \text{ Pd/C} \atop \text{MeOH, 16h, rt}$$

157 **159**
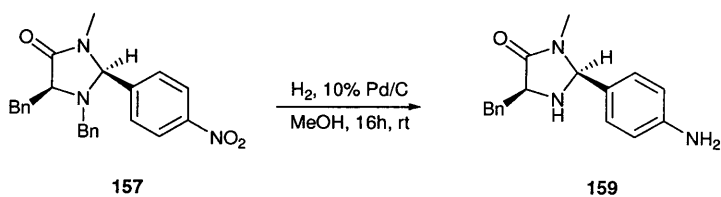
(Scheme 5.6)

To prepare catalyst **149** (*Figure 5.4*) we successfully attempted to deprotect **158** with Pd/C and H_2 indicating that the deprotection step was feasible. However, we sought to form the methyl ester before deprotection. To achieve this we used concentrated H_2SO_4 in methanol as a catalyst which gave a complex mixture of products. Subsequently, we used diazomethane to form the ester which appeared to be good method. Despite our efforts catalyst **149** was not isolated although it is our belief that another attempt using diazomethane to form the ester followed by deprotection would yield the catalyst. Regrettably, time restraints and more encouraging results meant that a final attempt was not conducted.

We also reacted the benzyl protected amine **156** with trifluoroacetone, ethyl glyoxylate, ethyl pyruvate, dibromoacetic acid, chloral, pentafluorobezaldehyde, benzophenone and hexafluoroactetone under MacMillans conditions all without any indication of the desired products.

Having succeeded in synthesising and isolating the imine precursor **152** we made a final attempt at the preparation of catalyst **146** by refluxing the starting materials in DMSO for 1 h and then reacted at 120 °C overnight which resulted in a small amount of desired catalyst **146** in 6% yield amidst numerous products.
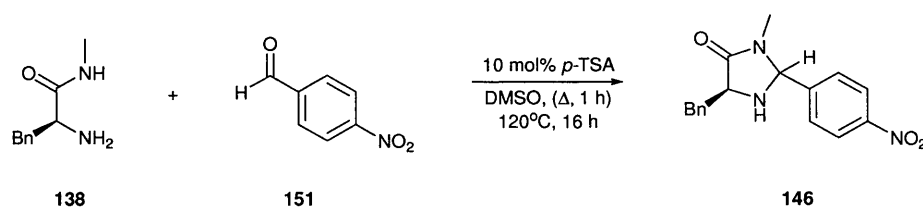
(Scheme 5.7)

The result of this experiment indicated to us that the reaction required large amounts of energy in order to proceed. This prompted us to use microwave technology in order to deliver sufficient energy to the substrates. Initial success affording cleaner transformations using DMSO prompted us to begin to optimise a microwave procedure.

Entry	Solvent	Temperature ºC	Time (mins)	Yield of **146**
1	**MeOH**	100	30	trace
2	**MeOH**	120	30	trace
3	**DMSO**	120	30	12%
4	**DMSO**	120	90	decomp
5	**DMSO**	180	30	decomp
6	**DMF**	120	30	25%

(Table 5.2)

Our brief optimisation indicated that MeOH was a poor solvent. The optimal temperature was found to be 120 °C as higher temperatures gave greater quantities of side products. DMF emerged as the solvent of choice affording a clean reaction mixture with only product, starting materials and imine present by ^{1}H NMR. Further optimisation was not conducted in the interest of time.

5.3.4 Catalyst Performance

Having synthesised catalyst **146** as a single diastereoisomer, we prepared the HCl salt and examined it in the standard Diels-Alder reaction between cinnamaldehyde and cyclopentadiene with a range of catalyst loadings.

Entry	Solvent	Catalyst loading (mol %)[a]	Time (h)	Conversion %[b]	*endo:exo*[c]
1	MeOH	10	6	99	65:35
2	MeOH	10	3	99	65:35
3	MeOH	5	3	82	65:35
4	MeOH	2.5	3	56	65:35
5	MeOH	1	3	23	67:33
6	MeOH/H$_2$O 19:1	10	3	78	68:32

(a) Catalyst **146** used as its HCl salt at 25 °C.

(b) Conversion determined by ^{1}H NMR of crude reaction mixture.

(c) *exo:endo* ratios determined by ^{1}H NMR of crude reaction mixture.

(Table 5.3)

MeOH proved to accelerate the reaction compared to MeOH/H$_2$O. It is also noteworthy that the *endo/exo* ratio observed for our catalysts was 2:1 whereas it was 1:1 for MacMillans original catalyst **7**. The conversion of 82% after 3 hours at 5 mol% loading is unprecedented and demonstrates superior activity to MacMillan catalyst **7** (99%, 24 h, 5 mol%). This result delighted us as we had only introduced a relatively weak EWG into the MacMillan scaffold. This result provided considerable encouragement form which to pursue some of the synthetically more challenging catalysts.

5.3.5 Testing the Predictive Model

The experiments demonstrated that catalyst **146** (82%, 3 h, 5 mol%) was indeed significantly more active than MacMillan's imidazolidinone **7** (89%, 6 h, 10 mol%) validating our design concept. The level of activity present at 5 mol% catalyst loading (82%, 3h) was sufficient to be a practical alternative to using higher loadings.

Synthesising an active catalyst gave us a chance to test our simplistic computational LUMO energy model. Pleasingly, the energy of the LUMO corresponding to the π* orbital of the iminium ion of **146** was -2.86 eV compared to that of the original catalyst **7** -2.72 eV. This is consistent with our hypothesis that the lower the energy level of the LUMO energy the more active the catalyst. The LUMO energy value obtained for the iminium ion of catalyst **146** was still significantly higher than that of proposed catalyst **135**, further highlighting **135** as a desirable catalyst to synthesise.

5.3.6 Asymmetric Induction

To establish the relative conformation of the catalyst **146** we used NOESY NMR. Analysis of the spectrum displayed an enhancement between H_a of the ring junction and H_b in the *ortho*-position of the nitrophenyl ring indicating that they are close in space (*Figure 5.7*). This observation is most consistent with that of the catalyst with the *trans*-conformation with respect to the benzyl and nitro phenyl groups.
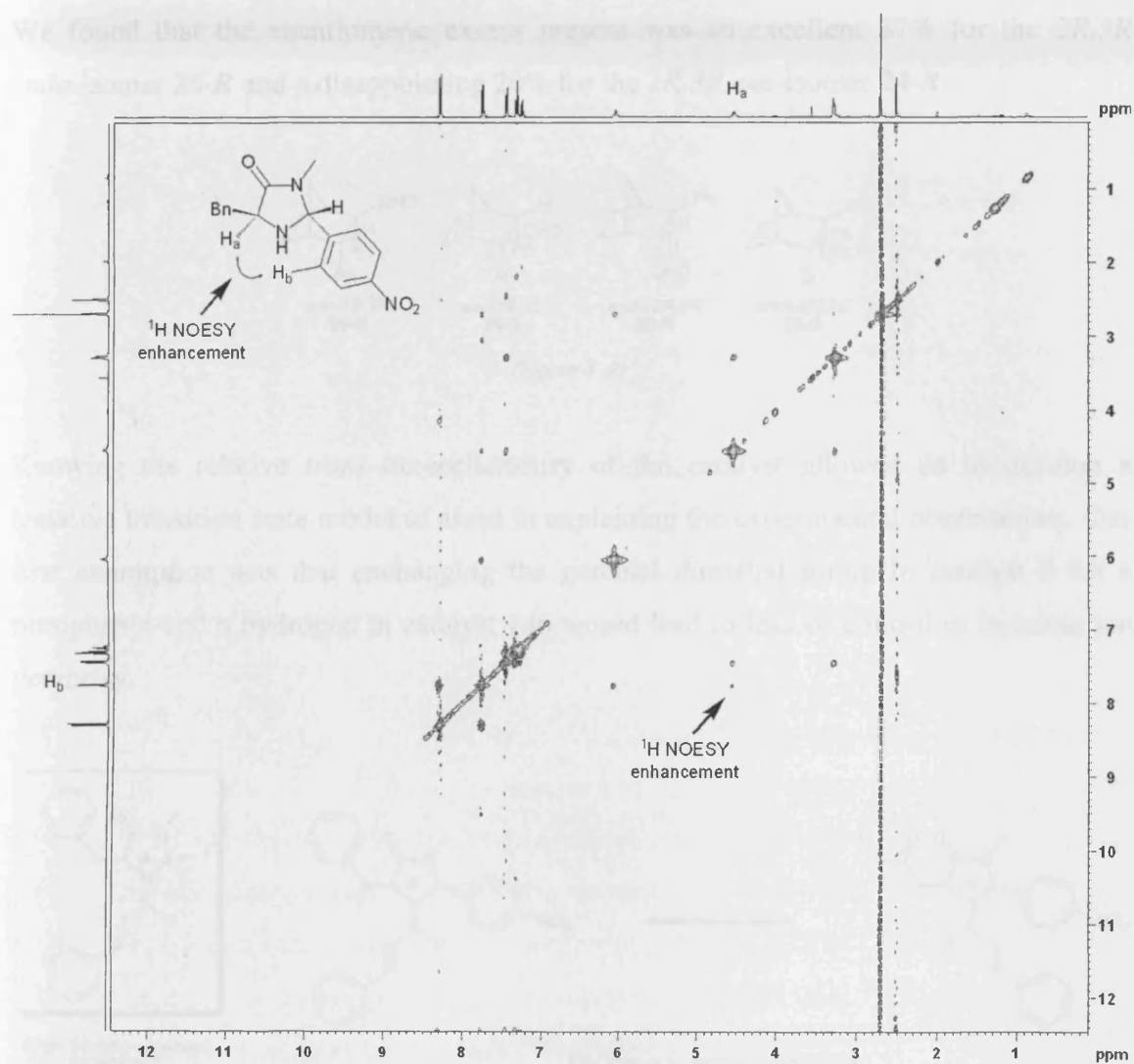
(Figure 5 .7)

To determine whether catalyst **146** had led to any asymmetric induction in the Diels-Alder cycloaddition reaction, we formed the corresponding 2,4-DNP derivatives[114] (**160**) (*Scheme 5.8*). Subsequent analysis of the derivatives by chiral phase HPLC was conducted in accordance to the methods developed by Cavill.[115]
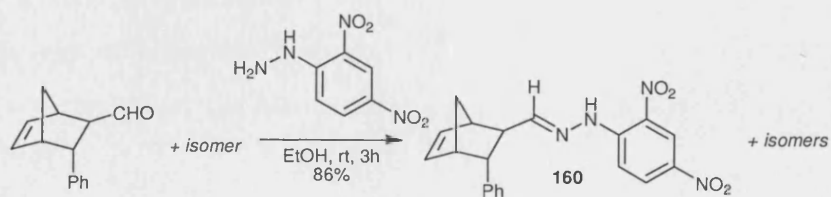
(Scheme 5.8)

We found that the enantiomeric excess present was an excellent 87% for the *2R,3R* *endo*-isomer **25-R** and a disappointing 26% for the *2R,3R exo*-isomer **24-R**.

exo-2R,3R   exo-2S,3S   endo-2R,3R   endo-2S,3S
24-R   **24-S**   **25-R**   **25-S**
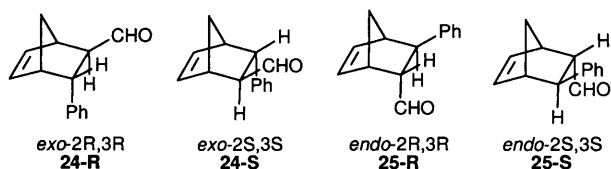
(Figure 5 .8)

Knowing the relative *trans*-stereochemistry of the catalyst allowed us to develop a tentative transition state model to assist in explaining the experimental observations. Our first assumption was that exchanging the geminal dimethyl group in catalyst **7** for a nitrophenyl and a hydrogen in catalyst **146** would lead to loss of control in iminium ion geometry.

Single E-iminium geometry
for catalyst **7**

Poor iminium ion control for catalyst **146**
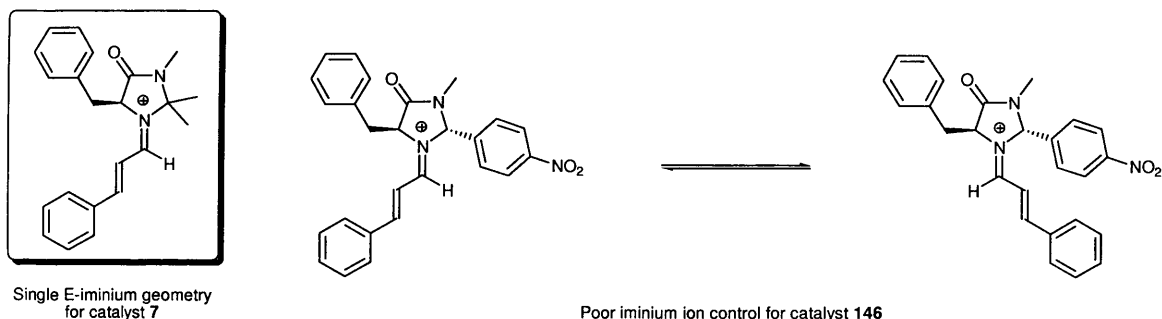
(Figure 5 .9)

Provided that both *E* and the *Z*-isomers of the iminium ion were present in solution there were eight transition-states that could lead to a product (*Figure 5.10*). The *Si* and *Re* labels refer to the face of the dienophile that is approached by the diene in order to provide the Diels-Alder cycloaddition products **24-S/25-S** and **24-R/25-R** respectively.

E-isomer-*Si*-endo
161

E-isomer-*Si*-exo
162

E-isomer-*Re*-exo
163

E-isomer-*Re*-endo
164

Z-isomer-*Si*-exo
165

Z-isomer-*Si*-endo
166

Z-isomer-*Re*-endo
167

Z-isomer-*Re*-exo
168
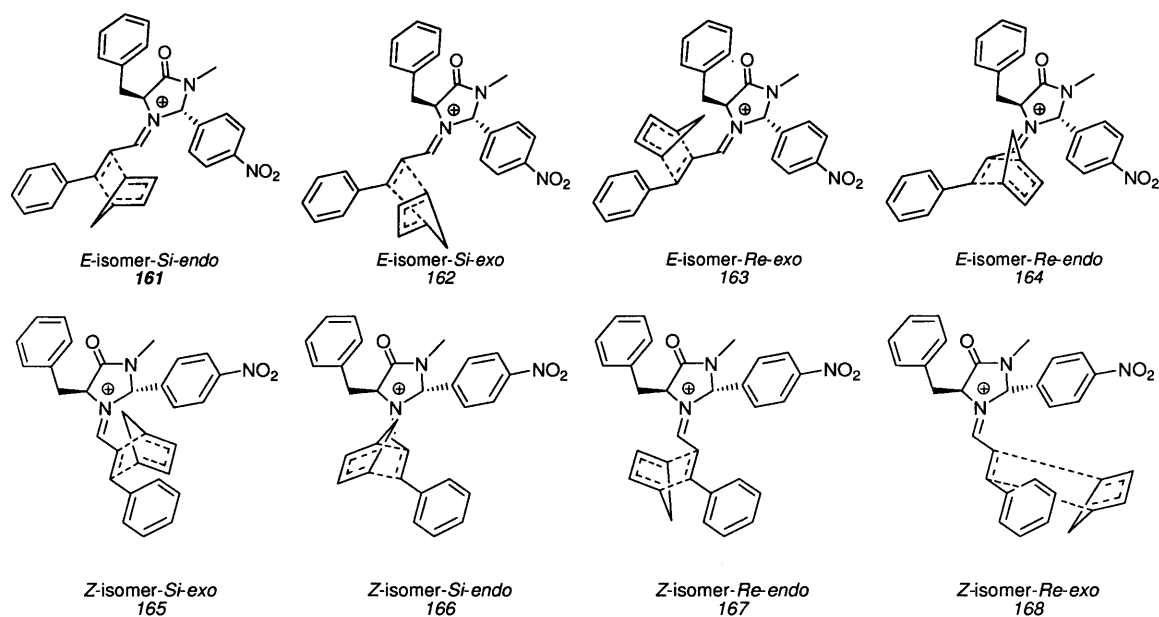
(Figure 5.10)

Without evidence to suggest the position of the benzyl arm in the reactive conformation of the iminium ion, it is difficult to discuss the mode of stereo-induction with any accuracy. The e.e, observed for the *endo* Diels-Alder product can be explained: in the *Si-endo* transition-states **161** and **166** the approach of the diene is hindered. This hindrance is not present in the *Re-endo* transition-states **164** and **167** promoting reaction at the *Re*-face of the iminium ion for *endo*-approach of the diene. Therefore the **25-R** Diels-Alder product is favoured consistent with our observation.

The selectivity observed for the *exo*-Diels-Alder product was much smaller and more difficult to rationalise. Transition-states **165** and **162** should be the most energetically favoured as approach of the diene is less hindered compared to **163** and **168**. The observation of this slight stereo enhancement indicates there must be a small energy difference between **165** and **162** compared to **163** and **168**. The origin of this energy difference is difficult to rationalise using basic modelling due to the large number of variables. The use of computational transition state modelling could provide a more detailed analysis that might explain the observed sense of asymmetric induction for the *exo* product **24-R**.

Interested by the levels of asymmetric induction observed with catalyst **146** we considered whether (*R*)-2-(trifluoromethyl)pyrrolidine **169** would yield enatioenriched products (*Figure 5.11*). We obtained commercially available **169** and prepared the corresponding HCl salt prior to utilising it as a catalyst in the reaction of cinnamaldehyde and cyclopentadiene at 25 °C in methanol.

169.HCl
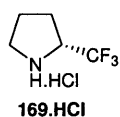
(Figure 5.11)

The Diels-Alder product was purified and a portion converted to the 2,4 DNP derivative **160** for analysis by chiral phase HPLC. We found a pleasing 84 % e.e. for the minor *endo* **25-R** isomer and 4 % e.e. for the major *exo* **24-R** product. Construction of a simple transition state model provides an explanation of the enantioinduction observed. Previous X-ray and spectroscopic data indicated that only the *E*-isomer was present in solution, therefore only four transition-states need be considered.

170   171   172   173
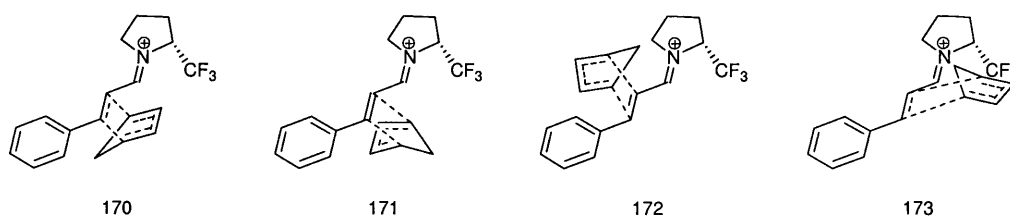
(Figure 5.12)

The steric differentiation for the transitions states with *exo* approach of the diene to the *Si* and the *Re* face **171** and **172** is minimal. Transition states **171** and **172** should therefore be of similar energy, consequently resulting in a low e.e. There is a larger steric differentiation between the *Si* and *Re* faces with *endo* attack of the diene. In the *Si-endo* transition state **170** the approach of the diene is hindered by the trifluoromethyl group. This hindrance is not present in the *Re-endo* transition state **173**. The additional steric hindrance in **170** raises its energy and therefore disfavours formation of the *endo 2S,3S* Diels-Alder product leading to the favoured *endo 2R, 3R* product **25-R**.

5.4 Conclusions

We have demonstrated that the inclusion of an additional β–EWG within the scaffold of the MacMillan imidazolidinone will increase catalyst activity consistent with our hypothesis. We failed to synthesise catalysts **134**, **135**, **136**, or **137** which are architecturally similar to MacMillan's imidazolidinone **7**. However, the catalyst **146** that we synthesised afforded good 87% e.e. for the **25-R** Diels-Alder adduct. Unfortunately, the e.e. for the **24-R** isomer, which was the major product, was found to be 26%. With the experimental observations obtained we were able to construct a transition state model to explain the observed sense of induction. Straightforward arguments could be invoked to explain the e.e, of the *endo* isomer **25-R** whereas the sense of asymmetric induction for the *exo* isomer **24-R** was more difficult to explain.

The calculated energy of the reactive LUMO of **146** is significantly lower than the calculated value for the corresponding LUMO energy of the iminium ion derived from MacMillan's catalyst **7**. This provides further evidence that lowering in the LUMO energy will increase activity provided a nucleophilic amine is present in the scaffold. This evidence also provides credibility to our simplistic model and as a consequence can be used with more confidence.

To achieve a highly active asymmetric catalyst compounds **134, 135, 136** and **137** should be targeted. The use of microwave technology could prove crucial in the synthesis of these molecules as it appears that large amounts of energy are needed to facilitate efficient cyclodehydration.

Chapter 6: Development of a Novel Catalytic Architecture for the Secondary Amine Catalysed Diels-Alder Reaction of Enones

6.1 The Aims of the Research

The aim of this study was to develop a piperazindione scaffold as a catalytic architecture, suitable upon modification, to facilitate the asymmetric organocatalysed Diels-Alder reactions of α,β-unsaturated ketones and aldehydes. We sought to synthesise a series of simple catalysts based around the piperazindione structure to obtain proof of concept by demonstrating their ability to catalyse Diels-Alder reactions involving aldehydes and ketones. Once achieved, synthesis of more challenging chiral variants would begin.

6.2 Introduction

To date, there have been a number of reports of organocatalysed Diels-Alder reaction with α,β–unsaturated aldehydes with excellent yields and selectivity.[116] However, this success has not been mirrored with more challenging α,β-unsaturated ketone substrates of which there is only one report.[117]

The group of MacMillan were the pioneers in this challenging area. Their initial investigations indicated that catalyst **7**, which had been successful for the asymmetric Diels-Alder reaction of α,β-unsaturated aldehydes, was not effective with α,β-unsaturated ketone substrates. Further investigations highlighted catalyst **9** with $HClO_4$ as the co-acid was the optimal catalyst-co-acid combination for the asymmetric Diels-Alder reactions of α,β-unsaturated ketones with cyclopentadiene (*Table 6.1*).
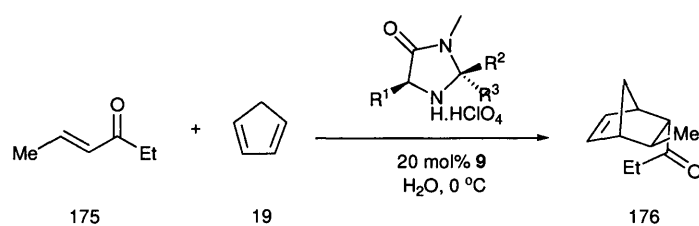
(Scheme 6.1)

Entry	Catalyst	R¹	R² (R³)	Time (h)	% Yield	*exo:endo*	e.e. %
1	7	Bn	Me (Me)	48	20	7:1	0
2	8	Bn	*t*-Bu (H)	48	27	9:1	0
3	177	Ph	Ph (H)	22	88	21:1	47
4	145	Bn	Ph (H)	42	83	23:1	82
5	9	Bn	5-Me-Furyl (H)	22	89	25:1	90

(Table 6.1)

It is clear from the results (*Table 6.1*) that the mode of asymmetric induction for reactions involving ketone substrates is different from that of aldehydes. The catalysts that provided the highest levels of enantioselectivity were **145** and **9** which both contain two sterically shielding groups *cis*-across the catalyst scaffold.
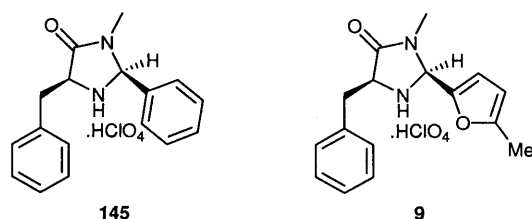
To explain the sense of asymmetric induction observed, MacMillan proposed a model which was supported by MM3 calculations. The structures obtained from these calculations are shown below (*Figure 6.1*).

cis-Iminium **179**   ● = H or Me   trans-Iminium **178**

178   **179**

└─ Re-face   └─ Si-face

● = Me   Re-face blocked   ● = Me   Si-face exposed
● = H   Re-face exposed   ● = H   Si-face exposed
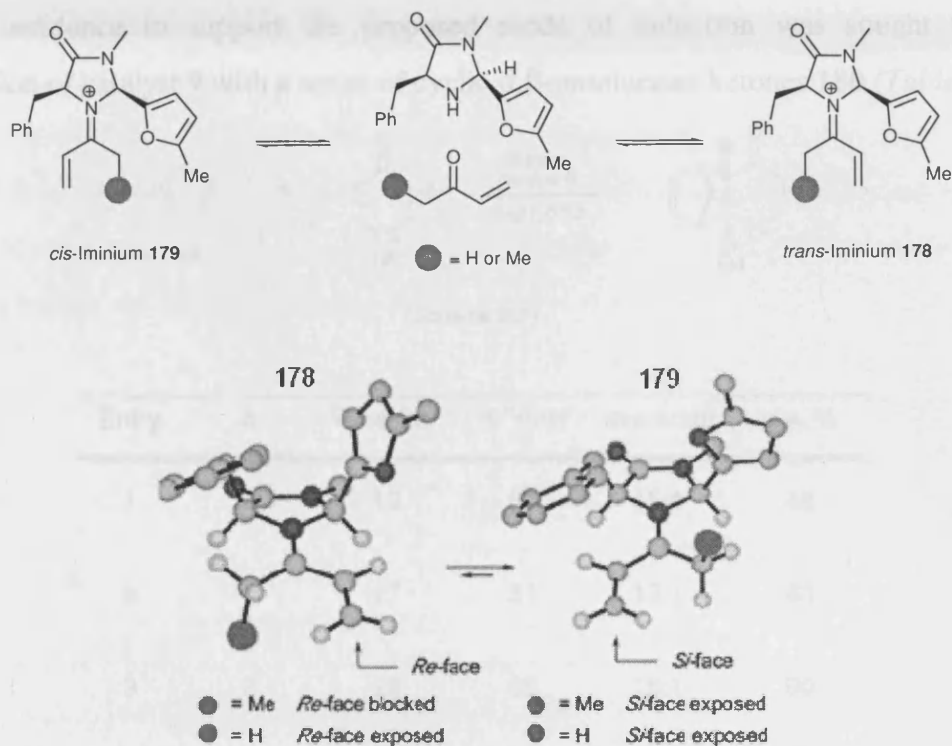
(*Figure 6.1*)

Importantly, the model provided an explanation as to why methyl ketones provided poor enantioselectivities. The model stated that both the *cis* and *trans* iminium ions **179** and **178** were accessible, but the *cis*-iminium ion **179** was favoured energetically. With methyl ketone substrates one face of the C=C bond was exposed for the *cis* and *trans* iminium ions **179** and **178** respectively. For the *cis*-iminium ion **179** it is the *Si*-face and for the *trans* iminium **178** the *Re*-face. Therefore low levels of asymmetric induction are observed. With ethyl ketone substrates the *cis* and *trans*-iminium ions **179** and **178** are also accessible. Crucially however, both faces of the *trans*-iminium ion **178** are blocked. The *Si*-face of the iminium ion **178** is blocked by the bulky furfural group and the *Re*-face by the terminal methyl group of the ethyl ketone substrate (*Figure 6.1*). The *Si*-face of *cis*-iminium ion **179** was exposed (analogous the methyl ketone substrates) and therefore reaction at this face predominates leading to the observed sense of asymmetric induction.

Further evidence to support the proposed mode of induction was sought through application of catalyst **9** with a series of cyclic α,β-unsaturated ketones **180** (*Table 6.2*).

$$\text{19} \quad + \quad \text{180} \xrightarrow[\text{H}_2\text{O, 0 °C}]{\substack{\text{20 mol\%}\\\text{catalyst 9}}} \text{181}$$

(Scheme 6.2)
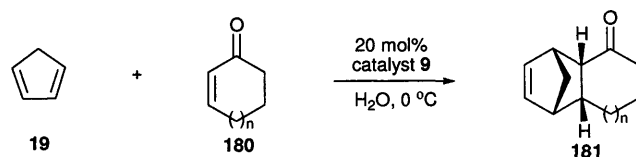
Entry	n	Time (h)	% Yield	exo:endo	e.e. %
1	0	12	81	15:1	48
2	1	17	81	12:1	63
3	2	28	85	18:1	90
4	3	72	83	6:1	91
5	10	72	88	5:1	93

(Table 6.2)

The observed increase in enantioselectivity with increasing ring size (*Table 6.2 entries 4 and 5*) was consistent with the proposed model. The large ring cyclic dieneophiles (n =3, 10, *entries 4 and 5*) possess a higher degree of rotational freedom about the N=C-alkyl bond of the iminium ion and therefore behave in a similar manner to the ethyl ketones with good *Re*-face coverage. However, dieneophiles with the smaller rings (n = 0, 1, *entries 1 and 2*) result in moderate enantioselectivities as a consequence of the restricted rotational freedom around the N=C-alkyl bond preventing effective coverage of the *Re*-face. The substrate specificity was therefore a consequence of the catalytic architecture of **9**. No conjugate additions to α,β-unsaturated ketones using the imidazolidinone architecture have been described to date. These observations revealed the opportunity to develop a universal catalyst that could tolerate both α,β-unsaturated aldehydes and ketones as substrates.

6.2.1 Catalyst Design

Having rationalised that an active asymmetric catalyst for Diels-Alder reaction with α,β-unsaturated ketones required the following elements: a nucleophilic nitrogen, a β-EWG and a chiral scaffold that could selectively hinder attack at one diasterotopic face of the iminium ion we proposed catalyst **185** as a novel candidate.
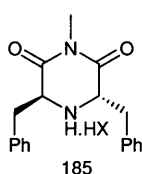
Piperidine is known to have a higher nucleophilicity than acyclic secondary amines. The piperazindione **185** should have a relatively flat geometry caused by the geometrically planar amides. This flattening of the ring should further expose the lone pair of the nitrogen and thus further increase the nucleophilicity. The scaffold of **185** also contains two β-EWG's which could facilitate a further increase in activity. Finally, the fact that the catalyst was C₂ symmetric dictates that independent of the geometry of the iminium ion, the same diastereotopic face should be shielded leading subsequent asymmetric reactions. For example, the iminium ions derived from **185** and cyclohexanone are identical and hence the stereochemical course of subsquent reactions would be the same (*Figure 6.2*).
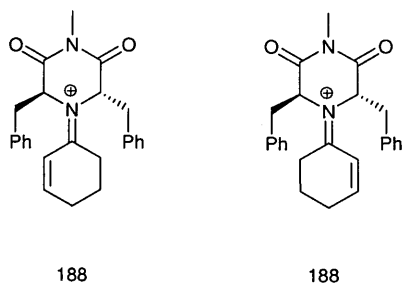
(*Figure 6.2*)

6.3 Results and Discussion

6.3.1 Preparation of Model Catalysts

Aware that synthesis of catalyst **185** may not be straightforward we set about synthesising a range of catalysts based around the piperazindione scaffold that would be synthetically more accessible to allow us to asses the feasibility of catalysts based around this scaffold.

189   **190**   **191**   **192**   **193**
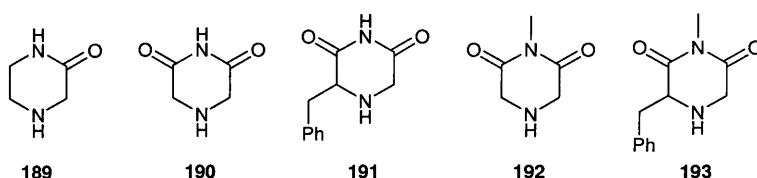
(*Figure 6.3*)

Piperazin-2-one **189** was obtained commercially. Compounds **190** and **191** were synthesised according to the procedure of Mancilla by reaction of glycine ethyl ester hydrochloride **186** and phenylalanine ethyl ester hydrochloride **187** respectively with 2-bromoacetamide **194** (*Scheme 6.3*).[118]

186 R = H
187 R = Bn

190 R = H 75%
191 R = Bn 11%
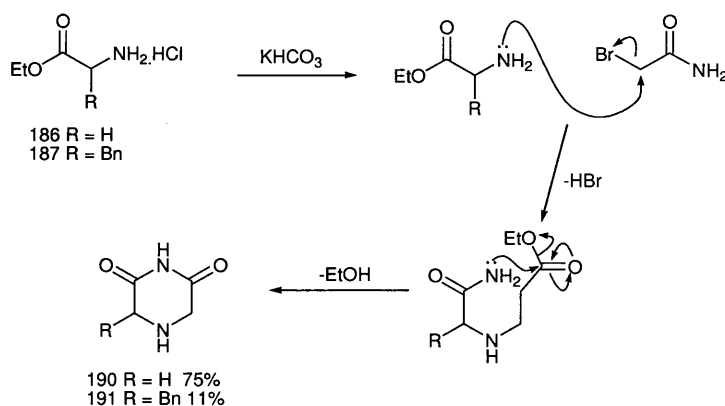
(*Scheme 6.3*)

Compounds **192** and **193** were synthesised in an analogous manner by reacting α–bromoester **195** with glycinamide **196** or phenylalaninamide **138** (*Scheme 6.4*).
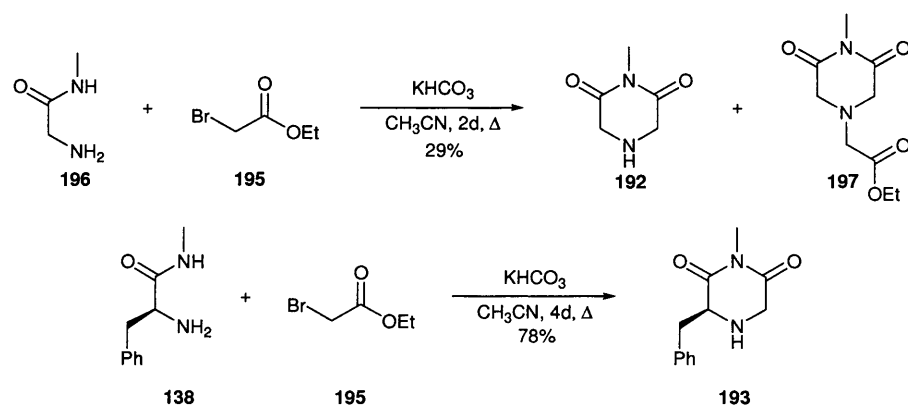
(Scheme 6.4)

Compound **193** was isolated in a respectable 78% yield while catalyst **192** was isolated in 29% along with 23% of the overalkylated byproduct **197**. Attempts to improve the yield using toluene as the solvent failed to provide any of catalyst **192** while a reductive amination protocol utilising ethyl glyoxylate also proved unsuccessful. Despite the low yield, sufficient quantities of **192** could be obtained using this method to pursue our studies.

6.3.2 Piperazindiones as Catalysts for Diels-Alder Reaction with α,β-aldehydes

Having obtained the catalysts we set about examining their activity with our standard Diels-Alder cycloaddition. Catalysts **189, 190-193** were converted to their hydrochloride salts by adding the free amines to 5 equivalents of HCl in ether. The catalysts were reacted at 10 mol% catalyst loading with (*E*)-cinnamaldehyde **20** and cyclopentadiene **19** in MeOH and MeOH/H$_2$O (19:1) as the solvents to gauge catalyst activity (*Table 6.3*).
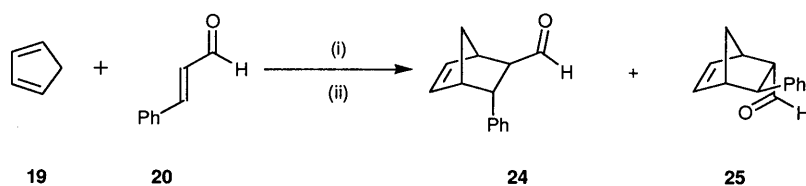
(i) Catalyst (10 mol%), solvent, 25 °C. (ii) TFA, CHCl$_3$, H$_2$O

(Scheme 6.5)

Entry	Catalyst[a]	Time (h)	Solvent	Conversion %[b]
1	**191**.HCl	6	MeOH	38
2	**191**.HCl	6	MeOH/H_2O 19:1l	18
3	**192**.HCl	6	MeOH	15
4	**192**.HCl	24	MeOH	32
5	**192**.HCl	6	MeOH/H_2O 19:1l	41
6	**192**.HCl	24	MeOH/H_2O 19:1l	54
7	**192**.HCl	24	MeOH/H_2O 19:1l	69[c]
8	**193**.HCl	6	MeOH	44
9	**193**.HCl	6	MeOH/H_2O 19:1l	22
10	**193**.HCl	24	MeOH	62

(a) catalyst used at 10 mol% loading as the HCl salt in the stated solvent at 25 °C with 2.5 equivalents **19** (b) conversion determined by ^{1}H NMR of the crude reaction mixture (c) reaction conducted at 20 mol% loading with 5 equivalents of **19**.

(*Table 6.3*)

Catalyst **189**.HCl and **190**.HCl proved inactive for the transformation with no reaction occurring after 6 h. This somewhat surprising result may be explained by the limited solubility of these catalysts in the reaction medium. Catalyst **191**.HCl displayed moderate activity (38 %, *Table 6.3, entry 1*) in MeOH and low activity in MeOH/H_2O (19:1) (18%, *Table 6.3, entry 2*). Catalysts **192**.HCl and **193**.HCl which both contain a methyl amide performed better. The optimal solvent for **192**.HCl was MeOH/H_2O (19:1) leading to modest conversion (54%, *Table 6.3, entry 6*) while for catalyst **193**.HCl the optimal solvent was MeOH (44%, *Table 6.3, entry 8*).

Examining the literature it was evident that there was no single co-acid that was efficient with all catalysts or indeed in every transformation. Therefore, we tested catalyst **192** with a range of co-acids in the standard Diels-Alder reaction with (*E*)-cinnamaldehyde **20** and cyclopentadiene **19** conducted in MeOH/H$_2$O (19:1) (*Table 6.4*).

Entry[a]	Co-acid	Conversion%[b]
1	**HCl**	41
2	**HClO$_4$**	22
3	**TFA**	33
4	**TCA**	25
5	**HPF$_6$**	4
6	**MsOH**	50
7	**BzOH**	0

(a) catalyst used at 10 mol% loading as stated salt in MeOH/H$_2$O (19:1) for
6 h at 25 °C with 2.5 equivalents **19** (b) conversion determined by ^{1}H NMR
of the crude reaction mixtures

(*Table 6.4*)

The study found that HCl and MsOH were the optimal co-acids for the standard Diels-Alder reaction (*entry 1 and 6*). Consistent with previous findings BzOH and HPF$_6$ were poor co-acids for the reaction.[119] TFA, TCA and HClO$_4$ all provided moderate yields for the reaction (*entries 2,3 and 4*). Given the similar activities of MsOH and HCl as co-acids, HCl was chosen as it allowed the convenient use of the preformed HCl salts of catalysts in the reactions.

6.3.3 X-Ray Study

A key feature in our design of catalyst **185** was the increased nucleophilicity of the nitrogen, facilitated by the flat geometry of the ring. To investigate the extent of this effect we attempted to form crystals of the iminium ions derived from the model catalyst **192** to allow further insight.
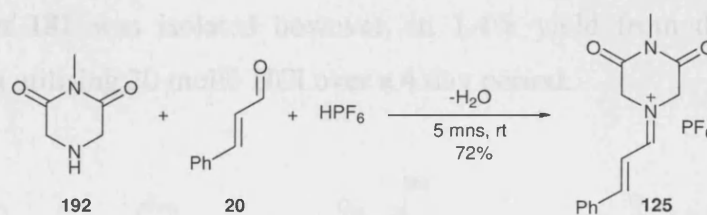
(Scheme 6.6)
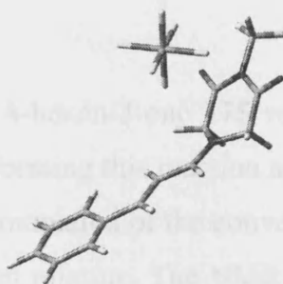
(Figure 6.4.)

We formed the iminium ion **125** by reaction of **192** with cinnamaldehyde **20** and HPF$_6$ cleanly in 72% yield (*Scheme 6.6*). Crystals suitable for X-ray crystallography were obtained by evaporation from CH$_3$CN. The crystal structure confirmed our hypothesis that the piperazindione ring would have a high degree of planarity and hence an enhanced nucleophilicity (*Figure 6.4*).

6.3.4 Diels-Alder Reactions with α,β-Unsaturated Ketones

Our initial aim was to develop a reaction that could be used as a benchmark to aid in the development of future catalysts for this class of transformation. We chose the literature reaction of cyclohexenone **198** and cyclopentadiene **19** to probe the reactivity of our catalysts (*Scheme 6.7*).[120]

106
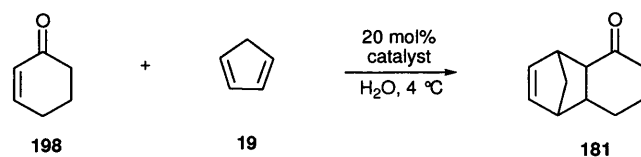
(Scheme 6.7)

Attempts using catalysts **112, 70, 7,** and **91** all failed to provide any indication of product **181**. The product **181** was isolated however, in 1.4% yield from the Brønsted acid catalysed reaction utilising 20 mol% HCl over a 4 day period.
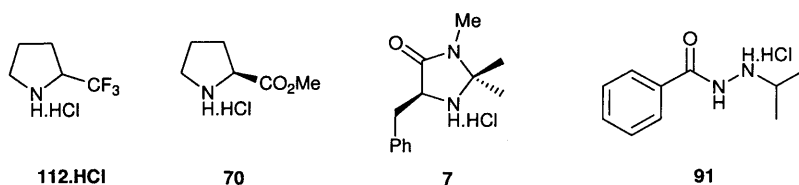
We then examined the reaction of 4-hexen-3-one **175** with cyclopentadiene **19** utilising MacMillans catalyst **9.HClO₄**. Performing this reaction and isolating the product allowed us to develop a method for the determination of the conversion of the reaction by analysis of the ^{1}H NMR of the crude reaction mixture. The NMR spectra of **175** (*Figure 6.5*) and **176** (*Figure 6.6*) display diagnostic peaks at 6.85 ppm for **175** and 5.83 ppm for **176** to allow for measurement of conversion.
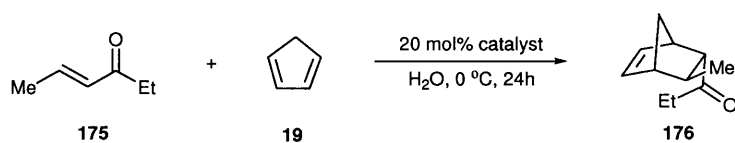
(Scheme 6.8)
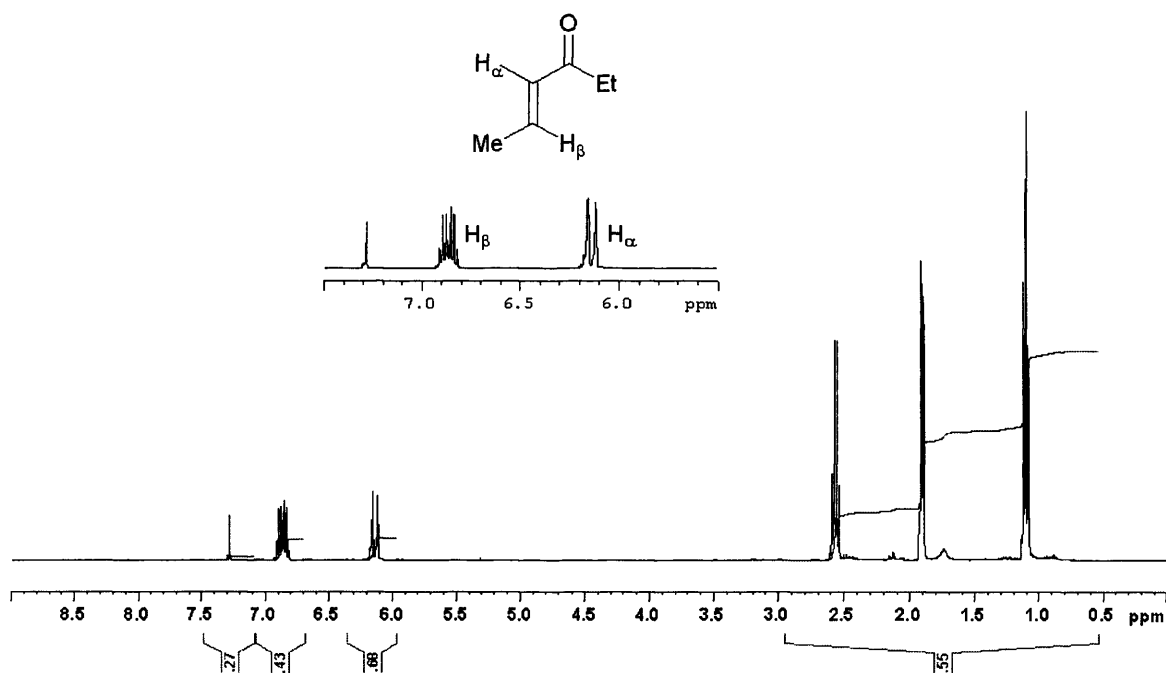
(Figure 6.5)
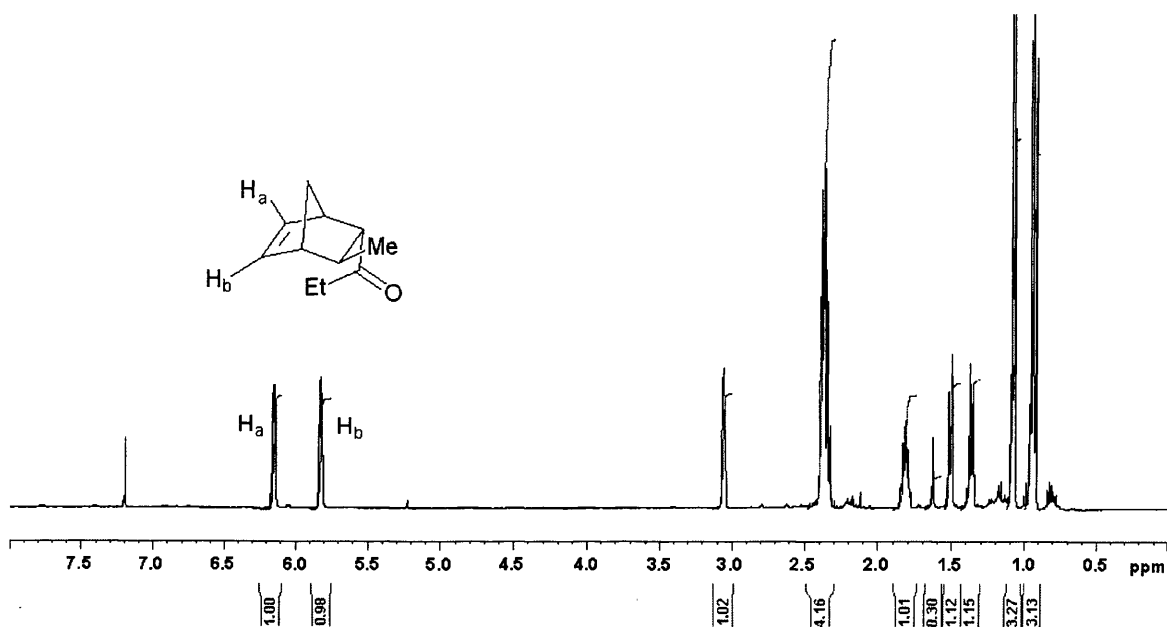
(Figure 6.6)

We then submitted our piperazindione catalyst **192**.HCl and **193**.HCl to the reaction conditions developed by MacMillan to discover whether our catalysts were active with ketone dienophiles. To our delight we obtained conversions of 21 and 26% for the transformation with catalysts **192**.HCl and **193**.HCl respectively (20 mol%, H$_2$O, 24h)

108

clearly demonstrating the ability of piperazin-2,6-diones to catalyse the organocatalysed Diels-Alder reaction with ketone dienophiles.

6.3.5 Development of an Asymmetric Piperazin-2,6-dione

Knowing that the catalysts based around the piperazin-2,6-dione scaffold were active for the reaction of ketone dienophiles in the Diels-Alder reaction we set about synthesising catalyst **185** as a chiral variant. Our first attempt was to perform a reported Ugi reaction that had been utilised to construct similar compounds (*Scheme 6.9*). Ugi had reported a one-pot synthesis of related non symmetrical compounds, however, the diastereoselectivity of these reactions was not discussed within the paper.[121]

(*Scheme 6.9*)
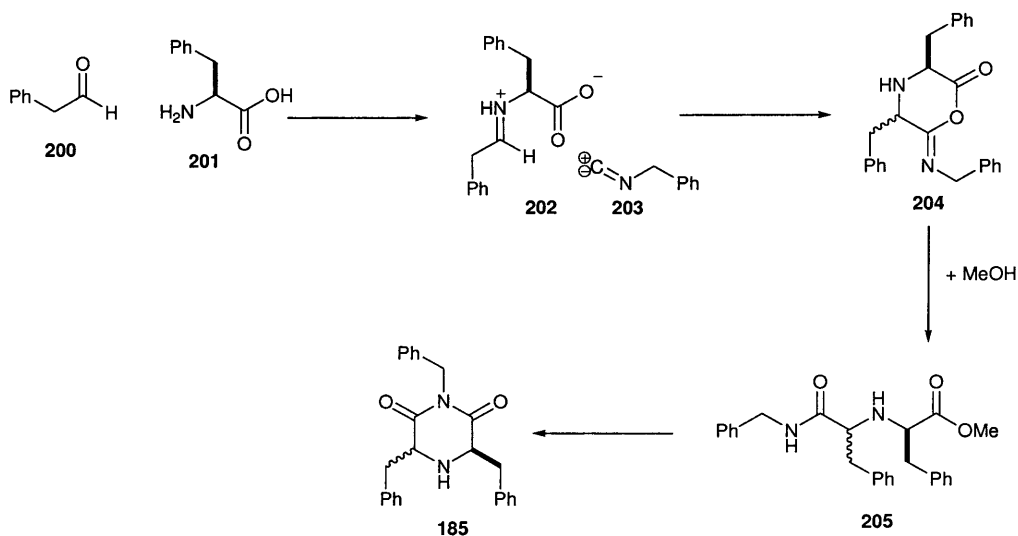
The procedure involved formation of iminium ion **202** from reaction of phenylacetaldehyde **200** with *L*-phenylalanine **201**. The iminium ion **202** can undergo attack from the isocyanide **203** followed by intramolecular attack of the carboxylic acid to form cyclic intermediate **204**. Hydrolysis of the intermediate with methanol leads to the acyclic precursor **205** which upon cyclisation with loss of methanol gives compound **185**, preferably with the desired *trans*-stereochemistry. Unfortunately, the reaction provided a complex mixture of compounds from which the desired product was not

isolated. This fact, coupled with the rancid stench of compound **203** led us to abandon this method as a route to **185**.

Our second approach was to modify the preparation that we had used to synthesise compounds **192** and **193**. To begin the synthesis we prepared bromo-ester **208** from keto-ester **206** and NBS *via* isolated intermediate **207** in 82% overall yield (*Scheme 6.10*).[122]
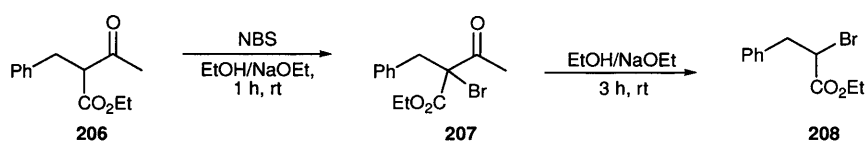
(Scheme 6.10)

The bromo-ester **208** was initially reacted with **138** in CH_3CN. This led to ethyl cinnamate **209** as the major isolated product *via* an elimination reaction (*Scheme 6.11*). The reaction yielded other unidentifiable spots by TLC whose spectroscopic data was not consistent with the desired product.
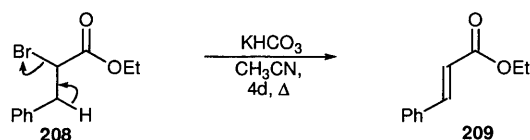
(Scheme 6.11)

The reaction was repeated in toluene which allowed isolation of a compound whose analytical data was consistent with that of the diasteriomeric uncyclised compound **210**, determined from ^1H, COSY and HSQC NMR spectra. However, full characterisation was not possible with the available data and without further purification. Time constraints ended our synthetic efforts at compound **185**.

210
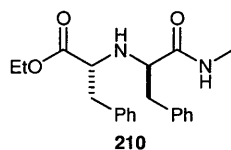
(Figure 6.7)

Future attempts at the preparation of catalyst **185** could use the work of MacMillan who has reported compound **211** as a catalyst for the Diels-Alder cycloaddition.[123]

211
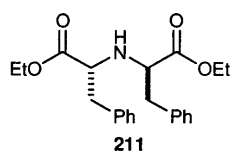
(Figure 6.8)

Adaptation of this methodology should allow for the synthesis of **185** with the desired *trans-* stereochemistry (*Scheme 6.12*). Evaluation of **185** as an asymmetric catalyst for the Diels-Alder reaction of α,β-unsaturated ketones and other iminium ion catalysed reactions could then be conducted.
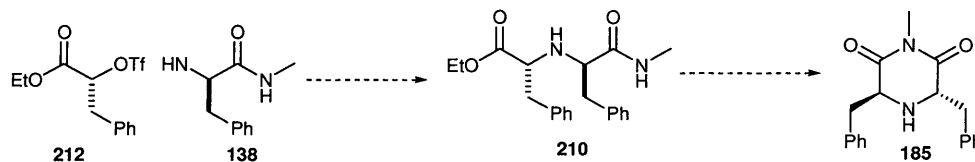
(Scheme 6.12)

6.4 Conclusions

The work to date has demonstrated that catalysts based on the piperazin-2,6-dione scaffold as their HCl salts can be effectively deployed to accelerate the Diels-Alder reaction of α,β-unsaturated aldehydes and ketones. We have developed a method for the rapid determination of catalyst activity based around conversions determined from the ^{1}H NMR spectrum of the crude reaction mixture. However, this method has yet to be fully validated. Structural studies on the iminium ion derived form catalyst **192** indicate that these cyclic catalysts have the desired flat geometry designed to increase the nucleophilicity of the active nitrogen. The synthesis of an asymmetric variant has to date proved elusive

111

Chapter 7: Investigations into an Organocatalytic Dynamic Resolution Procedure

7.1 The Aims of the Study

We sought to demonstrate the reversibility of an organocatalysed Michael addition reaction with a view to the development of an organocatalysed chiral dynamic resolution procedure.

7.2 Introduction

The notion of chiral dynamic resolution is an extremely attractive concept for organic synthesis. It allows for the installation of a racemic functionality early within a synthesis followed by chiral resolution in the final stages. With consideration of the complex and synthetically challenging compounds that are frequently targets in modern chemistry, development of such methods would provide a powerful alternative tool to aid the efficient synthesis of optically active compounds.

FG

R R

asymetric
catalyst
⟶

FG

R R

(Scheme 7.1)
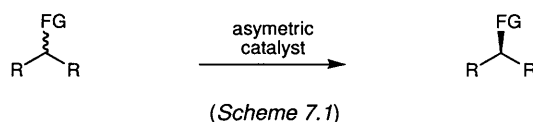
In order to afford dynamic chiral resolution, an asymmetric reagent or catalyst is required. Catalytic dynamic resolution is of course the more attractive. The search for a chiral resolution procedure should then begin with a search for an asymmetric transformation facilitated by a catalyst which could be reversible under the reaction conditions. Examination of the literature suggested that the Michael addition reaction would be a good candidate.

The reversibility of the Michael addition reaction is well documented.[124] There are examples of reversibility where cleavage of C-C,[125] C-N,[126] C-O[127] and C-S[128] bonds have occurred in a retro-Michael fashion. An example of this is with the naturally occurring alkaloid myrtine **215** which readily undergoes epimerisation under acidic or basic conditions *via* intermediate **216** to yield a 1:1 mixture of myrtine **215** and

epimyrtine **217**.[129] The proposed mechanism of this epimerisation was a retro-Michael reaction followed by a non selective Michael addition.
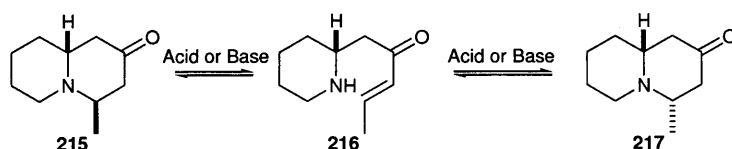
(Scheme 7.2)

A further example of the facility of these processes is the enzyme catalysed dynamic resolution of oxazole **218** which is believed to undergo a retro-Michael reaction to give **219** followed by a selective Michael addition to give **220** and finally hydrolysis to give **221**.[130]

Up to 90% e.e.
Up to 89% yield
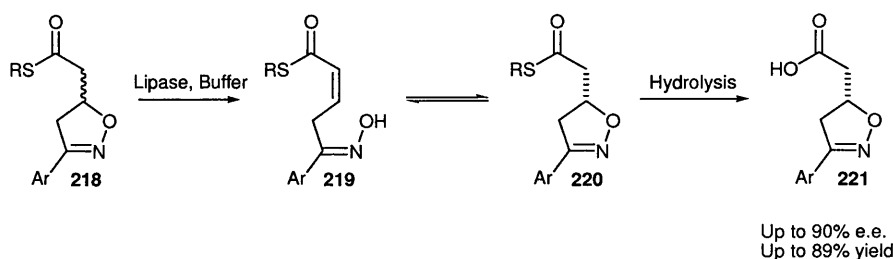
(Scheme 7.3)

Having examined the literature we rationalised that this type of process could be achieved utilising asymmetric organocatalysed Michael additions. We therefore set about finding a procedure that we could adapt to investigate the possibilities of organocatalysed dynamic resolution.

Within the field of organocatalysis Ogilvie began to develop a chiral dynamic resolution for the asymmetric Diels-Alder reaction catalysed by hydrazide **21** *(Scheme 7.4)*.[131]

114
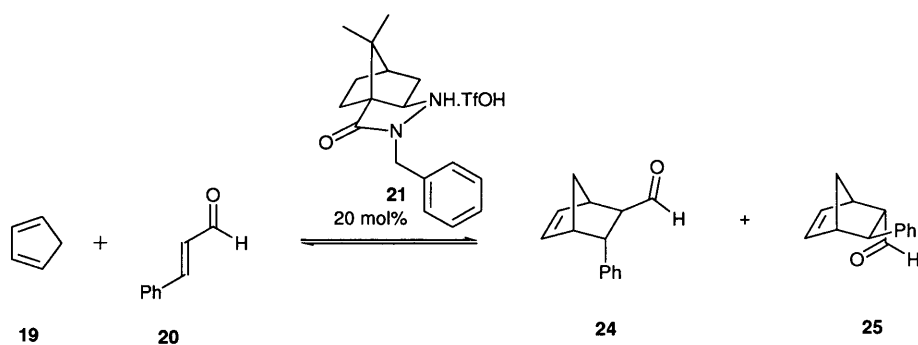
(Scheme 7.4)

Within his report Ogilvie stated that the iminium ion catalysed Diels-Alder reaction was reversible. He also concluded that the forward Diels-Alder reaction was catalysed by the hydrazide **21** while the retro-Diels-Alder reaction is primarily catalysed by the TfOH co-acid. Ogilvie demonstrated that on adding **21** to a racemic mixture of **24** and **25** under the standard reaction conditions for 48h a small increase in the e.e. was observed. Despite his initial success Ogilvie did not fully exploit this observation to develop an efficient dynamic resolution procedure, primarily due to the sluggish kinetics encountered for the reversible process.

We sought to obtain a proof of concept for a dynamic resolution procedure with an organocatalysed Michael addition reaction by demonstrating the reversibility of another process. Once this was achieved we could tune the reaction conditions to obtain a practical dynamic resolution procedure.

Our attention was drawn to the work of Jørgensen who had described asymmetric organocatalytic C-C bond forming Michael additions of nitroalkanes,[132] β-keto esters,[133] 1,3-dicarbonyls[134] and β-keto-sulphones[135] to α,β-unsaturated carbonyl compounds using imidazolidine based catalysts **10** and **222**.
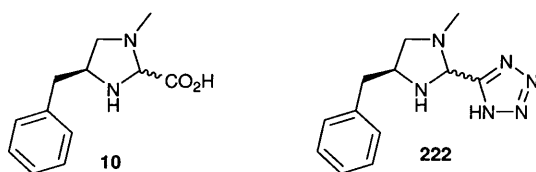
The mode of asymmetric induction of these catalysts was rationalised by comparing the calculated energy for the various iminium ion intermediates **223-226**.[16] PM3 semi

empirical calculations suggested that the *trans*-iminium ions **224** and **226** were considerably higher in energy (>3 kcal/mol) than **223** and **225** due to unfavourable steric interactions. Iminium ions **223** and **225** were of similar energy although **223** was slightly favoured.
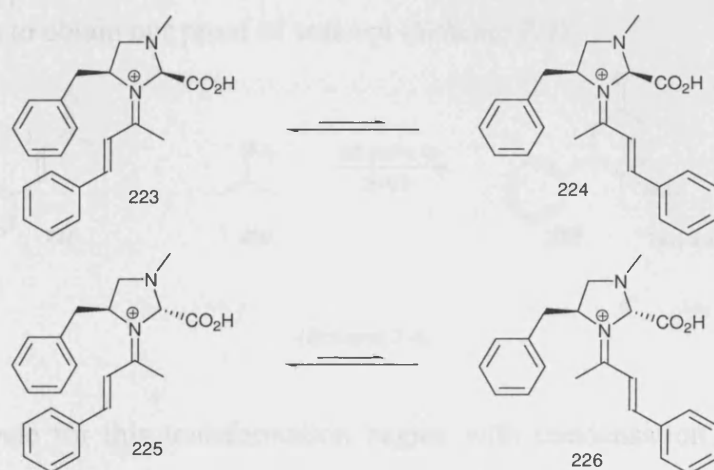
(Figure 7.1)

Constructing a model of iminium ion **223** demonstrates that the *Re*-face of the iminium ion intermediate was blocked by the benzyl group of the catalyst and that the *Si*-face was more exposed to nucleophilic attack (*Figure 7.2*). The proposed theoretical model was consistent with the observed asymmetric induction of the products determined by X-ray crystallography.
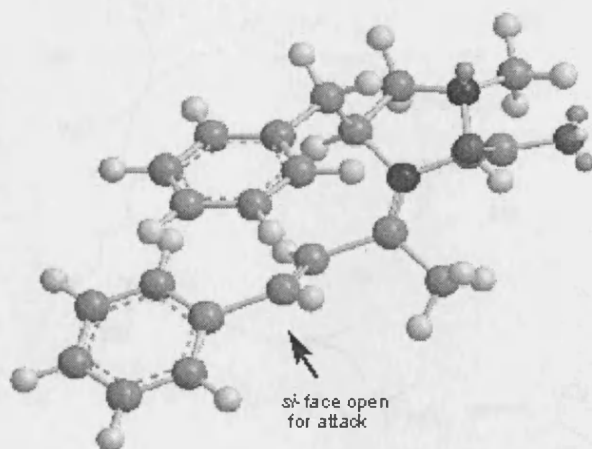
(Figure 7.2)

In particular, we were attracted by the Michael addition of nitroalkanes to α,β-unsaturated ketones principally due to the formation of the a C-C bond and the numerous

subsequent elaborations possible with the nitro group. Catalyst **10** took the reaction to 100% conversion with 79% e.e. over a period of 240 h with 20 mol% catalyst loading. The reaction times for a number of the reported transformations were extremely long (up to 300 h) to achieve modest yields. Therefore, we chose a system that was comparatively rapid to allow us to obtain our proof of concept (*Scheme 7.4*).
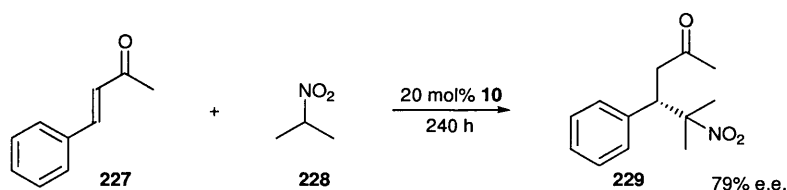
(*Scheme 7.4*)

The catalytic cycle for this transformation begins with condensation of the secondary amine with the enone **227** to generate the iminium ion **230** (*Scheme 7.5*). The Michael acceptor is now sufficiently activated for attack by the nucleophile. In this case, the deprotonated nitropropane **228** reacts. Upon attack of the nucleophile, the enamine **232** is formed. The catalytic cycle is then completed by hydrolysis of the enamine to yield the product **229** and regenerate the catalyst.

(*Scheme 7.5*)

117
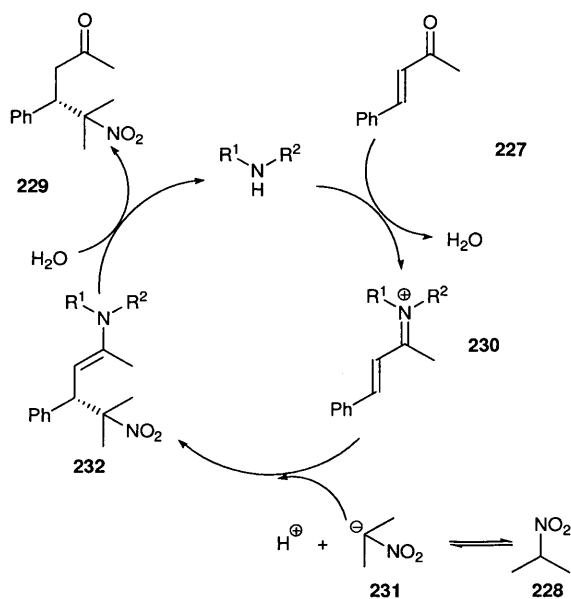
The proposed mechanism for the reversible Michael addition would begin by iminium ion formation by condensation of the secondary amine catalyst with the carbonyl of Michael adduct **229**. The resulting iminium would then form the enamine **232**. Donation of the lone pair of the nitrogen to form an iminium ion would displace electrons that in turn would displace the nitropropane anion **231** to generate the activated Michael acceptor **230**. The iminium ion could then be hydrolysed or undergo a Michael addition to reform **229** (*Scheme 7.6*).
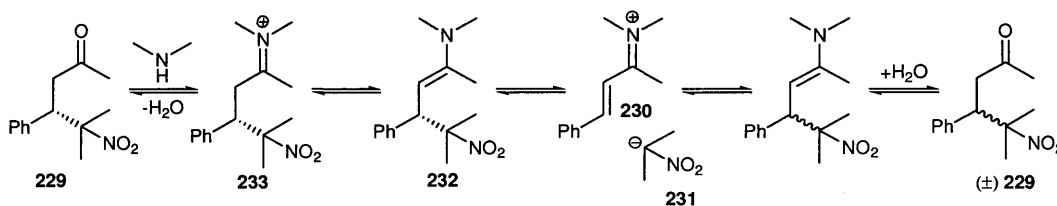
(*Scheme7.6*)

7.2.1 Experimental Design

In order to demonstrate the potential for dynamic resolution we designed three experiments that would give us proof of concept, or at least demonstrate the reversibility of the organocatalysed Michael addition.

Experiment I

The first and the most attractive would be to take a racemic Michael addition product from an organocatalysed reaction and submit this product to the optimal literature conditions for the asymmetric organocatalytic procedure in the presence of a chiral catalyst such as **10** (*Scheme 7.7*).

(*Scheme 7.7*)

118
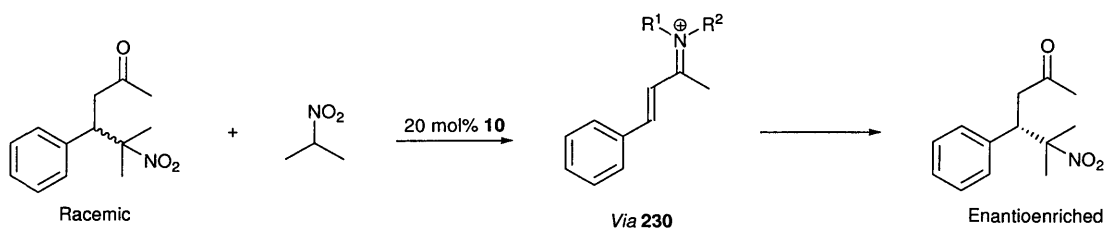
The observation of an increased e.e. in the Michael addition product would clearly indicate that intermediate **230** must have been formed with the reaction.

Experiment II

Another experiment very similar to experiment **II**, but less desirable, would be to subject an enantioenriched Michael addition adduct to an achiral catalyst under optimal reaction conditions and detect a decrease in the observed e.e. of the Michael adduct. As with experiment I this would clearly indicate that the intermediate iminium ion **230** must have been formed under the reaction conditions.

Experiment III

The third experiment would be to take the product of the Michael addition of a nucleophile and submit it to reaction conditions used for introducing an alternative nucleophile (*Scheme 7.8*). Detection of **234** would strongly indicate that the reaction was reversible as direct substitution would be unlikely.

(Scheme7.8)
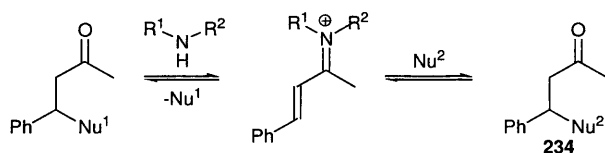
7.2.2 Selection of Catalyst for the Study

Our preferred choice of asymmetric catalyst was the imidazolidine **10**. In order to begin the research we had to prepare **10** which proved more difficult than expected. Preparation of **235** was straightforward and consistent with the literature. However, the cyclisation to afford **10** proved difficult and time consuming with many attempts conducted. It was found, however, that the glyoxylic acid starting material was the problem and on purchase of a fresh batch the synthesis was completed (*Scheme 7.9*).
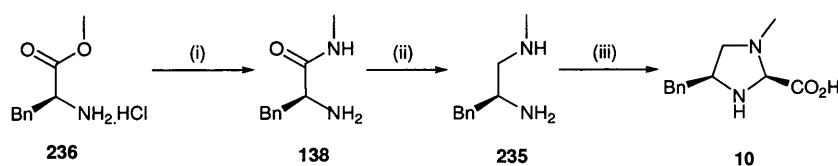
(i) NH_2Me(5 eq) in EtOH,16 h,rt 89%.(ii) $LiAlH_4$ (10 eq), THF, 16 h, reflux, 25%. (iii) $CHOCO_2H$, CH_2Cl_2, 16 h, rt, 62%.

(Scheme7.9)

We also required an achiral catalyst for Experiments **II** and **III** and therefore we proposed to use hydrazide catalyst **91** previously developed in the group as it was known to catalyse Michael addition reactions.[136] However, **91** proved inactive for the reaction of nitroalkanes with enones as the HCl salt and the free base. We also attempted using the MacMillan catalyst **7** to subsequently allow for preparation of an achiral variant but this also proved inactive. This may be for two reasons firstly; the catalysts were only sparingly soluble under reaction conditions. Secondly, the pK_a of the co-acid may have been too low as the majority of active catalysts for this transformation contain an internal carboxylic acid with a higher pK_a ($\approx$ 4). It is important to stress, however, that these organocatalysed Michael additions are slow, even under optimal conditions and therefore we could only realistically screen for the most active catalysts for this class of transformation.

We therefore targeted compound **237** as an achiral catalyst as it was structurally very similar to the chiral Jørgensen catalyst **10** and therefore should posses similar activity and be accessible by an analogous synthetic approach to catalyst **10**.
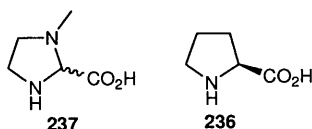
However, compound **237** proved elusive although much synthetic effort was deployed developing reaction conditions. In hindsight the most probable reason for this was a similar reaction to that discussed in (Chapter 8), however, due to the complex mixture of products obtained this was not clearly evident at the time. We therefore decided to use proline **236** as our 'achiral' catalyst as it was successful in catalysing the Michael addition reaction of nitropropane **228** and eneone **227** with low selectivity (e.e. $\approx$ 7%).

7.2.3 Obtaining the Compounds for the Experiments

Having found suitable catalysts **10** and **236** for this investigation, in order to conduct experiments **I-III** outlined earlier we need access to sufficient quantities of chiral and racemic Michael addition products. We obtained our chiral Michael addition product **229** by conducting the procedure reported by Jørgensen. Due to the lack of information in the literature on achiral organocatalysed Michael additions we obtained our racemic product **237** (equivalent to the reaction of **229** and nitromethane **238**) from an efficient proline catalysed conjugate addition of acetone to *trans*-nitrostyrene **239** (*Scheme 7.10*).[137]
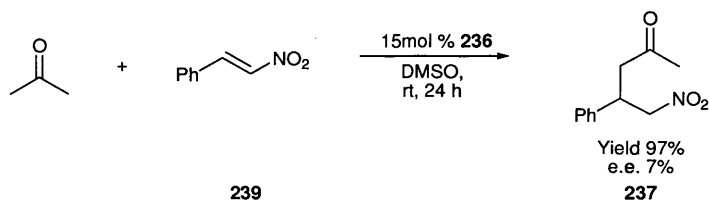
(Scheme 7.10)

7.2.4 Establishing a Method of Analysis

In his work Jørgensen determined the enantiomeric excess of the Michaels adducts using GC with a chirasil Dex-CB chiral stationary phase.[16] Without this apparatus we had to develop a novel procedure for analysis. To achieve this we repeated Jørgensen's procedure for the reaction and determined the e.e. by chiral phase HPLC. Comparing our observed values with those of the literature allowed us to validate our method and deduce the retention times of each enantiomer by analogy. An analogous procedure was conducted to establish the HPLC conditions for compound **237** using data provided by List (*see Appendix*).[137]

7.3 Results and Discussion

7.3.1 Reversibility Experiments

To satisfy the criteria of experiment **I** (*Section 7.2.1*) we took compound (±)**237** along with catalyst **10** and applied the reaction conditions provided for the transformation by Jørgensen. After a generous reaction time of 240h the reaction was stopped, columned

and analysed by HPLC. Disappointingly, the e.e. observed for the Michael addition adduct **237** was identical to the starting material (7%). Therefore, it can be concluded that this reaction is effectively irreversible at this time scale.
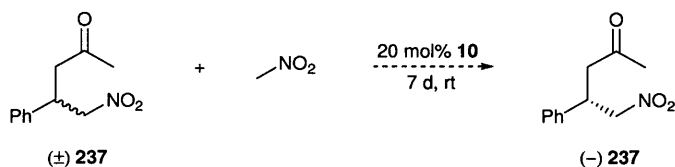
(Scheme 7.11)

To achieve proof of concept using experiment **II** we took the enantioenriched product **229** and subjected it to *D*-proline, *L*-proline and (±)-proline individually in 2-nitropropane for 3 weeks. Again, the e.e. of the products, determined by HPLC, obtained for all three catalysts was identical to that of the starting material.
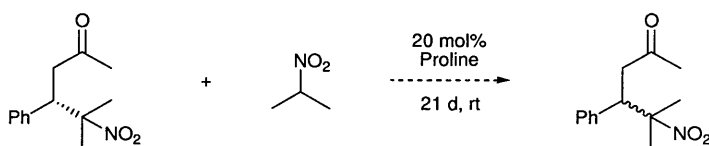
(Scheme 7.12)

Experiment **III** was conducted using the racemic compound (±)**237** which was stirred in diethyl malonate **240**, ethylacetoacectate **241** and nitropropane **228** in the presence of proline **236** for one week (*Scheme 7.13*).
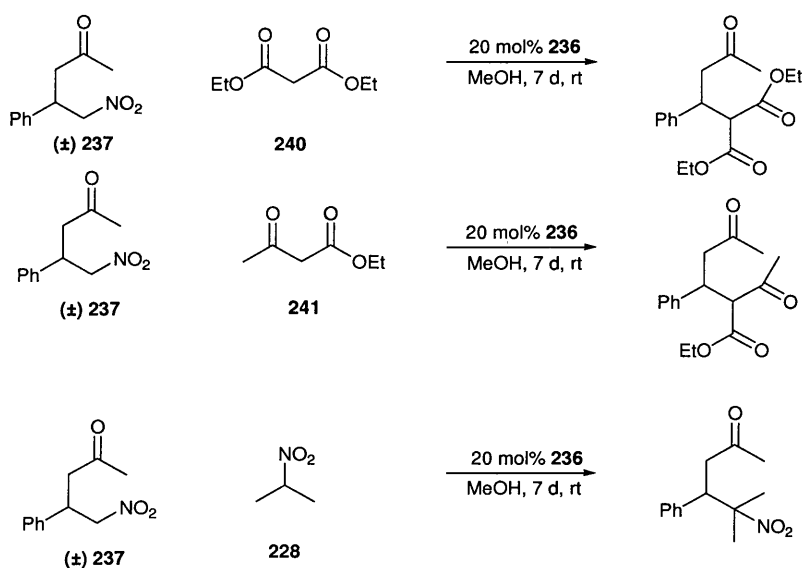
(Scheme 7.13)

Spectroscopic analysis provied no indication of the new products and the initial mass of racemic adduct was recovered. This experiment also indicated that the reaction was not reversible.

7.3.2 Effect of Methanol on Reaction Rate Of Michael Additions

The organocatalysed Michael additions involving nitroalkanes frequently use the nitroalkane as the solvent. In our investigations we made the observation that the catalyst did not appear to be well solubilised under the reaction conditions which could possibly explain the sluggish rate of reaction. We therefore added a small amount of methanol to see if this would accelerate the rate of reaction by making the catalyst more available in solution.

This proved successful and we managed to considerably lower the reaction time. In order to quantify this effect we did series of experiments where we altered the relative amount of methanol and nitroalkane (*Figure 7.3*).
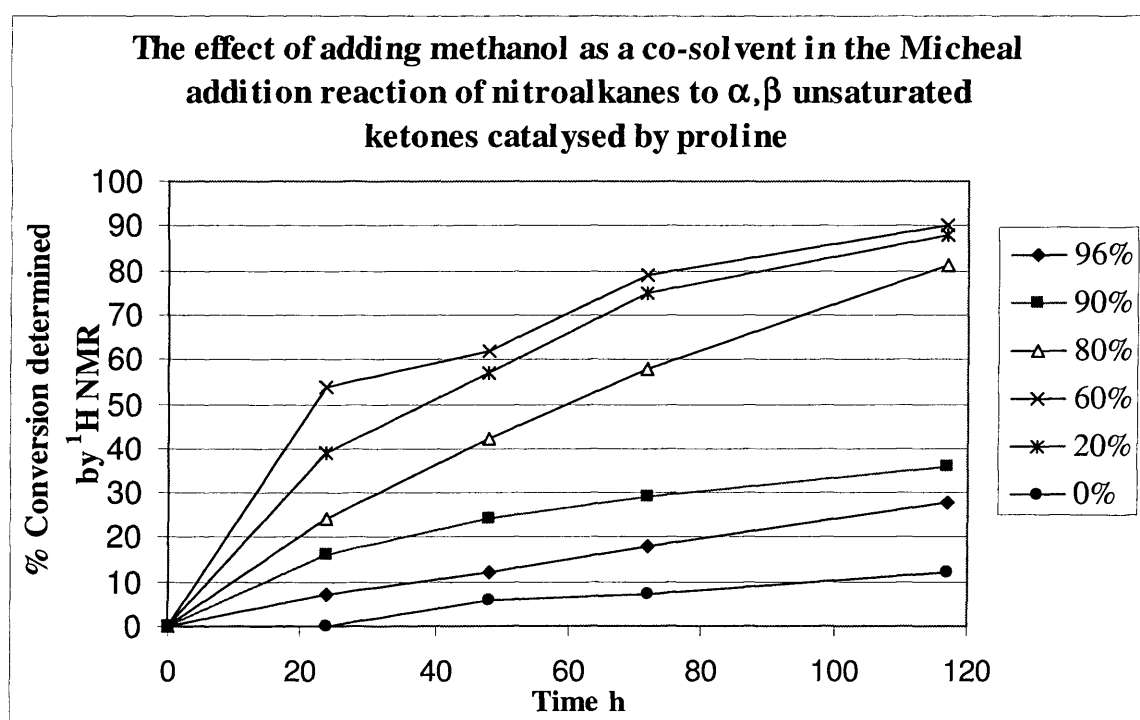
(*Figure 7.3*)

123

We discovered that the optimal amount of methanol for the reaction was 60 % (V/V MeOH/CH₃NO₂ although a similar acceleration was observed for 20% added methanol. Interestingly, addition of >60% methanol had a detrimental effect on the rate but was still superior than the levels of activity observed in the absence of co-solvent. An explanation for these observations may be that on addition of a greater portion of methanol there are fewer molar equivalents of nitropropane available for reaction, hence slowing the rate. This data suggested that with between 20-60% added methanol that all the catalyst was in solution. This was consistent with the physical observation of the transformation.

With these results in hand we believed that we might be able to accelerate the rate of the reactions and therefore added 60% methanol to reaction with the chiral **10**. Disappointingly, a significantly lower e.e. (21% compared to 80%) was observed rendering the discovery obsolete as a method to accelerate the rate of this class transformation.

It is noteworthy, that although the published catalyst loadings for these transformations is 20 mol%, in fact only a small fraction of this amount can be involved in the actual reaction due to an inherent lack of solubility of the catalyst.

7.3.3 Investigation of Alternative Catalysts for the Retro-Michael Reaction

Although we had failed to demonstrate the reversibility of the Michael addition with the published chiral catalyst **10** or proline **236** we rationalised that the requirements for a catalyst for the reverse reaction may be different to that of the forward reaction. There are examples in the literature of multiple organocatalysts selectively accelerating different reactions within a single reaction vessel.[138] We believed that we could exploit this concept to develop a dynamic resolution procedure. In order that an amine be efficient at facilitating the retro-Michael reaction, we rationalised that greater electron density associated with the lone pair of the nitrogen is desirable to facilitate elimination of the nucleophile(*Scheme 7.14*).
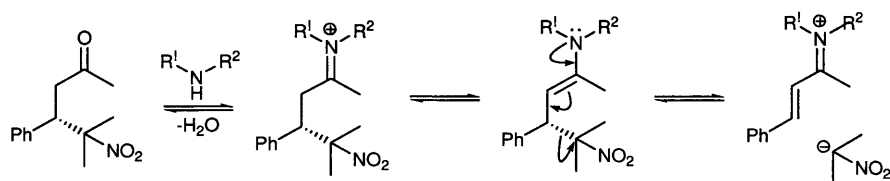
(Scheme 7.14)

To achieve our aims we selected a range of simple commercially available secondary amines with inductive electron donating groups. We also believed that the α-effect could encourage the retro-Michael reaction. We therefore selected a range of commercially available amines which would allow us to test this hypothesis (*Figure 7.4*).
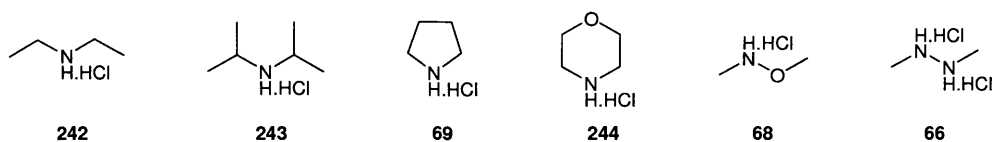
(Figure 7.4)

Initially, we examined the catalysts in the forward reaction of eneone **227** with nitromethane with 60% added methanol. No reaction was observed for any of the catalysts **242-244**, **66**, **68** and **69** after a 48 h period.

Having established that the catalysts **242-244**, **66**, **68** and **69** would not rapidly catalyse the Michael addition we sought to discover whether they could catalyse the retro-Michael reaction. We submitted compound **237** to the catalysts **242-244**, **66**, **68** and **69** at 20 mol% loading in deuterated solvent and monitored the reaction mixtures by ^{1}H NMR over a period of 7 d for the presence of eneone **227**. The presence of **227** was not observed in the ^{1}H NMR spectra for any of the catalysts. Furthermore, the initial spectrum was identical to all subsequent spectra. We therefore concluded that none of the catalysts employed could facilitate a retro-Michael addition reaction.

7.3.4 Iminium Ion Activation *vs* H-Bonding Activation

Subsequent to our investigations we became aware of work conducted by Lattanzi investigating the organocatalytic expoxidation of α,β-unsaturated ketones using peroxides (*Scheme 7.15*).[139]
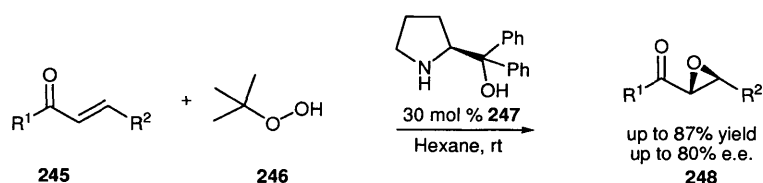
(*Scheme 7.15*)

Within this work Lattanzi conducted non linear studies and from the results postulated that catalyst **247** was acting as a bifunctional catalyst by simultaneously activating the ketone **245** and the peroxide **246** as outlined in the proposed catalytic cycle below (*Scheme 7.16*).
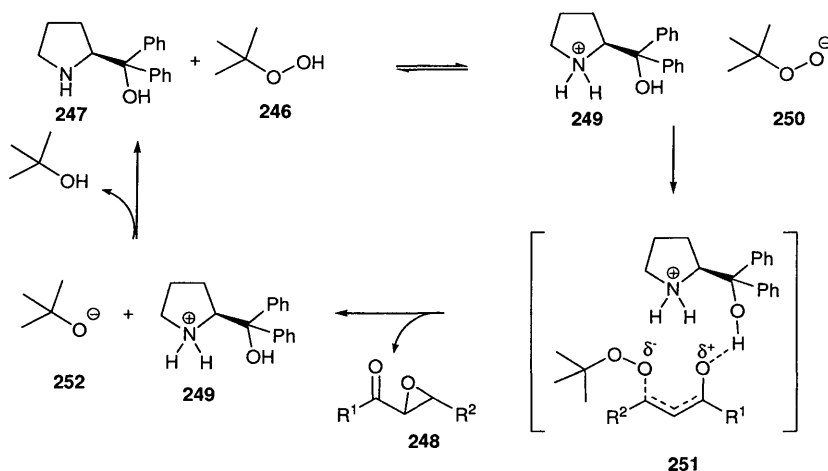
(*Scheme 7.16*)

The cycle is initiated through deprotonation of the peroxide **246** by catalyst **247** to form the active peroxide anion **250** and the corresponding ammonium cation **249** which forms a tight ion pair in the non-polar hexane medium. It was then believed that the hydroxyl group of the catalyst activates the α,β-unsaturated ketone through hydrogen bonding *via* the transition state **251**. Electrostatic interactions then arrange the reaction components to allow for the conjugate addition of peroxide anion **250** to form a hydrogen bond stabilised enolate, which subsequently attacks the O-O bond of the peroxide

intramolecularly generating the epoxide **248**, ammonium species **249** and the *tert*-butoxide anion **252**. The final step is regeneration of the catalyst **247** by deprotonation with the *tert*-butoxide anion **252**.

We began to consider whether catalyst **10** could be acting in a similar manner activating the α,β unsaturated carbonyl by hydrogen bonding (**254**) rather than activation *via* iminium ion formation (**253**) to nucleophiles (*Figure 7.5*).

| 10 | 253 | 254 |
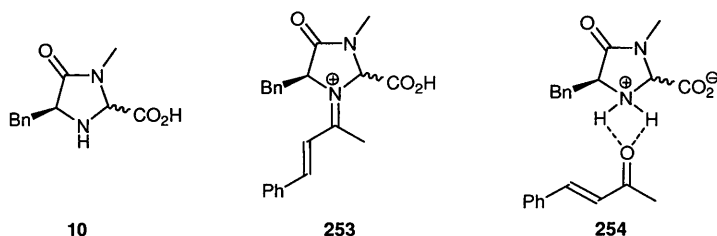
(*Figure 7.4*)

It is noteworthy that there has been no evidence presented that confirms the occurrence of iminium ion **253** within the organocatalysed Michael additions reported by Jørgensen. Through conducting our work we have not observed any indication of the presence of iminium ion **253** although we did not explicitly look for it. What is significant is that within our iminium ion catalysed Diels-Alder work, where we conducted detailed studies of iminium ions (*Chapter 2-5*), the presence of an iminium ion was clearly indicated by a strong yellow colour within the reaction. This yellow colouration was not observed within this Michael addition investigation. This argument may be easily discounted as the reaction medium and substrates have been altered considerably. It is also noteworthy that catalyst **91** which is known to be efficient at catalysing Michael additions to α,β-unsaturated aldehydes through iminium ion activation is inactive in this transformation.[140]

91
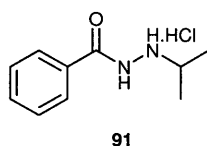
(*Figure 7.5*)

It may also be significant that the addition of MeOH as a co-solvent in the reaction increased the activity. This was thought to be due to solubility of the catalyst but it may well be that the MeOH present is contributing to the activation of the α,β-unsaturated ketone through hydrogen bonding. This is certainly consistent with the loss of asymmetry induced by adding MeOH (*see section 7.3.2*).

To discover whether or not catalyst **10** operates *via* iminium ion activation or through hydrogen bonding activation would require further experiments to be conducted. These additional experiments should be relatively straightforward to perform and certainly worthwhile.

7.4 Conclusions

Despite significant efforts to demonstrate the concept of dynamic resolution for the organocatalysed Michael addition reactions, proof remains elusive. It can be concluded that these reactions are effectively irreversible within the timescales that our experiments were conducted. Often, the forward organocatalysed Michael additions take several days for the reaction to achieve good yields. It has been shown that after an extended period of time excellent yields are obtained for these reactions (ca >95 %).[16] If these yields do in fact represent the equilibrium positions of the reactions, that suggests that the rate of the retro-Michael reaction is extremely slow given the sluggish rate at which the forward reaction takes place. It is primarily the slow rates of the organocatalysed Michael additions that will inevitably limit the practicality of any resolution procedure developed with the substrates used.

Chapter 8: Development of a Practical Method for the Carboxymethylation of Primary Amines[141]

8.1 The Aims of the Research

In this study we sought to explore the scope of a serendipitously discovered monocarboxymethylation reaction of primary amines. We then sought to extend our methodology to selectively synthesise piperazinones from diamines.

8.2 Introduction

In an attempt to synthesise catalyst **256** by reaction of glyoxylic **255** acid with **138**, for a project investigating organocatalysed Michael additions (*Chapter 7*), great difficulty was encountered in interpretation of the spectroscopic data obtained for the product.
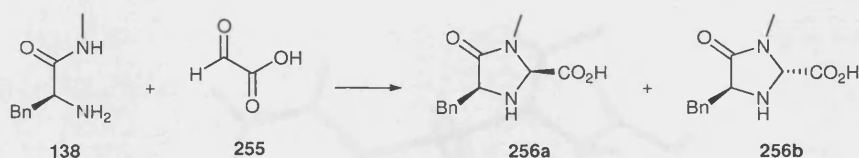
(Scheme 8.1)

The ^{1}H NMR data appeared to be generally consistent with a diastereotopic mixture of the isomers of **256a-b**. However, mass spectrometry failed to find the molecular ion for compound **256**. Not confident as to its structure we submitted the unidentified product as a catalyst for a Michael addition reaction in which it proved inactive. We therefore lost interest in the compound as a catalyst. Still unsure as to the compound's identity we attempted to grow crystals suitable for X-ray crystallography studies. The structure that was determined for the compound was that of **257** (*Figure 8.1*).
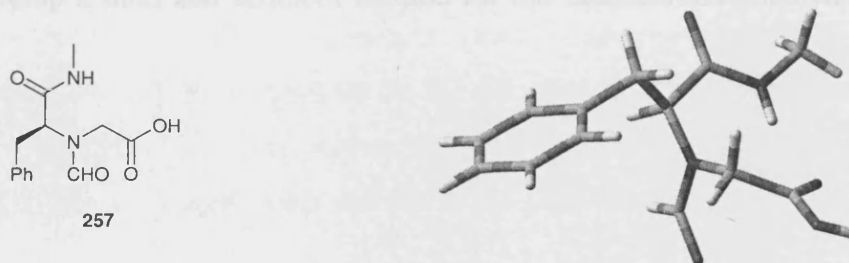
(Figure 8.1)

The result obtained was completely unexpected. Examining this result we rationalised that compound **257** must have reacted with two equivalents of glyoxylic acid **255** to give

compound **257**. In order to establish whether the reaction was reliable we reacted phenethylamine **258** with glyoxylic acid **255** (2 eq) and obtained the corresponding product **259** (63%).
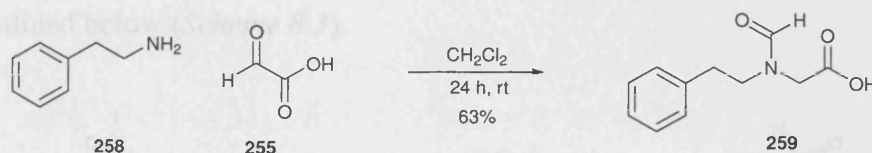
(Scheme 8.2)

Suitable crystals were also grown of this compound and X-ray crystallography confirmed that we had the desired product **259** (*Figure 8.2*).
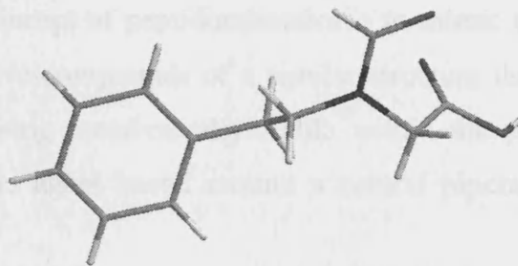
(Figure 8.2)

A literature search revealed that a monocarboxymethylation reaction of primary amines with glyoxylic acid had been previously reported.[142] However, we realised that the conditions used in the reported process were relatively harsh utilising formic or trifluoroacetic acid as the reaction medium at elevated temperatures (60-100 °C). The reaction that we had observed took place in CH_2Cl_2 at room temperature, presenting the opportunity to develop a mild and efficient method for the monocarboxymethylation of primary amines.

8.2.1 Potential Extension to Synthesise Piperazinones for Peptidomimetics

We hypothesised that the transformation had the potential to be developed as an efficient method for the formation of piperazinones **260** using diamines **261** and glyoxylic acid **255** as outlined below (*Scheme 8.3*).
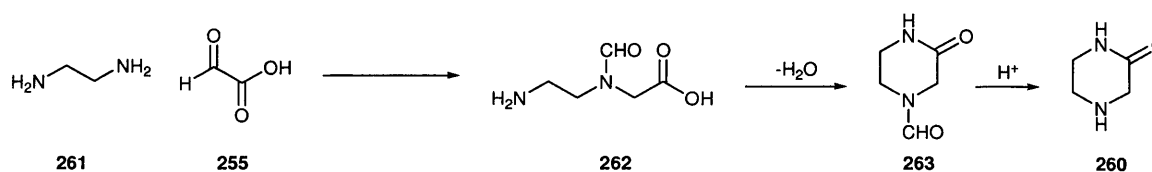
(Scheme 8.3)

The piperazinone ring as a structural motif is of importance in the field of peptidomimetics. The concept of peptidomimetics is to mimic the properties of peptides with therapeutically active compounds of a similar structure that have superior receptor binding ability while being metabolically stable within the physiological system. An example of a therapeutic agent based around a central piperazinone is TAK-024 **264** (*Figure 8.3*).[143]
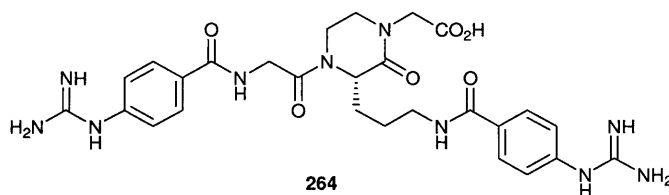
(Figure 8.3)

It is the potential of this class of peptidomimetic that fuels much of the research into the development of novel and efficient methods for the preparation of 2-piperazinones. A method frequently employed for the monocarboxymethylation of primary amines involves the use of α-halo carboxylic acids and esters **265** (*Scheme 8.4*)
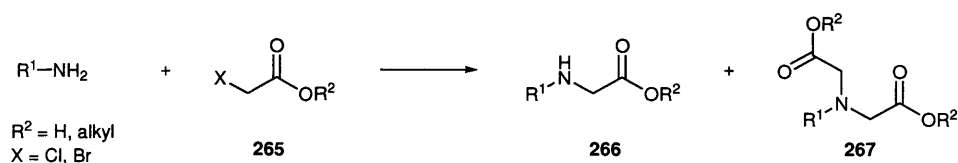
(Scheme 8.4)

However, these reactions are often inefficient due to the over alkylation of the amine which leads to compounds such as **267**. This can be overcome using protecting group strategies or adding an excess of the amine but both are undesirable in a multi-step synthesis. Therefore, methods providing a selective monocarboxymethylation are desired prompting our attempts to develop the reaction further.

8.3 Results and Discussion

8.3.1 The Mechanism

We began by considering the mechanism of the reaction. We believed that the first step of the reaction was formation of imine **269** by condensation of the amine **258** and a molecule of glyoxylic acid **255**. The imine then uncharacteristically acts as a nucleophile attacking a second molecule of glyoxylic acid **255** to yield iminium ion intermediate **270**. This intermediate was believed to decarboxylate evolving CO_2 (which is consistent with experimental observations.) The resulting enolate **271** can then be protonated restoring the carboxylic acid group while the iminium ion converts to the corresponding formamide to produce the observed structure **272**.
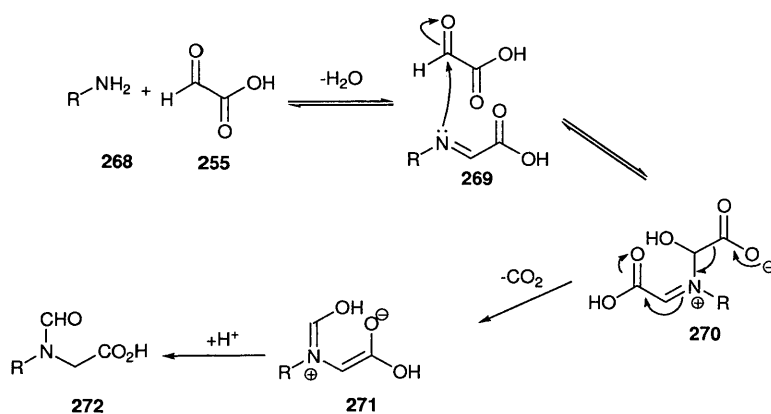
(Figure 8.4)

It is noteworthy that the glyoxylic acid **255** cannot be acting as a hydride source, in an analogous manner to formic acid reductions, due to the stoichiometry used within the reaction and the corresponding yields obtained.

8.3.2 Solvent Screen

Having realised the potential of the reaction we set about developing optimal conditions for the transformation. We selected the reaction of phenethylamine **258** and glyoxylic acid **255** as our standard, reacting for 24 h at 0.2 M in a range of solvents (*Table 8.1*).
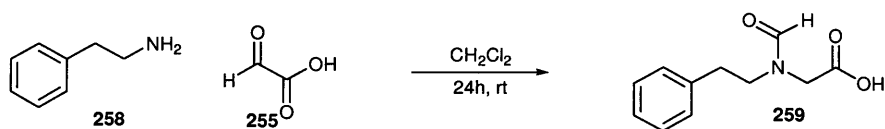
(Scheme 8.6)

Entry[a]	Solvent	conversion %
1	CH_2Cl_2	72
2	Et_2O	49
3	EtOAc	64
4	MeOH	23
5	MeCN	45
6	PhMe	43
7	THF	30
8	H_2O	75
9[b]	H_2O	77

(a) Glyoxylic acid monohydrate 99%
(b) 50% w/v of glyoxylic acid solution used

(*Table 8.1*)

The conversions were within 5% of the isolated yield of hydrolysed compound indicating the validity of the method for rapid analysis. The reaction tolerated a wide range of solvents with only MeOH (*Table 8.1, entry 4*) and THF (*Table 8.1, entry 7*) providing unsatisfactory yields in 24 h. This was most probably due to minor side reactions, as discolouration was observed in the reaction with these solvents. It was found that the optimal solvent was H_2O. This observation allowed us to develop a one-pot method for the monocarboxymethylation of primary amines as aqueous acid could be directly added to the reaction vessel to hydrolyse the formyl group after initial reaction. (*Scheme 8.6*). The method previously described involved isolation of the crude formamide intermediate before conducting the hydrolysis.
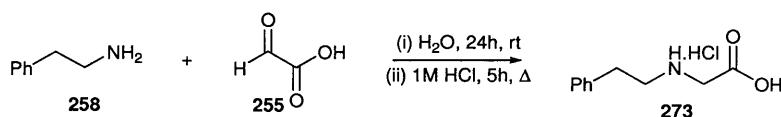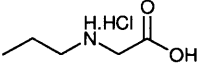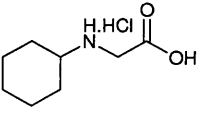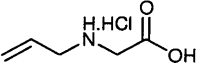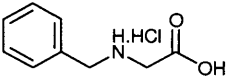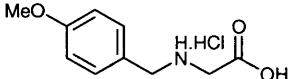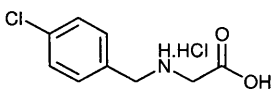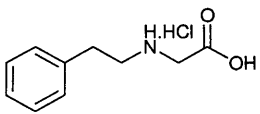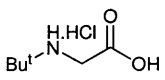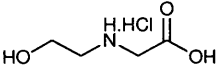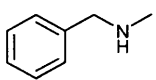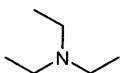
(*Scheme 8.6*)

We also examined the use of a commercially available solution of 50 % w/v glyoxylic acid in H_2O. Slightly better conversions were obtained (within experimental error) using the glyoxylic acid solution providing a more economical and convenient procedure.

8.3.3 Reaction with Primary Amines

Having established the optimal reaction conditions from our solvent and determined that we could conduct a subsequent hydrolysis in a single vessel, we set about discovering the substrate scope. Initially, we reacted a number of primary amines with glyoxylic acid which led to compounds **273-279** in good to excellent yields (*Table 8.2*).

Entry[a]	Product	Structure	Temp °C	Hydrolysis conditions[b]	Yield %
1	**274**		25	A	78
2	**275**		25	B	86
3	**276**		25	A	25
4	**277**		25	A	50
5	**278**		50	B	68
6	**279**		50	B	60
7	**273**		25	A	70
8	**280**		25	B	0
9	**281**		25	B	0
10	**282**		25	A	0
11	**283**		25	A	0

(a) Reactions conducted at stated temperature in H_2O for 24 h with 2.2 equivalents of glyoxylic acid. (b) A refers to hydrolysis in 1 M HCl at reflux for 18 h , B refers to hydrolysis with 2 M HCl at reflux for 18h.

(*Table 8.2*)

The reaction was shown to tolerate primary (*Table 8.2, entry 1*) and secondary (*Table 8.2, entry 2*) α-substituted amines with good yield. The lack or reactivity of *tert*-butyl amine (*Table 8.2, entry 8*) is most likely due to the steric bulk of the *tert*-butyl group hindering formation of the imine intermediate under the reaction conditions as the amine was present after reaction. Benzylamine reacted to give benzyl protected glycine **277** in 50%

yield (*Table 8.2, entry 4*). Reactions with *para*-substituted benzylamines containing electron donating methoxy and electron withdrawing chloro groups **278** and **279,** respectively, were successful (*Table 8.2, entry 5 and 6*). The reaction also tolerated allyl amine albeit with poor yield (*Table 8.2, entry 3*). Ethanolamine reacted with glyoxylic acid but the ^{1}H NMR indicated that numerous compounds had formed with isolation of the desired product proving too difficult.

The reaction of *N*-methyl benzylamine (*Table 8.2, entry 10*) and triethylamine (*Table 8.2, entry 11*) with glyoxylic acid yielded no products demonstrating the chemospecificity of the process for primary amines, a distinct advantage over other methods. This observation also provided further evidence for our proposed mechanism.

8.3.4 Reactions with Diamines

Having demonstrated that the reaction was efficient with a range of primary amines we set about reacting a series of 1,2 and 1,3 diamines with glyoxylic acid **255**. There are several possibilities for the course of the reaction of ethylene diamine with glyoxylic acid. For example, the monocarboxymethylation of a single amine (**284**), alternatively both amines could undergo a monocarboxymethylation reaction (**285**). A further possibility is that after monocarboxymethylation of a single amine an intramolecular cyclisation might occur to give piperzinone **260**. Dimerisation and polymerisation were also possible but less likely as it involves a more challenging intermolecular reaction (*Scheme 8.7*).
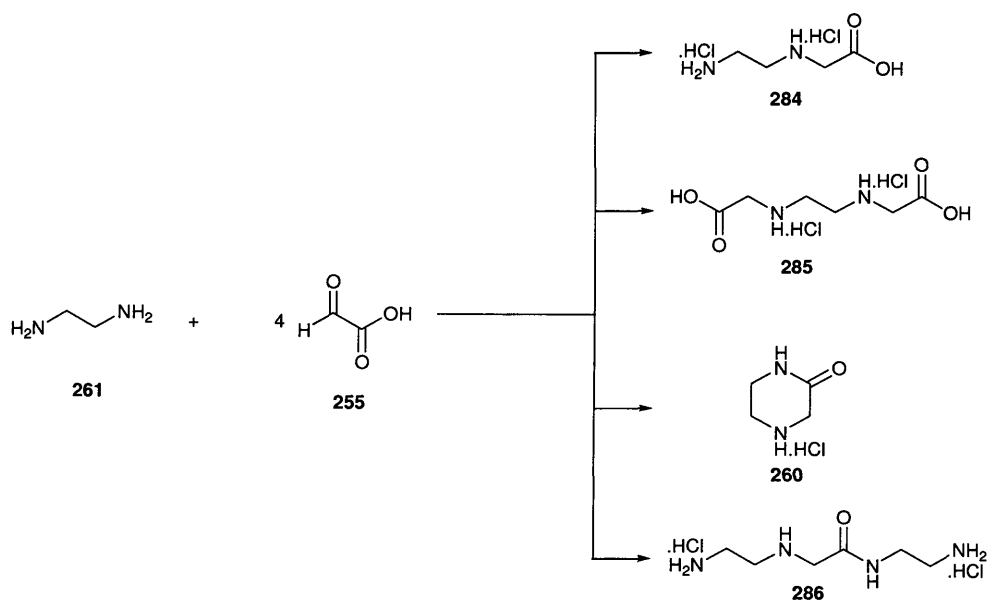
(Scheme 8.7)

On analysis of the reaction of ethylenediamine and glyoxylic (4 eq) acid we had to establish which product we had obtained. ^{1}H NMR allowed us to discount structures **285** and **286** as the correct structure. However, mass spectrometry failed to detect the molecular ion for either of structures **260** or **284**. Therefore, the correct structure **284** was determined by analogy to the commercially available product by comparing samples using ^{1}H and ^{13}C NMR as well as melting point and IR spectroscopy. Mass spectrometry also failed to detect the molecular ion of the commercially available sample. Products **284, 287-290** were easily characterised by conventional techniques.

Entry	Product	Structure	Equivalents of 251[a]	Hydrolysis conditions[b]	Yield %
1	**284**	.HCl H$_2$N⁓N(H.HCl)⁓C(O)OH	4.4	A	31
2	**287**	⁓N(H.HCl)⁓N(H.HCl)⁓C(O)OH	2.2	A	41
3	**288**	⁓N(.HCl)⁓N(H.HCl)⁓C(O)OH	2.2	B	68
4	**289**	⁓N(H.HCl)⁓N(H.HCl)⁓C(O)OH	4.4	B	44
5	**290**	⁓N(.HCl)⁓N(H.HCl)⁓C(O)OH	4.4	B	59

(a) Reactions conducted at 25°C in H$_2$O for 24h. (b) Conditions A refers to hydrolysis with 1M HCl at reflux for 18h, B refers to hydrolysis with 2M HCl at reflux for 18h.

(Table 8.3)

Although the yields obtained are only moderate attempting the monocarboxymethylation of these diamine substrates with α-halo acids/esters would undoubtedly produce even lower yields with numerous by-products forming.

Disappointingly, no evidence of a piperazinone was observed. However, further attempts within the group have subsequently been successful in synthesising piperazinone **260** from *N*-methyl ethylenediamine by altering the reaction conditions.

8.4 Conclusions

In summary, we have developed a mild and efficient method for a one-pot monocarboxymethylation of primary amines and diamines. The reaction is selective for primary amines without the need for protection of more nucleophilic secondary amines and can tolerate a range of amines. The reaction with ethylene diamine provides access to the monocarboxymethylated product in 31% isolated yield on addition of 4 equivalents of glyoxylic acid providing a remarkably selective process. This method has been subsequently been developed to allow for the synthesis of piperazinones.

Chapter 9: An Aminocatalytic Method for the Preparation of bis-Indoyl Alkanes[144]

9.1 Introduction

The importance of indoles as a structural motif in organic chemistry is well documented.[145] The indole unit is present in the naturally occurring and abundant amino acid tryptophan and is consequently found in many compounds of natural origin. Within this chapter an aminocatalytic method for the synthesis of a variety of bis-indole containing natural and non natural targets is reported.

9.1.1 Discovery

At the heart of much chemical research is the search for new synthetic methods. We began this research with a view to expand the existing reaction portfolio of iminium ion catalysed processes. Iminium ions have been successful in catalysing numerous reactions that traditionally utilise Lewis acids. With this in mind our attention was drawn to a Lewis acid catalysed process where nucleophilic attack of *N*-methyl indole facilitated cyclopropyl ring opening in a C-C bond forming process (*Scheme 9.1*).[146]
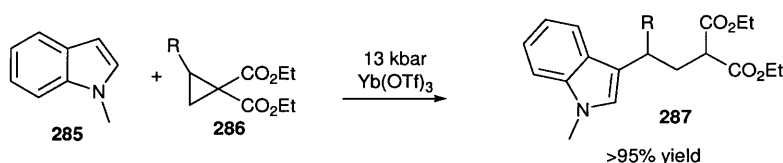
(Scheme 9.1)

To establish whether a similar procedure could be achieved using secondary amine catalysis we conducted a reaction between *N*-methylindole **291** and cyclopropyl carboxaldehyde **292** utilising catalyst **91** previously developed within the group (*Scheme 9.2*).
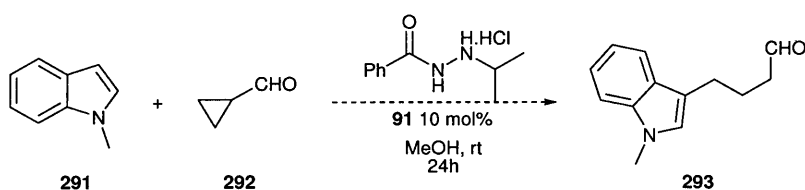
(Scheme 9.2)

142

It was evident from the appearance of the reaction mixture that reaction had taken place. However, on analysis of the purified product it was clear that an unexpected reaction had occurred (*Scheme 9.3*).
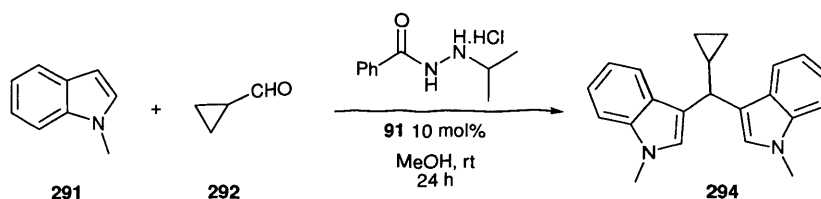
(Scheme 9.3)

The spectroscopic data measured for the product was consistent with that of compound **294**. Consulting the literature we found that this class of compound was known and that frequently they have a natural origin.

9.1.2 Biological Significance and Reported Procedures

Bis-indolylalkanes as a structural class contain some biologically important molecules. For example, diindolylalkane **295** has been identified as being active at promoting beneficial oestrogen metabolism in men and women[147] and has also been found to trigger apoptosis in human breast cancer cells.[148] The biological activity of these compounds has prompted numerous research groups to develop methods for their preparation.

295
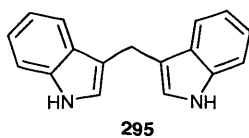
It has been reported that bisindolyl alkanes can be prepared using both Brønsted and Lewis acids to activate the carbonyl to attack by indole. Recent reports include the preparation of bisindolyl alkenes through heterogeneous catalysis using zeolites[149] and montmorillonite K10.[150] Lewis acids that have been utilised include $Zr(OTf)_3$,[151] $La(PFO)_3$[152] and $CeCl_3$.[153] The Brønsted catalysts reported include Amberlyst resins[154] and molecular iodine,[155] along with $KHCO_3$[156] also having reported as a catalyst. Of the

catalysts listed above, it is the heterogeneous catalysts that appear to be the most efficient with reaction times 10 min-6 h. However, large quantities of catalyst have to be used to accelerate the reaction with up to 9100% w/w of catalyst with respect to the aldehyde. To date there has been no report of secondary amines catalysing the reaction. We therefore set out to discover the potential of our aminocatalytic method for the preparation of bis-indolyl alkanes.

9.2. Results and Discussion

9.2.1 Proposed Mechanism

The initial work established the need for a secondary amine catalyst **91** in order for reaction to occur (*Table 9.1, entry 1*). Therefore, we conducted control reactions conducting the addition with no catalyst (*Table 9.1, entry 2*), triethylamine hydrochloride (*Table 9.1, entry 3*) and also acetic acid (*Table 9.1, entry 4*). These control reactions yielded no product, as expected, confirming that our catalyst **91** was responsible for the reactivity.
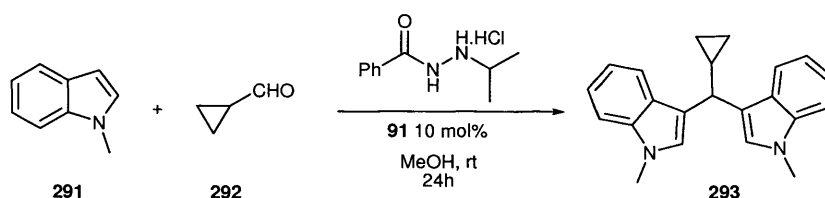
Entry	Catalyst	Catalyst Loading mol%	Yield %
1		10	74
2	No catalyst	10	0
3		10	0
4		10	0

(Table 9.1)

144

To explain the reactivity we proposed a mechanism where the activated iminium ion **296** formed by condensation of the secondary amine catalyst **91** and the carbonyl **298**. The iminium ion **299** is significantly more electrophilic than the corresponding aldehyde and therefore undergoes attack by the indole **300** to form the amine **301**. Protonation of the tertiary amine would allow for the lone pair of the indole nitrogen to push through the conjugated π-systems to eliminate and regenerate the catalyst **91**. The resulting α,β-unsaturated iminium ion **302** is sufficiently activated to undergo a nucleophilic Michael-type addition by a second molecule of indole **300** followed by rearomatisation of the indole to yield the observed product **303** (*Scheme 9.4*).
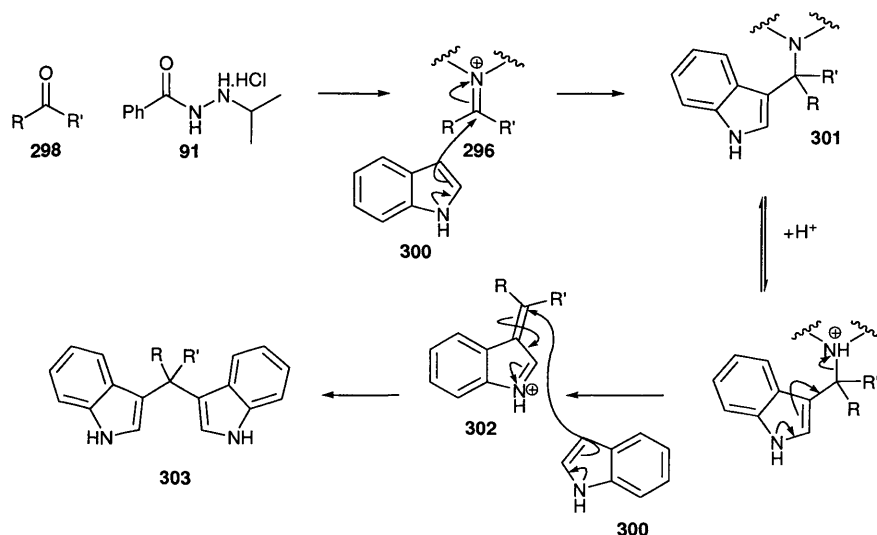
(Scheme 9.4)

It is thought that addition of the first indole is most likely to be the rate determining step. The tentative evidence for this is that the only compounds observed in the reaction mixture were the starting materials and the products. Attempts to facilitate mono addition of the indole by reducing the temperature and adding substoichiometric amounts of indole proved unfruitful; however, these studies were far from rigorous and comprehensive.

145

9.2.2 Effect of Solvent on Reaction

To discover the optimal solvent for the reaction we conducted a brief solvent screen. The reaction of propionaldehyde **304** and indole **300** with 5 mol% loading of catalyst **91** for a 24 h period was examined with a variety of solvents (*Table 9.2*).
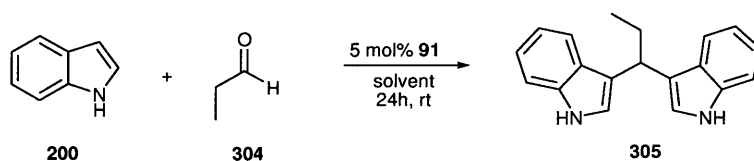
(Scheme 9.5)

Entry	Solvent	Catalyst Loading mol%	Yield %
1	CH₃CN	5	0
2	DMF	5	62
3	DMSO	5	55
4	H₂O	5	62
5	THF	5	39
6	MeOH	5	33
7	MeOH	10	84

(Table 9.2)

Acetonitrile was the worst solvent and failed to facilitate any significant reaction after a 24 h period (*Table 9.2, entry 1*). Polar solvents such a DMF, DMSO and H₂O (*Table 9.2, entries 2, 3 and 4*) all gave the product **305** in similar yields 55-62%. MeOH and THF (*Table 9.2, entries 6 and 7*) were less efficient as solvents, providing yields of 33 and 39% respectively.

It was MeOH that we selected as our solvent of choice (partly as we had synthesised a number of compounds in MeOH prior to commencing the solvent screen) as it was operationally simpler to use in the reaction than DMF, DMSO and H_2O. Using MeOH also provided the advantage that upon reaction a precipitate was observed for many of the substrates allowing a rapid qualitative indication of successful reaction. This precipitation was not apparent in THF for any substrate.

9.2.3 Variation of the Indole

Having established that the reaction worked for a few examples we sought to discover the tolerance of the reaction with derivatised indoles. We selected indole **300** as the standard, *N*-methylindole **291**, 5-methoxyindole **306**, 5-nitroindole **308** and 5-chloroindole **307** (*Figure 9.1*).
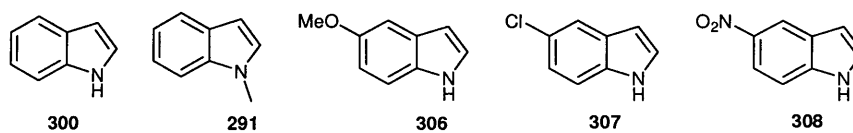
(Figure 9.1)

Propionaldehyde **304** was chosen as the reaction partner to allow direct comparison of the relative reactivity of the indoles (*Scheme 9.5*).

300 R = H R¹ = H
291 R = H R¹ = Me
306 R = OMe R¹ = H
307 R = Cl R¹ = H
308 R = NO₂ R¹ =H

305 R¹ = H R = H 84%
309 R¹ = H R = Me 81%
310 R ¹= H R = OMe 55%
311 R¹ = H R= Cl 42%
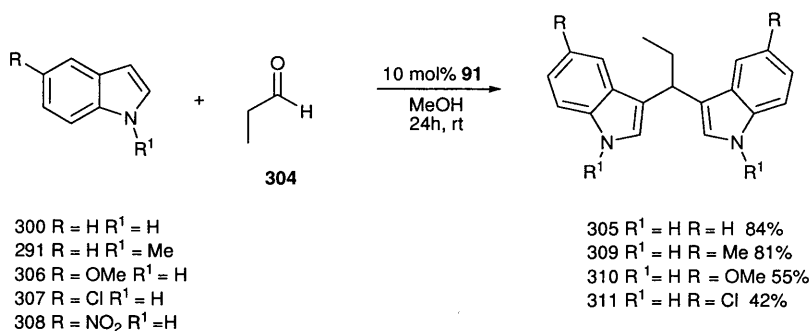
(Scheme 9.5)

No reaction occurred between 5-nitroindole **308** and propionaldehyde **304** after a 24 h period. The electron withdrawing effect of the nitro group considerably reduces the nucleophilicity of the indole and therefore reduces activity. The reaction did however tolerate the weaker EWG leading to 5-chloroindole derivative **311** in 42% yield after a

24h period. Addition of an alkyl group on the nitrogen of the indole had little effect on reactivity. The reactions with indole **300** and *N*-methylindole **291** with propionaldehyde **304** gave the expected products in 84 and 81% yield, respectively, after 24 h. The reaction also tolerated electron donating groups on the indole unit, 5-methoxyindole **306** reacted with propionaldehyde **304** to give the adduct **310** in 55% yield.

9.2.4 Variation of the Aldehyde
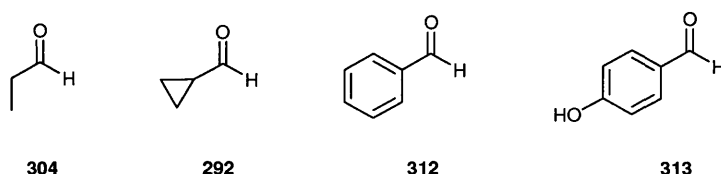
(Figure 9.2)

After our initial success in reacting a series of indoles we wanted to discover which carbonyl substrates would be tolerated. Four aldehydes were reacted with indole, propionaldehyde (**304**), cyclopropanecarboxaldehyde (**292**), benzaldehyde (**312**) and 4-hydroxybenzaldehyde (**313**) to give the products **305** and **314-316** in 74-89% yield (*Scheme 9.6*).

305 R = CH₂CH₃ 84%
314 R = CH(CH₂)₂ 74%
315 R = Ph 84%
316 R = 4-OH-C₆H₄ 89%

(Scheme 9.6)

148
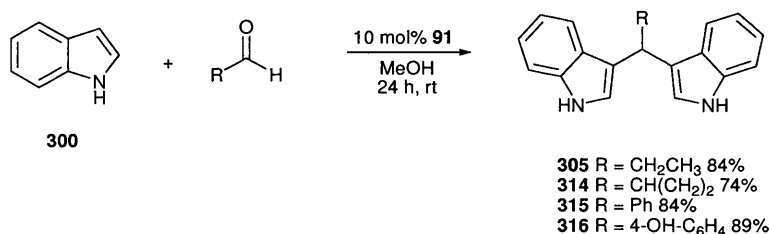
9.2.5 Reaction with Ketones
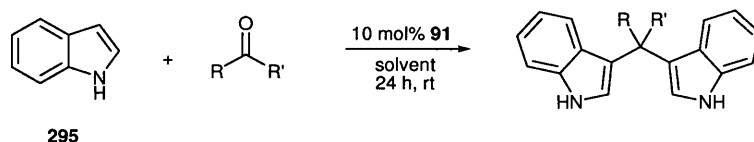
(Scheme 9.7)

Many of the examples in the literature to prepare bis-indolylalkanes did not report ketones as substrates. We therefore examined the more challenging ketone substrates within this organocatalysed reaction. In total three ketones were tested, methyl cyclopropyl ketone **317**, cyclohexanone **318** and cyclohexandione monoethylene ketal **319** with indole **300**. Methyl cyclopropyl ketone was also reacted with *N*-methylindole **291**.
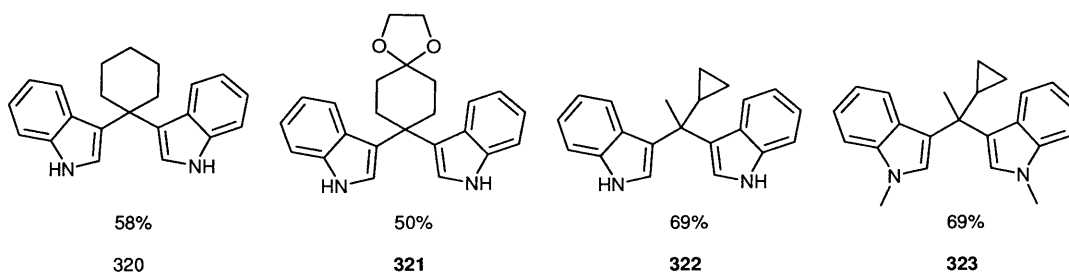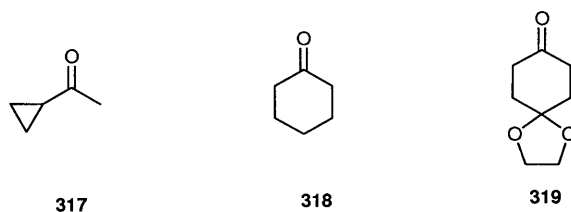
The reactions were all successful furnishing compounds **320-323** as the products. Indole **300** and *N*-methylindole **291** reacted with identical efficiency with methyl cyclopropyl ketone providing both **322** and **323** in 69% isolated yield. Reaction of cyclohexanone **318** with indole **300** gave the product **320** in 58% yield after 24 h. Pleasingly, compound **321** was also obtained in 50% yield from the corresponding ketone displaying that our synthetic method could tolerate the acid sensitive ketal functionality. Synthesis of **321** using the reported Brønsted and Lewis acid methods would in our opinion present a greater challenge. It is also noteworthy that the modest 50% isolated yield obtained for

321 is most likely a consequence of slower reactivity rather than side reactions or hydrolysis of the ketal (determined qualitatively by TLC).

9.2.6 Naturally Occurring Bis and Tris-Indolylalkanes

Having established that we had discovered a mild and efficient method for the synthesis for a range of bisindolylalkanes from aldehyde and ketone substrates we set about applying our methodology to synthesise a variety of naturally occurring compounds. There have been numerous bisindolylalkane natural products isolated and described.[157] Examining the literature we selected four targets to test our methodology **324-327** (*Figure 9.3*).

80%	77%	72%	51%
324	**325**	**326**	**327**
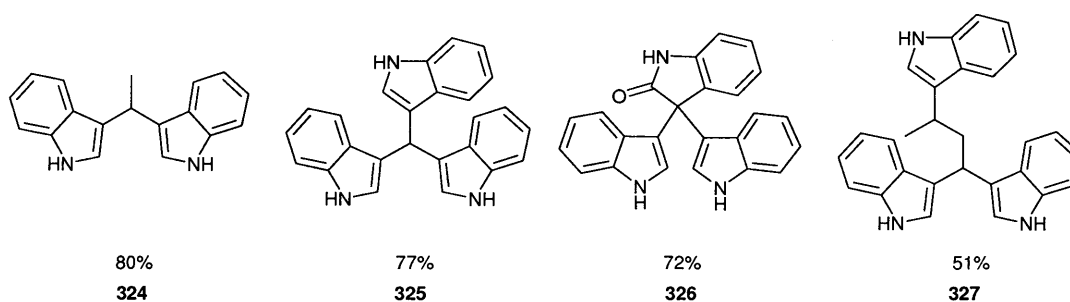
(Figure 9.3)

Vibrindole A **324** was first identified as a metabolite from the marine bacterium *vibrio paraheamolyitcus* and has also been detected in other marine organisms.[158] Our preparation afforded *Vibrindole A* **324** in 80% yield after a 24 h period under our standard reaction conditions at room temperature in methanol for 24 hours using 10 mol% of catalyst **91**.

The naturally occurring compounds **325**, **326** and **327** were all isolated from the marine bacterium *vibrio paraheamolyitcus*.[159] The tris-indolylalkane **325** was obtained by reaction of 3-indolecarboxaldehyde with 2 equivalents of indole in a respectable 77% yield. Compound **326** was synthesised by reaction of isatin with 2 equivalents of indole in 72% yield. The reaction of isatin at the ketone rather than the less reactive amide confirms the chemoselectivity of this process for aldehydes and ketones.

The highlight of our synthetic work was the synthesis of compound **327**. Previous experiments in the group had demonstrated that catalyst **91** could catalyse Michael additions to α,β-unsaturated carbonyl compounds. We recognised the opportunity to introduce the three indoles in one reaction vessel. This method was successful and gave **327** in a respectable 51% yield forming three C-C bonds in one pot.
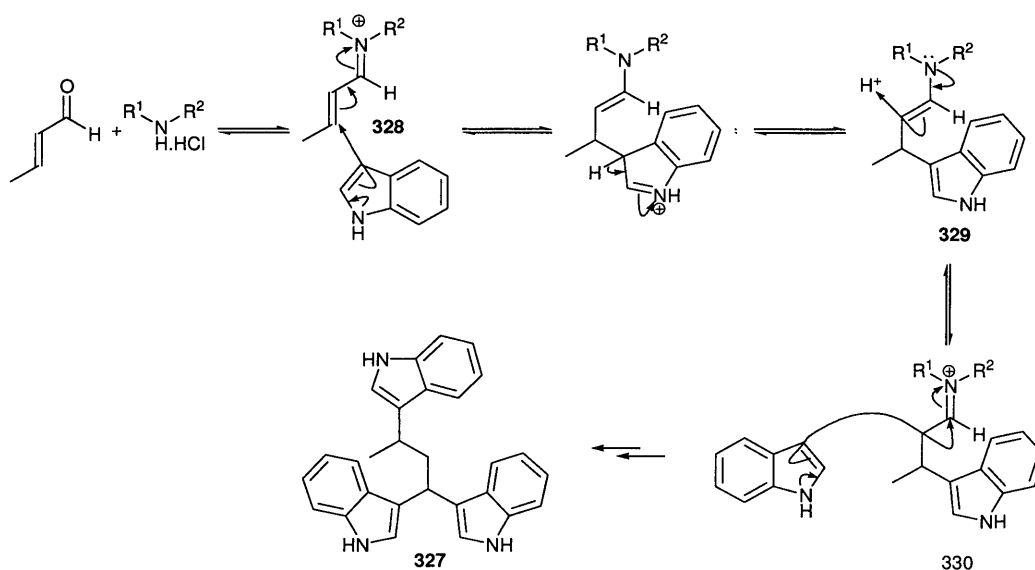
(Figure 9.4)

The first step in the mechanism is formation of the α,β-unsaturated iminium ion **328** which then undergoes the Michael addition reaction with a molecule of indole to give enamine **329**. The resulting enamine is in equilibrium with the corresponding iminium ion **330** which reacts by the same mechanism outlined above (*Scheme 9.4*) to give the product **327** (51%).

9.2.7 Catalyst Loading

To establish the activity of our catalyst in the transformation we conducted the reaction between benzaldehyde **312** and 2 equivalents of indole **300** in the presence of 1 mol% of **91**.
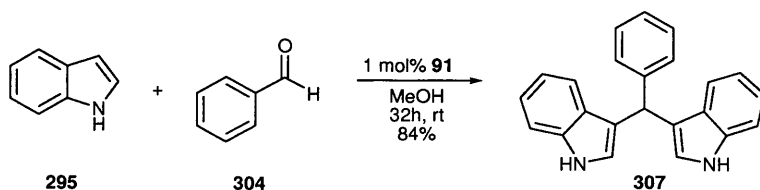
(*Scheme 9.9*)

The yield obtained after a 32 h period was 84% suggesting that catalyst **91** is particularly active for this transformation.

9.3 Conclusions

We have demonstrated the first aminocatalytic method for the preparation of bis and tris indolylalkanes. A variety of indoles, aldehydes and ketones are tolerated as substrates with acid sensitive groups such as ethylene ketals being compatible with the reaction conditions. The method was applied to the synthesis of a range of naturally occurring compounds including *vibrindole A*. The methodology can be further extended to facilitate a tandem Michaeladdition-bis-alkylation reaction in one-pot forming a total of three new C-C bonds. Significant reactivity was observed at 1 mol% catalyst loading.

Chapter 10: Experimental

Reagents were obtained from Aldrich, Lancaster and Fluka chemical suppliers. Solvents and reagents were purified according to the procedures of Perrin, Armarego and Perrin[160] Dichloromethane was dried by refluxing over, and distilling from calcium hydride. Ethanol was dried by refluxing over magnesium, followed by distillation. Toluene was dried over sodium wire for twenty-four hours prior to use. Anhydrous diethyl ether was obtained by distillation from sodium benzophenone ketyl.

All reactions using air/moisture sensitive reagents were performed in oven-dried or flame-dried apparatus, under a nitrogen atmosphere. Catalytic runs were performed using a Radley's carousel, which consists of twelve test tubes with suba-seals and nitrogen inlets, a stirrer plate and a bath for heating. All reactions were followed and monitored by TLC, ^{1}H NMR, ^{13}C NMR and mass spectrometry as appropriate.

TLC analysis refers to analytical thin layer chromatography, using aluminium-backed plates coated with Merck Kieselgel 60 GF_{254}. Product spots were viewed either by the quenching of UV fluorescence, or by staining with a solution of 2 % aqueous potassium permanganate. Chromatography refers to flash column chromatography using head pressure by means of compressed air according to the procedure of Still[161] using Merck Kieselgel 60 H silica or Matrix silica 60.

Melting points were recorded using a Kofler Heated Stage Micro Melting Point Apparatus and are uncorrected.

Infra-red spectra were recorded in the range 4000-600 cm^{-1} using a Perkin-Elmer 1600 series FTIR instrument either as a thin film, a nujol mull or dissolved in stated solvent between sodium chloride plates. All absorptions are quoted in wave numbers (cm^{-1}).

^{1}H NMR spectra (δ_H) were recorded using an Avance Bruker DPX 400 instrument (400 MHz) or an Avance Bruker DPX 500 (500MHz), with ^{13}C NMR spectra (δ_C) recorded at 100 MHz or 125 MHz respectively. Chemical shifts (δ_H and δ_C) were recorded in parts per million (ppm) from tetramethylsilane (or chloroform) and are corrected to 0.00 (TMS) and

7.26 (CHCl$_3$) for ^{1}H NMR and 77.30 (CHCl$_3$), centre line, for ^{13}C NMR. The abbreviations s, d, t, q, sept., m, bs and br, denote singlet, doublet, triplet, quartet, septet, multiplet, broad singlet and broadened resonances, respectively; all coupling constants were recorded in hertz (Hz).

Low resolution mass spectrometric data was determined using a Fisons VG Platform II Quadrapole instrument using atmospheric pressure chemical ionisation (APcI) unless otherwise stated. EI refers to electron ionisation and ES refers to electrospray. High resolution mass-spectrometric data was obtained courtesy of the EPSRC Mass Spectrometry Service at the University of Wales, Swansea, UK, using the ionisation methods specified. Calculated accurate masses are of the parent ion (exclusive of an electron, mass = 0.00055 Da).

Typical experimental procedure for catalytic runs

exo-isomer *endo*-isomer
24   **25**
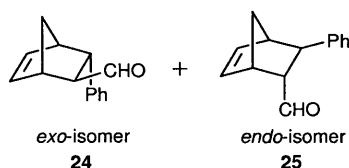
trans-Cinnamaldehyde **20** (252mg, 1.9 mmol, 0.24 mL, 1.0 eq) was added to a solution of catalyst (10 mol%, 0.19 mmol) in methanol (2.0 mL) at 25 °C and the resulting mixture was stirred for 5 minutes to initiate iminium ion formation. Freshly cracked cyclopentadiene **19** (323 mg, 4.9 mmol, 0.38 mL, 2.5 eq) was added in a single aliquot and stirring was continued for 24 hours. The volatiles were removed under reduced pressure and the resulting organics were hydrolysed in a chloroform (2 mL), water (1 mL) trifluoroacetic acid (1 mL) mixture over night. Saturated sodium hydrogen carbonate solution (18 mL) was added to neutralise the solution and the aqueous phase was extracted with dichloromethane (2x20 mL). The combined organics were washed with water (10 mL) and dried (Na$_2$SO$_4$) prior to the removal of the volatiles under reduced pressure. ^{1}H NMR of the crude reaction mixture was used to establish the conversion to the products and *exo:endo* ratios through the integration of aldehyde peaks at: δ_H (400 MHz, CDCl$_3$) 9.80 (*exo*) 9.65 (cinnamaldehyde) 9.53 (*endo*). The products were then purified by flash column

chromatography eluting with (9:1) ethyl acetate/petroleum ether resulting in a mixture of the *exo-* and *endo-* isomers of 3-phenyl-bicyclo[2.2.1]hept-5-ene-2-carboxaldehyde **24** and **25** as a pale yellow oil. ^{1}H NMR, ^{13}C NMR and IR data were consistent with previously reported literature values;[162] υ_{max} (liquid film)/cm^{-1} 1718, 1601, 1497; *exo*-isomer **24** ^{1}H NMR (400 MHz, CDCl$_3$) δ_H 9.85 (1H, d, *J* = 2.0, C$\underline{H}$O) 7.4-7.0 (5H, m, Ar-$\underline{H}$) 6.27 (1H, dd, *J* = 5.6 3.6, C$\underline{H}$=CH) 6.01 (1H, dd, *J* = 5.6 3.6, CH=C$\underline{H}$) 3.66 (1H, dd, *J* = 5.0 3.4, C$\underline{H}$Ph) 3.25-3.05 (2H, m, C$\underline{H}$CH$_2$) 2.55-2.45 (1H, m, C$\underline{H}$CHO) 1.65-1.45 (2H, m, C$\underline{H}_2$); *endo*-isomer **25** ^{1}H NMR (400 MHz, CDCl$_3$) δ_H 9.53 (1H, d, *J* = 2.1, C$\underline{H}$O) 7.4-7.0 (5H, m, Ar-$\underline{H}$) 6.36 (1H, dd, *J* = 5.6 3.6, C$\underline{H}$=CH) 6.10 (1H, dd, *J* = 5.6 3.6, CH=C$\underline{H}$) 3.26 (1H, m, C$\underline{H}$Ph) 3.05 (1H, m, C$\underline{H}$CH$_2$) 3.01 (1H, m, C$\underline{H}$CH$_2$) 2.91 (1H, m, C$\underline{H}$CHO) 1.46-1.49 (2H, m, C$\underline{H}_2$); *m/z* (EI) [M]$^+$ 198 (10%) 132 (89) 131 (100) 103 (52) 77 (21) 66 (54).

General Procedure 1

To a solution of *N,N'* dimethylhydrazine (1eq) in acetonitrile (40 mL) was added ethyl glyoxylate 50% w/w solution in toluene (1eq) and acetic acid (0.2 mL). The solution was stirred at ambient temperature overnight. Water (20 mL) was added and the aqueous layer extracted with ethyl acetate (3x30 mL). The organics were dried over MgSO$_4$, filtered and concentrated under reduced pressure to yield the crude imine as a pale yellow oil. The crude imine was analysed to determine reaction extent and was then dissolved in methanol and stirred at room temperature. To this was added sodium cyanoborohydride (1eq) followed by sufficient 2M HCl solution to maintain a pH 3-4 for a period of twenty minutes until a constant pH reading was obtained. A further equivalent of sodium cyanoborohydride was added and the procedure repeated to a total of three times. Once a constant pH was achieved after the third addition the reaction was allowed to stir at room temperature overnight. On reaction completion by TLC the mixture was quenched by adding sufficient 2M HCl to maintain pH 1 for five minutes. To this was added H$_2$O (20 mL), ethyl acetate (30 mL) and neutralised with 20% w/v Na$_2$CO$_3$ solution. The aqueous layer was extracted with ethyl acetate (3x30 mL). The organics were combined and dried over MgSO$_4$ and the volatiles removed under reduced pressure.

The HCl salt was prepared by adding 5 eq of HCl (in MeOH) to a solution of the free base in methanol with swirling for 10 minutes followed by removal of the volatiles under reduced pressure. The resulting solid was then washed with ether and dried *under reduced pressure*

General Procedure 2

To a stirred solution of *N-iso*-propylidene-*N'*-methyl-hydrazine **100** (1eq) and triethylamine (1eq) in dichloromethane (20 ml) in at 0 °C was added the acid chloride (1eq) in dichloromethane (5 mL) slowly over a period of five minutes, , the solution was then allowed to warm to room temperature and stirred overnight. Once the reaction appeared to be over by TLC H_2O (20 mL) was added and the aqueous solution extracted with dichloromethane (3x20 mL). The combined organics were dried over Na_2SO_4 and the volatiles removed under reduced pressure to yield the crude product. The crude product was analysed to determine reaction extent and was then dissolved in methanol and stirred at room temperature. To this was added sodium cyanoborohydride (1 eq) followed by sufficient 2M HCl solution to maintain a pH 3-4 for a period of twenty minutes until a constant pH reading was obtained. A further equivalent of sodium cyanoborohydride was added and the procedure repeated to a total of three times. Once a constant pH was achieved after the third addition the reaction was allowed to stir at room temperature overnight. On reaction completion by TLC the mixture was quenched by adding sufficient 2M HCl to maintain pH 1 for five minutes. To this was added H_2O (20 mL), ethyl acetate (30 mL) and neutralised with 20% w/v Na_2CO_3 solution. The aqueous layer was extracted with ethyl acetate (3x30 mL). The organics were combined and dried over $MgSO_4$ and the volatiles removed under reduced pressure.

The HCl salt was prepared by adding 5 eq of HCl (in MeOH) to a solution of the free base in methanol with swirling for 10 minutes followed by removal of the volatiles under reduced pressure. The resulting solid was then washed with ether and dried *under reduced pressure* to yield the title compound as a colourless solid.

Preparation of ethyl 2-(2,2-dimethylhydrazinyl)acetate hydrochloride 74.HCl[163]
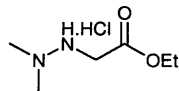
The *title compound* was prepared using general procedure 1. The crude residue was purified using column chromatography eluting with (1:1) petroleum ether/ethyl acetate to give the free base (137 mg, 2%)as a colourless oil. ^{1}H NMR (400MHz, CDCl$_3$) δ_H 6.32 (1H, bs, N<u>H</u>), 4.14 (2H, q, *J* = 7.2, C<u>H</u>$_2$CH$_3$), 3.50 (2H, s, NC<u>H</u>$_2$), 2.40 (6H, s, NC<u>H</u>$_3$), 1.21(3H, t, *J* = 7.5, CH$_2$C<u>H</u>$_3$) ^{13}C NMR (100MHz, CDCl$_3$) δ_C 169.4, 62.0, 51.4, 47.6, 14.0.

The HCl salt was prepared using general procedure 1 (93%). mp 71-73 °C.

Preparation of ethyl 2-(methoxyamino)acetate hydrochloride 75.HCl
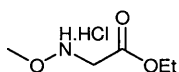
The *title compound* was prepared using general procedure 1. The resulting residue was purified by column chromatography eluting with (2:1) ethyl acetate/petroleum ether to afford the free base as a colourless oil (314 mg, 5%). ^{1}H NMR (400MHz, CDCl$_3$) δ_H 6.14 (1H, bs N<u>H</u>), 4.23 (2H, q, *J* = 7.1, C<u>H</u>$_2$CH$_3$), 3.62(2H, bd, *J* = 5.6, NHC<u>H</u>$_2$), 3.54 (3H, s OCH$_3$), 1.27 (3H, t, *J* = 7.1, CH$_2$C<u>H</u>$_3$).

The HCl salt was prepared using general procedure 1. (90%). mp 80-82 °C.

Preparation of 76.HCl
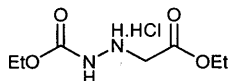
The *title compound* was prepared using general procedure 1. The resulting solid was purified by column chromatography eluting with (3:1) dichloromethane/diethyl ether to yield the free base(1.42 g, 26%) as a colourless solid. mp 88-89 °C; ^{1}H NMR (400MHz, CDCl$_3$) δ_H 6.48 (1H, bs, N<u>H</u>), 4.17-4.07 (5H, m, N<u>H</u>, C<u>H</u>$_2$CH$_3$), 3.59 (H, d, J = 4, NC<u>H</u>$_2$),

1.24-1.18 (6H, m, CH$_2$C$\underline{H}_3$); ^{13}C NMR (100MHz, CDCl$_3$) δ_C 171.3 (C), 156.9 (C), 61.5 (CH$_2$), 61.2 (CH$_2$), 52.8 (CH$_2$), 14.6 (CH$_3$), 14.2 (CH$_3$);

The HCl salt was prepared using general procedure 1. (95%). mp 115-118 °C.

Preparation of 77.HCl
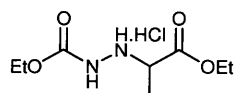
The *title compound* was prepared using general procedure 1. The resulting residue was purified by column chromatography eluting with (4:1) dichloromethane/diethyl ether to yield the free base (6.86g, 78%) as a colourless oil. υ_{max} (neat) /cm^{-1} 3320, 2937, 2908, 2882, 1728, 1530, 1554; ^{1}H NMR (400MHz, CDCl$_3$) δ_H 6.48 (1H, bs, N$\underline{H}$), 4.25-4.14 (5H, m, N$\underline{H}$, C$\underline{H}_2$CH$_3$), 3.76-3.75 (1H, m, NHC$\underline{H}$CH$_3$), 1.36-1.25 (9H, m, CHC$\underline{H}_3$, CH$_2$C$\underline{H}_3$); ^{13}C NMR (125MHz, CDCl$_3$) δ_C 173.4 (C), 157.1 (C), 61.5 (CH2), 61.2 (CH2), 58.4 (CH), 15.9 (CH$_3$), 14.6 (CH$_3$), 14.21 (CH$_3$).

The HCl salt was prepared using general procedure 1. (98%). mp 138 °C.

Preparation of 85.HCl
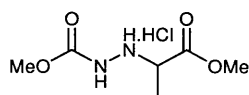
The *title compound* was prepared using general procedure 1. The resulting mixture was then purified by column chromatography eluting with (1:1) petroleum ether/ ethyl acetate to yield the free base (1.31 g, 38%) as a colourless oil. υ_{max} (CHCl$_3$) /cm^{-1} 3384, 2959, 1753, 1538, 1455, 1277, 1152; ^{1}H NMR (400MHz, CDCl$_3$) δ_H 6.78 (1H, bs, N$\underline{H}$), 4.31 (1H, bs, N$\underline{H}$), 3.84-3.71 (7H, m, C$\underline{H}$CH$_3$, OC$\underline{H}_3$), 1.36 (3H, d, J = 7.2, CHC$\underline{H}_3$); ^{13}C NMR (100MHz, CDCl$_3$) δ_C 174.3 (C), 157.6 (C), 58.2 (CH), 52.4 (CH$_3$), 52,0 (CH$_3$), 15.8 (CH$_3$); *m/z* (APCI) (M+H) 177; HRMS (ES) (found 177.0871 [M+H]$^+$; C$_6$H$_{13}$N$_2$O$_4$ requires 177.0870).

The HCl salt was prepared using general procedure 1.(92%). mp 133-134 °C.

2-Methyl-1-(propan-2-ylidene)hydrazine 100
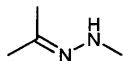
Methyl hydrazine (13.6g, 295 mmol, 15.7 mL) was added drop wise to acetone (23.7 g, 409 mmol, 30 mL) maintaining the reaction temperature below 35 °C. The solution was stirred for 1 hour after which the top layer was removed and allowed to stand over potassium hydroxide (5g) for a further 1 hour. The upper liquid was decanted from the lower aqueous phase and allowed to stand over two successive portions of potassium hydroxide (2x2.5g) for 30 minutes each. Purification was by distillation (1 atm., 110 °C) [lit.[118] b.pt. 116-118 °C] under nitrogen affording the *title compound* as a colourless oil (17.85g, 70%); v_{max} (liquid film)/cm^{-1} 3394, 3262, 2911, 1711, 1631; ^{1}H NMR (400 MHz, CDCl$_3$) δ_H 4.28 (1H, s br, N$\underline{H}$) 2.76 (3H, s, NHC$\underline{H}_3$) 1.88 (3H, s, N=CC$\underline{H}_3$ *trans*) 1.68 (3H, s, N=C-C$\underline{H}_3$ *cis*); ^{13}C NMR (100 MHz, CDCl$_3$) δ_C 146.4 (C) 37.9 (CH$_3$) 25.0 (CH$_3$) 15.5 (CH$_3$); *m/z* (APcI) [M+H]$^+$ 87 (100%); HRMS (EI) (found 86.0841 [M]$^+$; C$_4$H$_{10}$N$_2$ requires 86.0838).

Preparation of 1-isopropyl-2-methyl-4-phenylsemicarbazide 93
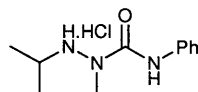
To a stirred solution of *N-iso*-propylidene-*N'*-methyl-hydrazine **100** (1.00 g, 11.6 mmol, 1.16 mL) **36** in dichloromethane (20 mL) at 0 °C was added phenyl isocyanate (1.38 g, 11.6 mmol, 1.26 mL) in dichloromethane (5 mL) slowly over a period of five minutes, the solution was then allowed to warm to room temperature and stirred overnight. Once the reaction appeared to be over by TLC H$_2$O (20 mL) was added and the aqueous solution extracted with dichloromethane (3x20 mL). The combined organics were dried over Na$_2$SO$_4$ and the volatiles removed under reduced pressure to yield the crude product. The crude product was analysed to determine reaction extent and was then dissolved in methanol (20 mL) and stirred at room temperature. To this was added sodium cyanoborohydride (0.72 g 11.6 mmol) followed by sufficient 2M HCl solution to maintain a pH 3-4 for a period of twenty minutes until a constant pH reading was obtained. A further equivalent of sodium

cyanoborohydride was added and the procedure repeated to a total of three times. Once a constant pH was achieved after the third addition the reaction was allowed to stir at room temperature overnight. On reaction completion by TLC the mixture was quenched by adding sufficient 2M HCl to maintain pH 1 for five minutes. To this was added H_2O (20 mL), ethyl acetate (30 mL) and neutralised with 20% w/v Na_2CO_3 solution. The aqueous layer was extracted with ethyl acetate (3x30 mL).The organics combined and dried over $MgSO_4$ and the volatiles removed under reduced pressure. The crude product was purified by column chromatography eluting with (2:1) petroleum ether/ethyl acetate resulting in the free base (1.97 g, 82%) as a colourless solid. mp 80-81 °C; v_{max} ($CDCl_3$)/cm^{-1} 3366, 2975, 2359, 1792, 1666, 1533; ^{1}H NMR (400 MHz, $CDCl_3$) δ_H 8.59 (1H, bs, N$\underline{H}$), 7.45 (2H, d, J = 8.6, Ar-$\underline{H}$), 7.29 (2H, m, Ar-H), 6.94 (1H, t, J = 7.4, Ar-H) 3.36-3.27 (2H, m, N$\underline{H}$, C$\underline{H}$), 3.16 (3H, s, NC$\underline{H}_3$), 1.11 (6H, d, J = 6.2, C$\underline{H}_3$); ^{13}C NMR (100 MHz, $CDCl_3$) δ_C 156.8(C), 139.2 (C), 128.9 (CH), 122.3 (C), 118.6 (CH), 47.1 (CH), 32.2 (CH_3), 20.5 (CH_3); m/z (ES) [M+H]$^+$; 208 (100%) HRMS (ES) (found 208.1446 [M+H]$^+$; $C_{11}H_{17}N_3O$ requires 208.1444).

The HCl salt was prepared by adding 5 eq of 3.8M HCl (in MeOH) to a solution of the free base in methanol with swirling for 10 minutes followed by removal of the volatiles under reduced pressure. The resulting solid was then washed with ether and dried *under reduced pressure* to yield the title compound as a colourless solid (96%). mp 149-150 °C.

Preparation of 4-(dimethylamino)-*N'*-isopropyl-*N*-methylbenzohydrazide 95
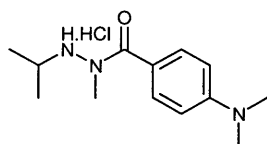
The title compound was prepared using general procedure 2. The crude product was purified by column chromatography eluting with (2:1) petroleum ether/ethyl acetate resulting in the free base (1.29 g, 63%) as an off white solid. mp 69-70 °C; v_{max} ($CDCl_3$)/cm^{-1} 3685, 3262, 3153, 2969, 2901, 2812, 2358, 1792, 1608, 1526, 1469, 1428; ^{1}H NMR (400 MHz, $CDCl_3$) δ_H 7.45 (2H, d, J = 8.7, Ar-$\underline{H}$), 6.60 (2H, d, J = 8.9, Ar-$\underline{H}$), 3.18 (4H, m, C$\underline{H}$, NC$\underline{H}_3$), 2.94 (6H, S, NC$\underline{H}_3$), 0.86 (6H, d, J = 6.2, C$\underline{H}_3$); ^{13}C NMR (62.5 MHz, $CDCl_3$) δ_C 171.9 (C),

151.7 (C), 130.0 (CH), 122.0 (C), 110.9 (CH), 49.6 (CH$_3$), 40.2 (CH$_3$), 39.8 (CH), 20.9 (CH$_3$); *m/z* (ES) [M+H]$^+$; 236 (100%) HRMS (ES) (found 236.1757 [M+H]$^+$; C$_{13}$H$_{21}$N$_3$O requires 236.1759).

The HCl salt was prepared using general procedure 2 (89%). mp 88 °C.

Preparation of *N'*-isopropyl-*N*-methyl-4-nitrobenzohydrazide 99
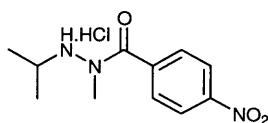
The title compound was prepared using general procedure 2. The crude product was purified by column chromatography eluting with (1:1) petroleum ether/ethyl acetate resulting in the free base (1.18 g, 33%) as an off white solid. mp 58 °C; ν_{max} (CDCl$_3$)/cm^{-1} 3434, 2968, 2106, 1636, 1520; ^{1}H NMR (400 MHz, DMSO) δ_H 8.19 (2H, d, *J* = 8.8, Ar-H̲), 7.67 (2H,d, *J* = 8.4, Ar-H̲), 5.04 (1H, s, NH̲), 3.14-3.11 (4H, m, CH̲, NCH̲$_3$), 0.66 (6H, d, *J* = 6.0, CH̲$_3$); ^{13}C NMR δ_C (62.5 MHz, DMSO) 170.2 (C), 147.6 (C), 144.4(C), 130.1 (CH), 123.0 (CH), 46.7 (CH$_3$), 33.0 (CH), 20.5 (CH$_3$); *m/z* (ES) [M+H]$^+$; 238 (100%) HRMS (ES) (found 238.1032 [M+H]$^+$; C$_{10}$H$_{15}$N$_3$O$_3$ requires 238.1030).

The HCl salt was prepared using general procedure 2. (93%). mp 144 °C.

Preparation of *N'*-isopropyl-4-methoxy-*N*-methylbenzohydrazide 77
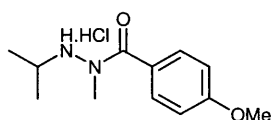
The title compound was prepared using general procedure 2 The crude product was purified by column chromatography eluting with (1:1) petroleum ether/ethyl acetate resulting in the free base (1.32 g, 51%) as a colourless solid. mp 42–44 °C; ν_{max} (CDCl$_3$)/cm^{-1} 3436, 3269, 3153, 2968, 2933, 2838, 1610, 1512, 1465; ^{1}H NMR (250 MHz, 35 °C, CDCl$_3$) δ_H 7.51

(2H, d, *J* = 8.5, Ar-H), 6.90 (2H, d, *J* = 8.8, Ar-H), 3.81 (3H, s, OCH₃), 3.27 - 3.15(4H, m,

CH, NCH₃), 1.06 (6H, d, J = 6.0, CH₃); ^{13}C NMR (100 MHz, CDCl₃) δ$_C$ 171.1 (C), 161.1

(C), 129.7 (CH), 127.6 (CH), 113.4 (C), 55.3 (CH₃), 49.6 (CH₃), 41.7 (CH), 20.8 (CH₃); *m/z*

(ES) [M+H]$^+$; 223 (100%) HRMS (ES) (found 223.1441 [M+H]$^+$; $C_{12}H_{18}N_2O_2$ requires

223.1441).

The HCl salt was prepared using general procedure 2 (91%). mp 130-133 °C.

Preparation of 4-chloro-*N'*-isopropyl-*N*-methylbenzohydrazide 97
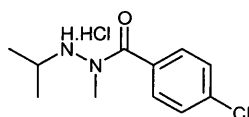
The title compound was prepared using general procedure 2 The crude product was purified

by column chromatography eluting with (5:1) ethyl acetate/petroleum ether resulting in the

title compound (1.13 g, 43%) as a colourless oil. Analysis of this compound clearly

indicated that it posses many rotational states in solution. v$_{max}$ (CDCl₃)/cm^{-1} 3420, 2105,

1639; ^{1}H NMR (500 MHz, DMSO) δ$_H$ 7.65-7.50 (2H, m, Ar-H), 7.41 (2H, bs, Ar-H), 4.98

(1H, bs, NH), 3.26-3.11 (4H, m, CH, NCH₃), 0.77 (6H, bs, CH₃); ^{13}C NMR (125 MHz,

DMSO) δ$_C$ 164.2 (C), 133.7 (C), 130.5 (CH), 129.1 (CH), 129.0 (CH), 127.3 (CH), 20.2

(CH₃), other carbons were not observed; *m/z* (ES) [M+H]$^+$; 227 (100%) HRMS (ES) (found

227.0946 [M+H]$^+$; $C_{11}H_{17}N_3O$ requires 227.0946).

The HCl salt was prepared in situ within the reaction flask of the catalytic run by adding 1

eq of HCl in methanol. The volume of methanol as a solvent was then adjusted to maintain

the correct reaction concentration.

Preparation of 2,3,4,5,6-pentafluoro-*N'*-isopropyl-*N*-methylbenzohydrazide 96
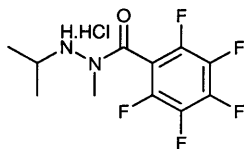
To a stirred solution of *N-iso*-propylidene-*N'*-methyl-hydrazine **100** (1 g, 11.6 mmol, 1.16 mL) and triethylamine (1.17g, 11.6 mmol, 1.61 mL) in dichloromethane (20 mL) at 0 °C was added 4 dimethylamino benzoyl chloride (2.67g, 11.6 mmol) in dichloromethane (5 mL) slowly over a period of five minutes, the solution was then allowed to warm to room temperature and stirred overnight. Once the reaction appeared to be over by TLC H$_2$O (20 mL) was added and the aqueous solution extracted with dichloromethane (3x20 mL). The combined organics were dried over Na$_2$SO$_4$ and the volatiles removed under reduced pressure to yield the crude product. The crude product was analysed to determine the extent of reaction and was then dissolved in a mixture of ethanol (12 mL) and acetic acid (6 mL). To this solution was added Platinium(IV) oxide (131 mg, 0.58 mmol, 5 mol%) and stirred at room temperature. The flask was then evacuated and back filled with an H$_2$ for a total of five times and allowed to stir at room temperature under an atmosphere of H$_2$ for 18hrs. The reaction mixture was then filtered through celite® and H$_2$O (10 mL) was added to the filtrate. The aqueous layer was then extracted with CHCl$_3$ (3x20 mL), the organics combined, dried over Na$_2$SO$_4$ and the volatiles removed under reduced pressure. The crude product was purified by column chromatography eluting with (4:1) petroleum ether/ethyl acetate resulting in the free base (2.59 g, 79%) as a pale pink solid. mp 77-77 °C; v$_{max}$ (CDCl$_3$)/cm^{-1} 3423, 2973, 2933, 1654, 1500; ^{1}H NMR (400 MHz, DMSO) δ$_H$ 5.49 (1H, bs, N<u>H</u>), 3.21-3.14 (4H, m, C<u>H</u>, NC<u>H$_3$</u>), 0.73 (6H, d, *J* = 6.0, C<u>H$_3$</u>); ^{13}C NMR (62.5 MHz, DMSO) δ$_C$ 160.2 (C), 45.6 (CH$_3$), 31.8 (CH), 19.6 (CH$_3$) *other carbons were not observed*; *m/z* (ES) [M+H]$^+$; 283; HRMS (ES) (found [M+H]$^+$; 283.0862 C$_{11}$H$_{11}$F$_5$N$_2$O requires 283.0864).

The HCl salt was prepared by adding 5 eq of HCl (in MeOH) to a solution of the free base in methanol with swirling for 10 minutes followed by removal of the volatiles under reduced pressure. The resulting solid was then washed with ether and dried *under reduced pressure* to yield the *title compound* as a colourless solid (93%). mp 111 °C.

N-Methyl-*N'-iso*-propyl benzoic hydrazide hydrochloride 90
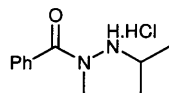
The *title compound* **90** was prepared using general procedure 2 affording the product (150 mg, 11%) as a colourless solid; mp 145-146 °C; v_{max} (nujol)/cm^{-1} 3408, 2923, 1638, 1460, 1377, 1333, 1122, 1077; ^{1}H NMR (400 MHz, CDCl$_3$) δ_H 7.51 (2H, d, *J* = 8.0, Ar-H), 7.49 (1H, t, *J* = 7.1, Ar-H), 7.42 (2H, m, Ar-H), 3.94 (1H, sept., *J* = 6.6 NCH(CH$_3$)$_2$), 3.61 (3H, s, NCH$_3$), 1.51 (6H, d, *J* = 6.6, NCH(CH$_2$)$_3$); ^{13}C NMR (100 MHz, CDCl$_3$) δ_C 170.8 (C), 132.3 (C), 130.7 (CH), 128.9 (CH), 128.2 (CH), 53.7 (CH$_3$), 38.6 (CH), 18.0 (CH$_3$); *m/z* (ES) [M+H-HCl]$^+$ 193 (100%); HRMS (ES) (found 193.1336 [M+H-HCl]$^+$; C$_{11}$H$_{17}$N$_2$O requires 193.1335).

N'-(Propan-2-ylidene)benzoic hydrazide 103
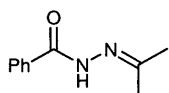
Benzoic hydrazide **102** (5.00 g, 36.7 mmol) was stirred in an excess of acetone (22 mL, 0.3 mmol), containing acetic acid (40 μL, 0.7 mmol), for 48 hours at ambient temperature. Water (30 mL) was added and the reaction mixture was extracted with dichloromethane (3x30 mL). The combined organic extracts were dried (Na$_2$SO$_4$) and reduced *in vacuo* to afford the *title compound* (5.57g, 86%) as a colourless solid; mp (petrol/ether) 141–143 °C [lit.[121] mp 142-143 °C]; v_{max} (nujol)/cm^{-1} 3221, 1655, 1578, 1578, 1531, 1490; ^{1}H NMR (400 MHz, CDCl$_3$) δ_H 8.70 (1H, s, NH), 7.79 (2H, d, *J* = 7.1, Ar-H), 7.52 (1H, t, *J* = 7.1, Ar-H), 7.44 (2H, t, *J* = 7.1, Ar-H), 2.15 (3H, s, CH$_3$), 1.97 (3H, s, CH$_3$); ^{13}C NMR (100 MHz, CDCl$_3$) δ_C 164.6 (C), 156.9 (C), 134.1 (C), 132.1 (CH), 129.0 (CH), 127.6 (CH), 26.0 (CH$_3$), 17.3 (CH$_3$); *m/z* (EI) [M]$^+$ 176 (8%), 161 (50), 105 (100); HRMS (EI) (found 176.0950 [M]$^+$; C$_{10}$H$_{12}$N$_2$O requires 176.0950).

N'-iso-Propylbenzoic hydrazide 91
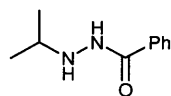
Platinum(IV) oxide (68 mg, 0.3 mmol) was placed in a nitrogen flushed flask with ethanol (12 mL) and acetic acid (6 mL). *N'*-(Propan-2-ylidene) benzoic hydrazide **103** (2.50 g, 14.2 mmol) was added, the flask was charged with hydrogen and stirred for 48 hours at ambient temperature. The reaction mixture was filtered over Celite and the filtrate was neutralised with saturated sodium bicarbonate solution (180 mL). The volatiles were removed under reduced pressure and the aqueous phase was extracted with diethyl ether (5x50 mL). The combined organic extracts were washed with brine (30 mL), dried (MgSO$_4$) and the volatiles were removed under reduced pressure to give the *title compound* (2.18 g, 86%) as a colourless powder; mp 110–112 °C; v$_{max}$ (nujol)/cm^{-1} 3289, 1640, 1537, 725, 693; ^{1}H NMR (400 MHz, CDCl$_3$) δ_H 7.70 (1H, s, N$\underline{H}$), 7.69 (2H, d, *J* = 7.7, Ar-$\underline{H}$), 7.46 (1H, t, *J* = 7.7, Ar-$\underline{H}$), 7.38 (2H, t, *J* = 7.7, Ar-$\underline{H}$), 4.81 (1H, s, N$\underline{H}$), 3.18 (1H, sept., *J* = 6.2, NC$\underline{H}$(CH$_3$)$_2$), 1.05 (6H, d, *J* = 6.2, NCH(C$\underline{H}_3$)$_2$); ^{13}C NMR (100 MHz, CDCl$_3$) δ_C 167.5 (C), 132.9 (C), 131.9 (CH), 128.7 (CH), 126.9 (CH), 51.4 (CH), 20.9 (CH$_3$); *m/z* (EI) [M]$^+$ 178 (3%), 163 (9), 122 (13), 105 (100); HRMS (EI) (found 178.1105 [M]$^+$; C$_{10}$H$_{14}$N$_2$O requires 178.1106).

Preparation of 3-naphthalen-2-yl-propenal
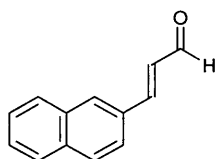
Compound **117** was prepared in accordance of the procedure of Cacchi.[164] To a stirred solution of 2 bromonapthalene (1.04 g, 5 mmol) in dry DMF (20 mL) was added acrolein diethylacetal(1.95 g, 15 mmol, 2.28 mL), ^{n}Bu$_4$NOAc (3.02 g, 10 mmol) , K$_2$CO$_3$(1.04 g, 10 mmol), KCl (0.37g, 5 mmol), and Pd(OAc)$_2$ (0.03 g, 15 mmol). The mixture was stirred for 16 h at 90 °C. The solution was allowed to cool and 2M HCl (5 mL)was added slowly and the reaction stirred at room temperature for 10 min to allow hydrolysis of the acetal. The reaction was then diluted with ether and washed with water. The organic layer was then dried over Na$_2$SO$_4$ and concentrated *in vacuo*. The crude product was purified by column

chromatography (9:1) petroleum ether/ethyl acetate to yield the title compound (0.62 g, 68%) as off white platy crystals; mp 125 °C,; ^{1}H NMR (400MHz, CDCl$_3$) δ_H 9.77 (1H, d, J =7.7), 7.97-7.55 (8H, m), 6.83 (1H, dd, J = 15.9, 7.7); ^{13}C (125 MHz, CDCl$_3$) δ_C 193.8, 152.8, 134.7, 133.3, 131.6, 130.8, 129.0, 128.9, 128.7, 127.9, 127.1, 123.6; m/z (APCI) 183 (M+H); HRMS (ES) (found 183.0804[M+H]$^+$;C$_{13}$H$_{10}$O requires 183.0804).

Preparation of (*E*)-3-(3-(trifluoromethyl)phenyl)acrylaldehyde 118
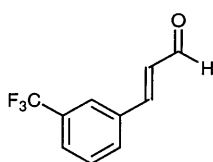
Compound **118** was prepared in accordance of the procedure of Cacchi.[164] To a stirred solution of 3-bromo benzotrifluoride (1.13 g, 5 mmol, 0.70mL) in dry DMF (20 mL) was added acrolein diethylacetal (1.95 g, 15 mmol, 2.28ml), ^{n}Bu$_4$NOAc (3.02 g, 10mmol) , K$_2$CO$_3$(1.04 g, 10 mmol), KCl (0.37g, 5 mmol), and Pd(OAc)$_2$ (0.03 g.15 mmol). The mixture was stirred for 3 h at 90 °C. The solution was allowed to cool and 2M HCl (5 mL) was added slowly and the reaction stirred at room temperature for 10 min to allow hydrolysis of the acetal. The reaction was then diluted with ether and washed with water. The organic layer was then dried over Na$_2$SO$_4$ and concentrated *in vacuo*. The crude product was purified by column chromatography (9:1) petroleum ether/ethyl acetate to yield the title compound (0.70 g, 70%) as a colourless oil. The data obtained is consistent with the reported values. υ_{max} (neat) /cm^{-1} 2683, 1334, 1168, 1125; ^{1}H NMR (400MHz, CDCl$_3$) δ_H 9.76 (1H, d, J = 7.5, CHO), 7.82-7.57 (4H, m, Ar-H), 7.53 (1H, d, J = 16.0, C=CHAr), 6.78 (1H, dd, J = 16.0, 7.5, CHOCH=C) ^{13}C NMR (100MHz, CDCl$_3$) δ_C 193.1, 150.4, 134.8, 131.7(q, J=32.8), 131.2, 130.0, 129.7, 127.5 (q, J=3.7), 125.2(q, J = 3.8), 123.7((q, J = 272.4).

Preparation of 122
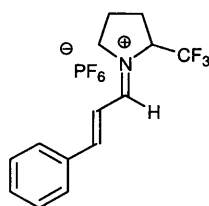
To a stirred solution of cinnamaldehyde(118 mg, 1.42 mmol, 122 μl) in methanol (2 mL) was added trifluoromethylpyrrolidine (198 mg, 1.42 mmol) and allowed to stir for 2 min. Then hexafluorophosphoric 60% w/w solution in H_2O (345 mg, 1.42 mmol, 210 μl) was added forming a yellow precipitate on reaction. The excess solvent was removed *under reduced pressure* and the crude mixture was recrystallised from the minimum amount of hot methanol. To yield *the title compound* (82%) as an of colourless solid. mp 125 °C; ^{1}H NMR (400MHz, CD_3CN) δ_H 8.64 (1H, d, J =10.6, N^+=C$\underline{H}$), 8.12 (1H, d, J = 15.2, CH=C$\underline{H}$Ar), 7.89 (2H, m, Ar-$\underline{H}$), 7.68(m, 1H, Ar-$\underline{H}$), 7.58 (m, 2H, Ar-$\underline{H}$), 7.32 (1H, dd, J = 10.6, 15.2, C$\underline{H}$=CHAr), 4.96 (1H, m, C$\underline{H}$CF$_3$), 4.41 (2H, m, N^+C$\underline{H}_2$), 2.41 (2H, m, CH_2CH_2), 2.26(2H, m, CH_2CH_2); ^{13}C (125 MHz, CD_3CN) δ_C 170.8, 165.3, 134.9, 131.2, 129.7, 125.1, 118.4, 66.8 (q, J = 31.3),53.3, 24.9, 22.6, 21.7; m/z (APCI) 254 (M-PF$_6$); HRMS (ES) (found 254.1152[M-PF$_6$]$^+$;$C_{14}H_{15}NF_3$ requires 254.1151).

Preparation of 3-(4-nitrophenyl)bicyclo[2.2.1]hept-5-ene-2-carbaldehyde
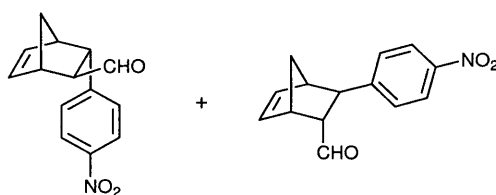
trans-4- Nitrocinnamaldehyde (390 mg, 1.9 mmol, 1.0 eq) was added to a solution of catalyst (10 mol%, 0.19 mmol) in methanol (2.0 mL) at 25 °C and the resulting mixture was stirred for 2 minutes to initiate iminium ion formation. Freshly cracked cyclopentadiene **19** (323 mg, 4.9 mmol, 0.38 mL, 2.5 eq) was added in a single aliquot and stirring was continued for 6 hours. The volatiles were removed under reduced pressure and the resulting organics were hydrolysed in a chloroform (2 mL), water (1 mL) trifluoroacetic acid (1 mL)

mixture over night. Saturated sodium hydrogen carbonate solution (18 mL) was added to neutralise the solution and the aqueous phase was extracted with dichloromethane (2x20 mL). The combined organics were washed with water (10 mL) and dried (Na_2SO_4) prior to the removal of the volatiles under reduced pressure. The data measured was consistent with the literature.[165] υ_{max} (liquid film)/cm^{-1} 1720, 1591, 1511, 1344.

exo-isomer ^1H NMR (400 MHz, $CDCl_3$) δ_H 9.87 (1H, d, J = 1.5) 8.06-8.01(2H, m,) 7.25 (1H, dd, J = 5.6 3.6) 6.36 (1H, dd, J = 5.7 3.3) 6.00 (1H, dd, J = 5.7, 2.7) 3.84 (1H, dd, J = 4.5, 4.5) 3.26-3.13 (2H, m), 2.59 (1H, dd, J = 5.1, 0.6) 1.74-1.63 (2H, m, C$\underline{H}_2$); ^{13}C (100 MHz, $CDCl_3$) δ_C 202.0(CH), 151.0(C), 146.8(C), 137.4(CH), 136.3(CH), 129.1(CH), 123.7(CH), 59.9(CH), 48.8(CH), 48.0(CH_2), 45.9(CH), 45.5(CH).

endo-isomer ^1H NMR (400 MHz, $CDCl_3$) δ_H 9.60 (1H, d, J = 1.5) 8.11-8.08(2H, m) 7.38 (1H, dd, J = 8.4, 0.6) 6.39 (1H, dd, J = 5.7 3.3) 6.15 (1H, dd, J = 5.7, 3.0) 3.84 (1H, br) 3.26-3.13 (2H, m), 2.59 (1H, dd, J = 5.1, 0.6) 2.94-2.90 (1H, m), 1.74-1.63 (2H, m); ^{13}C (100 MHz, $CDCl_3$) δ_C 202.6(CH), 152.0(C), 146.7(C), 139.4(CH), 134.3(CH), 128.6(CH), 124.1(CH), 61.5(CH), 48.3(CH), 47.5(CH_2), 45.9(CH), 45.4(CH).

Preparation of *L*-boc-phenylalaninemethylamide 154
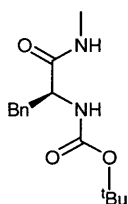
Di-tert-butyldicarbonate (2.44 g, 11.2mmol) was added to dry dichloromethane (70 mL) at 0 °C and stirred. To this was added *L*-phenylalaninmethylamide **138** (2 g, 11.2 mmol) in dichloromethane (10 mL) slowly over a period of 5 mins. The reaction was allowed to reach room temperature and stirred overnight. The volatiles were removed under reduced pressure to yield a crude colourless solid which was purified by column chromatography eluting with (1:1) ethyl aceatate/petroleum ether to tiled the title compound (2.16 g, 82%) as a colourless solid. Measured data is consistent with the literature.[166] Mp139-141 °C; ^1H NMR

(400MHz, CDCl₃) δ_H 7.30-7.14 (5H, m, Ar-H̲), 6.13 (1H, bs, NH̲), 5.22 (1H, bs, NH̲) 4.34 (1H, dd, J = 7.6, 7.2, CH̲CH₂) 3.03 (2H, m, CHCH̲₂) 2.71 (3H, d, J = 4.9, NCH̲₃), 1.38 (9H, s C(CH̲₃)₃); ¹³C NMR (100MHz, CDCl₃) δ_C 171.9(C), 155.2(C), 136.9(C), 128.2(CH), 128.5(CH), 126.8(CH), 80.0(C), 56.0(CH), 38.9(CH₂), 28.2(CH₃), 26.0(CH₃).

Preparation of benzyl (S)-1-(methylcarbamoyl)-2-phenylethylcarbamate 155
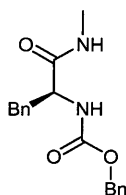
Benzyl chloroformate (3.84 g, 22.5 mmol, 3.21 mL) and triethylamine (2.28 g, 22.5 mmol, 3.14 mL) were added to dichloromethane (40 mL) and stirred at 0 °C. To this was added *L*-phenylalaninmethylamide **138** (4 g, 22.3 mmol) in dichloromethane (10 mL), allowed to warm to room temperature and stirred overnight resulting in significant quantities of a colourless precipitate. The precipitate was filtered and washed with H₂O and dichloromethane and subsequently purified by column chromatography eluting with (3:1) ethyl acetate/petroleum ether to yield the title compound (5.01 g, 72%) as a colourless solid. mp 163-164 °C; υ_max (KBr) /cm⁻¹ 3306, 2353, 1668.2, 1652, 1531, 1285, 1285, 1239, 1146; ¹H NMR (400MHz, CDCl₃) δ_H 7.30-7.18 (10H, m, Ar-H̲), 6.56 (1H, bs, NH̲), 5.82 (1H, bs, NH̲), 4.98 (2H, dd, J = 12.6, 28.4, OCH̲₂Ar), 4.24-4.18 (1H, m, CH̲CH₂), 3.09 (1H, dd, J = 5.0, 13.9, CHCH̲₂), 2.78 (1H, dd, J = 9.4, 13.9, CHCH̲₂), 2.62 (3H, d, J = 4.7, NHCH̲₃).

Preparation of (S)-2-(benzylamino)-N-methyl-3-phenylpropanamide 156
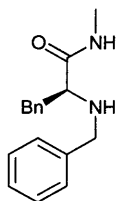
Benzyl bromide (5.73 g, 33.5 mmol, 3.98 mL), triethylamine (3.39 g, 33.5 mmol, 4.67 mL) and L-phenylalaninmethylamide **138** (6 g, 33.5 mmol) were added to toluene (70 mL) and refluxed with rigorous stirring overnight. The solution was allowed to cool and H_2O (30 mL) added. The resulting solution was extracted with ethyl acetate (3x50 mL), the organics combined and concentrated under reduced pressure to yield the crude colourless solid which was purified by column chromatography eluting with (1:1) ethyl acetate/petroleum ether to give the title compound (7.40 g, 82%) as a colourless solid.   mp 53-54 °C; υ_{max} (CHCl$_3$) /cm^{-1} 3377, 3017, 2942, 2854, 1950, 1666, 1531, 1496, 1454, 1412, 1332, 1117; ^{1}H NMR (400MHz, CDCl$_3$) δ_H 7.32-7.06 (10H, m, Ar-H), 3.72 (1H, d, J = 13.4, OCH$_2$Ar), 3.56 (1H, d, J = 13.4, OCH$_2$Ar), 3.42 (1H, dd. J = 4.2, 9.5, CHCH$_2$Ar), 3.26 (1H, dd, J = 4.2, 13.9, CHCH$_2$Ar), 2.83 (3H, d, J = 5.0, NCH$_3$), 2.77 (1H, dd, J = 9.5, 13.9, CHCH$_2$Ar), 1.75 (1H, bs, NH); m/z (APCI) (M+H) 269; HRMS (ES) (found 269.1650 [M+H]$^+$; C$_{17}$H$_{20}$N$_2$O requires 269.1648).

Preparation of (14E)-2-(2,4-dinitrophenyl)-1-((3-phenylbicyclo[2.2.1]hept-5-en-2-yl)methylene)hydrazine 160
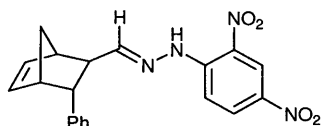
Compound **160** was prepared in accordance to the method developed by Cavill. 3-Phenylbicyclo[2.2.1]hept-5-ene-2-carboxaldehyde (**24** and **25**) was reacted with 2,4-dinitrophenylhydrazine to provide compound. Purification by flash chromatography on silica, eluting with ethyl acetate/petroleum ether (10:90), afforded the *title compound* as a yellow powder; Chiral HPLC analysis using a Chiralcel OD-R column, wavelength 215 nm,

eluting with acetonitrile/water (80:20), flow rate of 0.5 mL/min, separated the chiral sample, retention times of 30.7 and 36.5 minutes (*endo*-diastereoisomers), 41.8 and 51.4 minutes (*exo*-diastereoisomers)

Exo-**Diastereoisomer**; λ_{max} 215 nm (EtOH); mp 160-162°C; Found 379.1402 (MH$^+$ $C_{20}H_{18}N_4O_4$ requires 379.1401); ν_{max} (Nujol)/cm^{-1} 3289 , 1618 , 1586, 1518, 1502, 1334, 833, 743, 701; δ_H (400 MHz, CDCl$_3$) 9.05 (1H, d, J = 2.5, H-3'), 8.22 (1H, dd, J = 9.7, 2.5, H-5'), 7.85 (1H, d, J = 9.7, H-6'), 7.66 (1H, d, J = 6.1, N=CH), 7.21 (5H, m, Ar-H), 6.33 (1H, dd, J = 5.6, 3.1, C=CH), 6.03 (1H, dd, J = 5.6, 2.8, C=CH), 3.52 (1H, dd, J = 4.8, 3.7, H-3"), 3.21 (1H, br, C=CHCH), 2.99 (1H, br, C=CHCH), 2.63 (1H, ddd, J = 6.1, 4.8, 1.4, H-2"), 1.71 (1H, br, CH$_2$), 1.60 (1H, ddd, J = 9.4, 9.4, 1.6, CH$_2$); δ_C (100 MHz, CDCl$_3$) 154.9 (CH), 145.0 (C), 142.7 (C), 137.8 (C), 136.7 (CH), 135.9 (CH), 128.8 (C), 128.7 (CH), 128.2 (CH), 127.8 (CH), 126.4 (CH), 123.5 (CH), 116.6 (CH), 49.9 (CH), 48.9 (CH), 48.7 (CH), 48.1 (CH), 47.5 (CH$_2$); *m/z* (APcI) 378.9 (MH$^+$, 51%), 338.4 (40), 144.9 (35), 106.9 (100);

Endo-**Diastereoisomer**; λ_{max} 215 nm (EtOH); mp 160-162°C; Found 379.1402 (MH$^+$ $C_{20}H_{18}N_4O_4$ requires 379.1401); ν_{max} (nujol/cm^{-1}) 3289, 1618, 1586, 1518, 1502, 1334, 833, 743, 701; δ_H (400 MHz, CDCl$_3$) 11.04 (1H, s, NH), 9.05 (1H, d, J = 2.3 , H-3'), 8.22 (1H, dd, J = 9.6, 2.3, H-5'), 7.83 (1H, d, J = 9.6, H-6'), 7.18 (6H, m, N=CH, Ar-H), 6.44 (1H, dd, J = 5.5, 3.1, C=CH), 6.14 (1H, dd, J = 5.5, 2.6, C=CH), 3.09 (1H, br, C=CHCH), 3.07 (2H, br, C=CHCH, H-3"), 2.78 (1H, br, H-2"), 1.81 (1H, br, CH$_2$), 1.61 (1H, br, CH$_2$); δ_C (100 MHz, CDCl$_3$) 155.5 (CH), 145.0 (C), 143.6 (C), 139.6 (CH), 134.1 (CH), 130.0 (CH), 128.7 (CH), 127.3 (CH), 126.3 (CH), 123.5 (CH), 116.6 (CH), 51.1 (CH), 49.0 (CH), 48.4 (CH), 47.4 (CH), 47.3 (CH$_2$); other quaternary carbons not observed; *m/z* (APcI) 378.9 (MH$^+$, 51%), 338.4 (40), 144.9 (35), 106.9 (100).

Preparation of *L*-phenylalaninmethylamide 138
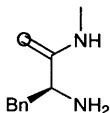
Compound **138** was prepared according to the procedure of MacMillan.[167] To a solution of *L*-phenylalanine methyl ester hydrochloride (2 g, 9.27 mmol) in ethanol (2 mL) was added methylamine 33% in ethanol solution (5 mL, 23.2 mmol) and the reaction stirred overnight at ambient temperature. The reaction mixture was then concentrated under reduced pressure to yield the crude reaction mixture. The mixture was purified by recrystallisation by displacement of the solid methylamine hydrochloride form solution with diethyl ether. The solid impurity was filtered and the filtrate concentrated under reduced pressure. The purification procedure was conducted as many times as necessary to yield the title compound(1.46 g, 81%) as a colourless solid. mp 62 °C. ^{1}H NMR (400MHz, CDCl$_3$) δ_H 7.39-7.16 (5H, m Ar-H), 3.72(1H, m, C$\underline{H}$) 3.27(1H, dd, J = 4.32,13.70,C$\underline{H}_2$) 2.80(3H, d, J 4.94, NC$\underline{H}_3$) 2.76(1H, dd, J = 9.16,13.70, C$\underline{H}_2$) 2.54 (2H, bs, N$\underline{H}_2$); ^{13}C NMR (125 MHz); δ_C 174.8 (C), 138.0(C), 129.3(CH), 128.7(CH), 126.8(CH), 56.5(CH), 41.0(CH$_2$), 25.8(CH$_3$); *m/z* (APCI) 179 (M+H); HRMS (ES) (found 179.1180[M+H]$^+$; C$_{10}$H$_{14}$N$_2$O requires 179.1179).

Preparation of (*S*)-2-(4-nitrobenzylideneamino)-*N*-methyl-3-phenylpropanamide 152
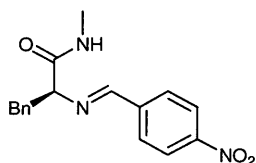
To a solution of *L*-phenylalaninemethylamide **183** (0.50 g, 2.8 mmol) and *p*-TSA (48 mg, 0.28 mmol) in MeOH (5 mL) was added 4-nitrobenzaldehyde **151** (0.42 g, 2.8mmol) and the reaction refluxed overnight. The reaction was allowed to cool and the volatiles removed under reduced pressure to yield the crude product. Purification was achieved using column chromatography eluting with ethyl acetate/petroleum ether (1:1) to afford the *title compound* as a viscous yellow oil. υ_{max} (CH$_2$Cl$_2$) /cm^{-1} 3414, 3054, 2363, 1676, 1348, 1265; ^{1}H NMR (400MHz, CDCl$_3$) δ_H 8.25 (2H, d, J = 8.8, Ar-$\underline{H}$), 7.75 (2H, d, J = 8.8, Ar-$\underline{H}$), 7.57 (1H, s,

N=CHAr), 7.26-7.17 (3H, m, Ar-H), 7.06 (2H, d, J = 8.0, Ar-H), 6.83 (1H, bs, NH), 4.02

(1H, dd, J = 3.0, 10.1, CHCH$_2$), 3.47 (1H, dd, J = 3.1, 13.3, CHCH$_2$), 2.95-2.90 (4H, m,

CHCH$_2$, NCH$_3$); m/z (EI) (M+) 311; HRMS (EI) (found 310.1186 [M-H]$^+$; C$_{17}$H$_1$N$_3$O$_3$

Preparation of (2R,5S)-5-benzyl-3-methyl-2-(4-nitrophenyl)imidazolidin-4-one hydrochloride 146
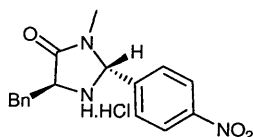
L-phenylalaninamethylamide **138** (400 mg, 2.23 mmol), p-nitrobenzaldehyde **151** (340 mg, 2.23 mmol) and p-TSA (42 mg, 0.22 mmol, 0.1eq) were dissolved in anhydrous DMF (2 mL) and heated to 120 °C for 30 minutes using microwave irradiation (max 100 watts). The reaction mixture was allowed to cool. H$_2$O (10 mL) and ethyl acetate (10 mL) were added and the aqueous layer extracted with ethyl acetate (3x10 mL). The organics were then combined, dried over MgSO$_4$, filtered and concentrated under reduced pressure. The resulting residue was purified using column chromatography eluting with (1:1) petroleum ether/ethyl acetate to yield the free base (94 mg, 25%) as a light yellow solid. ^{1}H NMR (500MHz, CDCl$_3$) δ_H 8.16 (2H, d, J = 8.8, Ar-H), 7.36 (2H, d, J = 8.8, Ar-H), 7.26-718 (5H, m, Ar-H), 4.88 (1H, s, CH(NR)$_2$Ar), 4.00-3.97 (1H, m, CHCH$_2$), 3.07 (1H, dd, J = 4.2, 13.8, CH$_2$CH), 2.96-2.92 (1H, m, CH$_2$CH), 2.52 (3H, s, NCH$_3$); ^{13}C NMR (125 MHz, CDCl$_3$); δ_C 174.0 (C), 148.5(C), 146.5(C), 137.0(C), 129.6(CH), 128.6(CH), 127.8(CH), 127.0(C), 124.3(CH), 76.5(CH), 59.7(CH), 38.5(CH$_2$), 27.3(CH$_3$) m/z (ES) 312 (M+H).

The HCl salt was prepared by treating the catalyst to 5 equivalents of 3.8M HCl in ether. The volatiles were removed under reduced pressure. The resulting solid was washed with ether and dried to yield the salt as a yellow solid (95%) mp 181-183 °C

Synthesis of piperazin-2,6-dione 190
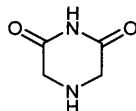
Glycine methyl ester hydrochloride **186** (1.00 g, 7.97 mmol) and potassium hydrogen carbonate (2.00 g, 19.93 mmol) was stirred in acetonitrile (60 mL). To this suspension 2-bromoacetamide **195** (1.10 g, 7.97 mmol) was added and the reaction mixture refluxed for 8 h. After cooling to room temperature the mixture was filtered and the solvent removed under reduced pressure. The resulting solid was washed with chloroform (5 mL) and acetone (5 mL) to yield the *title compound* (0.31 g, 34%) as a colourless solid. mp 100 °C (dec); v_{max} (Nujol) 3276, 1695 cm^{-1}; ^{1}H NMR (400 MHz, d-6 DMSO) δ_H 10.84 (1H, bs, NH), 3.42-3.32 (4H, m, NCH$_2$), 3.12-3.04 (1H, m, NH); ^{13}C NMR (62.5 MHz, DMSO) δ_C 173.3, 48.4. MS (ES) *m/z* = 114 [M]$^+$; HRMS (ES) (found [M]$^+$ 114.0424; C$_4$H$_6$N$_2$O$_2$ requires 114.0424).

Synthesis of piperazin-2,6-dione hydrochloride 190.HCl
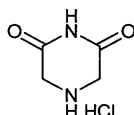
Piperazin-2,6-dione (0.20 g, 1.75 mmol) was stirred in a solution of HCl in diethyl ether (2.84 M, 8.75 mmol, 3 mL) for five minutes. Then the mixture was filtered and the product was washed with diethyl ether. The HCl-salt was isolated as a colourless solid in 74% yield (196mg). mp 130 °C (dec). v_{max} (Nujol)/cm^{-1}: 3295, 1692, 1267. ^{1}H NMR (400 MHz, d-6 DMSO) δ_H 10.92 (1H, bs, NH), 4.00-3.40 (2H, bs, NH), 3.39 (4H, s, CH$_2$); ^{13}C NMR (62.5 MHz, d-6 DMSO) δ_C 172.9, 48.1.

Synthesis of 3-benzylpiperazin-2,6-dione 191
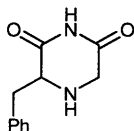
L-Phenylalanine ethyl ester hydrochloride **138** (1.83 g, 7.97 mmol) and potassium hydrogen carbonate (2.00 g, 19.93 mmol) were stirred in toluene (60 mL). To the suspension 2-bromoacetamide `95 (1.10 g, 7.97 mmol) was added and the reaction mixture refluxed for 4 d. After being cooled to room temperature the mixture was filtered and the solvent was evaporated. The solid collected was washed with chloroform (5 mL) then acetone(5 mL) and dried to yield *the title compound* (179 mg, 11%) as a colourless solid. mp 157 °C (dec); v_{max} (Nujol) 3282, 1697, 1226 cm^{-1}; ^{1}H NMR (400 MHz, d-6 DMSO) δ_H 10.78 (1H, bs, N$\underline{H}$), 7.29-7.17 (5H, m, Ar-$\underline{H}$), 3.60-3.54 (1H, m, NC$\underline{H}$), 3.47-3.31 (2H, m, NC$\underline{H}_2$), 3.16 (1H, dd, J = 3.8, 14.2, C$\underline{H}_2$Ar), 2.93-2.86 (1H, m, N$\underline{H}$), 2.75 (1H, dd, J = 9.7, 14.2, C$\underline{H}_2$Ar); ^{13}C NMR (100 MHz, d-6 DMSO) δ_C 173.8(C), 139.1(C), 129.8(CH), 128.5(CH), 126.6(CH), 58.6(CH), 48.1(CH$_2$), 35.6(CH$_2$); MS (ES) m/z = 246 [M+MeCN+H]$^+$, 205[M+H]$^+$; HRMS (ES) calculated for $C_{11}H_{12}N_2O_2$ [M]$^+$ 205.0972, found 205.0972.

Synthesis of 3-benzylpiperazin-2,6-dione hydrochloride 191.HCl
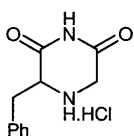
3-Benzylpiperazin-2,6-dione **191** (0.10 g, 0.49 mmol) was stirred in a solution of HCl in diethyl ether (2.84 M, 1.00 mL, 2.45 mmol) for five minutes. Then the mixture was filtered and the product was washed with diethyl ether. The HCl-salt was isolated (92 mg, 77%) as a colourless solid. v_{max} (Nujol) 3509, 3338, 1737, 1267 cm^{-1}; ^{1}H NMR (400 MHz, d-6 DMSO) δ_H 11.75 (1H, bs, N$\underline{H}$), 11.00-9.50 (2H, bs, N$\underline{H}$), 7.35-7.23 (5H, m, Ar-$\underline{H}$), 4.39 (1H, bs, NC$\underline{H}$), 3.99-3.88 (2H, m, NC$\underline{H}_2$), 3.37 (1H, dd, J = 6.2, 14.4, C$\underline{H}_2$Ar), 3.15 (1H, dd, J = 6.5, 14.3, C$\underline{H}_2$Ar); ^{13}C NMR (62.5 MHz, d-6 DMSO) δ_C 168.3, 166.6, 135.6, 129.6, 128.5, 127.0, 55.9, 44.5, 33.2; MS (ES) m/z = 246 [M+MeCN+H-HCl]$^+$, 205 [M+H-HCl]$^+$.

Synthesis of 2-amino-*N*-methylacetamide 196
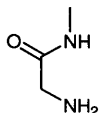
Glycine ethyl ester hydrochloride **186** (3.00 g, 21.50 mmol) was stirred in a solution of methylamine in ethanol (33%, 6.00 mL, 48.00 mmol) for 3 days. Then the solvent was removed under reduced pressure and the resulting residue dissolved in methanol. Diethyl ether was added slowly to the solution until the starting material began to precipitate as a colourless solid. The suspension was then filtered followed by concentration of the filtrate under reduced pressure to yield *the title compound* (1.17g, 25%) as a colourless oil. v_{max} (neat)/ cm^{-1}: 3298, 1651, 857, 831; ^{1}H NMR (400 MHz, d-6 DMSO) δ_H 7.64 (1H, bs, N$\underline{H}$), 2.91 (2H, s, C$\underline{H}_2$), 2.46 (3H, d, *J* = 6.5, NHC$\underline{H}_3$), 1.62 (2H, bs, N$\underline{H}$); ^{13}C NMR (62.5 MHz, d-6 DMSO) δ_C 173.3 (C) 44.8 (CH$_2$) 25.2 (CH$_3$); MS (ES) *m/z* = 88 [M]$^+$; HRMS (ES) calculated for C$_3$H$_8$N$_2$O [M]$^+$ 88.0631, found 88.0632.

Synthesis of 1-methylpiperazin-2,6-dione 192
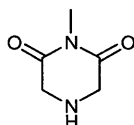
2-Amino-*N*-methylacetamide **196** (0.50 g, 5.67 mmol) and potassium hydrogen carbonate (1.40 g, 14.0 mmol) were stirred in acetronitrile (60 mL) and stirred vigorously to create a suspension. Ethylbromoacetate **195** (0.95 g, 5.67 mmol) was added and the reaction mixture was refluxed for 2 days. The reaction mixture was allowed to cool to room temperature and the precipitate filtered. The filtrate was concentrated under reduced pressure and the resulting residue purified by column chromatography eluting with ethyl acetate to provide the title compound (0.21 g, 29%) as a light purple solid. mp 78-82 °C; v_{max} (Nujol)/cm^{-1}: 3320, 1660, 1300, 1161; ^{1}H NMR (400 MHz, CDCl$_3$) δ_H 3.66 (s, 4H, NC$\underline{H}_2$), 3.09 (s, 3H, NC$\underline{H}_3$), 1.65 (1H, bs, N$\underline{H}$); ^{13}C NMR (62.5 MHz, CDCl$_3$) δ_C 171.4 (C) 49.7(CH$_2$) 25.4(CH$_3$) MS (ES) *m/z* = 128 [M]$^+$; HRMS (ES) calculated for C$_4$H$_8$N$_2$O$_2$ [M]$^+$ 128.0580, found 128.0578.

Synthesis of 1-methylpiperazin-2,6-dione hydrochloride 192.HCl
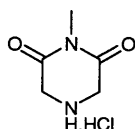
1-Methylpiperazin-2,6-dione **192** (0.15 g, 1.20 mmol) was stirred in a solution of HCl in diethyl ether (2.84 M, 2.50 mL, 6.00 mmol HCl) for five minutes. Then the mixture was filtered and the solid was washed with diethyl ether. The product was isolated as a light purple solid in 82% yield (0.16 g). mp >190 °C; v_{max} (Nujol)/ cm^{-1} 3319, 1667, 1166; ^{1}H NMR (400 MHz, d-6 DMSO) δ_H 10.21 (2H, bs, N$\underline{H}$), 4.07 (4H, s, NC$\underline{H_2}$), 3.03 (3H, s, NC$\underline{H_3}$); ^{13}C NMR (62.5 MHz, d-6 DMSO) δ_C 165.9(C), 44.6(CH$_2$), 25.6(CH$_3$). MS (ES) m/z = 128 [M-HCl]$^+$.

Synthesis of 3-benzyl-1-methylpiperazin-2,6-dione
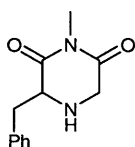
(*S*)-2-Amino-N-methyl-3-phenylpropanamide **193** (1.00 g, 5.61 mmol) and potassium hydrogen carbonate (1.40 g, 14.0 mmol) were stirred in acetonitrile (60 mL). To the suspension ethylbromoacetate **195** (0.95 g, 5.67 mmol) was added and the reaction mixture was refluxed for 3 d. The reaction mixture was allowed to cool to room temperature then the mixture was filtered and the solvent removed under reduced pressure. The residue was purified by column chromatography eluting with (1:1) ethyl acetate/petroleum ether to yield the title compound (0.88 g, 72%) as a light yellow solid. mp 49-52 °C; v_{max} (Nujol) 3295, 1660, 1292, 1127 cm^{-1}; ^{1}H NMR (400 MHz, CDCl$_3$) δ_H 7.37-7.26 (5H, m, Ar-$\underline{H}$), 3.82 (1H, d, *J* = 17.4, NC$\underline{H_2}$), 3.74-3.70 (1H, m, NC$\underline{H_2}$), 3.59 (1H, d, *J* = 17.5, NC$\underline{H}$), 3.42 (1H, dd, *J* = 4.0, 14.0, C$\underline{H_2}$Ar), 3.18 (3H, s, NC$\underline{H_3}$), 3.04 (1H, dd, *J* = 8.8, 14.0, C$\underline{H_2}$Ar), 1.67 (bs, 1H, N$\underline{H}$); ^{13}C NMR (100 MHz, CDCl$_3$) δ_C 172.5 (C), 171.1 (C), 136.7 (C), 129.4 (CH), 128.9 (CH), 127.2 (CH), 59.8(CH), 49.3 (CH$_2$), 36.6 (CH$_2$), 25.9 (CH$_3$). MS (ES) m/z = 260 [M+MeCN+H]$^+$, 219 [M+H]$^+$; HRMS (ES) calculated for C$_{12}$H$_{14}$N$_2$O$_2$ [M]$^+$ 219.1128, found 219.1127.

Synthesis of 3-benzyl-1-methylpiperazin-2,6-dione hydrochloride 193.HCl
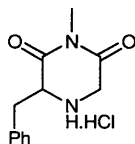
3-Benzyl-1-methylpiperazin-2,6-dione **193** (0.50 g, 2.30 mmol) was stirred in a solution of HCl in diethyl ether (2.84 M, 4.00 mL, 11.50 mmol HCl) for five minutes. Then the mixture was filtered and the solid was washed with diethyl ether. The product was isolated as a colourless solid in 87% yield (0.52 g). mp 170 °C (dec). v_{max} (Nujol) 3371, 1687 cm^{-1}. ^{1}H NMR (400 MHz, d-6 DMSO) δ_H 11.50-9.50 (2H, bs, N$\underline{H}$), 7.37-7.26 (5H, m, Ar-$\underline{H}$), 4.44 (1H, t, J = 5.8, NC$\underline{H}$), 4.04 (2H, s, NC$\underline{H}_2$), 3.39 (1H, dd, J = 6.5 , 14.4, C$\underline{H}_2$Ar), 3.18 (dd, J = 6.3, 14.3, C$\underline{H}_2$Ar), 3.03 (3H, s, NC$\underline{H}_3$). ^{13}C NMR (62.5 MHz, d-6 DMSO) δ_C 136.0 (C) 129.6 (CH) 128.4 (CH) 126.9 (CH) 56.8 (CH) 45.3(CH$_2$) 34.1(CH$_3$) 25.9 (CH$_2$) *carbonyl carbons were not observed*; MS (ES) *m/z* = 260 [M+MeCN+H-HCl]$^+$, 219 [M+H-HCl]$^+$.

Synthesis of piperazin-2-one hydrochloride 189.HCl
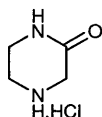
Piperazin-2-one **189** (0.25 g, 2.50 mmol) was stirred in a solution of HCl in diethyl ether (2.84 M, 4.40 mL, 12.50 mmol HCl) for five minutes. Then the mixture was filtered and the solid was washed with diethyl ether. The product was isolated as an orange solid in 60% yield (0.21 g). mp 96-98 °C; v_{max} (Nujol) 3301, 1651, 1120 cm^{-1}; ^{1}H NMR (400 MHz, d-6 DMSO) δ_H 7.78 (1H, bs, N$\underline{H}$), 6.00-4.00 (2H, bs, N$\underline{H}$), 3.25 (2H, s, C$\underline{H}_2$CO), 3.18-3.15 (2H, m, C$\underline{H}_2$CH$_2$), 2.88 (2H, t, J = 5.7, C$\underline{H}_2$CH$_2$); ^{13}C NMR (100 MHz, d-6 DMSO) δ_C 167.8(C), 48.7(CH$_2$), 41.7(CH$_2$), 41.2(CH$_2$).

Synthesis of (*E*)-4-methyl-3,5-dioxo-1-(3-phenylallylidene)piperazin-1-ium hexafluorophosphate 125
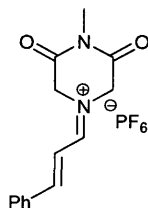
1-Methylpiperazin-2,6-dione **192** (0.05 mg, 0.39 mmol) was dissolved in methanol (5.00 mL) and (*E*)-cinnamaldehyde **20** (49.00 µL, 0.39 mmol) was added, followed by HPF$_6$ (60% in water, 57.00 µL, 0.39 mmol).After a few seconds a yellow precipitate was observed. The mixture was stirred for a further 5 minutes and then the precipitate was separated by filtration. The solid was washed with methanol to yield *the title compound* (0.11 g, 72%) as a yellow solid. v_{max} (Nujol)/ cm^{-1}: 3338, 1752, 1685, 1625; ^{1}H NMR (400 MHz, d-3 MeCN) δ_H 8.35 (1H, d, *J* = 10.8 N$^+$=C$\underline{H}$), 8.04 (1H, d, *J* = 15.0, CH=C$\underline{H}$Ar), 7.85 (2H, d, *J* = 7.4, Ar-$\underline{H}$), 7.65-7.61 (1H, m, Ar-$\underline{H}$), 7.55-7.51 (2H, m, Ar-$\underline{H}$), 7.37 (1H, dd, *J* = 10.8, 15.0, C$\underline{H}$=CHAr), 4.93 (2H, s, N$^+$C$\underline{H}_2$), 4.80 (2H, s, N$^+$C$\underline{H}_2$), 3.08 (3H, s, NC$\underline{H}_3$). ^{13}C NMR (125 MHz, d-3 MeCN) δ_C 171.0(CH), 165.0(CH), 134.9(CH), 133.5(C), 131.1(CH), 129.7(CH), 116.2(CH), 58.0(CH$_2$), 52.0(CH$_2$), 26.1(CH$_3$), *carbonyl carbons were not observed*; For X-ray structure see (*Appendix*)

Synthesis of ethyl 2-benzylbromoacetate 208
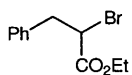
Under nitrogen and at -35 °C ethyl-2-benzylacetoacetate (10.00 g, 45.40 mmol) was added to a solution of sodium ethoxide (3.09 g, 45.50 mmol) in ethanol (75 mL). N-bromosuccinimide (8.08 g, 45.50 mmol) was added slowly and the resulting mixture was stirred for 1h at rt. After the addition of water (75 mL) the solution was extracted with diethyl ether (3x50 mL) and the organic layer was dried over NaSO$_4$. The intermediate **207** was purified by column chromatography (petroleum ether: dichloromethane 1.5:1). Then the bromonated intermediate was dissolved in a solution of sodium ethoxide (3.09 g, 45.50 mmol) in ethanol (75 mL) and was stirred for 3h. Water (75 mL) was added and the solution was extracted with diethyl ether (3x50 mL) and dried over NaSO$_4$, filtered and concentrated

under reduced pressure to yield the title compound (6.80 g, 82%) as a yellow liquid. IR (Nujol) 3295, 1739, 1605 cm^{-1}; ^{1}H NMR (400 MHz, CDCl$_3$) δ_H 7.26-7.14 (5H, m, Ar-H), 4.36-4.30 (1H, m, CHBr), 4.14-4.07 (2H, m, CO$_2$CH$_2$), 3.37 (1H, dd, *J* = 5.5, 14.1, Ar-CH$_2$), 3.17 (1H, dd, *J* = 7.1, 14.1, Ar-CH$_2$), 1.15 (3H, t, *J* = 3.9, CH$_2$CH$_3$); ^{13}C NMR (125 MHz, CDCl$_3$) δ_C 169.4(C), 136.8(C), 129.2(CH), 128.6(CH), 127.3(CH), 62.0(CH$_2$), 45.5(CH), 41.1(CH$_2$), 13.9(CH$_3$).

Synthesis of tricyclo[5.2.1.0~2,6~]dec-8-en-3-one
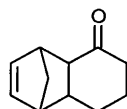
2-Cyclohexen-1-one **198** (290 mg, 3.00 mmol, 0.29 mL) was added to water (0.75 mL) at 4 °C, followed by conc. HCl (0.05 mL, 0.60 mmol). The mixture was stirred for five minutes and cyclopentadiene **19** (0.71 mL, 9.00 mmol) was added dropwise. The mixture was stirred for 4d and was then diluted with (5:1)petroleum ether/diethyl ether (12 mL) and submitted directly to column chromatography eluting with petroleum ether/diethyl ether (5:1) to yield the *title compound* (6.9 mg, 1.4%) as a yellow oil. Data was consistent with the literature.[168] ^{1}H NMR (400 MHz, CDCl$_3$) δ_H 6.13-6.11 (1H, m), 5.98-5.94 (1H, m), 4.14-4.07 (2H, m), 3.20 (1H, s), 2.82 (1H, s), 2.68-2.60 (2H, m), 2.28-2.23 (1H, m), 1.91-1.82 (2H, m), 1.73-1.59 (2H, m), 1.40-1.37 (1H, m), 125-1.23 (1H, m), 0.71-0.55 (1H, m); ^{13}C NMR (62.5 MHz, CDCl$_3$) δ_C 215.6, 137.7, 135.0, 51.7, 48.4, 46.6, 45.2, 41.4, 39.4, 28.0, 21.8; MS (ES) m/z = 162 [M]$^+$.

Synthesis of 1-(3-methylbicyclo[2.2.1]hept-5-en-2-yl)propan-1-one **176**
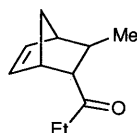
Catalyst (0.12 mmol) was dissolved in water (203.00 µL) and cooled to 4 °C. 4-hexen-3-one **175** (70.00 µL, 0.61 mmol) was added, followed by perchloric acid (70 % in water, 10.50 µL, 0.12 mmol) and the mixture was stirred for five minutes. Cyclopentadiene **19** (75.00 µL, 0.91 mmol) was added and the stirring was continued for 24h. Then the mixture was diluted

with petroleum ether/diethyl ether (9:1) and directly purified by column chromatography with the same solvent system to yield the *title compound* (32 mg, 16%) as a colourless liquid. Data was consistent with the literature.[168] ^{1}H NMR (400 MHz, CDCl$_3$) δ_H 6.17-6.15 (1H, m, CH=C<u>H</u>), 5.84-5.82 (1H, m, CH=C<u>H</u>), 3.06 (bs, 1H, CH=CHC<u>H</u>), 2.39-2.33 (4H, m, C<u>H</u>$_2$COC<u>H</u>, CH=CHC<u>H</u>,), 1.84-1.82 (1H, m, C<u>H</u>$_2$CH), 1.52 (1H, *m*, C<u>H</u>$_2$CH), 1.37 (1H, m, C<u>H</u>$_2$CH), 1.09 (3H, d, J = 7.0 CHC<u>H</u>$_3$), 0.95 (3H, t, J = 7.4, CH$_2$C<u>H</u>$_3$); ^{13}C NMR (62.5 MHz, CDCl$_3$) δ_C 211.7, 138.5, 132.5, 60.7, 49.0, 46.3, 35.7, 34.7, 21.0, 7.8.

Preparation of (S)-5-methyl-5-nitro-4-phenylhexan-2-one 229
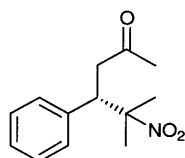
The enetaionenriched product was prepared in accordance with the method of Jorgensen.[169] *E*-4-phenylbut-3-en-2-one (37 mg, 0.25 mmol) was place in nitropropanane (496mg 5.5 mmol, 0.5 mL), To this was added 20 mol% of catalyst **10** (11mg g, 0.05 mmol) and the reaction allowed to stir at ambient temperature for 14 days. On completion of the reaction the volatiles were removed under reduced pressure. The resulting residue was purified by column chromatography eluting with. The e.e was determined by Chrial HPLC using Chiracel OJ column eluting 10% IPA in hexanes flow rate 1 mL min^{-1}. Enatiomers were determined by analogy. mp °C; ^{1}H NMR (400MHz, CDCl$_3$) δ_H 7.33-7.24 (3H, m, Ar-H), 7.21-7.16 (2H, m, Ar-H), 3.92 (1H, dd, J = 10.8, 3.6, CHC<u>H</u>$_2$), 3.09 (1H, dd, J = 16.8, 10.8, C<u>H</u>CH$_2$) 2.71, (1H, dd, J = 16.8, 3.0, CHC<u>H</u>$_2$) 2.03 (3H, s, COC<u>H</u>$_3$) 1.55 (3H, s, NO$_2$CC<u>H</u>$_3$) 1.47(3H, s, NO$_2$CC<u>H</u>$_3$) ^{13}C NMR (100MHz, CDCl$_3$)δ_C 205.2(C), 137.5(C), 129.1(CH), 128.5(CH), 127.9(C), 91.0(C), 48.8(CH$_2$), 44.0(CH), 30.3(CH$_3$), 25.8(CH$_3$), 22.3(CH$_3$).

Preparation of 5-nitro-4-phenylpentan-2-one 237
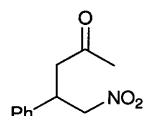
Compound **237** was prepared in accordance with the procedure of List.[170] To a suspension of *L*-proline (120mg 1.01mmol, 15mol%) in DMSO (54 mL) was added trans-beta nitro styrene (1 g, 6.7 mmol) and acetone (10.6 g, 182 mmol, 13.4 mL) and the mixture stirred overnight at room temperature. To this was added ethyl acetate (50 mL) and saturated NH_4Cl solution (50 mL). The aqueous layer was extracted with ethyl acetate (3x50 mL), the organics combined dried over $MgSO_4$ filtered and concentrated under reduced pressure. The resulting residue was purified using column chromatography eluting with (1:1) petroleum ether/ethyl acetate to yield the title compound (1.31 g, 95%) as a colourless solid. ^1H NMR (400MHz, $CDCl_3$) δ_H 7.35- 7.21 (5H, m Ar-H), 4.70 (1H, dd, J = 6.9, 6.9, $C\underline{H}_2NO_2$), 4.61 (1H, dd, J = 7.7, 7.7, $C\underline{H}_2NO_2$), 4.01 (1H, m, ArC$\underline{H}$CH_2), 2.93 (2h, d, J = 7.0, $C\underline{H}_2CO$), 2.13 (3H, s, COC$\underline{H}_3$).

Preparation of (S)-*N*-methyl-3-phenylpropane-1,2-diamine, 235
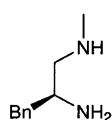
Compound **235** was prepared in accordance with the procedure of Jørgensen. *L*-phenylalaninmethylamide **138** (1 g, 5.6 mmol) was dissolved in anhydrous THF (30 mL) and lithium aluminium hydride (1.07g, 29.1 mmol, 5 eq) added. The reaction mixture was refluxed for 48h and allowed to cool before being filtered through celite. The filtrate was collected and concentrated under reduced pressure. The resulting oil was purified by column chromatography eluting with methanol to yield the title compound (0.23 g, 25%) as a colourless oil data consistent with reported values. ^1H NMR (400MHz, $CDCl_3$) δ_H 7.32-7.19 (5H, m, Ar-$\underline{H}$) 3.14-3.08 (1H, m, CH_2C$\underline{H}$CH_2), 2.80 (1H, dd, J = 4.9, 13.3, ArC$\underline{H}_2$) 2.67 (1H, dd, J = 3.9, 11.7, ArC$\underline{H}_2$), 2.53-2.44 (5H, m, NC$\underline{H}_3$, NC$\underline{H}_2$); ^{13}C NMR (125MHz,

CDCl$_3$); δ_C 139.0 (C), 129.3(CH), 128.5(CH), 126.3(C), 57.9(CH$_2$), 52.1(CH), 42.7(CH$_3$). *m/z* (APCI) (M+H) 165; HRMS (ES) (found 165.1386 [M+H]$^+$; C$_{10}$H$_{16}$N$_2$ requires 165.1386).

Preparation of 257
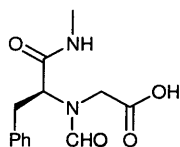
Glyoxylic acid monohydrate **255** (1.22 g, 13.2mmol) and *L*-phenylalaninmethylamide **138** (1 g, 6.6mmol) were dissolved in CH$_2$Cl$_2$ (100 mL) and stirred overnight at room temperature. The resulting solution was then concentrated under reduced pressure to yield *the title compound* (1.29 g, 74 %) as a colourless solid. For X-ray structure see *Appendix.* mp 175-177 °C; υ_{max} (CHCl$_3$) /cm^{-1} 3680, 1664, 1524, 1423, 1215, 1017; ^{1}H NMR (400MHz, CDCl$_3$) δ_H (*rotameric ratio* 2.58:1) 7.93 (1H, s, NC*H*O, *minor rotamer*), 7.85 (1H, s, CHO, *major rotamer*), 7.24-7.05 (5H, m, Ar-H, *major and minor*), 4.57 (1H, t, *J* = 8.4, C*H*CH$_2$, *minor*), 4.14 (1H, dd, *J* = 4.5, 10.9, C*H*CH$_2$, *major*) 3.96-3.65 (2H, m, C*H*$_2$COOH, *major and minor*)3.61-3.40 (1H, m, CHC*H*$_2$, major) 3.27-3.24 (1H, m, CHC*H*$_2$, *minor*) 300-2.95 (1H, m, CHC*H*$_2$, *minor*) 2.80-2.75 (4H, m, NC*H*$_3$, CHC*H*$_2$, *major*), 2.66-2.65 (3H, m, NC*H*$_3$, *minor*) ^{13}C NMR (100MHz, CDCl$_3$) δ_C 170.8, 169.5, 169.3, 163.9, 163.3, 136.9, 136.8, 129.0, 128.9, 128.7, 127.20, 126.9, 64.1, 52.8, 52.8, 47.4, 45.2, 36.1, 34.2, 26.5, 26.3; *m/z* (APCI) 264 (M+H); HRMS (EI) (found 264.1105 [M+H]$^+$; C$_{13}$H$_{16}$N$_2$O$_4$ requires 264.1103).

Synthesis of 2-(propylamino)acetic acid hydrochloride 273
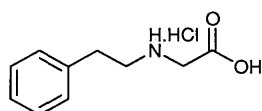
Glyoxylic acid monohydrate **255** (1.71 g, 19.0 mmol) was dissolved in distilled water (20 mL) at room temperature. Phenethylamine **258** (1.00 g, 8.25 mmol) was added and the resulting solution stirred for 24 hours. During this time the formation of a white precipitate

was observed. After this period 2M HCl (20 mL, 40 mmol) was added and the reaction mixture heated at reflux overnight. The solvent was removed under reduced pressure and the residue recrystallised from methanol/diethyl ether to give the *title compound* (1.24 g, 70%) as a colourless solid. mp 184°C; v_{max} (Nujol)/cm^{-1} 2924, 1748; ^{1}H NMR (500MHz, d-6 DMSO) δ_H 13.80 (1H, bs, CO$_2$<u>H</u>) 9.38 (2H, bs, N<u>H</u>), 7.36-7.24 (5H, m, Ar-<u>H</u>) 3.89 (2H, s, NC<u>H</u>$_2$CO$_2$H) 3.16 (2H, t, J = 10.0, NC<u>H</u>$_2$) 2.99 (2H, t, J = 10.0, C<u>H</u>$_2$Ar); ^{13}C NMR (125 MHz, d-6 DMSO) δ_C 168.5 (C) 137.6 (C) 129.1 (CH) 129.1 (CH) 127.3 (CH) 48.1 (CH$_2$) 47.3 (CH$_2$) 31.8 (CH$_2$); MS (ES) m/z = 180 [M + H - HCl]$^+$; HRMS (ES) (found 180.1019 [M + H - HCl]$^+$ C$_{10}$H$_{14}$NO$_2$; requires 180.1025)

Synthesis of 2-(propylamino)acetic acid hydrochloride 274
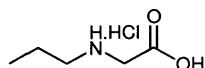
Glyoxylic acid monohydrate **255** (1.71 g, 19.0 mmol) was dissolved in distilled water (20 mL) at room temperature. Propylamine (0.50 g, 8.5 mmol) was added and the resulting solution stirred for 24 hours. After this period 2M HCl (20 mL, 40 mmol) was added and the reaction mixture heated at reflux overnight. The solvent was removed under reduced pressure and the residue recrystallised from methanol / diethyl ether to give the *title compound* (1.02 g, 78%) as a colourless solid. mp 197-198 °C; v_{max} (Nujol)/cm^{-1} 2924, 1753; ^{1}H NMR (400MHz, d-6 DMSO) δ_H 13.73 (1H, bs, CO$_2$<u>H</u>), 9.18 (2H, bs, N<u>H</u>), 3.84 (2H, s, NC<u>H</u>$_2$CO$_2$H), 2.85 (2H, t, J = 7.8, NC<u>H</u>$_2$), 1.69-1.61 (2H, m, C<u>H</u>$_2$CH$_3$), 0.89 (3H, t, J = 7.5, CH$_2$C<u>H</u>$_3$); ^{13}C NMR (62.5 MHz, d-6 DMSO) δ_C 167.9(C), 48.2(CH$_2$), 46.7(CH$_2$), 18.7(CH$_2$), 10.9(CH$_3$). MS (ES) m/z = 118 [M + H - HCl]$^+$; HRMS (ES) 118.0868 calculated for C$_5$H$_{11}$N$_1$O$_2$ [M + H - HCl]$^+$, found 118.0863.

Synthesis of 2-(cylohexylamino)acetic acid hydrochloride 275
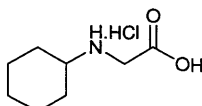
50%-Glyoxylic acid solution (0.82 g, 11.1 mmol) was added to distilled water (20 mL) at room temperature. Cyclohexylamine (0.50 g, 5.05 mmol) was added and the resulting solution stirred for 24 hours. The solvent was removed under reduced pressure to give a yellow oil. Then 2M HCl (20 mL, 40 mmol) was added and the reaction mixture heated at reflux overnight. The solvent was removed under reduced pressure and the residue recrystallised from methanol / diethyl ether to give the *title compound* (0.77g, 86%) as a colourless solid. mp 208 °C; v_{max} (Nujol)/cm^{-1} 2924, 1759; ^{1}H NMR (400MHz, d-6 DMSO) δ_H 13.77 (1H, bs, CO$_2$H), 9.09 (2H, bs, NH), 3.85 (s, 2H, NCH$_2$CO$_2$H), 3.03-2.90 (1H, m, NCH(CH$_2$)$_2$), 2.09-1.95 (2H, m, CHCH$_2$CH$_2$), 1.81-1.67 (2H, m, CHCH$_2$CH$_2$), 1.63-1.53 (1H, m, CH$_2$), 1.39-0.90 (5H, m, CH$_2$); ^{13}C NMR (125 MHz, d-6 DMSO) δ_C 167.7(C), 57.1(CH), 44.0(CH$_2$), 28.7(CH$_2$), 24.6(CH$_2$), 24.1(CH$_2$); MS (ES) m/z = 158 [M + H - HCl]$^+$; HRMS (ES) 158.1181 calculated for C$_8$H$_{15}$NO$_2$ [M + H - HCl]$^+$, found 158.1176.

Synthesis of 2-(allylamino)acetic acid hydrochloride 276
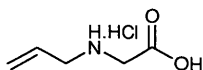
Glyoxylic acid monohydrate **255** (1.77g, 19.3 mmol) was dissolved in distilled water (20 mL) at room temperature. Allylamine (0.50 g, 8.76 mmol) was added and the resulting solution stirred for 24 hours. After this period 2M HCl (20 mL, 40 mmol) was added and the reaction mixture heated at reflux overnight. The solvent was removed under reduced pressure and the crude product dissolved in methanol and filtered through Celite®. The residue was recrystallised from methanol/diethyl ether to give the *title compound* (0.33 g, 25%) as a brownish solid. mp 163-164 °C; v_{max} (Nujol)/cm^{-1} 2912, 1752; ^{1}H NMR (400MHz, MeOD) δ_H 6.01-5.87 (1H, m, CH$_2$=CH), 5.56 (1H, dd, J =17.1, 0.9, CH$_2$=CH), 5.52 (1H, dd, J = 10.1, 0.8, CH$_2$=CH), 3.89 (2H, s, NCH$_2$CO$_2$H), 3.71 (2H, d, J = 7.7,

NC$\underline{H}_2$); ^{13}C NMR (62.5 MHz, MeOD) δ_C 167.5(C), 127.5(CH), 123.4(CH$_2$), 49.11(CH$_2$), 46.1(CH$_2$); MS (ES) m/z = 116 [M + H - HCl]$^+$; HRMS (ES) 116.0712 calculated for C$_5$H$_9$NO$_2$ [M + H - HCl]$^+$, found 116.0706.

Synthesis of 2-(benzylamino)acetic acid hydrochloride 277
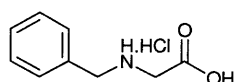
Glyoxylic acid monohydrate **255** (0.95 g, 10.3 mmol) was dissolved in distilled water (20 mL) at room temperature. Benzylamine (0.50 g, 4.67 mmol) was added and the resulting solution stirred for 24 hours. The solvent was removed under reduced pressure to give a yellow oil. Then 1N HCl (20 mL, 20 mmol) was added and the reaction mixture heated at reflux overnight. The solvent was removed under reduced pressure and the residue recrystallised from methanol / diethyl ether to give the *title compound* (0.47g, 50%) as a colourless solid. mp 221-222 °C; v_{max} (Nujol)/cm^{-1} 2924, 1747; ^{1}H NMR (400MHz, MeOD) δ_H 7.54-7.42 (5H, m, Ar-$\underline{H}$), 4.26 (2H, s, NC$\underline{H}_2$CO$_2$H), 3.92 (2H, s, NC$\underline{H}_2$Ar); ^{13}C NMR (125 MHz, MeOD) δ_C 167.3(C), 130.8(C), 129.7(CH), 129.5(CH), 129.0(CH), 50.6(CH$_2$), 46.2(CH$_2$); MS (ES) m/z = 166 [M + H - HCl]$^+$; HRMS (ES) 166.0868 calculated for C$_9$H$_{11}$NO$_2$ [M + H - HCl]$^+$, found 166.0863.

Synthesis of 2-(4-methoxybenzylamino)acetic acid hydrochloride 278
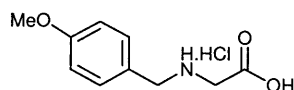
50%-Glyoxylic acid solution (0.59 g, 7.97 mmol) was added to distilled water (20 mL) at room temperature. 4-Methoxybenzylamine (0.50 g, 3.64 mmol) was added and the resulting solution stirred for 24 hours at 50 °C. The solvent was removed under reduced pressure to give a yellow oil. Then 2M HCl (20 mL, 40 mmol) was added and the reaction mixture heated at reflux overnight. The solvent was removed under reduced pressure and the residue recrystallised from methanol / diethyl ether to give the *title compound* (0.57g, 68%)

as a colourless solid. mp 200 °C; ν_{max} (Nujol)/cm^{-1} 2924, 1745 ; ^{1}H NMR (400MHz, MeOD) δ_H 7.45-7.38 (2H, m, Ar-H), 7.04-6.97 (2H, m, Ar-H), 4.19 (2H, s, NCH$_2$CO$_2$H), 3.88 (2H , s, NCH$_2$Ar), 3.83 (3H, s, OCH$_3$); ^{13}C NMR (125 MHz, d-6 DMSO) δ_C 168.2(C), 160.2(C), 132.3(CH), 123.8(C), 114.5(CH), 55.7(CH$_3$), 49.7(CH$_2$), 46.4(CH$_2$); MS (ES) m/z = 196 [M + H - HCl]$^+$; HRMS (ES) 196.0974 calculated for C$_{10}$H$_{13}$NO$_2$ [M + H - HCl]$^+$, found 196.0968.

Synthesis of 2-(4-chlorobenzylamino)acetic acid hydrochloride 279
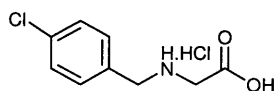
50%-Glyoxylic acid solution (0.58 g, 7.83 mmol) was added to distilled water (20 mL) at room temperature. 4-Chlorobenzylamine (0.50 g, 3.53 mmol) was added and the resulting solution stirred for 24 hours at 50 °C. The solvent was removed under reduced pressure to give a yellow oil. Then 2M HCl (20 mL, 40 mmol) was added and the reaction mixture heated at reflux overnight. The solvent was removed under reduced pressure and the residue recrystallised from methanol/diethyl ether to give the *title compound* (0.50 g, 60%) as a colourless solid. mp 216-217 °C; ν_{max} (Nujol)/cm^{-1} 2925, 1745; ^{1}H NMR (400MHz, MeOD) δ_H 7.57-7.41 (4H, m, Ar-H), 4.26 (s, 2H, NCH$_2$CO$_2$H), 3.94 (s, 2H, NCH$_2$Ar); ^{13}C NMR (125 MHz, MeOD) δ_C 167.3(C), 135.5(C), 131.6(CH), 129.5(C), 129.0(CH), 49.9(CH$_2$), 46.3(CH$_2$); MS (ES) m/z = 200 [M + H - HCl]$^+$; HRMS (ES) 200.0478 calculated for C$_9$H$_{10}$ClNO$_2$ [M + H - HCl]$^+$, found 200.0473.

Synthesis of 2-(2-aminoethylamino) acetic acid dihydrochloride 284
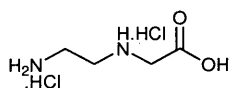
Glyoxylic acid monohydrate **255** (3.37g, 36.6 mmol) was dissolved in water (20 mL) at room temperature. Ethylenediamine (0.50 g, 8.32 mmol) was added and the resulting solution stirred for 24 hours. After that period 2M HCl (20 mL, 40 mmol) was added and

the reaction mixture heated at reflux overnight. The solvent was removed under reduced pressure and the residue recrystallised from methanol/diethyl ether to give the *title compound* (0.49 g, 31%) as a colourless solid. v_{max} (Nujol) 2923, 1719 cm^{-1}; ^{1}H NMR (400MHz, d-6 DMSO) δ_H 8.39 (bs, 4H, N$\underline{H}$), 4.03 (s, 2H, NC$\underline{H}_2$CO$_2$H), 3.46-3.39 (m, 2H, NC$\underline{H}_2$), 3.38-3.32 (m, 2H, NC$\underline{H}_2$); ^{13}C NMR (125 MHz, d-6 DMSO) δ_C 168.2(C), 47.4(CH$_2$), 44.3(CH$_2$), 35.5(CH$_2$);

Synthesis of 2-(2-(dimethylamino)ethylamino)acetic acid dihydrochloride 288
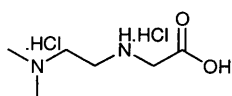
Glyoxylic acid monohydrate **255** (1.15 g, 12.5 mmol) was dissolved in water (20 mL) at room temperature. *N,N*-Dimethylethylenediamine (0.50 g, 5.67 mmol) was added and the resulting solution stirred for 24 hours. After that period 2M HCl (20 mL, 40 mmol) was added and the reaction mixture heated at reflux overnight. The solvent was removed under reduced pressure and the residue recrystallised from methanol/diethyl ether to give the *title compound* (0.71 g, 57%) as a colourless solid. mp 202 °C; v_{max} (Nujol)/cm^{-1} 2924, 1718; ^{1}H NMR (400MHz, MeOD) δ_H 4.05 (s, 2H, NC$\underline{H}_2$CO$_2$H), 3.62-3.52 (m, 4H, NCH$_2$), 2.99 (s, 6H, NCH$_2$); ^{13}C NMR (125 MHz, d-6 DMSO) δ_C 168.0(C), 52.5(CH$_2$), 47.3(CH$_2$), 42.9(CH$_3$), 41.4(CH$_2$); MS (ES) m/z = 147 [M + H - 2 HCl]$^+$. HRMS (ES) 147.1134 calculated for C$_6$H$_{14}$N$_2$O$_2$ [M + H - 2 HCl]$^+$, found 147.1128.

Synthesis of 2-(2-(methylamino)ethylamino)acetic acid dihydrochloride 287
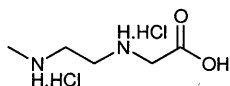
Glyoxylic acid monohydrate **255** (1.37g, 14.9 mmol) was dissolved in water (20 mL) at room temperature. *N*-Methylethylenediamine (0.50 g, 6.75 mmol) was added and the resulting solution stirred for 24 hours. The solvent was removed under reduced pressure to give a brown oil. Then 2M HCl (30 mL, 60 mmol) was added and the reaction mixture

heated at reflux overnight. The solvent was removed under reduced pressure and the residue recrystallised from methanol / diethyl ether to give the *title compound* (0.57g, 41%) as a brownish solid. mp 192-194 °C; v_{max} (Nujol)/cm^{-1} 2923, 1736; ^{1}H NMR (400MHz, MeOD) δ_H 4.01 (2H, s, NC$\underline{H}_2$CO$_2$H), 3.50-3.37 (4H, m, NC$\underline{H}_2$), 2.79 (s, 3H, NC$\underline{H}_3$); ^{13}C NMR (125 MHz, d-6 DMSO) δ_C 168.2(C), 47.3(CH$_2$), 44.3(CH$_2$), 42.9(CH$_2$), 32.7(CH$_3$).

Synthesis of 2-(3-(dimethylamino)propylamino)acetic acid dihydrochloride 290
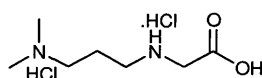
Glyoxylic acid monohydrate **255** (1.98 g, 21.5 mmol) was dissolved in water (20 mL) at room temperature. 3-Dimethylaminopropylamine (0.50 g, 4.89 mmol) was added and the resulting solution stirred for 24 hours. The solvent was removed under reduced pressure to give a brown oil. Then 2M HCl (25 mL, 50 mmol) was added and the reaction mixture heated at reflux overnight. The solvent was removed under reduced pressure and the residue recrystallised from methanol/diethyl ether to give the *title compound* (0.57g, 50%) as a colourless solid. mp 194 °C; v_{max} (Nujol)/cm^{-1} 2924, 1754; ^{1}H NMR (400MHz, MeOD) δ_H 3.99 (2H, s, NC$\underline{H}_2$CO$_2$H), 3.26 (2H, t, J = 7.9, NC$\underline{H}_2$), 3.19 (2H, t, J = 8.0, C$\underline{H}_2$CH$_2$N), 2.93 (6H, s, NC$\underline{H}_3$), 2.27-2.12 (2H, m, (CH$_3$)$_2$NC$\underline{H}_2$). ^{13}C NMR (125 MHz, d-6 DMSO) δ_C 168.2(C), 53.8(CH$_2$), 47.2(CH$_2$), 44.3(CH$_2$), 42.3(CH$_3$), 20.8(CH$_2$). MS (ES) m/z = 161 [M + H - 2 HCl]$^+$. HRMS (ES) 161.1290 calculated for C$_7$H$_{16}$N$_2$O$_2$ [M + H - 2 HCl]$^+$, found 161.1284.

Synthesis of 2-(3-(methylamino)propylamino)acetic acid dihydrochloride 289
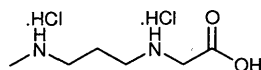
Glyoxylic acid monohydrate **255** (2.30 g, 25.0 mmol) was dissolved in water (20 mL) at room temperature. 3-Dimethylaminopropylamine (0.50 g, 5.67 mmol) was added and the resulting solution stirred for 24 hours. The solvent was removed under reduced pressure to give a brown oil. Then 2M HCl (30 mL, 60 mmol) was added and the reaction mixture

heated at reflux overnight. The solvent was removed under reduced pressure and the residue recrystallised from methanol/diethyl ether to give the *title compound* (0.55 g, 44%) as a colourless solid. mp 199 °C; v_{max} (Nujol)/cm^{-1} 2923, 1741 cm^{-1}. ^{1}H NMR (400MHz, MeOD) δ_H 3.97 (2H, s, NC$\underline{H}_2$ CO$_2$H), 3.19 (2H, t, J = 7.9, NC$\underline{H}_2$), 3.12 (2H, t, J = 7.8, NC$\underline{H}_2$), 2.74 (3H, s, NC$\underline{H}_3$), 2.19-2.08 (2H, m, NCH$_2$C$\underline{H}_2$). ^{13}C NMR (125 MHz, d-6 DMSO) δ_C 168.3(C), 47.2(CH$_2$), 45.6(CH$_2$), 44.3(CH$_2$), 32.6(CH$_3$), 22.4(CH$_2$). MS (ES) m/z = 147 [M + H - 2 HCl]$^+$. HRMS (ES) 147.1134 calculated for C$_6$H$_{14}$N$_2$O$_2$ [M + H - 2 HCl]$^+$, found 147.1128.

Synthesis of 5-methoxy-3-(1-(5-methoxy-1*H*-indol-3-yl)propyl)-1*H*-indole 310
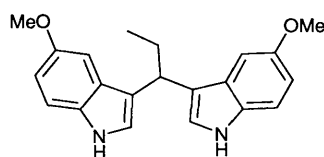
5-Methoxyindole **306** (200 mg, 1.35 mmol) was added to methanol (2.5 mL) and benzoic acid *N'*-isopropylhyrdazide **91** (14.5 mg, 0.0675 mmol, 0.1eq) and stirred at 25 °C. Propionaldehyde **304** (39 mg, 0.675 mmol, 0.049 mL,) was added, the reaction tube sealed and allowed to stir for 24hrs at ambient temperature. The solvent was removed under reduced pressure and the resulting mixture was then purified by flash column chromatography eluting with 3:1 petroleum ether/ethyl acetate to yield the *title compound* (124 mg, 55%) as an off white solid. mp 70-72 °C; v_{max} (nujol) /cm^{-1} 3403, 2360, 1622, 1579, 1483, 1435, 1288, 1208, 1171, 1096cm^{-1}; ^{1}H NMR (400MHz, CDCl$_3$) 7.81 (2H, bs, N$\underline{H}$) 7.24 (2H, d, Ar$\underline{H}$, J = 9.04) 7.02 (2H, dd, , J = 13.1, 2.5, Ar-$\underline{H}$) 6.83 (2H, dd, Ar$\underline{H}$, J = 8.5, 2.51), 4.27 (1H, t, J = 7.5, C$\underline{H}$), 3.76 (6H, s, OC$\underline{H}_3$), 2.23(2H, m, C$\underline{H}_2$) 1.01(3H, t, J = 7.5, C$\underline{H}_3$); ^{13}C NMR (100MHz, CDCl$_3$) δ 154.4(C), 131.8(C), 127.5(C), 122.1(CH), 120.0(C), 111.6(CH), 101.8(CH), 55.9(CH$_3$), 35.8(CH), 28.2(CH$_2$), 13.1(CH$_3$). m/z (APCI) 335 (M+H); HRMS (ES) (found 335.1752 [M+H]$^+$; C$_{21}$H$_{22}$N$_2$O$_2$ requires 335.1754).

Synthesis of 3-(1-(1*H*-indol-3-yl)propyl)-1*H*-indole 305
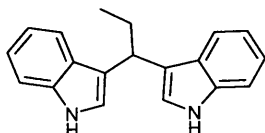
Indole **300** (158 mg, 1.35 mmol) was added to methanol (2.5 mL) and benzoic acid *N'*-isopropylhyrdazide **91** (14.5 mg, 0.0675 mmol, 0.1eq) and stirred at 25 °C. Propionaldehyde **304** (39 mg, 0.675 mmol, 0.049 mL,) was added, the reaction tube sealed and allowed to stir for 24hrs at ambient temperature. The solvent was removed under reduced pressure and the resulting mixture was then purified by flash column chromatography eluting with 3:1 petroleum ether/ethyl acetate to yield the *title compound* (156 mg, 84%) as an off white solid. mp 131-133 °C; υ_{max} (CHCl$_3$) /cm^{-1} 3478, 3418, 3058, 3047, 2962, 2931, 2872, 1731, 1618, 1456, 1447; ^{1}H NMR (400MHz, CDCl$_3$) δ_H 7.89 (2H, bs, N$\underline{H}$), 7.60 (2H, d, *J* = 7.7, Ar-H), 7.53-7.00 (8H, m, Ar-H), 4.39 (1H, t, *J* = 7.4, C$\underline{H}$CH$_2$), 2.30-2.22 (2H, m, C$\underline{H}_2$CH$_3$), 1.02 (3H, t, *J* = 7.4, CH$_2$C$\underline{H}_3$); ^{13}C NMR (100MHz, CDCl$_3$) δ_C 136.6(C), 127.2(C), 121.7(CH), 121.5(CH), 120.3(C), 119.7(CH), 119.0(CH), 111.1(CH), 35.9(CH), 28.7(CH$_2$), 13.1(CH$_3$).

Synthesis of 5-chloro-3-(1-(5-chloro-1*H*-indol-3-yl)propyl)-1*H*-indole 311
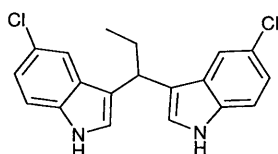
5-Chloroindole **307** (200 mg, 1.32 mmol) was added to methanol (3.0 mL) and benzoic acid *N'*-isopropylhyrdazide **91** (14.1 mg, 0.066 mmol, 0.1eq) and stirred at 25 °C. Propionaldehyde **304** (39 mg, 0.660 mmol, 0.05 mL,) was added, the reaction tube sealed and allowed to stir for 24hrs at ambient temperature. The solvent was removed under reduced pressure and the resulting mixture was then purified by flash column chromatography eluting with 3:1 petroleum ether/ethyl acetate to yield the *title compound* (190 mg, 42%) as an off white solid. mp 88 °C; ; ^{1}H NMR (400MHz, CDCl$_3$) δ_H 7.98 (2H,

bs, N$\underline{H}$), 7.49 (2H, d, J = 1.9, Ar-$\underline{H}$), 7.26-7.24 (2H, m, Ar-H), 7.11-7.06 (4H, m, Ar-$\underline{H}$), 4.23 (1H, t, J = 7.4, C$\underline{H}$CH$_2$), 2.24-2.17 (2H, m, CHC$\underline{H}_2$CH$_3$), 1.21 (3H, t, J = 7.0, CH$_2$C$\underline{H}_3$)

Synthesis of 1-methyl-3-(1-(1-methyl-1H-indol-3-yl)propyl)-1H-indole
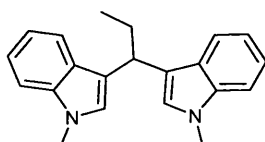
N-Methylindole **291** (177 mg, 1.35 mmol) was added to methanol (2.5 mL) and benzoic acid N'-isopropylhyrdazide **91** (14.5 mg, 0.0675 mmol, 0.1eq) and stirred at 25 °C. Propionaldehyde **304** (39 mg, 0.675 mmol, 0.049 mL,) was added and allowed to stir for 24hrs at ambient temperature. The solvent was removed under reduced pressure and the resulting mixture was then purified by flash column chromatography eluting with 10:1 petroleum ether/ethyl acetate to yield the *title compound* (165 mg, 81%) as an off white solid. mp 142-144 °C; ^{1}H NMR (400MHz, CD$_3$OD) δ_H 7.46 (2H, d, J = 8.0, Ar-$\underline{H}$), 7.11 (2H, d, J = 8.2, Ar-$\underline{H}$), 7.05-7.03 (2H, m, Ar-$\underline{H}$), 6.90-6.88 (2H, m, Ar-H), 6.68 (2H, s, Ar-$\underline{H}$), 4.21 (1H, t, J = 7.4, C$\underline{H}$CH$_2$), 3.53 (6H, s, NC$\underline{H}_3$) 2.09-2.09 (2H, m, CHC$\underline{H}_2$CH$_3$), 0.85 (3H, t, J = 7.4, CH$_2$C$\underline{H}_3$).

Synthesis of 3-(cyclopropyl(1H-indol-3-yl)methyl)-1H-indole 293
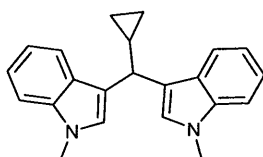
N-Methyl indole **291** (177 mg, 1.35 mmol) was added to methanol (2.5 mL) and benzoic acid N'-isopropylhyrdazide **91**(14.5 mg, 0.0675 mmol, 0.1eq) and stirred at 25 °C. cyclopropanecarboxaldehyde **292** (47 mg, 0.675 mmol) was added, the reaction tube sealed and allowed to stir for 24hrs at ambient temperature. The solvent was removed under reduced pressure and the resulting mixture was then purified by flash column chromatography eluting with 3:1 petroleum ether/ethyl acetate to yield the *title compound*

(157 mg, 74%) as an off white solid. mp 124-125 °C; υ_{max} (CHCl$_3$) /cm^{-1} 2359, 1734, 1473, 1423, 1372, 1327; ^{1}H NMR (400MHz, CDCl$_3$) δ_H 7.35 (2H, d, J = 7.6, Ar-H), 7.06 (2H, d, J = 7.7, Ar-H), 6.97-6.93 (2H, m, Ar-H), 6.78-6.73 (4H, m, Ar-H), 3.75 (1H, d, *J* = 8.4, CHCH(Ar)$_2$), 3.51 (6H, s, NCH$_3$), 1.30-1.26 (1H, m, CHCH(CH)$_2$), 0.41-0.36 (2H, m, CH$_2$CH$_2$) 0.17-0.05, (2H, m, CH$_2$CH$_2$); ^{13}C NMR (100MHz, CDCl$_3$) δ_C 137.2 (C), 127.7 (C), 126.7 (CH), 121.2 (CH), 120.0 (CH), 118.7 (C), 118.4 (CH), 109.0 (CH), 38.0 (CH), 32.7 (CH$_3$), 17.2 (CH), 4.95 (CH$_2$).

Synthesis of 3-(cyclopropyl(1-methyl-1*H*-indol-3-yl)methyl)-1-methyl-1*H*-indole 323
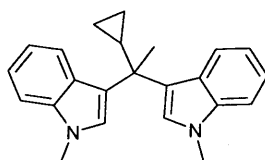
N-methyl indole **291** (0.52 g, 4.0 mmol, 2eq) was added to methanol (4 mL) and benzoic acid *N'*-isopropylhyrdazide **91** (43 mg, 0.2 mmol, 0.1eq) and stirred at 25 °C. Cyclopropyl methyl ketone **317** (170 mg, 2.0 mmol, 0.2 mL) was added, the reaction tube sealed and allowed to stir for 24hrs at ambient temperature. The solvent was removed *under reduced pressure* and the resulting mixture was then purified by flash column chromatography eluting with 3:1 petroleum ether/ethyl acetate to yield the *title compound* (453 mg, 69%) as an off white solid. mp 59 °C; υ_{max} (CHCl$_3$) /cm^{-1} 3416, 3049, 3006, 2935, 2821, 1681, 1631 1465, 1372, 1323, 1215, 1095, 1016; ^{1}H NMR (400MHz, CDCl$_3$) δ_H 7.19-7.15 (4H, m, Ar-H), 7.02-6.98 (2H, m, Ar-H), 6.93 (2H, s, Ar-H), 6.74-6.70 (2H, m, Ar-H), 3.70 (6H, s, NCH$_3$), 1.67-1.64 (4H, m, CH(CH$_2$)$_2$, CH$_3$), 0.41-0.38 (2H, m, CH$_2$) 0.24-0.23 (2H, m, CH$_2$); *m/z* (APCI) (M+H) 328;

Synthesis of 3-((1*H*-indol-3-yl)(phenyl)methyl)-1*H*-indole 315
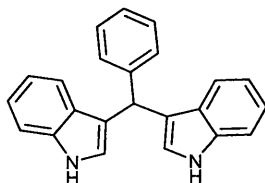
Indole **300** (500 mg, 4.27 mmol, 2eq) was added to methanol (5 mL) and benzoic acid *N'*-isopropylhyrdazide **91** (46 mg, 0.214 mmol, 0.1eq) and stirred at 25 °C. Benzaldehyde **312** (230 mg, 2.14 mmol, 0.22 mL,) was added, the reaction tube sealed and allowed to stir for 24hrs at ambient temperature. The solvent was removed *under reduced pressure* and the resulting mixture was then purified by flash column chromatography eluting with 3:1 petroleum ether/ethyl acetate to yield the *title compound* (570 mg, 84%) as a red solid. Measured data is consistent with literature values.[171] mp 157 °C; υ_{max} (KBr) /cm^{-1}; 3416, 1634, 1378, 737. ^{1}H NMR (400MHz, CDCl$_3$) δ_H 7.88 (2H, bs, N$\underline{H}$), 7.42-7.14 (11H, m, Ar-H), 7.04-6.98 (2H, m, Ar-H), 6.65 (2H, d, J = 2.4, Ar-H), 5.89 (1H, s, (Ar)$_3$C$\underline{H}$) ^{13}C NMR (125MHz, CDCl$_3$) δ_C 145.5 (C), 137.0 (C), 128.8 (CH), 128.5 (CH), 127.1 (C), 126.3 (CH), 124.0 (CH), 121.3 (CH) 119.6 (CH), 118.6 (CH), 118.5 (C), 111.9 (CH), 40.2 (CH); *m/z* (APCI) (M+H$^+$) 321.

Synthesis of 4-(di(1*H*-indol-3-yl)methyl)phenol 316
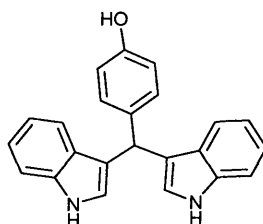
Indole **300** (250 mg, 2.13 mmol, 2 eq) was added to methanol (2.5 mL) and benzoic acid *N'*-isopropylhyrdazide **91** (14.5 mg, 0.0675 mmol, 0.1eq) and stirred at 25 °C. *p*-Hydroxy benzaldehyde **313** (130 mg, 1.07 mmol) was added, the reaction tube sealed and allowed to stir for 24hrs at ambient temperature. The solvent was removed under reduced pressure and the resulting mixture was then purified by flash column chromatography eluting with (2:1) petroleum ether/ethyl acetate to yield the *title compound* (322 mg, 89%) as an off white solid. mp 118-122 °C; ^{1}H NMR (400MHz, CDCl$_3$) δ_H 7.82 (2H, bs, NH), 7.40-7.35 (4H, m,

Ar-$\underline{H}$), 7.21-7.15 (4H, m, Ar-$\underline{H}$), 7.00 (2H, t, J = 7.8, Ar-$\underline{H}$), 6.75 (2H, d, J = 8.5, Ar-$\underline{H}$), 6.66 (2H, d, J = 1.5, Ar-$\underline{H}$), 5.82 (1H, s, C$\underline{H}$), 4.67 (1H, bs, O$\underline{H}$). ^{13}C NMR (100MHz, CDCl$_3$) δ_C 129.8 (CH), 123.5 (CH), 121.9 (CH), 120.0 (CH), 119.2 (CH), 115.0 (CH), 31.0 (CH). *None of the quaternary carbons were observed*; m/z (APCI) $(M+H)^+$ 339.

Synthesis of 3-(1-(1*H*-indol-3-yl)cyclohexyl)-1*H*-indole 320
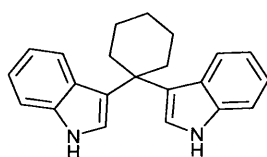
Indole **300** (500 mg, 4.27 mmol, 2eq) was added to methanol (5.0 mL) and benzoic acid N'-isopropylhyrdazide **91** (45.9 mg, 0.214 mmol, 0.1eq) and stirred at 25 °C. Cyclohexanone **318** (210 mg, 2.14 mmol, 0.22 mL,) was added, the reaction tube sealed and allowed to stir for 24hrs at ambient temperature. The solvent was removed under reduced pressure and the resulting mixture was then purified by flash column chromatography eluting with 3:1 petroleum ether/ethyl acetate to yield the *title compound* (393 mg, 59%) as an off white solid. mp 146°C; υ_{max} (CHCl$_3$) /cm^{-1} 3477, 3018, 2934, 2856, 2356, 1456, 1415, 1215, 1100; ^{1}H NMR (400MHz, CDCl$_3$) δ_H 7.92 (2H, bs, N$\underline{H}$), 7.56 (2H, d, J = 8.0, Ar-$\underline{H}$), 7.31 (2H, d, J = 8.1, Ar-$\underline{H}$), 7.11, (2H, d, J = 2.4, Ar-$\underline{H}$), 7.04 (2H, t, J = 7.6, Ar-$\underline{H}$), 6.89 (2H, t, J = 7.9, Ar-$\underline{H}$), 2.56-2.52 (4H, m, CC$\underline{H_2}$), 1.66-1.57 (6H, m, C$\underline{H_2}$) ^{13}C NMR (100MHz, CDCl$_3$) δ_C 137.0(C), 126.2(C), 123.6(C), 122.0(CH), 121.4(CH), 121.2(CH), 118.5(CH), 111.0(CH), 39.5(C), 36.8(CH$_2$), 26.8(CH$_2$) 23.0(CH$_2$).

Synthesis of 3-(1-(1*H*-indol-3-yl)cyclohexan-4-one ethylene acetal)-1*H*-indole 321
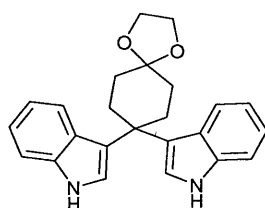
Indole **300** (250 mg, 2.13 mmol, 2eq) was added to methanol (3 mL) and benzoic acid N'-isopropylhyrdazide **91** (23 mg, 0.11 mmol, 0.1eq) and stirred at 25 °C. 1,4 cyclohexadione monoethylene ketal **319** (170 mg, 1.07 mmol)was added, the reaction tube, sealed and allowed to stir for 24hrs at ambient temperature. The solvent was removed *under reduced*

pressure and the resulting mixture was then purified by flash column chromatography eluting with (3:1) petroleum ether/ethyl acetate to yield the *title compound* (200 mg, 50%) as an off white solid. mp 228 °C; υ_{max} (CHCl$_3$) /cm^{-1} 3477, 3415, 3019, 2932, 2329, 1722, 1456, 1215; ^{1}H NMR (400MHz, CDCl$_3$) δ_H 7.94 (2H, s, N<u>H</u>), 7.59 (2H, d, J = 8.1, Ar-<u>H</u>), 7.31 (2H, d, J = 8.1, Ar-<u>H</u>), 7.10-7.06 (4H, m, Ar-<u>H</u>), 6.94-6.90 (2H, m, Ar-<u>H</u>), 4.00 (4H, s, O(C<u>H</u>$_2$)$_2$O), 2.73-.2.70 (4H, m, OC<u>H</u>$_2$CH$_2$), 1.83-1.80 (4H, m, OCH$_2$C<u>H</u>$_2$); ^{13}C NMR (100MHz, d6 acetone) δ_C 139.4(C), 128.2(C) 124.1(CH), 122.8(CH), 122.4(CH), 119.7(CH), 133.1(CH), 110.6(C), 56.7(CH$_2$), 40.3(C), 35.9(CH$_2$), 33.7(CH$_2$) *the other quaternary carbon was not observed. m/z* (APCI) (M+H); HRMS (ES) (found [M+H]$^+$ 373.1914; C$_{21}$H$_{22}$N$_2$O$_2$ requires 373.1911).

Synthesis of *vibrandole A* 324
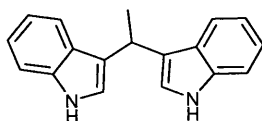
Indole **300** (500 mg, 4.27 mmol, 2eq) was added to methanol (2.5 mL) and benzoic acid *N'*-isopropylhyrdazide **91** (46 mg, 0.214 mmol, 0.1eq) and stirred at 25 °C. Acetylaldehyde (94 mg, 2.14 mmol, 0.12 mL,) was added, the reaction tube sealed and allowed to stir for 24hrs at ambient temperature. The solvent was removed *under reduced pressure* and the resulting mixture was then purified by flash column chromatography eluting with 3:1 petroleum ether/ethyl acetate to yield the *title compound* (450 mg, 80%) as an off white solid. mp 155 °C; υ_{max} (CHCl$_3$) /cm^{-1} 3479, 3417, 3018, 1455, 1416, 1092; ^{1}H NMR (500MHz, CDCl$_3$) δ_H 7.81 (1H, bs, NH), 7.52 (2H, d, J = 7.9, Ar-H), 7.29 (2H, d, J = 8.1, Ar-H), 7.10,(2H, t, J = 8.1, Ar-H), 6.97 (2H, t, J = 8.0, Ar-H), 6.86 (2H, d, J = 2.4, Ar-H), 4.61 (1H, q, J = 7.1, CH), 1.75(3H, d, J = 7.1, CH$_3$).^{13}C NMR (125MHz, CDCl$_3$) δ_C 136.7 (C), 126.9 (C). 121.8 (CH), 121.7 (C), 121.2 (CH), 119.8 (CH), 119.0 (CH), 111.1 (CH), 28.1 (CH), 21.8 (CH$_3$).

Synthesis of 3-(1,3-di(1*H*-indol-3-yl)butyl)-1*H*-indole 327
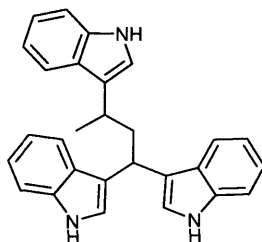
Indole **300** (0.5 g, 4.27 mmol) was added to methanol (5 mL) and benzoic acid N'-isopropylhyrdazide **91** (30.5 mg, 0.142 mmol, 0.1eq) and stirred at 25 °C. Crotonaldheyde (100 mg, 1.42 mmol, 0.12 mL,) was added, the reaction tube sealed and allowed to stir for 24hrs at ambient temperature. The solvent was removed *under reduced pressure* and the resulting mixture was then purified by flash column chromatography eluting with (3:1) petroleum ether/ethyl acetate to yield the *title compound* (290 mg, 51%) as an off white solid. The measured data is consistent with literature values[172] mp 151-154 °C; ^{1}H NMR (400MHz, CDCl$_3$) δ_H 7.60-7.43(4H, m, 3(NH), Ar-H) 7.43(1H, d, J = 7.8, Ar-H), 7.41 (1H, d, J = 7.8, Ar-H) 7.25-7.05 (6H, m, Ar-H), 7.04-6.90 (3H, m, Ar-H), 6.76 (1H, d, J = 2.0, Ar-H), 6.70 (1H, d, J = 2.0, Ar-H), 6.65(1H, d, J = 2.0, Ar-H), 4.50 (1H, t, J = 7.8, Ar$_2$-CH), 3.00 (1H, m, CH$_3$CH), 2.60 (1H, m, CHCH$_2$), 2.40 (1H, m, CHCH$_2$), 1.38 (3H, d, J = 7.0, CH$_3$CH).

Synthesis of tri(1*H*-indol-3-yl)methane 325
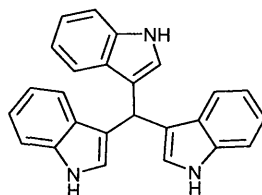
Indole **300** (500 mg, 4.27 mmol, 2 eq) was added to methanol (5 mL) and benzoic acid N'-isopropylhyrdazide **91** (46 mg, 0.214 mmol, 0.1 eq) and stirred at 25 °C. Indole-3-carboxaldehyde (310 mg, 2.14 mmol) was added, the reaction tube sealed and allowed to stir for 24hrs at ambient temperature. The solvent was removed *under reduced pressure* and the resulting mixture was then purified by flash column chromatography eluting with 3:1 petroleum ether/ethyl acetate to yield the *title compound* (590 mg, 77%) as an off white solid. ^{1}H NMR (400MHz, CDCl$_3$) δ_H 10.8 (3H, d, J = 1.9, NH), 7.43 (3H, d, J = 8.0, Ar-H),

7.39 (3H, d, *J* = 8.0, Ar-H̲), 7.07-7.05 (3H, m, Ar-H̲), 6.99 (3H, d, *J* = 2.0, Ar-H̲), 6.92-6.88

(3H, m, Ar-H̲), 6.10 (3H, s, Ar₃CH̲) ^{13}C NMR (100MHz, CDCl₃) δ$_C$ 136.7(C), 127.1(C),

123.3(CH), 121.7(CH), 120.0(CH), 119.3(C), 199.0(CH), 111.0(CH), 31.2(CH).

Preparation of 3,3-di(1*H*-indol-3-yl)indolin-2-one 326
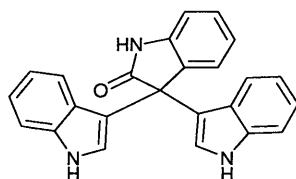
Indole **300** (250 mg, 2.13 mmol, 2eq) was added to methanol (5.0 mL) and benzoic acid *N'*-isopropylhyrdazide **91** (23.0 mg, 0.107 mmol, 0.1 eq) and stirred at 25 °C. Isatin (160 mg, 1.07 mmol) was added, the reaction tube sealed and allowed to stir for 24hrs at ambient temperature. The solvent was removed under reduced pressure and the resulting mixture was then purified by flash column chromatography eluting with 3:1 petroleum ether/ethyl acetate to yield the *title compound* (280 mg, 72%) as an off white solid. mp 286 °C; ^{1}H NMR (400MHz, CD₃OD) δ$_H$ 7.32 (2H, m, Ar-H), 7.27-7.25(4H, m, Ar-H), 7.05-7.03 (3H, m, Ar-H), 6.99-6.96(1H, m) , 6.90(2H, s, Ar-H), 6.82-6.81 (2H, m Ar-H); ^{13}C NMR (125MHz, CD₃OD) δ$_C$ 183.4(C), 143.1(C), 139.6(C), 137.5(C), 129.8(CH), 128.1(C), 127.3(CH), 126.4(CH), 124.1(CH), 123.2(CH), 122.9(CH), 120.3(CH), 116.5(C), 113.1(CH), 111.8(CH),55.7(CH).

Appendix

Equation to determine rate of iminium ion formation

For a reaction where the initial concentration of A and B are identical

$$A + B \rightarrow P \tag{1}$$

Where A and B are the starting materials and P is the product the rate of the reaction is given by

$$-\frac{d[A]}{dt} = k \times [A][B] \tag{2}$$

This can be rewritten as

$$-\frac{d[A]}{dt} = k \times [A]^2 \tag{3}$$

Through mathematical separation of the variables and integration gives

$$\frac{1}{[A]} = kt + C \tag{4}$$

Provided that $[A] = [A]_0$ at $t = 0$ the constant of integration becomes $1/[A]_0$ and therefore the integrated second order equation becomes

$$\frac{1}{[A]} - \frac{1}{[A]_o} = kt \tag{5}$$

A plot of $1/[A]$ *vs* t should therefore be a straight line for a second order process and have slope k. The rate constants k were measured using data points up to 50% conversion.

Equation to determine the rate constant of the Diels-Alder cycloaddition

For the reaction where the initial concentration of A and B are in equivalent the variable x is introduced to give.

$$\frac{dx}{dt} = k([A]_0 - x)([B]_0 - x) \tag{6}$$

x is the decrease in the concentration of A and B therefore $[A]_0 - x = [A]$ and $[B]_0 - x = [B]$. If equation is treated mathematically with separation of the variables and partial fraction expansion it can then be integrated to give

$$\frac{1}{[A]_0 - [B]_0} \ln \frac{[A]_0 - x}{[B]_0 - x} = kt + C \tag{7}$$

The constant of integration C can then be found using the condition $x = 0$ when $t = 0$ by equation (8)

$$C = \frac{1}{[A]_0 - [B]_0} \ln \frac{[A]_0}{[B]_0} \tag{8}$$

When this is substituted into equation (7) we get

$$\ln \frac{[A]_0 - x}{[B]_0 - x} = kt([A]_0 - [B]_0) + \ln \frac{[A]_0}{[B]_0} \tag{9}$$

Therefore if [A] > [B] then a plot of $\ln(([A]_0-x)/([B]_0-x))$ *vs* t will have positive slope, equal to $([A]_0 - [B]_0)k$. The rate constant k was measured using data points up to 50% conversion.

The Arrhenius Equation

The Arrhenius equation relates rate to activation energy is often written in the form

$$\ln k = -\frac{E_a}{RT} + \ln A$$

<div align="right">(10)</div>

Where k is the rate constant, E_a is the activation energy, R is the gas constant, T is the temperature and A is the Arrhenius pre-exponential factor. Using this equation a plot of $\ln k$ vs $1/T$ gives a slope of $-E_a/R$ with an intercept lnA.

NOSEY CD₃CN, 500 MHz **122**.

g-NOESY
500 MHz

ppm

BRUKER

203

Progress of reaction for iminium ion formation (293K Run 1)
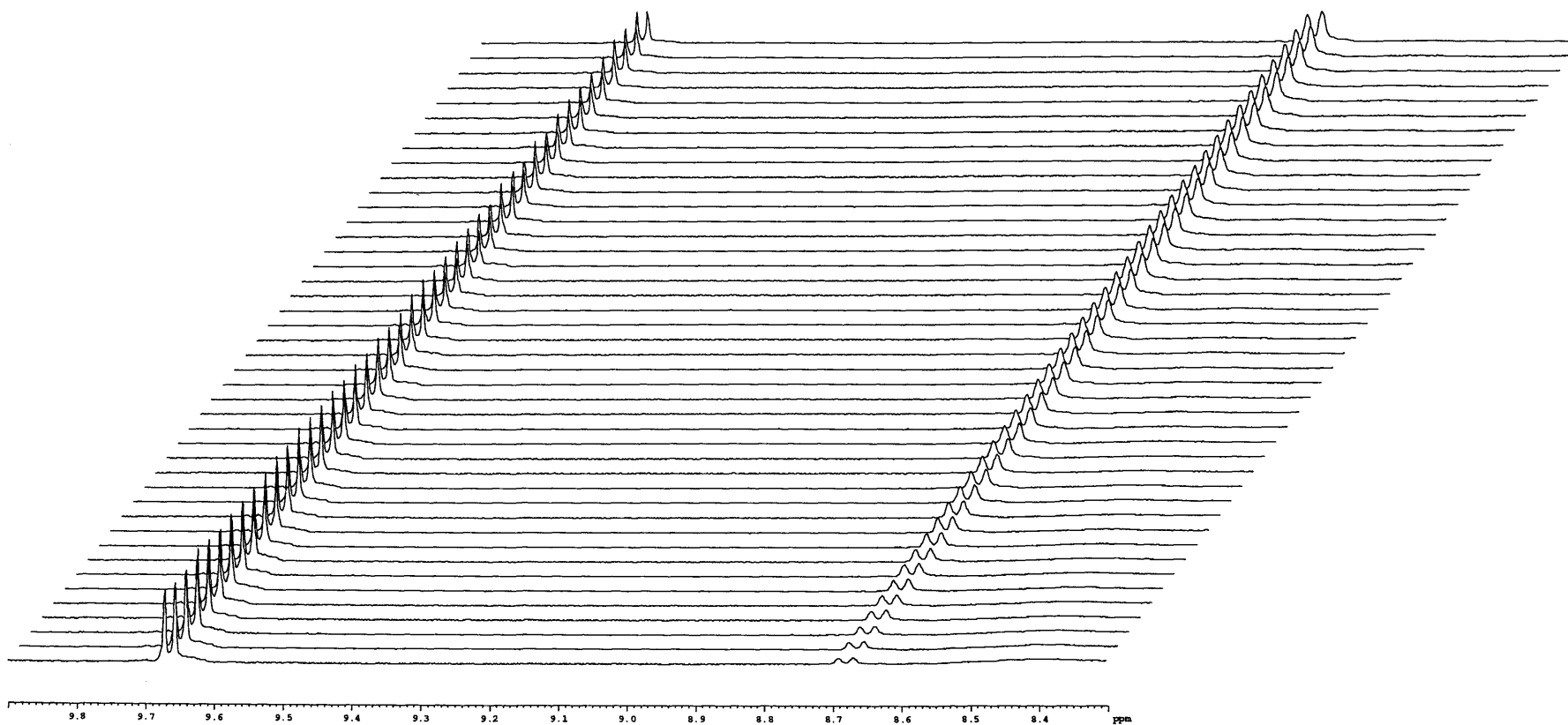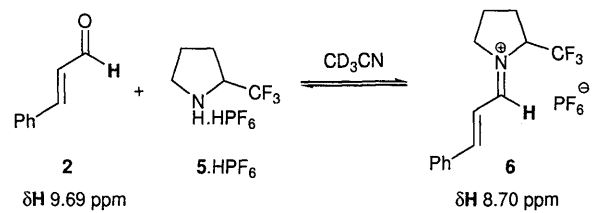
2nd Order Rate Plot for Iminium Ion formation at 293K
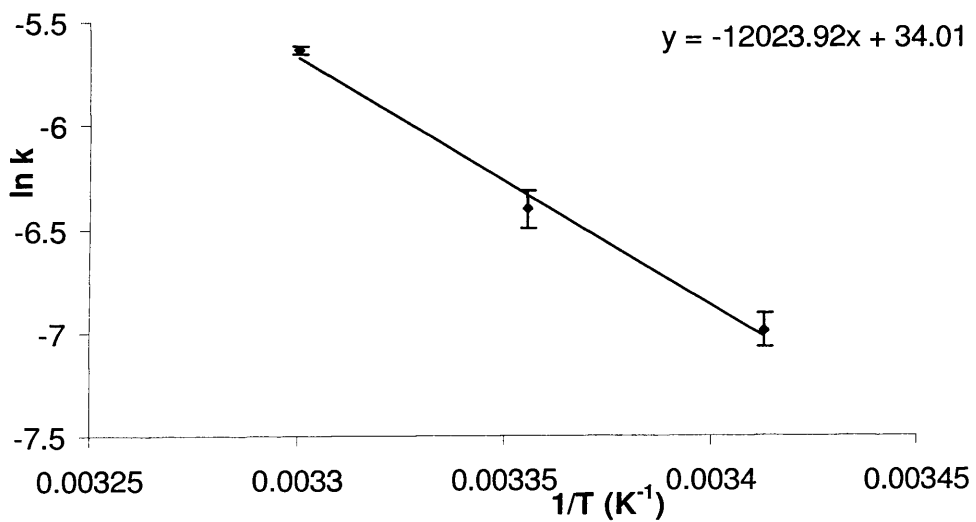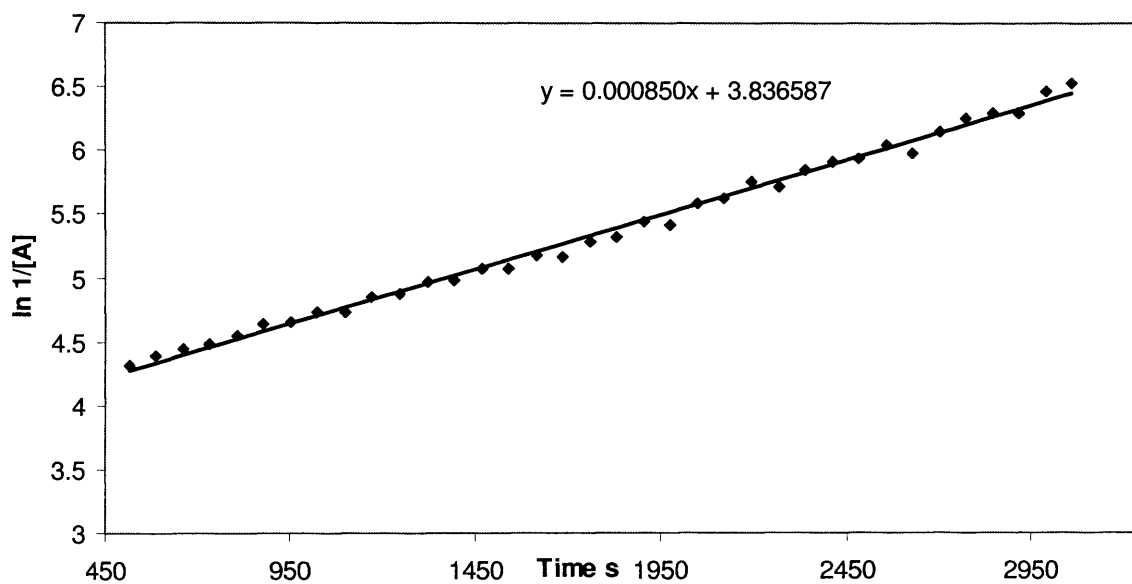
$y = 0.000850x + 3.836587$

$y = -12023.92x + 34.01$

Kinetic data for iminium ion formation at 293K (Run 1)

ne	Integration cinnamaldehyde	Integration iminium	Total integration	Integration cinnamaldehyde/ Total integration	Integration iminium/Total integration	[Iminium]	1/[Imini
)	1	0	1	1	1	0	0
4	1	0.0786616	1.0786616	0.927074812	0.072925188	0.018231297	54.85C
7	0.975638	0.0954952	1.0711332	0.910846569	0.089153431	0.022288358	44.866
0	0.974936	0.106356	1.081292	0.90163989	0.09836011	0.024590027	40.666
3	0.959829	0.116821	1.07665	0.891495844	0.108504156	0.027126039	36.864
6	0.965788	0.133105	1.098893	0.878873557	0.121126443	0.030281611	33.02C
9	0.937286	0.148708	1.085994	0.863067383	0.136932617	0.034233154	29.211
2	0.930808	0.153153	1.083961	0.858709861	0.141290139	0.035322535	28.31C
25	0.931484	0.170722	1.102206	0.845108809	0.154891191	0.038722798	25.824
98	0.8834	0.160245	1.043645	0.84645641	0.15354359	0.038385898	26.051
71	0.902673	0.192012	1.094685	0.824596117	0.175403883	0.043850971	22.804
44	0.881297	0.192969	1.074266	0.820371305	0.179628695	0.044907174	22.266
17	0.876085	0.211909	1.087994	0.805229624	0.194770376	0.048692594	20.5C
90	0.848822	0.207038	1.05586	0.803915292	0.196084708	0.049021177	20.39C
63	0.866961	0.232523	1.099484	0.788516249	0.211483751	0.052870938	18.91C
36	0.829297	0.221371	1.050668	0.789304519	0.210695481	0.05267387	18.984
09	0.810011	0.237827	1.047838	0.773030755	0.226969245	0.056742311	17.62C
82	0.808783	0.235496	1.044279	0.774489385	0.225510615	0.056377654	17.737
55	0.798519	0.256306	1.054825	0.757015619	0.242984381	0.060746095	16.461
28	0.780611	0.259038	1.039649	0.750840909	0.249159091	0.062289773	16.0C
01	0.803918	0.289411	1.093329	0.735293768	0.264706232	0.066176558	15.111
74	0.790241	0.27926	1.069501	0.738887575	0.261112425	0.065278106	15.31C
47	0.783533	0.309042	1.092575	0.717143446	0.282856554	0.070714139	14.141
20	0.767473	0.312511	1.079984	0.710633676	0.289366324	0.072341581	13.82C
93	0.764613	0.336035	1.100648	0.69469349	0.30530651	0.076326628	13.101
66	0.745143	0.320089	1.065232	0.699512407	0.300487593	0.075121898	13.31
39	0.72069	0.332389	1.053079	0.684364611	0.315635389	0.078908847	12.672
2	0.715529	0.342035	1.057564	0.676582221	0.323417779	0.080854445	12.36
35	0.727121	0.351789	1.07891	0.673940366	0.326059634	0.081514909	12.267
38	0.724685	0.371061	1.095746	0.661362214	0.338637786	0.084659447	11.812
31	0.709422	0.350005	1.059427	0.669628016	0.330371984	0.082592996	12.107
04	0.685013	0.368386	1.053399	0.650288257	0.349711743	0.087427936	11.437

206

777	0.67552	0.379978	1.055498	0.640001213	0.359998787	0.089999697	11.111
350	0.695931	0.39885	1.094781	0.635680561	0.364319439	0.09107986	10.979
923	0.669385	0.383779	1.053164	0.635594266	0.364405734	0.091101433	10.976
996	0.666577	0.410277	1.076854	0.619004062	0.380995938	0.095248985	10.498
069	0.644206	0.407436	1.051642	0.612571579	0.387428421	0.096857105	10.324

Kinetic data for iminium ion formation at 293K (Run 1)

[Cinnamaldehyde]	1/[Cinnamaldehyde]	Time	1/[Cinnamaldehyde]	Time	Conversion to iminium
0.25	1	0	4	0	0
0.231769	4.314646	514	4.314646	514	119.1291
0.227712	4.391519	587	4.391519	587	133.6667
0.22541	4.436361	660	4.436361	660	148.7706
0.222874	4.486841	733	4.486841	733	163.3666
0.219718	4.55128	806	4.55128	806	177.093
0.215767	4.634632	879	4.634632	879	189.6591
0.214677	4.658151	952	4.658151	952	204.3729
0.211277	4.733118	1025	4.733118	1025	216.5591
0.211614	4.725583	1098	4.725583	1098	232.3523
0.206149	4.85086	1171	4.85086	1171	241.4005
0.205093	4.875841	1244	4.875841	1244	255.1355
0.201307	4.967527	1317	4.967527	1317	265.1219
0.200979	4.975649	1390	4.975649	1390	279.3606
0.197129	5.072819	1463	5.072819	1463	288.3998
0.197326	5.067753	1536	5.067753	1536	303.0929
0.193258	5.174438	1609	5.174438	1609	310.9516
0.193622	5.164693	1682	5.164693	1682	325.6728
0.189254	5.283907	1755	5.283907	1755	332.1406
0.18771	5.32736	1828	5.32736	1828	343.1343
0.183823	5.440003	1901	5.440003	1901	349.4484
0.184722	5.413543	1974	5.413543	1974	364.641
0.179286	5.577685	2047	5.577685	2047	366.9982
0.177658	5.628779	2120	5.628779	2120	376.6358
0.173673	5.757935	2193	5.757935	2193	380.8657
0.174878	5.718269	2266	5.718269	2266	396.2738
0.171091	5.844838	2339	5.844838	2339	400.1822
0.169146	5.912068	2412	5.912068	2412	407.9791
0.168485	5.935243	2485	5.935243	2485	418.6855
0.165341	6.048123	2558	6.048123	2558	422.9411
0.167407	5.973466	2631	5.973466	2631	440.4478
0.162572	6.151118	2704	6.151118	2704	439.5949
0.16	6.249988	2777	6.249988	2777	444.3208
0.15892	6.292469	2850	6.292469	2850	452.9224

0.158899	6.293323	2923	6.293323	2923	464.4605
0.154751	6.461993	2996	6.461993	2996	463.634
0.153143	6.529849	3069	6.529849	3069	469.9955
0.231769	4.314646	514	4.314646	514	119.1291
0.227712	4.391519	587	4.391519	587	133.6667
0.22541	4.436361	660	4.436361	660	148.7706
0.222874	4.486841	733	4.486841	733	163.3666
0.219718	4.55128	806	4.55128	806	177.093
0.215767	4.634632	879	4.634632	879	189.6591
0.214677	4.658151	952	4.658151	952	204.3729

Kinetic data for iminium ion formation at 293K (Run 2)

me	Integration cinnamaldehyde	Integration iminium	Total integration	Integration cinnamaldehyde / Total integration	Integration iminium/ Total integration	[iminium]	1/[iminiu
)	1	0	1	1	1	0	0
:2	1	0.0525211	1.052521	0.9501	0.049900282	0.012475071	80.159E
)5	0.976773	0.0563195	1.033093	0.945485	0.054515448	0.013628862	73.373
i8	0.954415	0.0573704	1.011785	0.943298	0.056702143	0.014175536	70.544C
l1	0.950905	0.0833145	1.03422	0.919442	0.080557851	0.020139463	49.6537
4	0.935718	0.102005	1.037723	0.901703	0.098296944	0.024574236	40.693C
i7	0.927286	0.117216	1.044502	0.887778	0.112221901	0.028055475	35.6436
i0	0.906985	0.133437	1.040422	0.871747	0.128252767	0.032063192	31.1884
i3	0.906053	0.152904	1.058957	0.855609	0.144391132	0.036097783	27.702E
)6	0.896053	0.161474	1.057527	0.84731	0.152690191	0.038172548	26.196E
'9	0.868374	0.171544	1.039918	0.835041	0.16495916	0.04123979	24.2484
i2	0.858046	0.176109	1.034155	0.829707	0.170292654	0.042573164	23.488S
25	0.854173	0.195951	1.050124	0.813402	0.186597964	0.046649491	21.4364
38	0.833209	0.209131	1.04234	0.799364	0.200636069	0.050159017	19.936E
71	0.821795	0.222229	1.044024	0.787142	0.212858134	0.053214533	18.791E
44	0.804798	0.229205	1.034003	0.778332	0.221667635	0.055416909	18.045C
17	0.787319	0.230004	1.017323	0.773913	0.226087486	0.056521872	17.692Z
30	0.777969	0.24731	1.025279	0.758788	0.241212392	0.060303098	16.582!
63	0.774994	0.259439	1.034433	0.749197	0.250803097	0.062700774	15.9487
36	0.785654	0.268687	1.054341	0.745161	0.254838805	0.063709701	15.696:
09	0.749746	0.283626	1.033372	0.725533	0.274466504	0.068616626	14.5737
32	0.728995	0.274805	1.0038	0.726235	0.273764694	0.068441174	14.611C
55	0.725611	0.299039	1.02465	0.708155	0.29184502	0.072961255	13.705!
28	0.717782	0.306193	1.023975	0.700976	0.299023902	0.074755975	13.376E
01	0.700969	0.306338	1.007307	0.695884	0.304115826	0.076028956	13.152E
74	0.696942	0.328612	1.025554	0.679576	0.320423888	0.080105972	12.4834
47	0.690886	0.32511	1.015996	0.680009	0.319991417	0.079997854	12.500:
20	0.695492	0.346814	1.042306	0.667263	0.332737219	0.083184305	12.021!
93	0.663821	0.338093	1.001914	0.662553	0.337447126	0.084361782	11.8537
66	0.668502	0.360286	1.028788	0.649796	0.350204318	0.08755108	11.421!
39	0.649619	0.353584	1.003203	0.647545	0.352455086	0.088113772	11.348S
l2	0.654922	0.361241	1.016163	0.644505	0.355495132	0.088873783	11.251S

35	0.640255	0.38727	1.027525	0.623104	0.376895939	0.094223985	10.613C
58	0.629395	0.396955	1.02635	0.613236	0.386763775	0.096690944	10.3422
31	0.630692	0.402422	1.033114	0.610477	0.389523325	0.097380831	10.2689
04	0.612024	0.398681	1.010705	0.605542	0.394458324	0.098614581	10.1404
77	0.608491	0.407083	1.015574	0.59916	0.400840313	0.100210078	9.97903
50	0.58768	0.408425	0.996105	0.589978	0.410022036	0.102505509	9.75557
23	0.5987	0.425149	1.023849	0.584754	0.415245803	0.103811451	9.63284
96	0.592189	0.43644	1.028629	0.575707	0.424292918	0.10607323	9.42744
69	0.587037	0.439659	1.026696	0.571773	0.428227051	0.107056763	9.34083
42	0.578097	0.449466	1.027563	0.56259	0.437409677	0.109352419	9.14474
15	0.559014	0.438187	0.997201	0.560583	0.439416928	0.109854232	9.10297

Kinetic data for iminium ion formation at 293K (Run 2)

[Cinnamaldehyde]	1/[Cinnamaldehyde]	Time	1/[Cinnamaldehyde]	Time	Conversion to iminium
0.25	1	0	4	0	0
0.237525	4.210084	222	4.210084	222	0.049900282
0.236371	4.230635	295	4.230635	295	0.054515448
0.235824	4.240442	368	4.240442	368	0.056702143
0.229861	4.350464	441	4.350464	441	0.080557851
0.225426	4.43605	514	4.43605	514	0.098296944
0.221945	4.50563	587	4.50563	587	0.112221901
0.217937	4.588486	660	4.588486	660	0.128252767
0.213902	4.675033	733	4.675033	733	0.144391132
0.211827	4.720823	806	4.720823	806	0.152690191
0.20876	4.790185	879	4.790185	879	0.16495916
0.207427	4.820977	952	4.820977	952	0.170292654
0.203351	4.917617	1025	4.917617	1025	0.186597964
0.199841	5.003979	1098	5.003979	1098	0.200636069
0.196785	5.081676	1171	5.081676	1171	0.212858134
0.194583	5.139193	1244	5.139193	1244	0.221667635
0.193478	5.168543	1317	5.168543	1317	0.226087486
0.189697	5.271567	1390	5.271567	1390	0.241212392
0.187299	5.33905	1463	5.33905	1463	0.250803097
0.18629	5.367966	1536	5.367966	1536	0.254838805
0.181383	5.513184	1609	5.513184	1609	0.274466504
0.181559	5.507857	1682	5.507857	1682	0.273764694
0.177039	5.648481	1755	5.648481	1755	0.29184502
0.175244	5.706329	1828	5.706329	1828	0.299023902
0.173971	5.748083	1901	5.748083	1901	0.304115826
0.169894	5.886022	1974	5.886022	1974	0.320423888
0.170002	5.882279	2047	5.882279	2047	0.319991417
0.166816	5.99464	2120	5.99464	2120	0.332737219
0.165638	6.037254	2193	6.037254	2193	0.337447126
0.162449	6.155781	2266	6.155781	2266	0.350204318
0.161886	6.177178	2339	6.177178	2339	0.352455086
0.161126	6.206315	2412	6.206315	2412	0.355495132
0.155776	6.419473	2485	6.419473	2485	0.376895939
0.153309	6.522772	2558	6.522772	2558	0.386763775
0.152619	6.552257	2631	6.552257	2631	0.389523325
0.151385	6.605656	2704	6.605656	2704	0.394458324

0.14979	6.676017	2777	6.676017	2777	0.400840313
0.147494	6.779914	2850	6.779914	2850	0.410022036
0.146189	6.840481	2923	6.840481	2923	0.415245803
0.143927	6.947978	2996	6.947978	2996	0.424292918
0.142943	6.995784	3069	6.995784	3069	0.428227051
0.140648	7.109969	3142	7.109969	3142	0.437409677
0.140146	7.135428	3215	7.135428	3215	0.439416928

Kinetic data for iminium ion formation at 298K (Run 1)

Time	Integration cinnamaldehyde	Integration iminium	Total integration	Integration Iminium/ Total Integration	Integration Cinnamaldehyde/ Total Integration	[iminium]	1/[iminiun
0	1	0	1	0	1	0	0
148	1	0.0381273	1.038127	0.036726999	0.963273	0.00918175	108.9117
221	0.977101	0.068101	1.045202	0.065155826	0.934844	0.016288957	61.3912C
294	0.944072	0.0890635	1.033136	0.086206988	0.913793	0.021551747	46.39995
367	0.927927	0.110772	1.038699	0.106644947	0.893355	0.026661237	37.50764
440	0.901843	0.136438	1.038281	0.131407586	0.868592	0.032851897	30.43964
513	0.895628	0.159392	1.05502	0.1510796	0.84892	0.0377699	26.47611
586	0.880292	0.172619	1.052911	0.163944531	0.836055	0.040986133	24.3985
659	0.851433	0.202143	1.053576	0.19186371	0.808136	0.047965927	20.84813
732	0.833351	0.204827	1.038178	0.197294684	0.802705	0.049323671	20.27424
805	0.825531	0.214549	1.04008	0.206281248	0.793719	0.051570312	19.391
878	0.799671	0.246174	1.045845	0.235382872	0.764617	0.058845718	16.99359
951	0.789724	0.262774	1.052498	0.249666983	0.750333	0.062416746	16.02134
1024	0.777948	0.277229	1.055177	0.262732224	0.737268	0.065683056	15.22463
1097	0.760145	0.299082	1.059227	0.282358739	0.717641	0.070589685	14.16638
1170	0.735175	0.30465	1.039825	0.292981992	0.707018	0.073245498	13.65272
1243	0.730068	0.316186	1.046254	0.302207686	0.697792	0.075551921	13.23593
1316	0.694745	0.323989	1.018734	0.318031007	0.681969	0.079507752	12.57739
1389	0.701208	0.341494	1.042702	0.327508723	0.672491	0.081877181	12.21342
1462	0.692057	0.360264	1.052321	0.342351811	0.657648	0.085587953	11.68389
1535	0.685448	0.376786	1.062234	0.354710921	0.645289	0.08867773	11.27679
1608	0.673502	0.386399	1.059901	0.364561407	0.635439	0.091140352	10.97209
1681	0.644835	0.387832	1.032667	0.375563468	0.624437	0.093890867	10.65066
1754	0.634209	0.410421	1.04463	0.392886477	0.607114	0.098221619	10.18106
1827	0.619857	0.407543	1.0274	0.396674129	0.603326	0.099168532	10.08384
1900	0.604452	0.409388	1.01384	0.403799416	0.596201	0.100949854	9.905908
1973	0.615885	0.441054	1.056939	0.417293713	0.582706	0.104323428	9.585575
2046	0.593532	0.435814	1.029346	0.42338922	0.576611	0.105847305	9.447572
2119	0.581948	0.454921	1.036869	0.438744914	0.561255	0.109686228	9.116915
2192	0.5725	0.465287	1.037787	0.448345373	0.551655	0.112086343	8.921693
2265	0.555753	0.478724	1.034477	0.462769109	0.537231	0.115692277	8.64361S
2338	0.557002	0.483413	1.040415	0.464634785	0.535365	0.116158696	8.608912

214

2411	0.54596	0.490692	1.036652	0.473343031	0.526657	0.118335758	8.450531
2484	0.547975	0.503603	1.051578	0.478902183	0.521098	0.119725546	8.352436
2557	0.509369	0.477541	0.98691	0.483874923	0.516125	0.120968731	8.266599
2630	0.512666	0.504277	1.016943	0.495875383	0.504125	0.123968846	8.066543
2703	0.510927	0.51026	1.021187	0.499673419	0.500327	0.124918355	8.005229
2776	0.502922	0.523368	1.02629	0.509961122	0.490039	0.127490281	7.843735
2849	0.488333	0.528361	1.016694	0.519685372	0.480315	0.129921343	7.696965
2922	0.479294	0.537184	1.016478	0.528475776	0.471524	0.132118944	7.568937
2995	0.481056	0.547697	1.028753	0.532389213	0.467611	0.133097303	7.5133
3068	0.476493	0.56941	1.045903	0.544419511	0.45558	0.136104878	7.347275
3141	0.469258	0.556244	1.025502	0.542411424	0.457589	0.135602856	7.374476

Kinetic data for iminium ion formation at 298K (Run 1)

[Cinnamaldehyde]	1/[Cinnamaldehyde]	Time	1/[Cinnamaldehyde]	Time	Conversion to iminium
0.25	4	0	4	0	0
0.240818	4.152509	148	4.152509	148	0.036727
0.233711	4.278788	221	4.278788	221	0.065156
0.228448	4.377359	294	4.377359	294	0.086207
0.223339	4.477503	367	4.477503	367	0.106645
0.217148	4.605152	440	4.605152	440	0.131408
0.21223	4.711867	513	4.711867	513	0.15108
0.209014	4.784372	586	4.784372	586	0.163945
0.202034	4.94966	659	4.94966	659	0.191864
0.200676	4.983149	732	4.983149	732	0.197295
0.19843	5.039568	805	5.039568	805	0.206281
0.191154	5.231376	878	5.231376	878	0.235383
0.187583	5.330966	951	5.330966	951	0.249667
0.184317	5.425437	1024	5.425437	1024	0.262732
0.17941	5.573816	1097	5.573816	1097	0.282359
0.176755	5.657565	1170	5.657565	1170	0.292982
0.174448	5.732365	1243	5.732365	1243	0.302208
0.170492	5.865369	1316	5.865369	1316	0.318031
0.168123	5.948033	1389	5.948033	1389	0.327509
0.164412	6.082279	1462	6.082279	1462	0.342352
0.161322	6.198772	1535	6.198772	1535	0.354711
0.15886	6.294865	1608	6.294865	1608	0.364561
0.156109	6.405775	1681	6.405775	1681	0.375563
0.151778	6.588554	1754	6.588554	1754	0.392886
0.150831	6.629916	1827	6.629916	1827	0.396674
0.14905	6.709151	1900	6.709151	1900	0.403799
0.145677	6.864522	1973	6.864522	1973	0.417294
0.144153	6.937088	2046	6.937088	2046	0.423389
0.140314	7.126884	2119	7.126884	2119	0.438745
0.137914	7.250914	2192	7.250914	2192	0.448345
0.134308	7.445588	2265	7.445588	2265	0.462769
0.133841	7.471535	2338	7.471535	2338	0.464635
0.131664	7.595077	2411	7.595077	2411	0.473343
0.130274	7.676102	2484	7.676102	2484	0.478902

0.129031	7.750059	2557	7.750059	2557	0.483875
0.126031	7.934546	2630	7.934546	2630	0.495875
0.125082	7.994778	2703	7.994778	2703	0.499673
0.12251	8.162618	2776	8.162618	2776	0.509961
0.120079	8.327875	2849	8.327875	2849	0.519685
0.117881	8.483127	2922	8.483127	2922	0.528476
0.116903	8.554123	2995	8.554123	2995	0.532389
0.113895	8.780007	3068	8.780007	3068	0.54442
0.114397	8.741477	3141	8.741477	3141	0.542411

Kinetic data for iminium ion formation at 298K (Run 2)

me	Integration cinnamaldehyde	Integration iminium	Total integration	Integration iminium/ Total integration	Integration cinnamaldehyde/ Total integration	[Iminium]	1/[Iminium
0	1		1	0	1	0	0
16	1	0.0705531	1.070553	0.06590341	0.934097	0.016475853	60.69489
89	0.973304	0.104543	1.077847	0.09699243	0.903008	0.024248108	41.24033
62	0.948847	0.128629	1.077476	0.119379921	0.88062	0.02984498	33.50647
35	0.910521	0.150602	1.061123	0.141926996	0.858073	0.035481749	28.1835
08	0.896143	0.172831	1.068974	0.16167933	0.838321	0.040419832	24.74033
81	0.874285	0.192482	1.066767	0.180434903	0.819565	0.045108726	22.16866
54	0.849718	0.217178	1.066896	0.203560609	0.796439	0.050890152	19.65017
27	0.831153	0.235786	1.066939	0.220992953	0.779007	0.055248238	18.10012
00	0.800476	0.242617	1.043093	0.232593834	0.767406	0.058148458	17.19736
73	0.78471	0.280492	1.065202	0.263322825	0.736677	0.065830706	15.19048
46	0.770275	0.297911	1.068186	0.278894312	0.721106	0.069723578	14.34235
19	0.74892	0.308191	1.057111	0.291540813	0.708459	0.072885203	13.72021
92	0.724236	0.316609	1.040845	0.304184581	0.695815	0.076046145	13.14991
65	0.727113	0.351275	1.078388	0.325740828	0.674259	0.081435207	12.2797
38	0.69251	0.351875	1.044385	0.336920772	0.663079	0.084230193	11.87223
11	0.65095	0.352897	1.003847	0.351544608	0.648455	0.087886152	11.37836
84	0.678897	0.39428	1.073177	0.367395127	0.632605	0.091848782	10.88746
57	0.635938	0.390678	1.026616	0.3805493	0.619451	0.095137325	10.51112
30	0.638093	0.425213	1.063306	0.399897113	0.600103	0.099974278	10.00257
03	0.620677	0.428597	1.049274	0.408470047	0.59153	0.102117512	9.79264
76	0.622848	0.440722	1.06357	0.414379872	0.58562	0.103594968	9.652979
49	0.569515	0.438564	1.008079	0.435049237	0.564951	0.108762309	9.194362
22	0.586092	0.464447	1.050539	0.44210353	0.557896	0.110525882	9.047655
95	0.586715	0.483447	1.070162	0.45175123	0.548249	0.112937808	8.854431
68	0.577458	0.488218	1.065676	0.458129863	0.54187	0.114532466	8.731149
41	0.545846	0.494477	1.040323	0.475311033	0.524689	0.118827758	8.415542
14	0.542624	0.508636	1.05126	0.483834637	0.516165	0.120958659	8.267287
87	0.545096	0.503786	1.048882	0.480307604	0.519692	0.120076901	8.327996
60	0.530972	0.528254	1.059226	0.498716988	0.501283	0.124679247	8.020581
33	0.510325	0.5307	1.041025	0.509786028	0.490214	0.127446507	7.846429
06	0.506187	0.536307	1.042494	0.514446126	0.485554	0.128611532	7.775353

479	0.507857	0.547137	1.054994	0.51861622	0.481384	0.129654055	7.712832
552	0.499314	0.56139	1.060704	0.529261698	0.470738	0.132315424	7.557698
625	0.486593	0.560334	1.046927	0.535217833	0.464782	0.133804458	7.473593
698	0.476103	0.568149	1.044252	0.544072695	0.455927	0.136018174	7.351959
771	0.468767	0.586491	1.055258	0.555779724	0.44422	0.138944931	7.197096
844	0.445948	0.583674	1.029622	0.566881827	0.433118	0.141720457	7.056144
917	0.452698	0.606701	1.059399	0.572684135	0.427316	0.143171034	6.984653
990	0.453399	0.582676	1.036075	0.562387858	0.437612	0.140596965	7.112529
063	0.44701	0.599515	1.046525	0.572862569	0.427137	0.143215642	6.982478
136	0.427333	0.612589	1.039922	0.589072065	0.410928	0.147268016	6.790341
209	0.425571	0.61778	1.043351	0.59211138	0.407889	0.148027845	6.755486

Kinetic data for iminium ion formation at 298K (Run 2)

[Cinnamaldehyde]	1/[Cinnamaldehyde]	Time	1/[Cinnamaldehyde]	Time	Conversion to iminium
0.25	4	0	4	0	0
0.233524	4.282212	216	4.282212	216	0.065903
0.225752	4.429642	289	4.429642	289	0.096992
0.220155	4.542254	362	4.542254	362	0.11938
0.214518	4.661608	435	4.661608	435	0.141927
0.20958	4.771444	508	4.771444	508	0.161679
0.204891	4.880637	581	4.880637	581	0.180435
0.19911	5.022353	654	5.022353	654	0.203561
0.194752	5.134742	727	5.134742	727	0.220993
0.191852	5.212364	800	5.212364	800	0.232594
0.184169	5.429787	873	5.429787	873	0.263323
0.180276	5.547037	946	5.547037	946	0.278894
0.177115	5.646056	1019	5.646056	1019	0.291541
0.173954	5.748651	1092	5.748651	1092	0.304185
0.168565	5.932437	1165	5.932437	1165	0.325741
0.16577	6.032462	1238	6.032462	1238	0.336921
0.162114	6.168504	1311	6.168504	1311	0.351545
0.158151	6.323062	1384	6.323062	1384	0.367395
0.154863	6.457334	1457	6.457334	1457	0.380549
0.150026	6.665524	1530	6.665524	1530	0.399897
0.147882	6.762126	1603	6.762126	1603	0.40847
0.146405	6.830366	1676	6.830366	1676	0.41438
0.141238	7.080263	1749	7.080263	1749	0.435049
0.139474	7.169789	1822	7.169789	1822	0.442104
0.137062	7.295958	1895	7.295958	1895	0.451751
0.135468	7.381842	1968	7.381842	1968	0.45813
0.131172	7.623564	2041	7.623564	2041	0.475311
0.129041	7.749455	2114	7.749455	2114	0.483835
0.129923	7.696861	2187	7.696861	2187	0.480308
0.125321	7.979524	2260	7.979524	2260	0.498717
0.122553	8.159702	2333	8.159702	2333	0.509786
0.121388	8.238015	2406	8.238015	2406	0.514446
0.120346	8.309378	2479	8.309378	2479	0.518616
0.117685	8.49729	2552	8.49729	2552	0.529262

0.116196	8.606182	2625	8.606182	2625	0.535218
0.113982	8.773328	2698	8.773328	2698	0.544073
0.111055	9.004542	2771	9.004542	2771	0.55578
0.10828	9.235355	2844	9.235355	2844	0.566882
0.106829	9.360757	2917	9.360757	2917	0.572684
0.109403	9.140514	2990	9.140514	2990	0.562388
0.106784	9.364667	3063	9.364667	3063	0.572863
0.102732	9.734067	3136	9.734067	3136	0.589072
0.101972	9.806599	3209	9.806599	3209	0.592111

Kinetic data for iminium ion formation at 303K (Run 1)

ıe	Integration cinnamaldehyde	Integration iminium	Total integration	Integration iminium/ Total integration	Integration cinnamaldehyde/ Total integration	[Iminium]	1/[Imini
	1	1	1	0	1	0	0
3	1	0.0901037	1.090104	0.082656081	0.917344	0.02066402	48.393
5	0.964781	0.143097	1.107878	0.129163139	0.870837	0.032290785	30.968
9	0.907487	0.178053	1.08554	0.164022514	0.835977	0.041005629	24.38€
2	0.856561	0.241803	1.098364	0.22014833	0.779852	0.055037082	18.169
5	0.819382	0.275352	1.094734	0.251524115	0.748476	0.062881029	15.903
3	0.760271	0.286789	1.04706	0.273899299	0.726101	0.068474825	14.603
1	0.745521	0.335275	1.080796	0.310211178	0.689789	0.077552794	12.894
4	0.703929	0.368981	1.07291	0.343906758	0.656093	0.08597669	11.631
7	0.668953	0.395704	1.064657	0.371672755	0.628327	0.092918189	10.762
)	0.627587	0.410407	1.037994	0.395384752	0.604615	0.098846188	10.116
3	0.637699	0.457356	1.095055	0.417655734	0.582344	0.104413934	9.5772
5	0.616577	0.471962	1.088539	0.433573809	0.566426	0.108393452	9.225€
9	0.604825	0.507397	1.112222	0.45620119	0.543799	0.114050298	8.7680
2	0.566877	0.530449	1.097326	0.483401469	0.516599	0.120850367	8.2746
5	0.544459	0.529283	1.073742	0.492933125	0.507067	0.123233281	8.1146
8	0.539165	0.553629	1.092794	0.506617899	0.493382	0.126654475	7.8954
1	0.510997	0.563222	1.074219	0.524308358	0.475692	0.131077089	7.6290
4	0.482115	0.580638	1.062753	0.546352727	0.453647	0.136588182	7.3212
7	0.473249	0.598312	1.071561	0.558355521	0.441644	0.13958888	7.1638
0	0.479658	0.605995	1.085653	0.558184798	0.441815	0.139546199	7.1660
3	0.444531	0.61556	1.060091	0.580667131	0.419333	0.145166783	6.8886
6	0.452681	0.626872	1.079553	0.580677373	0.419323	0.145169343	6.8885
9	0.426774	0.643525	1.070299	0.601257219	0.398743	0.150314305	6.6527
2	0.43909	0.653521	1.092611	0.598127787	0.401872	0.149531947	6.6875
5	0.420399	0.655627	1.076026	0.60930405	0.390696	0.152326013	6.5648
3	0.388653	0.655905	1.044558	0.627925879	0.372074	0.15698147	6.3701
1	0.384896	0.678521	1.063417	0.638057319	0.361943	0.15951433	6.2690
4	0.379119	0.695412	1.074531	0.647177234	0.352823	0.161794308	6.1806
7	0.38128	0.687933	1.069213	0.643401268	0.356599	0.160850317	6.216९
)	0.358461	0.692381	1.050842	0.658882115	0.341118	0.164720529	6.0708
3	0.350027	0.689689	1.039716	0.663343644	0.336656	0.165835911	6.0300

406	0.341765	0.71051	1.052275	0.675213228	0.324787	0.168803307	5.9240
479	0.328437	0.718539	1.046976	0.686299399	0.313701	0.17157485	5.828₃
552	0.342062	0.728263	1.070325	0.680412959	0.319587	0.17010324	5.8787
525	0.325008	0.719611	1.044619	0.688874125	0.311126	0.172218531	5.8065
598	0.322701	0.727793	1.050494	0.69281024	0.30719	0.17320256	5.7735
771	0.314953	0.738144	1.053097	0.700926885	0.299073	0.175231721	5.7067
844	0.308657	0.742736	1.051393	0.706430421	0.29357	0.176607605	5.662₂
917	0.304859	0.744226	1.049085	0.709404862	0.290595	0.177351216	5.6385
990	0.298109	0.747843	1.045952	0.714987877	0.285012	0.178746969	5.594
063	0.283406	0.748465	1.031871	0.725347451	0.274653	0.181336863	5.5145
36	0.283381	0.745474	1.028855	0.72456663	0.275433	0.181141657	5.5205

Kinetic data for iminium ion formation at 303K (Run 1)

[Cinnamaldehyde]	1/[Cinnamaldehyde]	Time	1/[Cinnamaldehyde]	Time	Conversion to iminium
0.25	4	0	4	0	0
0.229336	4.360415	143	4.360415	143	0.082656
0.217709	4.593283	216	4.593283	216	0.129163
0.208994	4.784818	289	4.784818	289	0.164023
0.194963	5.129181	362	5.129181	362	0.220148
0.187119	5.344194	435	5.344194	435	0.251524
0.181525	5.508878	508	5.508878	508	0.273899
0.172447	5.798876	581	5.798876	581	0.310211
0.164023	6.096694	654	6.096694	654	0.343907
0.157082	6.366109	727	6.366109	727	0.371673
0.151154	6.615778	800	6.615778	800	0.395385
0.145586	6.868789	873	6.868789	873	0.417656
0.141607	7.06182	946	7.06182	946	0.433574
0.13595	7.355662	1019	7.355662	1019	0.456201
0.12915	7.742957	1092	7.742957	1092	0.483401
0.126767	7.888506	1165	7.888506	1165	0.492933
0.123346	8.107307	1238	8.107307	1238	0.506618
0.118923	8.408809	1311	8.408809	1311	0.524308
0.113412	8.817423	1384	8.817423	1384	0.546353
0.110411	9.057059	1457	9.057059	1457	0.558356
0.110454	9.053559	1530	9.053559	1530	0.558185
0.104833	9.538961	1603	9.538961	1603	0.580667
0.104831	9.539194	1676	9.539194	1676	0.580677
0.099686	10.03153	1749	10.03153	1749	0.601257
0.100468	9.953413	1822	9.953413	1822	0.598128
0.097674	10.23814	1895	10.23814	1895	0.609304
0.093019	10.75055	1968	10.75055	1968	0.627926
0.090486	11.05147	2041	11.05147	2041	0.638057
0.088206	11.33714	2114	11.33714	2114	0.647177
0.08915	11.21709	2187	11.21709	2187	0.643401
0.085279	11.72615	2260	11.72615	2260	0.658882
0.084164	11.88155	2333	11.88155	2333	0.663344
0.081197	12.31577	2406	12.31577	2406	0.675213
0.078425	12.75101	2479	12.75101	2479	0.686299

0.079897	12.51615	2552	12.51615	2552	0.680413
0.077781	12.85653	2625	12.85653	2625	0.688874
0.076797	13.02127	2698	13.02127	2698	0.69281
0.074768	13.37466	2771	13.37466	2771	0.700927
0.073392	13.62539	2844	13.62539	2844	0.70643
0.072649	13.76486	2917	13.76486	2917	0.709405
0.071253	14.03449	2990	14.03449	2990	0.714988
0.068663	14.56386	3063	14.56386	3063	0.725347
0.068858	14.52257	3136	14.52257	3136	0.724567

Kinetic data for iminium ion formation at 303K (Run 2)

Time	Integration cinnamaldehyde	Integration iminium	Total integration	Integration iminium/ Total integration	Integration cinnamaldehyde/ Total integration	[Iminium]	1/[Iminium]
0	1		1	0	1	0	0
230	1	0.163228	1.163228	0.140323307	0.859676693	0.0350808	28.50559953
303	0.962368	0.219744	1.182112	0.185891015	0.814108985	0.0464728	21.51798456
376	0.924426	0.265949	1.190375	0.22341615	0.77658385	0.055854	17.90380862
449	0.881526	0.308666	1.190192	0.25934135	0.74065865	0.0648353	15.42368774
522	0.821678	0.350713	1.172391	0.299143375	0.700856625	0.0747858	13.3715146
595	0.790433	0.404799	1.195232	0.338678181	0.661321819	0.0846695	11.81062206
668	0.759024	0.430771	1.189795	0.362054808	0.637945192	0.0905137	11.04805105
741	0.734027	0.455591	1.189618	0.382972517	0.617027483	0.0957431	10.4446137
814	0.687468	0.472025	1.159493	0.407096032	0.592903968	0.101774	9.825691436
887	0.663333	0.511782	1.175115	0.435516524	0.564483476	0.1088791	9.184496524
960	0.645477	0.535298	1.180775	0.453344625	0.546655375	0.1133362	8.823309633
1033	0.625652	0.546298	1.17195	0.46614446	0.53385554	0.1165361	8.581030866
1106	0.604054	0.586793	1.190847	0.492752637	0.507247363	0.1231882	8.117663299
1179	0.576299	0.59951	1.175809	0.509870226	0.490129774	0.1274676	7.845133526
1252	0.563836	0.636919	1.200755	0.530432103	0.469567897	0.132608	7.5410217
1325	0.544572	0.640737	1.185309	0.540565372	0.459434628	0.1351413	7.399660079
1398	0.53979	0.654131	1.193921	0.547884659	0.452115341	0.1369712	7.300806719
1471	0.523341	0.675546	1.198887	0.563477625	0.436522375	0.1408694	7.098773437
1544	0.504036	0.678466	1.182502	0.573754632	0.426245368	0.1434387	6.971621275
1617	0.480303	0.697507	1.17781	0.592206723	0.407793277	0.1480517	6.754398164
1690	0.4718	0.711698	1.183498	0.601351249	0.398648751	0.1503378	6.65168653
1763	0.443569	0.716596	1.160165	0.617667315	0.382332685	0.1544168	6.475978096
1836	0.452493	0.741603	1.194096	0.621058106	0.378941894	0.1552645	6.440621195
1909	0.43994	0.746351	1.186291	0.629146643	0.370853357	0.1572867	6.357818238
1982	0.431272	0.741282	1.172554	0.632194338	0.367805662	0.1580486	6.327168338
2055	0.425618	0.751212	1.17683	0.638335189	0.361664811	0.1595838	6.266300325
2128	0.406439	0.759162	1.165601	0.651305206	0.348694794	0.1628263	6.141513932
2201	0.401245	0.78128	1.182525	0.660687935	0.339312065	0.165172	6.054295515
2274	0.401387	0.792153	1.19354	0.663700421	0.336299579	0.1659251	6.026815527
2347	0.392661	0.7909	1.183561	0.668237632	0.331762368	0.1670594	5.985894551
2420	0.387922	0.800155	1.188077	0.673487493	0.326512507	0.1683719	5.939234273

2493	0.38571	0.806335	1.192045	0.676430001	0.323569999	0.1691075	5.913398277
2566	0.377009	0.818333	1.195342	0.684601562	0.315398438	0.1711504	5.8428146
2639	0.360539	0.83209	1.192629	0.697693918	0.302306082	0.1744235	5.733173094
2712	0.353074	0.824649	1.177723	0.700206245	0.299793755	0.1750516	5.712602574
2785	0.363757	0.83316	1.196917	0.696088367	0.303911633	0.1740221	5.746396851
2858	0.34824	0.83048	1.17872	0.70456088	0.29543912	0.1761402	5.677295058
2931	0.359567	0.84659	1.206157	0.701890384	0.298109616	0.1754726	5.698895569
3004	0.328763	0.841457	1.17022	0.719058809	0.280941191	0.1797647	5.562827334
3077	0.361945	0.868937	1.230882	0.70594663	0.29405337	0.1764867	5.666150711
3150	0.337369	0.850687	1.188056	0.716032746	0.283967254	0.1790082	5.58633669
3223	0.333659	0.868738	1.202397	0.722505129	0.277494871	0.1806263	5.536292875

Kinetic data for iminium ion formation at 303K (Run 2)

[Cinnamaldehyde]	1/[Cinnamaldehyde]	Time	1/[Cinnamaldehyde]	Time	Conversion to iminium
0.25	4	0	4	0	0
0.214919	4.652912	230	4.652912	230	0.140323
0.203527	4.913347	303	4.913347	303	0.185891
0.194146	5.150764	376	5.150764	376	0.223416
0.185165	5.400599	449	5.400599	449	0.259341
0.175214	5.707301	522	5.707301	522	0.299143
0.16533	6.048492	595	6.048492	595	0.338678
0.159486	6.270131	668	6.270131	668	0.362055
0.154257	6.482693	741	6.482693	741	0.382973
0.148226	6.746455	814	6.746455	814	0.407096
0.141121	7.086124	887	7.086124	887	0.435517
0.136664	7.317224	960	7.317224	960	0.453345
0.133464	7.492664	1033	7.492664	1033	0.466144
0.126812	7.885699	1106	7.885699	1106	0.492753
0.122532	8.161104	1179	8.161104	1179	0.50987
0.117392	8.51847	1252	8.51847	1252	0.530432
0.114859	8.706353	1325	8.706353	1325	0.540565
0.113029	8.8473	1398	8.8473	1398	0.547885
0.109131	9.163333	1471	9.163333	1471	0.563478
0.106561	9.384266	1544	9.384266	1544	0.573755
0.101948	9.808891	1617	9.808891	1617	0.592207
0.099662	10.0339	1690	10.0339	1690	0.601351
0.095583	10.46209	1763	10.46209	1763	0.617667
0.094735	10.55571	1836	10.55571	1836	0.621058
0.092713	10.78593	1909	10.78593	1909	0.629147
0.091951	10.87531	1982	10.87531	1982	0.632194
0.090416	11.05996	2055	11.05996	2055	0.638335
0.087174	11.47135	2128	11.47135	2128	0.651305
0.084828	11.78856	2201	11.78856	2201	0.660688
0.084075	11.89416	2274	11.89416	2274	0.6637
0.082941	12.05682	2347	12.05682	2347	0.668238
0.081628	12.25068	2420	12.25068	2420	0.673487
0.080892	12.36209	2493	12.36209	2493	0.67643
0.07885	12.68237	2566	12.68237	2566	0.684602

0.075577	13.23162	2639	13.23162	2639	0.697694
0.074948	13.34251	2712	13.34251	2712	0.700206
0.075978	13.16172	2785	13.16172	2785	0.696088
0.07386	13.53917	2858	13.53917	2858	0.704561
0.074527	13.41788	2931	13.41788	2931	0.70189
0.070235	14.23786	3004	14.23786	3004	0.719059
0.073513	13.60297	3077	13.60297	3077	0.705947
0.070992	14.08613	3150	14.08613	3150	0.716033
0.069374	14.41468	3223	14.41468	3223	0.722505

Progress of reaction for Diels-Alder cycloaddition (293K Run 1)

2nd Order Rate Plot for Diels-Alder Cycloaddition at 293K

y = -5428.43x + 10.63
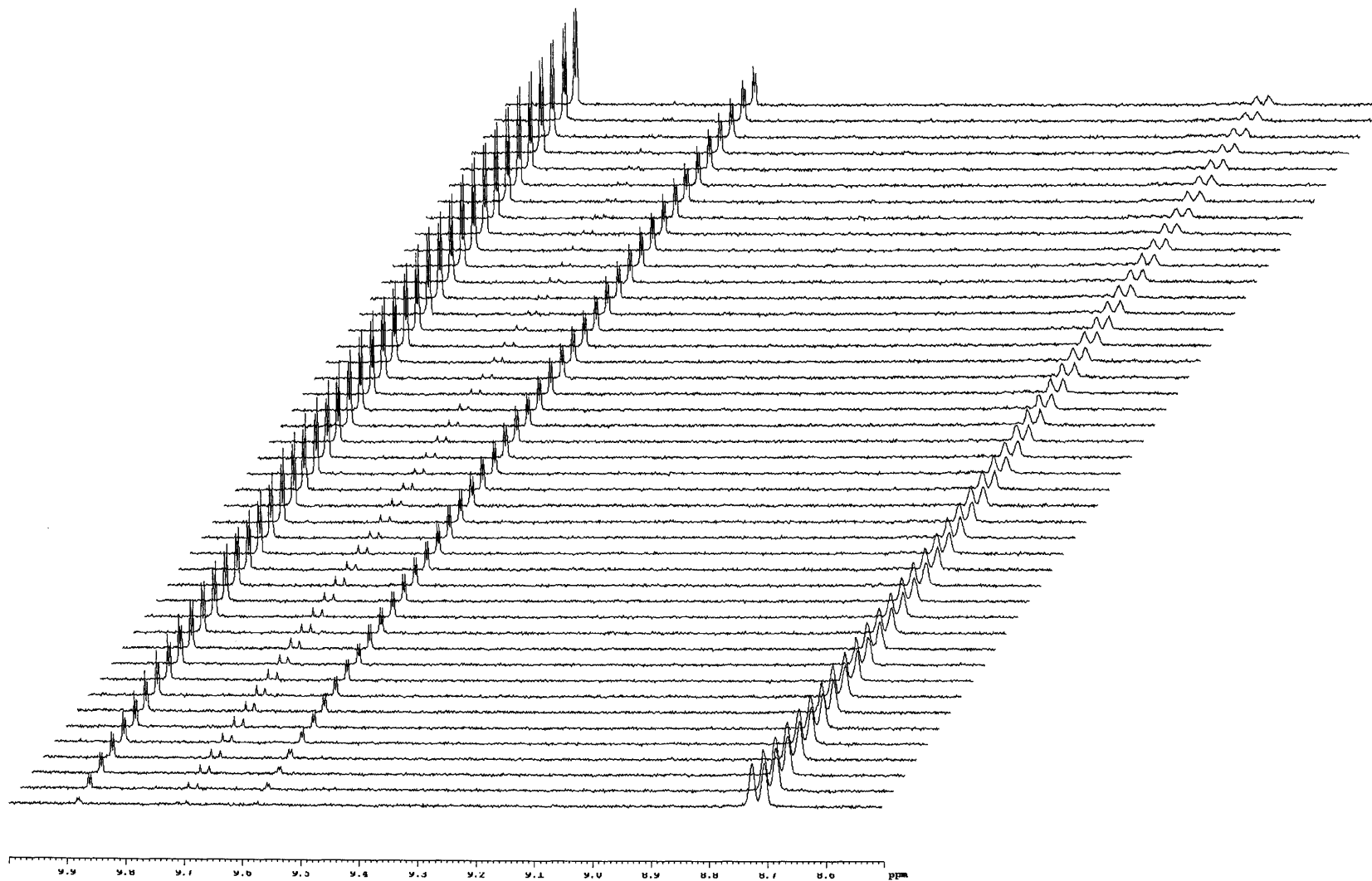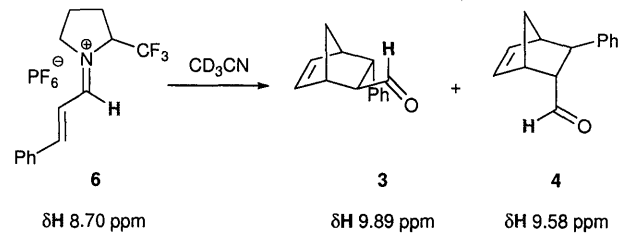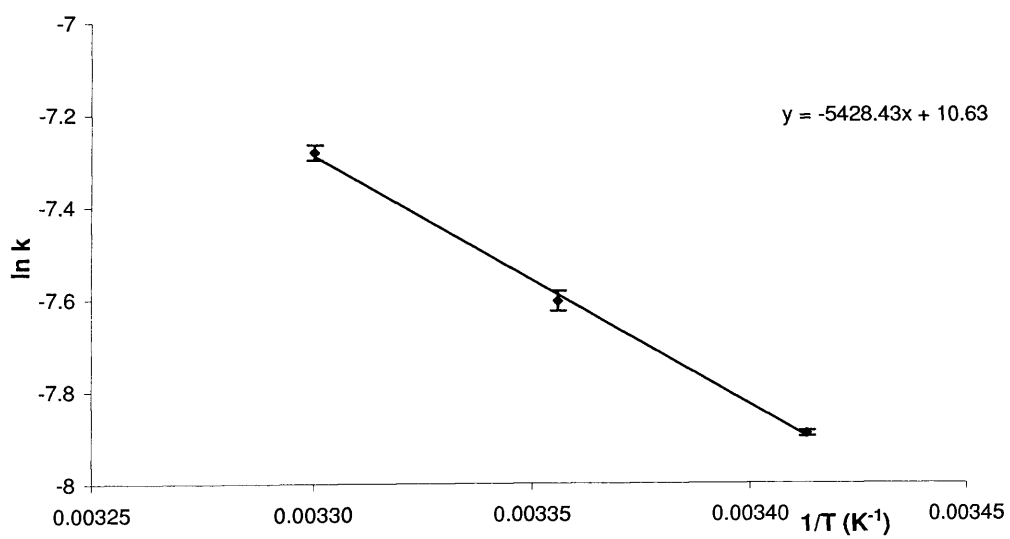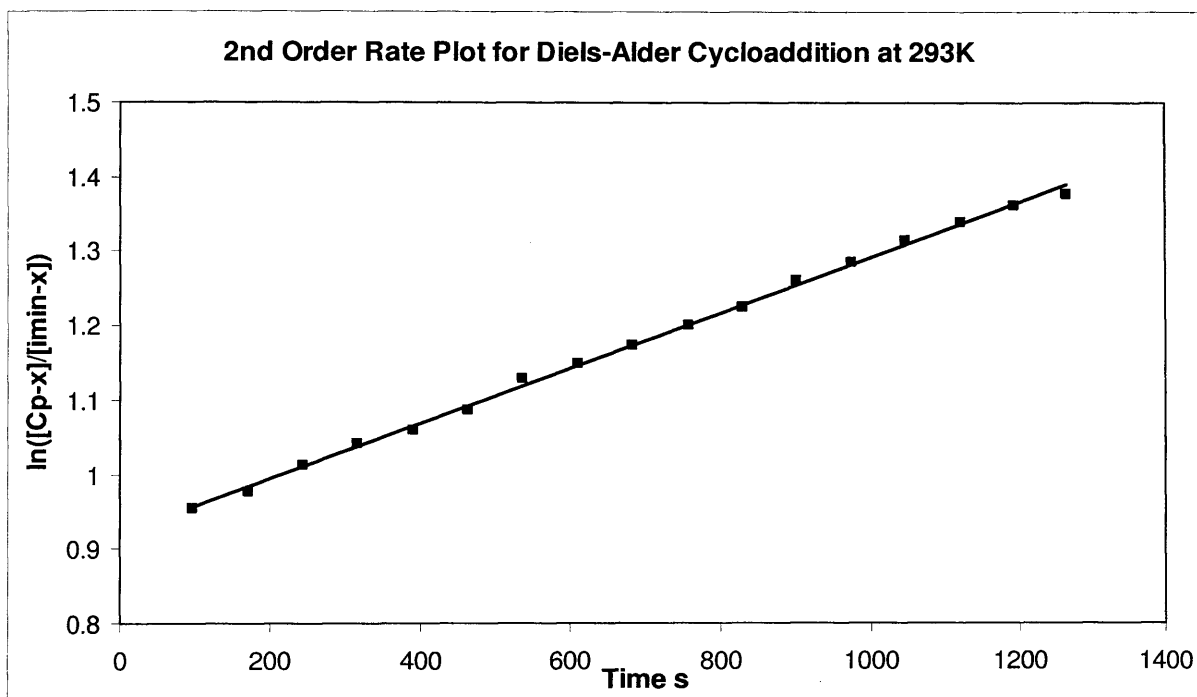
Kinetic data for Diels-Alder cycloaddition at 293K (Run 1)

Time (s)	Integration of the *exo* product	Integration of cinnamaldehyde	Integration of the *endo* product	Integration of the iminium ion	Integration of the exo and endo products	Total integration
132	1	0.443178	0.314401	19.9132	1.314401	21.227601
205	1.5281	0.633787	0.41473	18.8209	1.94283	20.76373
278	2.0545	0.726718	0.903806	17.697	2.958306	20.655306
351	2.48329	0.770859	1.1683	16.4122	3.65159	20.06379
424	2.84032	0.859304	1.24855	15.8221	4.08887	19.91097
497	3.10956	0.756098	1.36814	14.5266	4.4777	19.0043
570	3.83278	0.888352	1.77336	14.1804	5.60614	19.78654
643	4.10522	0.990289	1.88705	13.8015	5.99227	19.79377
716	4.47477	0.808459	1.81848	12.9319	6.29325	19.22515
789	4.63335	0.947674	2.1003	12.3074	6.73365	19.04105
862	4.98822	0.788095	2.1244	11.8066	7.11262	18.91922
935	5.38899	0.919572	2.42932	11.3805	7.81831	19.19881
1008	5.46939	0.953847	2.59327	10.865	8.06266	18.92766
1081	5.99213	0.685697	2.49926	10.4356	8.49139	18.92699
1154	5.97561	0.625884	2.80706	10.0179	8.78267	18.80057
1227	6.19115	0.646107	2.83301	9.68277	9.02416	18.70693
1300	6.37306	0.832465	2.84055	9.45022	9.21361	18.66383
1373	6.62413	0.850626	3.01164	9.05988	9.63577	18.69565
1446	6.64276	0.630097	3.05003	8.43732	9.69279	18.13011
1519	7.0151	0.777956	3.11684	8.29454	10.13194	18.42648
1592	7.0876	0.51669	3.4369	8.49082	10.5245	19.01532
1665	7.06853	0.499362	3.26604	7.8275	10.33457	18.16207
1738	7.39644	0.513954	3.41204	7.45658	10.80848	18.26506
1811	7.47012	0.486778	3.47047	7.43117	10.94059	18.37176
1884	7.48556	0.324261	3.38135	7.03816	10.86691	17.90507
1957	7.62022	0.525984	3.53411	7.04086	11.15433	18.19519
2030	7.89744	0.679776	3.54282	6.87238	11.44026	18.31264
2103	7.86037	0.386134	3.67879	6.74693	11.53916	18.28609
2176	8.16861	0.514953	3.60814	6.4286	11.77675	18.20535
2249	7.97014	0.310302	3.66812	6.20622	11.63826	17.84448
2322	8.1258	0.42108	3.64404	5.88301	11.76984	17.65285
2395	8.18489	0.260208	3.60635	5.90892	11.79124	17.70016
2468	8.16034	0.100944	3.76929	5.78053	11.92963	17.71016
2541	8.3345	0.194453	3.69758	5.55221	12.03208	17.58429

2614	8.53592	0.476606	3.89941	5.70902	12.43533	18.14435
2687	8.42668	0.47604	3.8157	5.33601	12.24238	17.57839
2760	8.57247	0.400387	3.78431	5.1553	12.35678	17.51208
2833	8.57508	0.285465	3.87256	4.85637	12.44764	17.30401
2906	8.61132	0.179459	3.9837	5.08617	12.59502	17.68119
2979	8.68236	0.244203	4.01059	4.75732	12.69295	17.45027
3052	8.8846	0.173319	4.04224	4.67276	12.92684	17.5996
3125	8.93811	0.218495	4.09827	4.74538	13.03638	17.78176
3198	8.91594	0.174362	3.94794	4.39183	12.86388	17.25571
3271	9.07006	0.175409	4.21481	4.76245	13.28487	18.04732
3344	8.87158	0.147853	3.91455	4.43572	12.78613	17.22185

233

Kinetic data for Diels-Alder cycloaddition at 293K (Run 1)

Conversion	Extent of reaction [x]	[iminium]-[x]	[cyclopentadiene]-[x]	Time (s)	ln([cp-x]/[imin-x])
0.06191943	0.01548	0.23452	0.60952	98	0.955130518
0.09356845	0.023392	0.226608	0.601608	171	0.976384726
0.14322257	0.035806	0.214194	0.589194	244	1.011872292
0.18199901	0.0455	0.2045	0.5795	317	1.041596907
0.20535765	0.051339	0.198661	0.573661	390	1.060440132
0.2356151	0.058904	0.191096	0.566096	463	1.085986974
0.28333099	0.070833	0.179167	0.554167	536	1.129146801
0.30273515	0.075684	0.174316	0.549316	609	1.147803295
0.32734465	0.081836	0.168164	0.543164	682	1.172472274
0.35363859	0.08841	0.16159	0.53659	755	1.20017051
0.37594679	0.093987	0.156013	0.531013	828	1.224845795
0.40722889	0.101807	0.148193	0.523193	901	1.261436013
0.42597236	0.106493	0.143507	0.518507	974	1.284570167
0.44863922	0.11216	0.13784	0.51284	1047	1.313869277
0.46714913	0.116787	0.133213	0.508213	1120	1.338952871
0.48239663	0.120599	0.129401	0.504401	1193	1.360456382
0.49366127	0.123415	0.126585	0.501585	1266	1.376860939
0.51540171	0.12885	0.12115	0.49615	1339	1.409851522
0.53462389	0.133656	0.116344	0.491344	1412	1.440592999
0.5498576	0.137464	0.112536	0.487536	1485	1.466093691
0.55347478	0.138369	0.111631	0.486631	1558	1.472305236
0.56901939	0.142255	0.107745	0.482745	1631	1.499720141
0.59175716	0.147939	0.102061	0.477061	1704	1.542075922
0.59551126	0.148878	0.101122	0.476122	1777	1.54934498
0.60691804	0.15173	0.09827	0.47327	1850	1.571943308
0.61303729	0.153259	0.096741	0.471741	1923	1.584395455
0.62471932	0.15618	0.09382	0.46882	1996	1.608839396
0.63103485	0.157759	0.092241	0.467241	2069	1.622437959
0.64688402	0.161721	0.088279	0.463279	2142	1.657827257
0.65220505	0.163051	0.086949	0.461949	2215	1.67013521
0.6667388	0.166685	0.083315	0.458315	2288	1.704925166
0.66616573	0.166541	0.083459	0.458459	2361	1.70351961
0.67360374	0.168401	0.081599	0.456599	2434	1.721987881
0.68425168	0.171063	0.078937	0.453937	2507	1.749307523
0.6853555	0.171339	0.078661	0.453661	2580	1.75220142

0.6964449	0.174111	0.075889	0.450889	2653	1.781951899
0.70561464	0.176404	0.073596	0.448596	2726	1.807528163
0.71935002	0.179838	0.070162	0.445162	2799	1.847625474
0.71234006	0.178085	0.071915	0.446915	2872	1.826883738
0.72737843	0.181845	0.068155	0.443155	2945	1.872130201
0.73449624	0.183624	0.066376	0.441376	3018	1.894562338
0.73313215	0.183283	0.066717	0.441717	3091	1.890210101
0.74548541	0.186371	0.063629	0.438629	3164	1.93058934
0.73611317	0.184028	0.065972	0.440972	3237	1.899754754
0.7424365	0.185609	0.064391	0.439391	3310	1.920417455

Kinetic data for Diels-Alder cycloaddition at 293K (Run 2)

Time (s)	Integration of the *exo* product	Integration of cinnamaldehyde	Integration of the *endo* product	Integration of the iminium ion	Integration of the exo and endo products	Total integration
115	1	1.1977	0.588322	33.7338	1.588322	35.322122
188	1.97878	1.09731	0.569363	30.6192	2.548143	33.167343
261	2.77687	1.19328	1.4394	29.4255	4.21627	33.64177
334	3.83312	1.49192	1.52667	27.6966	5.35979	33.05639
407	4.79735	1.59608	1.91962	26.1127	6.71697	32.82967
480	5.33093	1.63499	2.33374	24.8816	7.66467	32.54627
553	5.83677	1.42367	2.60002	23.5417	8.43679	31.97849
626	6.6899	1.57599	3.01422	22.5281	9.70412	32.23222
699	7.43091	1.55895	3.21669	21.9246	10.6476	32.5722
772	7.98625	1.74427	3.44161	20.8478	11.42786	32.27566
845	7.9136	1.4436	3.61764	19.1402	11.53124	30.67144
918	8.90324	1.44959	3.96748	19.7038	12.87072	32.57452
991	9.14003	1.50054	4.3442	18.4598	13.48423	31.94403
1064	9.41085	1.59847	4.36509	17.7059	13.77594	31.48184
1137	9.77863	1.25328	4.46319	17.1776	14.24182	31.41942
1210	9.94212	1.41886	4.68691	15.737	14.62903	30.36603
1283	10.1965	1.29494	4.74496	15.1833	14.94146	30.12476
1356	10.8873	1.43864	5.05094	15.052	15.93824	30.99024
1429	10.8351	1.23221	4.85884	14.3643	15.69394	30.05824
1502	10.9914	1.10448	5.12397	14.0891	16.11537	30.20447
1575	11.8753	1.19271	5.16815	13.1102	17.04345	30.15365
1648	11.6855	1.2669	5.43089	12.9065	17.11639	30.02289
1721	12.1996	1.12174	5.68624	12.9837	17.88584	30.86954
1794	12.1255	0.912212	5.6435	12.1288	17.769	29.8978
1867	12.4235	0.831865	5.74079	11.7876	18.16429	29.95189
1940	12.3562	0.85857	5.46775	11.1637	17.82395	28.98765
2013	12.8894	0.913403	6.07531	11.6558	18.96471	30.62051
2086	13.0927	0.910045	5.96973	11.2524	19.06243	30.31483
2159	13.4647	1.0471	6.24542	10.6116	19.71012	30.32172
2232	13.1309	0.521987	5.94959	9.75125	19.08049	28.83174
2305	13.5171	0.787979	6.10488	9.68629	19.62198	29.30827
2378	13.8017	0.535886	6.16776	9.43089	19.96946	29.40035
2451	14.111	0.542592	6.49218	9.65886	20.60318	30.26204
2524	13.6493	0.464769	6.27454	8.91436	19.92384	28.8382

2597	13.7468	0.599861	6.30728	8.46443	20.05408	28.51851
2670	14.1562	0.539094	6.31019	8.42941	20.46639	28.8958
2743	14.6246	0.749743	6.76512	8.68289	21.38972	30.07261
2816	13.9492	0.429609	6.56668	8.33204	20.51588	28.84792
2889	14.4107	0.351022	6.51465	7.74285	20.92535	28.6682
2962	14.4168	0.532449	6.60905	7.60123	21.02585	28.62708
3035	14.7398	0.251386	6.64956	7.65496	21.38936	29.04432
3108	14.6981	0.571086	6.8424	7.39724	21.5405	28.93774
3181	14.8833	0.355521	6.83105	6.75029	21.71435	28.46464
3254	15.34	0.36123	6.87116	7.04841	22.21116	29.25957
3327	14.6411	0.161429	6.4516	6.44895	21.0927	27.54165

Kinetic data for Diels-Alder cycloaddition at 293K (Run 2)

Conversion	Extent of reaction [x]	[iminium]-[x]	[cyclopentadiene]-[x]	Time (s)	ln([cp-x]/[imin-x])
0.04496678	0.011242	0.238758	0.613758	98	0.944149445
0.07682687	0.019207	0.230793	0.605793	171	0.965016378
0.12532842	0.031332	0.218668	0.593668	244	0.998765949
0.16214081	0.040535	0.209465	0.584465	317	1.026140862
0.20460059	0.05115	0.19885	0.57385	390	1.059817755
0.23550072	0.058875	0.191125	0.566125	463	1.085887861
0.26382703	0.065957	0.184043	0.559043	536	1.111056082
0.30106893	0.075267	0.174733	0.549733	609	1.146174519
0.32689226	0.081723	0.168277	0.543277	682	1.172008152
0.35407053	0.088518	0.161482	0.536482	755	1.200637737
0.37596018	0.09399	0.15601	0.53101	828	1.224860946
0.39511618	0.098779	0.151221	0.526221	901	1.246979149
0.4221205	0.10553	0.14447	0.51947	974	1.279737815
0.4375837	0.109396	0.140604	0.515604	1047	1.299391211
0.45328081	0.11332	0.13668	0.51168	1120	1.320058082
0.48175642	0.120439	0.129561	0.504561	1193	1.359537539
0.49598603	0.123997	0.126003	0.501003	1266	1.380303442
0.5142987	0.128575	0.121425	0.496425	1339	1.408133597
0.52211773	0.130529	0.119471	0.494471	1412	1.420417584
0.53354255	0.133386	0.116614	0.491614	1485	1.438822152
0.56522013	0.141305	0.108695	0.483695	1558	1.492908981
0.57011134	0.142528	0.107472	0.482472	1631	1.501691343
0.57940092	0.14485	0.10515	0.48015	1704	1.518712369
0.59432467	0.148581	0.101419	0.476419	1777	1.547038561
0.60644888	0.151612	0.098388	0.473388	1850	1.570998264
0.61488082	0.15372	0.09628	0.47128	1923	1.588193478
0.61934664	0.154837	0.095163	0.470163	1996	1.597485384
0.62881534	0.157204	0.092796	0.467796	2069	1.617627333
0.65003305	0.162508	0.087492	0.462492	2142	1.665084321
0.66178767	0.165447	0.084553	0.459553	2215	1.692874922
0.66950318	0.167376	0.082624	0.457624	2288	1.711745661
0.67922525	0.169806	0.080194	0.455194	2361	1.736278206
0.68082588	0.170206	0.079794	0.454794	2434	1.740401111
0.69088362	0.172721	0.077279	0.452279	2507	1.766875976
0.70319522	0.175799	0.074201	0.449201	2580	1.800690637
0.70828252	0.177071	0.072929	0.447929	2653	1.815144121

0.71126916	0.177817	0.072183	0.447183	2726	1.82376671
0.71117363	0.177793	0.072207	0.447207	2799	1.823489314
0.72991503	0.182479	0.067521	0.442521	2872	1.88004621
0.73447414	0.183619	0.066381	0.441381	2945	1.89449163
0.73643866	0.18411	0.06589	0.44089	3018	1.900804391
0.74437396	0.186093	0.063907	0.438907	3091	1.926865181
0.76285349	0.190713	0.059287	0.434287	3164	1.991320978
0.75910753	0.189777	0.060223	0.435223	3237	1.977802534

Kinetic data for Diels-Alder cycloaddition at 298K (Run 1)

Time (s)	Integration of the *exo* product	Integration of cinnamaldehyde	Integration of the *endo* product	Integration of the iminium ion	Integration of the exo and endo products	Total integration
257	1.05014	0.568175	0.429233	10.9229	1.479373	12.402273
330	1.51128	0.63491	0.702269	9.74399	2.213549	11.957539
403	1.82365	0.564261	0.825886	9.00445	2.649536	11.653986
476	2.1374	0.608931	0.967224	8.09036	3.104624	11.194984
549	2.47616	0.585157	1.12501	7.66519	3.60117	11.26636
622	2.52258	0.510535	1.17381	6.87672	3.69639	10.57311
695	2.62174	0.599926	1.32525	6.37829	3.94699	10.32528
768	2.7211	0.488499	1.51313	5.8567	4.23423	10.09093
841	2.99779	0.516527	1.5448	5.95424	4.54259	10.49683
914	3.03841	0.520903	1.58483	5.54047	4.62324	10.16371
987	3.11679	0.37729	1.60035	4.992	4.71714	9.70914
1060	3.19429	0.423254	1.69892	4.8132	4.89321	9.70641
1133	3.24389	0.328069	1.67503	4.39346	4.91892	9.31238
1206	3.34994	0.272149	1.80893	4.20195	5.15887	9.36082
1279	3.57951	0.324634	1.80032	4.20275	5.37983	9.58258
1352	3.80965	0.357925	1.97626	4.09311	5.78591	9.87902
1425	3.8302	0.305604	2.0592	4.15209	5.8894	10.04149
1498	4.12016	0.217452	2.08327	3.82053	6.20343	10.02396
1571	4.17007	0.191647	2.13767	3.92606	6.30774	10.2338
1644	4.4001	0.278559	2.24493	3.7863	6.64503	10.43133
1717	4.79209	0.328737	2.15222	3.74801	6.94431	10.69232
1790	4.84675	0.26315	2.16867	3.52333	7.01542	10.53875
1863	5.06768	0.20256	2.41277	3.64323	7.48045	11.12368
1936	4.94053	0.235318	2.23653	3.34327	7.17706	10.52033
2009	5.1689	0.259431	2.38515	3.44932	7.55405	11.00337
2082	5.13933	0.150331	2.30868	3.11546	7.44801	10.56347
2155	5.01954	0.194659	2.26493	3.1442	7.28447	10.42867
2228	4.92869	0.134416	2.41037	2.73745	7.33906	10.07651
2301	4.44973	0.187652	2.24419	2.75107	6.69392	9.44499
2374	4.24017	0.0865062	2.14613	2.33208	6.3863	8.71838
2447	4.12144	0.0956692	2.18952	2.2114	6.31096	8.52236
2520	4.0661	0.0393535	2.15212	2.16495	6.21822	8.38317
2593	4.30019	0.082393	2.18357	2.22753	6.48376	8.71129
2666	4.25577	0.0416384	2.22883	2.2233	6.4846	8.7079

2739	4.41392	0.0813617	2.22712	2.03468	6.64104	8.67572
2812	4.72656	-0.0375703	2.46217	2.12988	7.18873	9.31861
2885	4.99499	0.131605	2.50267	2.32027	7.49766	9.81793
2958	5.43016	0.165122	2.48033	2.42774	7.91049	10.33823
3031	5.47156	0.0418692	2.58885	2.26193	8.06041	10.32234
3104	5.46794	0.0642045	2.52735	2.12589	7.99529	10.12118
3177	5.3256	0.0748257	2.43836	2.14574	7.76396	9.9097
3250	5.40339	0.0543981	2.64202	2.10903	8.04541	10.15444

Kinetic data for Diels-Alder cycloaddition at 298K (Run 1)

Conversion	Extent of reaction [x]	[iminium]-[x]	[cyclopentadiene]-[x]	Time (s)	ln([cp-x]/[imin-x])
0.11928241	0.029821	0.220179	0.595179	257	0.994420211
0.18511744	0.046279	0.203721	0.578721	330	1.04407023
0.2273502	0.056838	0.193162	0.568162	403	1.078875833
0.27732277	0.069331	0.180669	0.555669	476	1.123505019
0.31963917	0.07991	0.17009	0.54509	549	1.164622374
0.34960291	0.087401	0.162599	0.537599	622	1.195824711
0.38226469	0.095566	0.154434	0.529434	695	1.232042487
0.41960751	0.104902	0.145098	0.520098	768	1.276607269
0.43275827	0.10819	0.14181	0.51681	841	1.293184957
0.45487721	0.113719	0.136281	0.511281	914	1.322202032
0.4858453	0.121461	0.128539	0.503539	987	1.365430684
0.5041215	0.12603	0.12397	0.49897	1060	1.392508651
0.52821298	0.132053	0.117947	0.492947	1133	1.430167874
0.55111304	0.137778	0.112222	0.487222	1206	1.468242608
0.5614177	0.140354	0.109646	0.484646	1279	1.486164728
0.58567651	0.146419	0.103581	0.478581	1352	1.530472533
0.58650658	0.146627	0.103373	0.478373	1425	1.532044273
0.61886021	0.154715	0.095285	0.470285	1498	1.596466935
0.61636342	0.154091	0.095909	0.470909	1571	1.591263847
0.63702615	0.159257	0.090743	0.465743	1644	1.635598543
0.64946709	0.162367	0.087633	0.462633	1717	1.663774349
0.66567857	0.16642	0.08358	0.45858	1790	1.702326997
0.67247979	0.16812	0.08188	0.45688	1863	1.719165489
0.68220864	0.170552	0.079448	0.454448	1936	1.743982433
0.68652149	0.17163	0.07837	0.45337	2009	1.755271307
0.70507229	0.176268	0.073732	0.448732	2082	1.805989756
0.69850422	0.174626	0.075374	0.450374	2155	1.787616567
0.72833352	0.182083	0.067917	0.442917	2228	1.87510076
0.70872706	0.177182	0.072818	0.447818	2301	1.816421022
0.73250994	0.183127	0.066873	0.441873	2374	1.888233363
0.74051788	0.185129	0.064871	0.439871	2447	1.914087012
0.74175044	0.185438	0.064562	0.439562	2520	1.918147606
0.7442939	0.186073	0.063927	0.438927	2593	1.92659765
0.74468012	0.18617	0.06383	0.43883	2666	1.92788919
0.76547422	0.191369	0.058631	0.433631	2739	2.000923812
0.77143801	0.19286	0.05714	0.43214	2812	2.023237676

0.76367014	0.190918	0.059082	0.434082	2885	1.994300356
0.7651687	0.191292	0.058708	0.433708	2958	1.999798067
0.78087042	0.195218	0.054782	0.429782	3031	2.05991015
0.78995631	0.197489	0.052511	0.427511	3104	2.09695864
0.78347074	0.195868	0.054132	0.429132	3177	2.070333974
0.79230465	0.198076	0.051924	0.426924	3250	2.106827637

Kinetic data for Diels-Alder cycloaddition at 298K (Run 2)

Time (s)	Integration of the *exo* product	Integration of cinnamaldehyde	Integration of the *endo* product	Integration of the iminium ion	Integration of the exo and endo products	Total integration
184	1	0.617481	0.303014	11.7723	1.303014	13.075314
257	1.39986	0.623436	0.567036	10.9337	1.966896	12.900596
330	1.72921	0.778468	0.814944	10.3887	2.544154	12.932854
403	2.20689	0.713036	1.08432	9.47829	3.29121	12.7695
476	2.60725	0.683518	1.17424	8.66667	3.78149	12.44816
549	2.81504	0.739291	1.37266	8.4328	4.1877	12.6205
622	3.07085	0.711366	1.49662	7.95526	4.56747	12.52273
695	3.37578	0.548659	1.48714	7.2982	4.86292	12.16112
768	3.62921	0.657811	1.68779	7.08246	5.317	12.39946
841	3.91802	0.553304	1.75937	6.59007	5.67739	12.26746
914	4.09506	0.543954	1.9386	6.46684	6.03366	12.5005
987	4.25479	0.385424	1.91287	6.32179	6.16766	12.48945
1060	4.21536	0.492054	1.90166	5.87398	6.11702	11.991
1133	4.44024	0.60114	1.83456	5.51464	6.2748	11.78944
1206	4.21839	0.29801	1.90968	5.13518	6.12807	11.26325
1279	4.66625	0.563785	1.93933	5.31234	6.60558	11.91792
1352	4.6803	0.365043	2.10178	5.50598	6.78208	12.28806
1425	4.53321	0.286121	1.82928	5.05673	6.36249	11.41922
1498	4.73631	0.393185	2.16885	5.08405	6.90516	11.98921
1571	4.71146	0.41166	2.1836	5.06629	6.89506	11.96135
1644	4.7605	0.399322	2.01284	4.65744	6.77334	11.43078
1717	4.96761	0.367229	2.20662	4.62894	7.17423	11.80317
1790	5.14617	0.225882	2.34412	4.75469	7.49029	12.24498
1863	5.12305	0.201425	2.28066	4.34588	7.40371	11.74959
1936	5.24365	0.214372	2.35038	4.38729	7.59403	11.98132
2009	5.07096	0.2994	2.33554	4.44344	7.4065	11.84994
2082	5.30453	0.336778	2.36224	4.06168	7.66677	11.72845
2155	5.29879	0.094489	2.36504	3.93017	7.66383	11.594
2228	5.49052	0.149918	2.35154	3.84398	7.84206	11.68604
2301	5.29584	0.11285	2.42161	3.74948	7.71745	11.46693
2374	5.32107	0.125611	2.35833	3.84952	7.6794	11.52892
2447	5.54984	0.165606	2.47455	3.7881	8.02439	11.81249
2520	5.62915	0.199216	2.58591	3.64913	8.21506	11.86419
2593	5.53311	0.137472	2.62978	3.4282	8.16289	11.59109

2666	5.57873	0.0186666	2.55815	3.27397	8.13688	11.41085
2739	5.62756	0.200425	2.5535	3.21401	8.18106	11.39507
2812	5.6102	0.038692	2.44476	3.08591	8.05496	11.14087
2885	5.75015	0.0652576	2.47362	3.17309	8.22377	11.39686
2958	5.71579	-0.0371191	2.47743	3.07326	8.19322	11.26648
3031	5.81946	0.0527227	2.64216	3.13048	8.46162	11.5921
3104	6.01637	0.115045	2.66996	3.20585	8.68633	11.89218

Kinetic data for Diels-Alder cycloaddition at 298K (Run 2)

Conversion	Extent of reaction [x]	[iminium]-[x]	[cyclopentadiene]-[x]	Time (s)	ln([cp-x]/[imin-x])
0.09965451	0.024914	0.225086	0.600086	184	0.980589392
0.15246551	0.038116	0.211884	0.586884	257	1.018789372
0.19672023	0.04918	0.20082	0.57582	330	1.053386313
0.25773993	0.064435	0.185565	0.560565	403	1.105539913
0.30377903	0.075945	0.174055	0.549055	476	1.148826328
0.33181728	0.082954	0.167046	0.542046	549	1.177082972
0.36473437	0.091184	0.158816	0.533816	622	1.212303105
0.39987435	0.099969	0.150031	0.525031	695	1.25261341
0.428809	0.107202	0.142798	0.517798	768	1.288155424
0.46280078	0.1157	0.1343	0.5093	841	1.332962193
0.48267349	0.120668	0.129332	0.504332	914	1.360854186
0.49382959	0.123457	0.126543	0.501543	987	1.377109527
0.51013427	0.127534	0.122466	0.497466	1060	1.401691106
0.53223902	0.13306	0.11694	0.49194	1133	1.436694179
0.54407653	0.136019	0.113981	0.488981	1206	1.456292761
0.55425611	0.138564	0.111436	0.486436	1279	1.473655099
0.55192439	0.137981	0.112019	0.487019	1352	1.469635304
0.55717378	0.139293	0.110707	0.485707	1425	1.478721597
0.57594787	0.143987	0.106013	0.481013	1498	1.512332335
0.57644497	0.144111	0.105889	0.480889	1571	1.513246878
0.59255274	0.148138	0.101862	0.476862	1644	1.543609611
0.60782231	0.151956	0.098044	0.473044	1717	1.573768624
0.61170292	0.152926	0.097074	0.472074	1790	1.581659966
0.63012497	0.157531	0.092469	0.467469	1863	1.620461678
0.63382248	0.158456	0.091544	0.466544	1936	1.628529276
0.62502426	0.156256	0.093744	0.468744	2009	1.609489673
0.65368996	0.163422	0.086578	0.461578	2082	1.673609908
0.66101691	0.165254	0.084746	0.459746	2155	1.691017794
0.67106222	0.167766	0.082234	0.457234	2228	1.715622027
0.67301797	0.168254	0.081746	0.456746	2301	1.720515516
0.66609882	0.166525	0.083475	0.458475	2374	1.703355687
0.67931401	0.169829	0.080171	0.455171	2447	1.736506217
0.69242485	0.173106	0.076894	0.451894	2520	1.771022087
0.70423834	0.17606	0.07394	0.44894	2593	1.803630612
0.71308272	0.178271	0.071729	0.446729	2666	1.829053284
0.71794732	0.179487	0.070513	0.445513	2739	1.843427316

0.72300996	0.180752	0.069248	0.444248	2812	1.858694682
0.72158208	0.180396	0.069604	0.444604	2885	1.85435616
0.72722092	0.181805	0.068195	0.443195	2958	1.871641473
0.72994712	0.182487	0.067513	0.442513	3031	1.880146907
0.73042369	0.182606	0.067394	0.442394	3104	1.88164392
0.75218413	0.188046	0.061954	0.436954	3177	1.953436204

Kinetic data for Diels-Alder cycloaddition at 303K (Run 1)

Time (s)	Integration of the *exo* product	Integration of cinnamaldehyde	Integration of the *endo* product	Integration of the iminium ion	Integration of the exo and endo products	Total integration
184	1	0.411761	0.519678	8.84649	1.519678	10.366168
257	1.52154	0.580055	0.622719	7.98402	2.144259	10.128279
330	1.89861	0.600281	0.858788	7.15802	2.757398	9.915418
403	2.23546	0.617828	0.990452	6.6279	3.225912	9.853812
476	2.47537	0.458713	1.05817	6.11517	3.53354	9.64871
549	2.81319	0.54425	1.27326	5.63236	4.08645	9.71881
622	2.98469	0.414501	1.43704	5.24318	4.42173	9.66491
695	3.23056	0.370209	1.54418	4.94985	4.77474	9.72459
768	3.36991	0.384487	1.48031	4.70621	4.85022	9.55643
841	3.50289	0.383477	1.54111	4.22507	5.044	9.26907
914	3.67118	0.346429	1.69118	4.02078	5.36236	9.38314
987	3.85086	0.407948	1.6758	3.82373	5.52666	9.35039
1060	3.90466	0.266436	1.82203	3.75004	5.72669	9.47673
1133	3.92278	0.283751	1.77076	3.4688	5.69354	9.16234
1206	3.99832	0.26852	1.88336	3.2691	5.88168	9.15078
1279	4.11886	0.192361	1.81609	3.13087	5.93495	9.06582
1352	4.17592	0.274056	1.95652	2.9809	6.13244	9.11334
1425	4.2737	0.148861	1.95331	2.93651	6.22701	9.16352
1498	4.22025	0.194625	1.90704	2.85008	6.12729	8.97737
1571	4.34327	0.159192	1.89775	2.72828	6.24102	8.9693
1644	4.41781	0.114091	1.92767	2.67168	6.34548	9.01716
1717	4.36781	0.126512	1.977	2.60163	6.34481	8.94644
1790	4.39061	0.169025	2.00379	2.67802	6.3944	9.07242
1863	4.41802	0.165651	2.13537	2.61968	6.55339	9.17307
1936	4.40808	0.169097	2.07055	2.40184	6.47863	8.88047
2009	4.51248	0.0530001	2.05467	2.43435	6.56715	9.0015
2082	4.54513	0.208635	2.0955	2.31993	6.64063	8.96056
2155	4.50076	0.142176	2.06152	2.17135	6.56228	8.73363
2228	4.55608	0.158693	2.06776	2.19528	6.62384	8.81912
2301	4.57147	0.0742623	2.18265	2.13236	6.75412	8.88648
2374	4.62788	0.147124	2.10001	2.14687	6.72789	8.87476
2447	4.56756	0.116401	2.21251	2.08649	6.78007	8.86656
2520	4.67312	-0.0165822	2.09703	2.05455	6.77015	8.8247
2593	4.63966	0.0384821	2.12657	2.0652	6.76623	8.83143

2666	4.7579	0.0146899	2.11469	1.90538	6.87259	8.77797
2739	4.73657	-0.0737908	2.21514	1.92246	6.95171	8.87417
2812	4.72842	0.0363881	2.19363	1.98309	6.92205	8.90514
2885	4.70708	0.00864628	2.20825	1.81459	6.91533	8.72992
2958	4.68277	0.123942	2.21647	1.79733	6.89924	8.69657
3031	4.71327	0.060859	2.25193	1.78694	6.9652	8.75214
3104	4.76054	-0.0220905	2.0897	1.68341	6.85024	8.53365

Kinetic data for Diels-Alder cycloaddition at 303K (Run 1)

Conversion	Extent of reaction [x]	[iminium]-[x]	[cyclopentadiene]-[x]	Time (s)	ln([cp-x]/[imin-x])
0.14659978	0.03665	0.21335	0.58835	98	1.014387839
0.2117101	0.052928	0.197072	0.572072	171	1.065694137
0.27809196	0.069523	0.180477	0.555477	244	1.124223818
0.32737706	0.081844	0.168156	0.543156	317	1.172505539
0.3662189	0.091555	0.158445	0.533445	390	1.213947227
0.42046814	0.105117	0.144883	0.519883	463	1.277677445
0.45750348	0.114376	0.135624	0.510624	536	1.325746458
0.49099654	0.122749	0.127251	0.502251	609	1.372939266
0.50753472	0.126884	0.123116	0.498116	682	1.397704021
0.54417541	0.136044	0.113956	0.488956	755	1.45645911
0.57148886	0.142872	0.107128	0.482128	828	1.504186822
0.59106198	0.147765	0.102235	0.477235	901	1.540738746
0.60428967	0.151072	0.098928	0.473928	974	1.566666429
0.62140676	0.155352	0.094648	0.469648	1047	1.601816113
0.64275177	0.160688	0.089312	0.464312	1120	1.648420352
0.65465121	0.163663	0.086337	0.461337	1193	1.675868684
0.67290807	0.168227	0.081773	0.456773	1266	1.720239601
0.67954345	0.169886	0.080114	0.455114	1339	1.737095904
0.68252617	0.170632	0.079368	0.454368	1412	1.744807431
0.69582019	0.173955	0.076045	0.451045	1485	1.780242353
0.70371159	0.175928	0.074072	0.449072	1558	1.802144482
0.70919941	0.1773	0.0727	0.4477	1631	1.817780291
0.70481746	0.176204	0.073796	0.448796	1704	1.805268038
0.71441622	0.178604	0.071396	0.446396	1777	1.832965254
0.72953684	0.182384	0.067616	0.442616	1850	1.878860559
0.72956174	0.18239	0.06761	0.44261	1923	1.87893857
0.74109542	0.185274	0.064726	0.439726	1996	1.915986928
0.75138058	0.187845	0.062155	0.437155	2069	1.950658569
0.7510772	0.187769	0.062231	0.437231	2142	1.949612543
0.76004447	0.190011	0.059989	0.434989	2215	1.981161227
0.75809261	0.189523	0.060477	0.435477	2288	1.974181037
0.76467875	0.19117	0.05883	0.43383	2361	1.997996225
0.76718189	0.191795	0.058205	0.433205	2434	2.007246812
0.76615339	0.191538	0.058462	0.433462	2507	2.003432292
0.78293615	0.195734	0.054266	0.429266	2580	2.06817948
0.78336453	0.195841	0.054159	0.429159	2653	2.069905448

0.77730951	0.194327	0.055673	0.430673	2726	2.045859712
0.79214128	0.198035	0.051965	0.426965	2799	2.106137035
0.79332886	0.198332	0.051668	0.426668	2872	2.111171234
0.79582822	0.198957	0.051043	0.426043	2945	2.121872815
0.80273271	0.200683	0.049317	0.424317	3018	2.152215154
0.78587263	0.196468	0.053532	0.428532	3091	2.080088398

Kinetic data for Diels-Alder cycloaddition at 303K (Run 2)

Time (s)	Integration of the *exo* product	Integration of cinnamaldehyde	Integration of the *endo* product	Integration of the iminium ion	Integration of the exo and endo products	Total integration
102	1	1.70731	0.602389	24.6436	1.602389	26.245989
175	2.18514	1.54899	0.888656	21.5688	3.073796	24.642596
248	3.48476	1.57842	1.51398	19.3979	4.99874	24.39664
321	4.29983	1.66131	1.83014	17.2627	6.12997	23.39267
394	5.27288	1.44818	2.3872	16.6192	7.66008	24.27928
467	6.02307	1.0864	2.54141	14.7662	8.56448	23.33068
540	6.56928	1.43667	2.89315	13.9631	9.46243	23.42553
613	7.20941	1.50606	3.28602	13.1772	10.49543	23.67263
686	7.65345	1.07714	3.71487	12.0481	11.36832	23.41642
759	8.02601	1.29979	3.98826	11.1164	12.01427	23.13067
832	8.40285	0.981851	3.96891	10.7386	12.37176	23.11036
905	8.77222	0.882777	3.69827	10.0099	12.47049	22.48039
978	9.04088	0.771884	4.43107	9.46524	13.47195	22.93719
1051	9.33634	0.951116	4.23953	8.86197	13.57587	22.43784
1124	9.80761	0.603918	4.42215	8.5009	14.22976	22.73066
1197	9.76211	0.793144	4.35524	8.20221	14.11735	22.31956
1270	9.79634	0.459518	4.56534	7.90611	14.36168	22.26779
1343	10.3127	0.643226	4.57718	7.29526	14.88988	22.18514
1416	10.3579	0.447227	5.13141	7.22655	15.48931	22.71586
1489	10.4681	0.580607	4.89958	6.62652	15.36768	21.9942
1562	10.6647	0.349698	4.81496	6.60603	15.47966	22.08569
1635	10.6862	0.18903	5.00502	5.899	15.69122	21.59022
1708	10.7884	0.505039	5.37554	5.57429	16.16394	21.73823
1781	10.9719	0.421715	5.33455	5.92042	16.30645	22.22687
1854	11.2169	0.263083	5.14199	5.48633	16.35889	21.84522
1927	11.3467	0.511007	5.12723	5.50552	16.47393	21.97945
2000	11.2044	0.392757	5.25786	5.49768	16.46226	21.95994
2073	11.1483	0.397373	5.27965	5.01623	16.42795	21.44418
2146	11.493	0.155555	5.6701	5.14695	17.1631	22.31005
2219	11.4408	0.00884792	5.23873	4.90797	16.67953	21.5875
2292	11.4738	0.0150697	5.42898	4.36039	16.90278	21.26317
2365	11.4571	0.262941	5.34878	4.69083	16.80588	21.49671
2438	11.4768	0.21012	5.07697	4.23516	16.55377	20.78893
2511	11.5839	0.0393883	5.53946	4.11497	17.12336	21.23833

2584	11.7375	-0.153986	5.58891	4.28569	17.32641	21.6121
2657	11.567	0.106337	5.42094	4.02404	16.98794	21.01198
2730	11.6907	0.111804	5.58598	4.08215	17.27668	21.35883
2803	11.636	0.133164	5.60553	3.78351	17.24153	21.02504
2876	11.8589	-0.305899	5.56972	4.02366	17.42862	21.45228
2949	11.5401	0.0219436	5.76508	3.75631	17.30518	21.06149
3022	11.8321	-0.302145	5.47577	3.65036	17.30787	20.95823

Kinetic data for Diels-Alder cycloaddition at 303K (Run 2)

Conversion	Extent of reaction [x]	[iminium]-[x]	[cyclopentadiene]-[x]	Time (s)	ln([cp-x]/[imin-x])
0.06105272	0.015263	0.234737	0.609737	98	0.954562449
0.12473507	0.031184	0.218816	0.593816	171	0.998337644
0.20489461	0.051224	0.198776	0.573776	244	1.06005937
0.26204662	0.065512	0.184488	0.559488	317	1.109436402
0.31549865	0.078875	0.171125	0.546125	390	1.160452247
0.36709089	0.091773	0.158227	0.533227	463	1.214915276
0.40393665	0.100984	0.149016	0.524016	536	1.25746931
0.44335716	0.110839	0.139161	0.514161	609	1.306906429
0.48548497	0.121371	0.128629	0.503629	682	1.364909
0.51940865	0.129852	0.120148	0.495148	755	1.416133411
0.53533394	0.133833	0.116167	0.491167	828	1.441758564
0.55472748	0.138682	0.111318	0.486318	901	1.474470853
0.58734091	0.146835	0.103165	0.478165	974	1.533627938
0.60504353	0.151261	0.098739	0.473739	1047	1.568175597
0.62601614	0.156504	0.093496	0.468496	1120	1.611609206
0.63251023	0.158128	0.091872	0.466872	1193	1.625654955
0.64495309	0.161238	0.088762	0.463762	1266	1.653415345
0.67116457	0.167791	0.082209	0.457209	1339	1.715877259
0.68187205	0.170468	0.079532	0.454532	1412	1.743108989
0.69871512	0.174679	0.075321	0.450321	1485	1.788199238
0.70089094	0.175223	0.074777	0.449777	1558	1.794238596
0.72677444	0.181694	0.068306	0.443306	1631	1.870257829
0.74357204	0.185893	0.064107	0.439107	1704	1.924189686
0.73363681	0.183409	0.066591	0.441591	1777	1.891817263
0.74885444	0.187214	0.062786	0.437786	1850	1.941992769
0.74951512	0.187379	0.062621	0.437621	1923	1.944249527
0.74964959	0.187412	0.062588	0.437588	1996	1.944709702
0.76607965	0.19152	0.05848	0.43348	2069	2.003159565
0.76929904	0.192325	0.057675	0.432675	2142	2.01515945
0.7726476	0.193162	0.056838	0.431838	2215	2.027843862
0.79493227	0.198733	0.051267	0.426267	2288	2.118019799
0.78178847	0.195447	0.054553	0.429553	2361	2.063574303
0.79627812	0.19907	0.05093	0.42593	2434	2.123814728
0.80624795	0.201562	0.048438	0.423438	2507	2.168122241
0.80169951	0.200425	0.049575	0.424575	2580	2.147599816
0.8084883	0.202122	0.047878	0.422878	2653	2.178429004

0.80887764	0.202219	0.047781	0.422781	2726	2.180233854
0.82004743	0.205012	0.044988	0.419988	2799	2.23382752
0.81243672	0.203109	0.046891	0.421891	2872	2.19692464
0.82165032	0.205413	0.044587	0.419587	2945	2.241820139
0.82582689	0.206457	0.043543	0.418543	3018	2.263024991
0.83186909	0.207967	0.042033	0.417033	3091	2.294716138

X-Ray data for iminium ion 122aq

Table 1. Crystal data and structure refinement.

Identification code	**2007src0354 (TG 3.399)**
Empirical formula	$C_{14}H_{15}F_9NP$
Formula weight	399.24
Temperature	120(2) K
Wavelength	0.71073 Å
Crystal system	Monoclinic
Space group	$P2_1/c$
Unit cell dimensions	$a = 18.5797(5)$ Å $\quad \alpha = 90°$
	$b = 10.6257(3)$ Å $\quad \beta = 98.718(2)°$
	$c = 8.38670(10)$ Å $\quad \gamma = 90°$
Volume	1636.59(7) Å^3
Z	4
Density (calculated)	1.620 Mg / m^3
Absorption coefficient	0.260 mm^{-1}
$F(000)$	808
Crystal	Block; colourless
Crystal size	$0.50 \times 0.20 \times 0.10$ mm^3
θ range for data collection	2.93 – 27.49°
Index ranges	$-23 \leq h \leq 24, -12 \leq k \leq 13, -10 \leq l \leq 10$
Reflections collected	19829
Independent reflections	3737 [$R_{int} = 0.0411$]
Completeness to $\theta = 27.49°$	99.5 %
Absorption correction	Semi–empirical from equivalents
Max. and min. transmission	0.9745 and 0.8810
Refinement method	Full-matrix least-squares on F^2
Data / restraints / parameters	3737 / 0 / 226
Goodness-of-fit on F^2	1.047
Final R indices [$F^2 > 2\sigma(F^2)$]	$R1 = 0.0395, wR2 = 0.0978$
R indices (all data)	$R1 = 0.0530, wR2 = 0.1047$
Largest diff. peak and hole	0.328 and -0.442 e Å^{-3}

Diffractometer: *Nonius KappaCCD* area detector (ϕ scans and ω scans to fill *asymmetric unit* sphere). **Cell determination:** DirAx (Duisenberg, A.J.M.(1992). J. Appl. Cryst. 25, 92-96.) **Data collection:** Collect (Collect: Data collection software, R. Hooft, Nonius B.V., 1998). **Data reduction and cell refinement:** *Denzo* (Z. Otwinowski & W. Minor, *Methods in Enzymology* (1997) Vol. **276:** *Macromolecular Crystallography*, part A, pp. 307–326; C. W. Carter, Jr. & R. M. Sweet, Eds., Academic Press). **Absorption correction:** *SADABS Version 2.10.* (G. M. Sheldrick (2003)) Bruker AXS Inc., Madison, Wisconsin, USA. **Structure solution:** *SHELXS97* (G. M. Sheldrick, Acta Cryst. (1990) A46 467–473). **Structure refinement:** *SHELXL97* (G. M. Sheldrick (1997), University of Göttingen, Germany). **Graphics:** *PLATON* (A.L. Spek, J. Appl. Crystallogr. 2003, 36, 7).

Table 2. Atomic coordinates [× 10⁴], equivalent isotropic displacement parameters [$\text{Å}^2 \times 10^3$] and site occupancy factors. U_{eq} is defined as one third of the trace of the orthogonalized U^{ij} tensor.

Atom	x	y	z	U_{eq}	S.o.f.
C1	727(1)	−1336(2)	8711(2)	32(1)	1
C2	1163(1)	−514(2)	7734(2)	22(1)	1
C3	826(1)	790(2)	7369(2)	28(1)	1
C4	1162(1)	1603(2)	8795(2)	30(1)	1
C5	1935(1)	1102(2)	9224(2)	23(1)	1
C6	2418(1)	−1030(2)	8872(2)	18(1)	1
C7	3121(1)	−768(2)	9732(2)	19(1)	1
C8	3640(1)	−1664(2)	9809(2)	20(1)	1
C9	4386(1)	−1573(2)	10632(2)	19(1)	1
C10	4642(1)	−547(2)	11617(2)	23(1)	1
C11	5364(1)	−508(2)	12334(2)	26(1)	1
C12	5839(1)	−1474(2)	12086(2)	28(1)	1
C13	5595(1)	−2485(2)	11113(2)	28(1)	1
C14	4870(1)	−2536(2)	10399(2)	24(1)	1
N1	1882(1)	−232(1)	8680(2)	18(1)	1
F1	2456(1)	976(1)	5693(1)	34(1)	1
F2	3301(1)	−168(1)	4637(2)	40(1)	1
F3	2573(1)	1180(1)	3070(1)	44(1)	1
F4	2418(1)	−935(1)	2728(1)	36(1)	1
F5	1581(1)	209(1)	3791(2)	47(1)	1
F6	2320(1)	−1137(1)	5358(1)	32(1)	1
F7	1030(1)	−2469(1)	9007(2)	50(1)	1
F8	645(1)	−838(1)	10133(1)	43(1)	1
F9	57(1)	−1528(1)	7902(2)	50(1)	1
P1	2440(1)	24(1)	4207(1)	21(1)	1

257

Table 3. Bond lengths [Å] and angles [°].

C1–F8	1.334(2)	C9–C14	1.396(2)
C1–F7	1.335(2)	C9–C10	1.407(2)
C1–F9	1.340(2)	C10–C11	1.386(2)
C1–C2	1.514(2)	C11–C12	1.389(3)
C2–N1	1.4784(19)	C12–C13	1.384(3)
C2–C3	1.532(2)	C13–C14	1.390(2)
C3–C4	1.530(2)	F1–P1	1.6026(10)
C4–C5	1.521(2)	F2–P1	1.5990(11)
C5–N1	1.487(2)	F3–P1	1.5979(11)
C6–N1	1.299(2)	F4–P1	1.6009(10)
C6–C7	1.419(2)	F5–P1	1.5940(12)
C7–C8	1.351(2)	F6–P1	1.6027(10)
C8–C9	1.455(2)		
F8–C1–F7	107.06(16)	C2–N1–C5	111.68(12)
F8–C1–F9	106.81(15)	F5–P1–F3	90.86(7)
F7–C1–F9	106.84(15)	F5–P1–F2	179.53(7)
F8–C1–C2	113.48(15)	F3–P1–F2	89.56(7)
F7–C1–C2	112.08(15)	F5–P1–F4	90.10(6)
F9–C1–C2	110.22(15)	F3–P1–F4	90.87(6)
N1–C2–C1	109.90(13)	F2–P1–F4	90.10(6)
N1–C2–C3	103.47(13)	F5–P1–F1	89.55(6)
C1–C2–C3	113.19(14)	F3–P1–F1	89.56(6)
C4–C3–C2	104.38(13)	F2–P1–F1	90.25(6)
C5–C4–C3	104.27(14)	F4–P1–F1	179.45(6)
N1–C5–C4	104.22(13)	F5–P1–F6	90.02(7)
N1–C6–C7	124.26(15)	F3–P1–F6	179.11(7)
C8–C7–C6	118.74(15)	F2–P1–F6	89.56(6)
C7–C8–C9	126.72(15)	F4–P1–F6	89.29(6)
C14–C9–C10	118.83(15)	F1–P1–F6	90.28(6
C14–C9–C8	118.21(14)		
C10–C9–C8	122.94(14)		
C11–C10–C9	119.84(15)		
C10–C11–C12	120.50(16)		
C13–C12–C11	120.29(15)		
C12–C13–C14	119.54(16)		
C13–C14–C9	120.99(16)		
C6–N1–C2	123.22(13)		
C6–N1–C5	124.80(13)		

258

Table 4. Anisotropic displacement parameters [$\mathrm{\AA}^2 \times 10^3$]. The anisotropic displacement factor exponent takes the form: $-2\pi^2[h^2 a^{*2} U^{11} + \cdots + 2\, h\, k\, a^*\, b^*\, U^{12}]$.

Atom	U^{11}	U^{22}	U^{33}	U^{23}	U^{13}	U^{12}
C1	18(1)	23(1)	52(1)	3(1)	4(1)	0(1)
C2	18(1)	23(1)	24(1)	−2(1)	1(1)	1(1)
C3	22(1)	26(1)	35(1)	5(1)	−1(1)	2(1)
C4	25(1)	20(1)	46(1)	−3(1)	3(1)	4(1)
C5	24(1)	17(1)	27(1)	−4(1)	2(1)	0(1)
C6	20(1)	16(1)	20(1)	2(1)	7(1)	−1(1)
C7	20(1)	19(1)	19(1)	1(1)	4(1)	−1(1)
C8	21(1)	19(1)	19(1)	1(1)	5(1)	−2(1)
C9	19(1)	20(1)	19(1)	4(1)	5(1)	−1(1)
C10	25(1)	22(1)	22(1)	3(1)	4(1)	1(1)
C11	26(1)	29(1)	22(1)	2(1)	1(1)	−6(1)
C12	19(1)	40(1)	24(1)	7(1)	2(1)	−3(1)
C13	22(1)	32(1)	29(1)	4(1)	6(1)	7(1)
C14	24(1)	25(1)	24(1)	−1(1)	5(1)	1(1)
N1	18(1)	18(1)	18(1)	1(1)	4(1)	−1(1)
F1	45(1)	29(1)	29(1)	−13(1)	7(1)	−2(1)
F2	25(1)	34(1)	61(1)	−2(1)	7(1)	0(1)
F3	81(1)	22(1)	29(1)	6(1)	8(1)	−6(1)
F4	64(1)	25(1)	22(1)	−6(1)	13(1)	−5(1)
F5	28(1)	38(1)	67(1)	−14(1)	−12(1)	8(1)
F6	46(1)	26(1)	25(1)	4(1)	12(1)	−4(1)
F7	33(1)	23(1)	97(1)	17(1)	15(1)	2(1)
F8	38(1)	50(1)	46(1)	8(1)	23(1)	−2(1)
F9	21(1)	40(1)	84(1)	2(1)	−3(1)	−10(1)
P1	27(1)	17(1)	18(1)	−1(1)	3(1)	1(1)

X-Ray data for iminium ion 123

Table 1. Crystal data and structure refinement.

Identification code	**2007src0546 (TG 3.415)**	
Empirical formula	$C_{13}H_{16}F_6NP$	
Formula weight	331.24	
Temperature	120(2) K	
Wavelength	0.71073 Å	
Crystal system	Monoclinic	
Space group	$P2_1/c$	
Unit cell dimensions	$a = 18.0459(5)$ Å	$\alpha = 90°$
	$b = 16.9680(5)$ Å	$\beta = 97.198(2)°$
	$c = 9.58230(10)$ Å	$\gamma = 90°$
Volume	2911.00(12) Å^3	
Z	8	
Density (calculated)	1.512 Mg / m^3	
Absorption coefficient	0.247 mm^{-1}	
$F(000)$	1360	
Crystal	Block; colourless	
Crystal size	$0.20 \times 0.12 \times 0.04$ mm^3	
θ range for data collection	$3.31 - 27.50°$	
Index ranges	$-23 \leq h \leq 23, -22 \leq k \leq 22, -12 \leq l \leq 11$	
Reflections collected	40070	
Independent reflections	6664 [$R_{int} = 0.0556$]	
Completeness to $\theta = 27.50°$	99.5 %	
Absorption correction	Semi–empirical from equivalents	
Max. and min. transmission	0.9902 and 0.9523	
Refinement method	Full-matrix least-squares on F^2	
Data / restraints / parameters	6664 / 0 / 416	
Goodness-of-fit on F^2	1.040	
Final R indices [$F^2 > 2\sigma(F^2)$]	$R1 = 0.0552, wR2 = 0.1405$	
R indices (all data)	$R1 = 0.0825, wR2 = 0.1583$	
Largest diff. peak and hole	0.783 and -0.775 e Å^{-3}	

Diffractometer: *Nonius KappaCCD* area detector (φ scans and ω scans to fill *asymmetric unit* sphere). **Cell determination:** DirAx (Duisenberg, A.J.M.(1992). J. Appl. Cryst. 25, 92-96.) **Data collection:** Collect (Collect: Data collection software, R. Hooft, Nonius B.V., 1998). **Data reduction and cell refinement:** *Denzo* (Z. Otwinowski & W. Minor, *Methods in Enzymology* (1997) Vol. 276: *Macromolecular Crystallography*, part A, pp. 307–326; C. W. Carter, Jr. & R. M. Sweet, Eds., Academic Press). **Absorption correction:** *SADABS Version 2.10.* (G. M. Sheldrick (2003)) Bruker AXS Inc., Madison, Wisconsin, USA. **Structure solution:** *SHELXS97* (G. M. Sheldrick, Acta Cryst. (1990) A46 467–473). **Structure refinement:** *SHELXL97* (G. M. Sheldrick (1997), University of Göttingen, Germany). **Graphics:** *PLATON* (A.L. Spek, J. Appl. Crystallogr. 2003, 36, 7).

Table 2. Atomic coordinates [$\times 10^4$], equivalent isotropic displacement parameters [$\text{Å}^2 \times 10^3$] and site occupancy factors. U_{eq} is defined as one third of the trace of the orthogonalized U^{ij} tensor.

Atom	x	y	z	U_{eq}	$S.o.f.$
F7	3133(2)	8267(1)	994(3)	47(1)	0.774(8)
F9	4209(2)	8860(2)	690(4)	46(1)	0.774(8)
F10	3596(3)	9702(2)	−844(3)	49(1)	0.774(8)
F12	2517(1)	9118(2)	−556(4)	51(1)	0.774(8)
F7'	2604(10)	8543(8)	633(12)	75(6)	0.226(8)
F9'	3870(16)	8633(12)	1331(16)	142(12)	0.226(8)
F10'	3941(18)	9511(19)	−200(40)	214(18)	0.226(8)
F12'	2820(15)	9495(11)	−953(11)	108(9)	0.226(8)
F8	3456(1)	8385(1)	−1140(2)	37(1)	1
F11	3233(1)	9612(1)	1342(1)	36(1)	1
P2	3351(1)	8995(1)	111(1)	26(1)	1
C14	2796(1)	3187(2)	−2677(3)	30(1)	1
C15	3295(2)	2729(2)	−3554(3)	34(1)	1
C16	3385(1)	3288(2)	−4774(2)	30(1)	1
C17	2621(1)	3664(2)	−5106(2)	27(1)	1
C18	1851(1)	4196(1)	−3365(2)	23(1)	1
C19	1443(1)	4739(1)	−4299(2)	22(1)	1
C20	955(1)	5238(1)	−3800(2)	22(1)	1
C21	521(1)	5844(1)	−4618(2)	21(1)	1
C22	560(1)	5954(1)	−6056(2)	25(1)	1
C23	132(1)	6529(2)	−6800(2)	29(1)	1
C24	−338(1)	7007(1)	−6112(3)	28(1)	1
C25	−387(1)	6898(1)	−4698(2)	27(1)	1
C26	37(1)	6319(1)	−3943(2)	24(1)	1
N2	2364(1)	3725(1)	−3696(2)	22(1)	1
F1	640(1)	4022(1)	591(2)	68(1)	1
F3	1610(1)	3417(1)	−269(2)	72(1)	1
F4	2409(1)	4095(1)	1212(3)	76(1)	1
F6	1515(1)	4721(1)	2054(2)	71(1)	1
F2	1516(1)	3394(1)	2040(2)	43(1)	1
F5	1527(1)	4758(1)	−274(2)	48(1)	1
P1	1516(1)	4075(1)	882(1)	27(1)	1
C1	2080(1)	6585(1)	1178(2)	24(1)	1
C2	1405(1)	6795(2)	120(2)	28(1)	1
C3	1766(1)	7029(2)	−1180(2)	28(1)	1
C4	2407(1)	6445(1)	−1207(2)	26(1)	1
C5	3064(1)	5662(1)	731(2)	20(1)	1
C6	3532(1)	5245(1)	−123(2)	21(1)	1

262

C7	3980(1)	4673(1)	479(2)	22(1)	1
C8	4473(1)	4158(1)	−205(2)	21(1)	1
C9	4868(1)	3569(1)	597(3)	27(1)	1
C10	5336(1)	3057(1)	−19(3)	30(1)	1
C11	5425(1)	3137(1)	−1422(3)	28(1)	1
C12	5047(1)	3732(1)	−2230(2)	26(1)	1
C13	4575(1)	4237(1)	−1632(2)	23(1)	1
N1	2578(1)	6189(1)	281(2)	19(1)	1

Table 3. Bond lengths [Å] and angles [°].

F7–P2	1.575(2)	C24–C25	1.381(3)
F9–P2	1.594(3)	C25–C26	1.392(3)
F10–P2	1.604(3)	F1–P1	1.5742(19)
F12–P2	1.573(3)	F3–P1	1.5935(18)
F7'–P2	1.681(9)	F4–P1	1.603(2)
F9'–P2	1.532(10)	F6–P1	1.5693(17)
F10'–P2	1.436(15)	F2–P1	1.6024(15)
F12'–P2	1.560(12)	F5–P1	1.6051(16)
F8–P2	1.6128(15)	C1–N1	1.480(3)
F11–P2	1.6114(14)	C1–C2	1.526(3)
C14–N2	1.485(3)	C2–C3	1.529(3)
C14–C15	1.520(4)	C3–C4	1.527(3)
C15–C16	1.529(3)	C4–N1	1.485(3)
C16–C17	1.517(3)	C5–N1	1.289(3)
C17–N2	1.486(3)	C5–C6	1.434(3)
C18–N2	1.292(3)	C6–C7	1.347(3)
C18–C19	1.425(3)	C7–C8	1.461(3)
C19–C20	1.351(3)	C8–C9	1.400(3)
C20–C21	1.461(3)	C8–C13	1.409(3)
C21–C22	1.400(3)	C9–C10	1.393(3)
C21–C26	1.405(3)	C10–C11	1.380(3)
C22–C23	1.385(3)	C11–C12	1.397(3)
C23–C24	1.397(3)	C12–C13	1.383(3)
F10'–P2–F9'	90.2(18)	F7–P2–F9	89.84(18)
F10'–P2–F12'	86.9(18)	F10'–P2–F10	33(2)
F9'–P2–F12'	169.7(7)	F9'–P2–F10	123.4(13)
F10'–P2–F12	122(2)	F12'–P2–F10	54.0(11)
F9'–P2–F12	145.5(13)	F12–P2–F10	89.3(2)
F12'–P2–F12	35.3(10)	F7–P2–F10	176.70(17)
F10'–P2–F7	146(2)	F9–P2–F10	88.92(18)
F9'–P2–F7	56.3(13)	F10'–P2–F11	85.6(7)
F12'–P2–F7	127.1(11)	F9'–P2–F11	80.0(4)
F12–P2–F7	91.75(18)	F12'–P2–F11	89.9(4)
F10'–P2–F9	56(2)	F12–P2–F11	90.23(12)
F9'–P2–F9	37.1(13)	F7–P2–F11	92.95(11)
F12'–P2–F9	142.8(11)	F9–P2–F11	92.85(14)
F12–P2–F9	176.46(16)	F10–P2–F11	90.17(13)

F10'–P2–F8	94.6(7)	F6–P1–F4	86.30(14)
F9'–P2–F8	101.1(4)	F1–P1–F4	177.61(11)
F12'–P2–F8	89.0(4)	F3–P1–F4	87.74(13)
F12–P2–F8	88.79(12)	F2–P1–F4	88.01(10)
F7–P2–F8	87.53(11)	F6–P1–F5	89.49(10)
F9–P2–F8	88.12(14)	F1–P1–F5	91.03(10)
F10–P2–F8	89.37(13)	F3–P1–F5	90.96(9)
F11–P2–F8	178.92(9)	F2–P1–F5	179.30(10)
F10'–P2–F7'	168.9(9)	F4–P1–F5	91.29(11)
F9'–P2–F7'	91.4(12)	N1–C1–C2	102.29(17)
F12'–P2–F7'	89.6(11)	C1–C2–C3	102.49(19)
F12–P2–F7'	54.5(7)	C4–C3–C2	104.22(18)
F7–P2–F7'	38.5(6)	N1–C4–C3	103.89(17)
F9–P2–F7'	127.6(7)	N1–C5–C6	125.16(19)
F10–P2–F7'	143.2(7)	C7–C6–C5	118.37(19)
F11–P2–F7'	83.9(3)	C6–C7–C8	127.3(2)
F8–P2–F7'	95.9(3)	C9–C8–C13	118.8(2)
N2–C14–C15	104.42(19)	C9–C8–C7	118.6(2)
C14–C15–C16	103.50(19)	C13–C8–C7	122.6(2)
C17–C16–C15	103.9(2)	C10–C9–C8	120.4(2)
N2–C17–C16	102.56(18)	C11–C10–C9	120.2(2)
N2–C18–C19	125.1(2)	C10–C11–C12	120.1(2)
C20–C19–C18	119.4(2)	C13–C12–C11	120.1(2)
C19–C20–C21	125.5(2)	C12–C13–C8	120.3(2)
C22–C21–C26	119.2(2)	C5–N1–C1	123.95(17)
C22–C21–C20	122.2(2)	C5–N1–C4	125.04(18)
C26–C21–C20	118.6(2)	C1–N1–C4	110.91(17
C23–C22–C21	120.4(2)		
C22–C23–C24	119.9(2)		
C25–C24–C23	120.1(2)		
C24–C25–C26	120.4(2)		
C25–C26–C21	119.9(2)		
C18–N2–C14	123.51(19)		
C18–N2–C17	125.51(19)		
C14–N2–C17	110.95(18)		
F6–P1–F1	94.34(14)		
F6–P1–F3	174.03(14)		
F1–P1–F3	91.61(13)		
F6–P1–F2	90.46(10)		
F1–P1–F2	89.67(10)		
F3–P1–F2	89.01(10)		

Table 4. Anisotropic displacement parameters [$\text{Å}^2 \times 10^3$]. The anisotropic displacement factor exponent takes the form: $-2\pi^2[h^2 a^{*2} U^{11} + \cdots + 2\,h\,k\,a^*\,b^*\,U^{12}]$.

Atom	U^{11}	U^{22}	U^{33}	U^{23}	U^{13}	U^{12}
F7	74(2)	34(1)	38(1)	1(1)	29(1)	−9(1)
F9	30(1)	57(2)	47(2)	−13(1)	−10(1)	5(1)
F10	91(3)	27(1)	32(1)	4(1)	23(1)	−1(2)
F12	28(1)	68(2)	53(2)	−33(2)	−10(1)	18(1)
F7'	104(12)	70(8)	63(7)	−50(6)	63(8)	−65(9)
F9'	230(20)	128(15)	49(8)	−44(8)	−72(11)	151(17)
F10'	170(20)	230(30)	290(30)	−190(30)	210(20)	−160(20)
F12'	200(20)	95(12)	23(5)	−5(6)	−8(8)	84(14)
F8	42(1)	34(1)	35(1)	−8(1)	4(1)	11(1)
F11	49(1)	37(1)	21(1)	−7(1)	5(1)	−6(1)
P2	29(1)	26(1)	21(1)	0(1)	1(1)	1(1)
C14	28(1)	31(1)	30(1)	11(1)	−2(1)	4(1)
C15	31(1)	26(1)	44(1)	2(1)	0(1)	5(1)
C16	26(1)	34(1)	29(1)	−5(1)	1(1)	4(1)
C17	28(1)	33(1)	21(1)	−3(1)	1(1)	5(1)
C18	22(1)	26(1)	21(1)	3(1)	2(1)	−5(1)
C19	23(1)	23(1)	21(1)	3(1)	2(1)	−2(1)
C20	21(1)	24(1)	22(1)	2(1)	1(1)	−3(1)
C21	20(1)	21(1)	23(1)	0(1)	3(1)	−3(1)
C22	25(1)	27(1)	24(1)	5(1)	7(1)	4(1)
C23	30(1)	31(1)	27(1)	9(1)	7(1)	1(1)
C24	26(1)	20(1)	38(1)	6(1)	4(1)	1(1)
C25	24(1)	22(1)	34(1)	−5(1)	4(1)	0(1)
C26	21(1)	24(1)	26(1)	−5(1)	2(1)	−2(1)
N2	22(1)	23(1)	19(1)	2(1)	−1(1)	−1(1)
F1	37(1)	84(2)	79(1)	27(1)	−7(1)	−5(1)
F3	138(2)	37(1)	49(1)	−11(1)	41(1)	−15(1)
F4	36(1)	53(1)	142(2)	18(1)	20(1)	−8(1)
F6	140(2)	44(1)	31(1)	−12(1)	14(1)	4(1)
F2	49(1)	44(1)	31(1)	12(1)	−8(1)	−21(1)
F5	82(1)	34(1)	27(1)	4(1)	9(1)	−15(1)
P1	32(1)	28(1)	21(1)	−1(1)	6(1)	−7(1)
C1	29(1)	26(1)	20(1)	0(1)	9(1)	5(1)
C2	26(1)	31(1)	28(1)	4(1)	7(1)	6(1)
C3	29(1)	31(1)	23(1)	4(1)	3(1)	3(1)
C4	28(1)	32(1)	17(1)	3(1)	3(1)	5(1)
C5	20(1)	21(1)	19(1)	−1(1)	2(1)	−3(1)
C6	20(1)	26(1)	18(1)	−2(1)	5(1)	−1(1)

C7	21(1)	23(1)	22(1)	−1(1)	3(1)	−2(1)
C8	17(1)	23(1)	24(1)	−1(1)	3(1)	−2(1)
C9	27(1)	25(1)	29(1)	5(1)	6(1)	−1(1)
C10	27(1)	24(1)	40(1)	5(1)	6(1)	5(1)
C11	25(1)	25(1)	35(1)	−7(1)	7(1)	2(1)
C12	22(1)	32(1)	25(1)	−5(1)	2(1)	−1(1)
C13	20(1)	26(1)	22(1)	−2(1)	0(1)	0(1)
N1	19(1)	23(1)	15(1)	−1(1)	5(1)	−1(1)

X-Ray data for iminium ion 126

Table 1. Crystal data and structure refinement.

Identification code	2007src1313 (TG3-446)	
Empirical formula	$C_{16}H_{20}F_9N_2P$	
Formula weight	442.31	
Temperature	120(2) K	
Wavelength	0.71073 Å	
Crystal system	Monoclinic	
Space group	$P2_1/c$	
Unit cell dimensions	$a = 20.7923(9)$ Å	$\alpha = 90°$
	$b = 10.7114(5)$ Å	$\beta = 94.923(3)°$
	$c = 8.4013(3)$ Å	$\gamma = 90°$
Volume	1864.19(14) Å^3	
Z	4	
Density (calculated)	1.576 Mg / m^3	
Absorption coefficient	0.238 mm^{-1}	
F(000)	904	
Crystal	Blade; orange	
Crystal size	$0.40 \times 0.20 \times 0.04$ mm^3	
θ range for data collection	$3.09 - 27.50°$	
Index ranges	$-26 \le h \le 26, -13 \le k \le 13, -10 \le l \le 10$	
Reflections collected	30035	
Independent reflections	4260 [$R_{int} = 0.0644$]	
Completeness to $\theta = 27.50°$	99.7 %	
Absorption correction	Semi–empirical from equivalents	
Max. and min. transmission	0.9905 and 0.9108	
Refinement method	Full-matrix least-squares on F^2	
Data / restraints / parameters	4260 / 0 / 255	
Goodness-of-fit on F^2	1.025	
Final R indices [$F^2 > 2\sigma(F^2)$]	$R1 = 0.0520, wR2 = 0.1308$	
R indices (all data)	$R1 = 0.0690, wR2 = 0.1421$	
Largest diff. peak and hole	0.530 and −0.493 e Å^{-3}	

Diffractometer: *Nonius KappaCCD* area detector (ϕ scans and ω scans to fill *asymmetric unit* sphere). **Cell determination:** DirAx (Duisenberg, A.J.M.(1992). J. Appl. Cryst. 25, 92-96.) **Data collection:** Collect (Collect: Data collection software, R. Hooft, Nonius B.V., 1998). **Data reduction and cell refinement:** *Denzo* (Z. Otwinowski & W. Minor, *Methods in Enzymology* (1997) Vol. 276: *Macromolecular Crystallography*, part A, pp. 307–326; C. W. Carter, Jr. & R. M. Sweet, Eds., Academic Press). **Absorption correction:** *SADABS Version 2.10.* (G. M. Sheldrick (2003)) Bruker AXS Inc., Madison, Wisconsin, USA. **Structure solution:** *SHELXS97* (G. M. Sheldrick, Acta Cryst. (1990) A46 467–473). **Structure refinement:** *SHELXL97* (G. M. Sheldrick (1997), University of Göttingen, Germany). **Graphics:** *PLATON* (A.L. Spek, J. Appl. Crystallogr. 2003, 36, 7).

Special details:

Table 2. Atomic coordinates [× 10^4], equivalent isotropic displacement parameters [$\text{Å}^2 \times 10^3$] and site occupancy factors. U_{eq} is defined as one third of the trace of the orthogonalized U^{ij} tensor.

Atom	x	y	z	U_{eq}	S.o.f.
C1	−3299(1)	6047(2)	−1052(3)	35(1)	1
C2	−3984(1)	6504(2)	−1341(3)	46(1)	1
C3	−4279(1)	5676(2)	−2697(3)	40(1)	1
C4	−3956(1)	4404(2)	−2400(3)	33(1)	1
C5	−4332(1)	3559(2)	−1377(3)	42(1)	1
C6	−2839(1)	3942(2)	−1397(2)	29(1)	1
C7	−2234(1)	4223(2)	−589(2)	29(1)	1
C8	−1747(1)	3375(2)	−574(2)	29(1)	1
C9	−1106(1)	3504(2)	190(2)	27(1)	1
C10	−632(1)	2620(2)	−131(3)	30(1)	1
C11	−2(1)	2716(2)	512(2)	30(1)	1
C12	192(1)	3707(2)	1561(2)	27(1)	1
C13	−285(1)	4603(2)	1885(2)	29(1)	1
C14	−907(1)	4497(2)	1216(2)	28(1)	1
C15	1297(1)	2893(2)	1866(3)	38(1)	1
C16	994(1)	4802(2)	3354(3)	36(1)	1
N1	−3325(1)	4715(2)	−1544(2)	27(1)	1
N2	810(1)	3805(2)	2229(2)	32(1)	1
F1	−4436(1)	4057(2)	36(2)	54(1)	1
F2	−4913(1)	3303(2)	−2123(2)	64(1)	1
F3	−4038(1)	2462(1)	−1083(2)	60(1)	1
F4	2744(1)	1243(1)	2317(2)	58(1)	1
F5	2577(1)	1001(1)	−347(2)	51(1)	1
F6	2040(1)	−213(2)	1317(2)	51(1)	1
F7	2811(1)	−1054(1)	−76(2)	50(1)	1
F8	2987(1)	−816(1)	2590(2)	44(1)	1
F9	3523(1)	386(2)	935(2)	59(1)	1
P1	2783(1)	95(1)	1126(1)	33(1)	1

270

Table 3. Bond lengths [Å] and angles [°].

C1–N1	1.486	C1–C2		C10–C11	1.377(3)
C2–C3	1.529(4)			C11–C12	1.416(3)
C3–C4	1.530(3)			C12–N2	1.361(3)
C4–N1	1.479(3)			C12–C13	1.424(3)
C4–C5	1.511(3)			C13–C14	1.370(3)
C5–F1	1.337(3)			C15–N2	1.459(3)
C5–F3	1.337(3)			C16–N2	1.456(3)
C5–F2	1.342(3)			F4–P1	1.5920(15)
C6–N1	1.304(3)			F5–P1	1.6017(14)
C6–C7	1.410(3)			F6–P1	1.5994(15)
C7–C8	1.360(3)			F7–P1	1.5958(15)
C8–C9	1.436(3)			F8–P1	1.5985(14)
C9–C14	1.408(3)			F9–P1	1.5919(16)
C9–C10	1.410(3)				

N1–C1–C2	104.83(18)
C1–C2–C3	104.1(2)
C2–C3–C4	104.63(19)
N1–C4–C5	109.78(18)
N1–C4–C3	103.77(17)
C5–C4–C3	112.67(19)
F1–C5–F3	107.0(2)
F1–C5–F2	106.7(2)
F3–C5–F2	106.6(2)
F1–C5–C4	113.4(2)
F3–C5–C4	112.5(2)
F2–C5–C4	110.2(2)
N1–C6–C7	124.2(2)
C8–C7–C6	119.6(2)
C7–C8–C9	127.0(2)
C14–C9–C10	116.87(19)
C14–C9–C8	123.93(18)
C10–C9–C8	119.17(19)
C11–C10–C9	122.1(2)
C10–C11–C12	120.67(19)
N2–C12–C11	121.50(19)
N2–C12–C13	121.18(19)
C11–C12–C13	117.32(19)
C14–C13–C12	120.99(19)
C13–C14–C9	122.00(19)
C6–N1–C4	123.46(18)
C6–N1–C1	125.05(18)
C4–N1–C1	111.14(16)
C12–N2–C16	120.77(18)
C12–N2–C15	120.69(19)
C16–N2–C15	118.51(18)
F4–P1–F9	90.78(10)
F4–P1–F7	179.19(10)
F9–P1–F7	89.91(9)
F4–P1–F8	90.70(8)
F9–P1–F8	90.07(9)
F7–P1–F8	89.72(8)
F4–P1–F6	89.69(10)
F9–P1–F6	179.39(10)
F7–P1–F6	89.62(9)
F8–P1–F6	89.55(8)

F4–P1–F5	89.56(9)
F9–P1–F5	90.03(9)
F7–P1–F5	90.03(8)
F8–P1–F5	179.73(10)
F6–P1–F5	90.36(8)

Symmetry transformations used to generate equivalent atoms:

Table 4. Anisotropic displacement parameters [$\text{Å}^2 \times 10^3$]. The anisotropic displacement factor exponent takes the form: $-2\pi^2[h^2 a^{*2} U^{11} + \cdots + 2\, h\, k\, a^*\, b^*\, U^{12}]$.

Atom	U^{11}	U^{22}	U^{33}	U^{23}	U^{13}	U^{12}
C1	33(1)	28(1)	44(1)	–3(1)	5(1)	0(1)
C2	37(1)	35(1)	65(2)	–4(1)	1(1)	3(1)
C3	32(1)	40(1)	48(1)	6(1)	1(1)	3(1)
C4	28(1)	35(1)	36(1)	–3(1)	2(1)	–1(1)
C5	27(1)	36(1)	64(2)	1(1)	7(1)	–2(1)
C6	28(1)	28(1)	32(1)	2(1)	10(1)	–2(1)
C7	29(1)	29(1)	31(1)	1(1)	7(1)	–2(1)
C8	31(1)	27(1)	30(1)	1(1)	9(1)	–3(1)
C9	27(1)	25(1)	30(1)	3(1)	8(1)	0(1)
C10	33(1)	25(1)	34(1)	–1(1)	7(1)	1(1)
C11	32(1)	25(1)	34(1)	1(1)	9(1)	5(1)
C12	26(1)	28(1)	27(1)	4(1)	7(1)	–1(1)
C13	32(1)	26(1)	29(1)	0(1)	8(1)	–1(1)
C14	29(1)	26(1)	30(1)	2(1)	10(1)	4(1)
C15	31(1)	38(1)	45(1)	4(1)	7(1)	6(1)
C16	33(1)	37(1)	37(1)	2(1)	3(1)	–4(1)
N1	25(1)	28(1)	29(1)	0(1)	6(1)	–2(1)
N2	29(1)	32(1)	35(1)	2(1)	4(1)	1(1)
F1	46(1)	60(1)	60(1)	7(1)	24(1)	–2(1)
F2	31(1)	59(1)	102(1)	0(1)	–4(1)	–15(1)
F3	41(1)	35(1)	104(1)	16(1)	18(1)	–1(1)
F4	92(1)	37(1)	46(1)	–9(1)	1(1)	7(1)
F5	62(1)	51(1)	40(1)	17(1)	3(1)	–3(1)
F6	37(1)	66(1)	53(1)	13(1)	13(1)	1(1)
F7	67(1)	45(1)	40(1)	–10(1)	16(1)	–8(1)
F8	55(1)	42(1)	36(1)	6(1)	7(1)	9(1)
F9	39(1)	66(1)	73(1)	9(1)	6(1)	–15(1)
P1	38(1)	32(1)	30(1)	1(1)	7(1)	–3(1)

X-Ray data for Indanone for 125

274

X-Ray data for iminium ion 124

Table 1. Crystal data and structure refinement for nct0601.

Identification code	nct0601
Empirical formula	C22 H25 F6 N2 O P
Formula weight	478.41
Temperature	150(2) K
Wavelength	0.71073 Å
Crystal system	Orthorhombic
Space group	P 212121
Unit cell dimensions	a = 9.7220(3) Å α= 90°.
	b = 13.2520(4) Å β= 90°.
	c = 17.4010(5) Å γ = 90°.
Volume	2241.87(12) Å^3
Z	4
Density (calculated)	1.417 Mg/m^3
Absorption coefficient	0.189 mm^{-1}
F(000)	992
Crystal size	0.40 x 0.28 x 0.25 mm^3
Theta range for data collection	3.72 to 26.37°.
Index ranges	-11<=h<=12, -16<=k<=16, -21<=l<=21
Reflections collected	13712
Independent reflections	4572 [R(int) = 0.0925]
Completeness to theta = 26.37°	99.5 %
Absorption correction	Semi-empirical from equivalents
Max. and min. transmission	0.9543 and 0.9282
Refinement method	Full-matrix least-squares on F^2
Data / restraints / parameters	4572 / 0 / 292
Goodness-of-fit on F^2	1.079
Final R indices [I>2sigma(I)]	R1 = 0.0486, wR2 = 0.1037
R indices (all data)	R1 = 0.0666, wR2 = 0.1117
Absolute structure parameter	0.04(12)
Largest diff. peak and hole	0.204 and -0.292 e.Å^{-3}

Table 2. Atomic coordinates (x 10^4) and equivalent isotropic displacement parameters ($\mathring{A}^2$x 10^3) for nct0601. U(eq) is defined as one third of the trace of the orthogonalized U^{ij} tensor.

	x	y	z	U(eq)
C(1)	1785(3)	8179(2)	5405(2)	26(1)
C(2)	1876(3)	8783(2)	6689(1)	23(1)
C(3)	2417(3)	8135(2)	7345(2)	34(1)
C(4)	1959(3)	9906(2)	6882(2)	29(1)
C(5)	304(3)	8192(2)	5663(1)	22(1)
C(6)	4061(3)	8688(2)	5880(2)	37(1)
C(7)	-565(3)	8930(2)	5189(2)	27(1)
C(8)	-83(3)	10012(2)	5214(1)	29(1)
C(9)	-779(3)	10730(2)	5641(2)	39(1)
C(10)	-303(4)	11711(2)	5693(2)	49(1)
C(11)	871(4)	11997(2)	5311(2)	47(1)
C(12)	1559(4)	11309(2)	4864(2)	46(1)
C(13)	1094(3)	10325(2)	4813(2)	33(1)
C(14)	-496(3)	8353(2)	7003(1)	26(1)
C(15)	-1787(3)	7876(2)	6912(2)	26(1)
C(16)	-2550(3)	7717(2)	7545(2)	27(1)
C(17)	-3771(3)	7092(2)	7622(2)	25(1)
C(18)	-4405(3)	7018(2)	8342(2)	31(1)
C(19)	-5509(3)	6359(2)	8455(2)	35(1)
C(20)	-5957(3)	5782(2)	7849(2)	37(1)
C(21)	-5351(3)	5849(2)	7133(2)	36(1)
C(22)	-4263(3)	6502(2)	7017(1)	27(1)
N(1)	437(2)	8473(2)	6482(1)	22(1)
N(2)	2586(2)	8536(2)	5974(1)	24(1)
O(1)	2167(2)	7916(1)	4765(1)	30(1)
P(1)	-907(1)	10124(1)	8875(1)	32(1)
F(1)	-823(2)	9951(2)	9774(1)	57(1)
F(2)	-1792(2)	11127(1)	9004(1)	54(1)
F(3)	471(2)	10771(1)	8889(1)	51(1)
F(4)	-15(2)	9120(1)	8729(1)	42(1)
F(5)	-2291(2)	9474(1)	8848(1)	46(1)
F(6)	-1016(2)	10280(1)	7967(1)	47(1)

276

Table 3. Bond lengths [Å] and angles [°] for nct0601.

C(1)-O(1)	1.224(3)
C(1)-N(2)	1.346(3)
C(1)-C(5)	1.508(4)
C(2)-N(2)	1.459(3)
C(2)-N(1)	1.502(3)
C(2)-C(3)	1.523(4)
C(2)-C(4)	1.527(4)
C(5)-N(1)	1.478(3)
C(5)-C(7)	1.533(3)
C(6)-N(2)	1.458(3)
C(7)-C(8)	1.510(4)
C(8)-C(9)	1.384(4)
C(8)-C(13)	1.402(4)
C(9)-C(10)	1.383(4)
C(10)-C(11)	1.374(5)
C(11)-C(12)	1.372(5)
C(12)-C(13)	1.384(4)
C(14)-N(1)	1.293(3)
C(14)-C(15)	1.415(4)
C(15)-C(16)	1.344(4)
C(16)-C(17)	1.453(4)
C(17)-C(22)	1.396(4)
C(17)-C(18)	1.401(4)
C(18)-C(19)	1.397(4)
C(19)-C(20)	1.374(4)
C(20)-C(21)	1.381(4)
C(21)-C(22)	1.381(4)
P(1)-F(1)	1.5843(18)
P(1)-F(3)	1.5906(19)
P(1)-F(6)	1.5966(17)
P(1)-F(5)	1.5984(19)
P(1)-F(2)	1.5996(19)
P(1)-F(4)	1.6073(17)

O(1)-C(1)-N(2)	126.5(3)
O(1)-C(1)-C(5)	124.3(2)
N(2)-C(1)-C(5)	109.2(2)
N(2)-C(2)-N(1)	100.09(19)
N(2)-C(2)-C(3)	110.5(2)
N(1)-C(2)-C(3)	110.3(2)
N(2)-C(2)-C(4)	112.4(2)
N(1)-C(2)-C(4)	111.6(2)
C(3)-C(2)-C(4)	111.5(2)
N(1)-C(5)-C(1)	101.9(2)
N(1)-C(5)-C(7)	114.0(2)
C(1)-C(5)-C(7)	111.9(2)
C(8)-C(7)-C(5)	114.8(2)
C(9)-C(8)-C(13)	117.6(3)
C(9)-C(8)-C(7)	121.0(3)
C(13)-C(8)-C(7)	121.3(2)
C(10)-C(9)-C(8)	121.1(3)
C(11)-C(10)-C(9)	120.4(3)
C(12)-C(11)-C(10)	119.8(3)
C(11)-C(12)-C(13)	120.2(3)
C(12)-C(13)-C(8)	120.9(3)
N(1)-C(14)-C(15)	126.8(2)
C(16)-C(15)-C(14)	117.9(2)
C(15)-C(16)-C(17)	128.0(2)
C(22)-C(17)-C(18)	119.0(2)
C(22)-C(17)-C(16)	122.0(2)
C(18)-C(17)-C(16)	118.8(2)
C(19)-C(18)-C(17)	120.5(3)
C(20)-C(19)-C(18)	119.0(3)
C(19)-C(20)-C(21)	121.4(3)
C(20)-C(21)-C(22)	120.0(3)
C(21)-C(22)-C(17)	120.2(2)
C(14)-N(1)-C(5)	125.7(2)
C(14)-N(1)-C(2)	121.3(2)
C(5)-N(1)-C(2)	112.40(19)
C(1)-N(2)-C(6)	122.3(2)

C(1)-N(2)-C(2)	115.6(2)
C(6)-N(2)-C(2)	122.0(2)
F(1)-P(1)-F(3)	91.07(11)
F(1)-P(1)-F(6)	178.80(11)
F(3)-P(1)-F(6)	90.10(11)
F(1)-P(1)-F(5)	89.66(11)
F(3)-P(1)-F(5)	179.26(11)
F(6)-P(1)-F(5)	89.16(10)
F(1)-P(1)-F(2)	90.45(11)
F(3)-P(1)-F(2)	90.14(10)
F(6)-P(1)-F(2)	89.75(10)
F(5)-P(1)-F(2)	89.92(10)
F(1)-P(1)-F(4)	90.48(10)
F(3)-P(1)-F(4)	89.72(10)
F(6)-P(1)-F(4)	89.32(9)
F(5)-P(1)-F(4)	90.21(10)
F(2)-P(1)-F(4)	179.07(10)

Symmetry transformations used to generate equivalent atoms:

Table 4. Anisotropic displacement parameters ($\mathring{A}^2$x 10^3)for nct0601. The anisotropic displacement factor exponent takes the form: $-2\pi^2[\ h^2a^{*2}U^{11} + ... + 2\ h\ k\ a^*\ b^*\ U^{12}\ ]$

	U^{11}	U^{22}	U^{33}	U^{23}	U^{13}	U^{12}
C(1)	32(2)	18(1)	29(2)	0(1)	1(1)	0(1)
C(2)	21(1)	26(1)	23(1)	-4(1)	1(1)	-2(1)
C(3)	29(2)	42(2)	31(2)	4(1)	-2(1)	2(1)
C(4)	26(1)	28(1)	32(1)	-8(1)	1(1)	-5(1)
C(5)	27(2)	18(1)	21(1)	-4(1)	-1(1)	-4(1)
C(6)	22(1)	44(2)	45(2)	-2(1)	6(1)	-3(1)
C(7)	24(1)	30(1)	28(1)	1(1)	-3(1)	-4(1)
C(8)	34(2)	29(1)	24(1)	1(1)	-5(1)	6(1)
C(9)	37(2)	36(2)	44(2)	-3(1)	0(2)	12(1)
C(10)	68(3)	30(2)	51(2)	-8(2)	-9(2)	25(2)
C(11)	73(3)	24(2)	44(2)	4(1)	-14(2)	-1(2)
C(12)	61(2)	35(2)	40(2)	5(2)	4(2)	-4(2)
C(13)	46(2)	26(1)	28(1)	3(1)	1(1)	2(1)
C(14)	29(2)	25(1)	24(1)	-4(1)	0(1)	-1(1)
C(15)	26(1)	26(1)	28(1)	-4(1)	-2(1)	-4(1)
C(16)	24(1)	29(1)	28(1)	-6(1)	0(1)	2(1)
C(17)	21(1)	25(1)	29(1)	1(1)	-2(1)	2(1)
C(18)	27(2)	37(2)	29(1)	-1(1)	0(1)	3(1)
C(19)	30(2)	41(2)	35(2)	10(1)	6(1)	0(1)
C(20)	25(2)	38(2)	49(2)	11(1)	1(1)	-6(1)
C(21)	31(2)	35(2)	41(2)	0(1)	-7(1)	-3(1)
C(22)	24(1)	29(1)	27(1)	2(1)	-1(1)	-1(1)
N(1)	22(1)	22(1)	22(1)	0(1)	2(1)	-2(1)
N(2)	23(1)	25(1)	25(1)	-2(1)	6(1)	-2(1)
O(1)	41(1)	28(1)	22(1)	-5(1)	6(1)	3(1)
P(1)	36(1)	27(1)	33(1)	-7(1)	2(1)	-2(1)
F(1)	71(1)	68(1)	30(1)	-9(1)	2(1)	-18(1)
F(2)	50(1)	34(1)	76(1)	-18(1)	19(1)	1(1)
F(3)	44(1)	44(1)	66(1)	-10(1)	7(1)	-15(1)
F(4)	49(1)	36(1)	41(1)	-4(1)	-5(1)	13(1)
F(5)	42(1)	37(1)	58(1)	-10(1)	-2(1)	-10(1)
F(6)	56(1)	49(1)	36(1)	4(1)	-1(1)	15(1)

Table 5. Hydrogen coordinates (x 10^4) and isotropic displacement parameters (Å^2x 10^3)
for nct0601.

	x	y	z	U(eq)
H(3A)	2229	7423	7236	51
H(3B)	1959	8330	7825	51
H(3C)	3411	8236	7397	51
H(4A)	2908	10080	7018	43
H(4B)	1352	10054	7317	43
H(4C)	1672	10303	6435	43
H(5)	-92	7498	5621	27
H(6A)	4561	8165	6164	55
H(6B)	4316	9354	6079	55
H(6C)	4299	8647	5333	55
H(7A)	-568	8701	4648	33
H(7B)	-1525	8902	5377	33
H(9)	-1598	10545	5904	47
H(10)	-791	12190	5994	59
H(11)	1205	12668	5356	57
H(12)	2358	11510	4589	55
H(13)	1578	9854	4503	40
H(14)	-293	8612	7500	31
H(15)	-2106	7674	6419	32
H(16)	-2255	8054	7997	32
H(18)	-4082	7418	8758	37
H(19)	-5942	6311	8942	42
H(20)	-6701	5327	7924	45
H(21)	-5682	5447	6721	43
H(22)	-3848	6549	6524	32

X-ray structure for compound 257

Table 1. Crystal data and structure refinement.

Identification code	**2006src0812 / TG218**	
Empirical formula	$C_{13}H_{16}N_2O_4$	
Formula weight	264.28	
Temperature	120(2) K	
Wavelength	0.71073 Å	
Crystal system	Orthorhombic	
Space group	$P2_12_12_1$	
Unit cell dimensions	$a = 8.1869(3)$ Å	$\alpha = 90°$
	$b = 10.1197(3)$ Å	$\beta = 90°$
	$c = 15.8896(4)$ Å	$\gamma = 90°$
Volume	1316.44(7) Å^3	
Z	4	
Density (calculated)	1.333 Mg / m^3	
Absorption coefficient	0.100 mm^{-1}	
F(000)	560	
Crystal	Slab; Colourless	
Crystal size	$0.62 \times 0.36 \times 0.09$ mm^3	
θ range for data collection	3.26 – 27.48°	
Index ranges	$-10 \leq h \leq 10, -13 \leq k \leq 13, -20 \leq l \leq 20$	
Reflections collected	13552	
Independent reflections	1744 $[R_{int} = 0.0402]$	
Completeness to $\theta = 27.48°$	99.7 %	
Absorption correction	Semi−empirical from equivalents	
Max. and min. transmission	0.9911 and 0.9407	
Refinement method	Full-matrix least-squares on F^2	
Data / restraints / parameters	1744 / 0 / 175	
Goodness-of-fit on F^2	1.045	
Final R indices $[F^2 > 2\sigma(F^2)]$	$R1 = 0.0323, wR2 = 0.0770$	
R indices (all data)	$R1 = 0.0437, wR2 = 0.0823$	
Absolute structure parameter	?	
Extinction coefficient	0.016(3)	
Largest diff. peak and hole	0.183 and −0.156 e Å^{-3}	

Diffractometer: *Nonius KappaCCD* area detector (ϕ scans and ω scans to fill *asymmetric unit* sphere). **Cell determination**: DirAx (Duisenberg, A.J.M.(1992). J. Appl. Cryst. 25, 92-96.) **Data collection**: Collect (Collect: Data collection software, R. Hooft, Nonius B.V., 1998). **Data reduction and cell refinement**: *Denzo* (Z. Otwinowski & W. Minor, *Methods in Enzymology* (1997) Vol. **276**: *Macromolecular Crystallography*, part A, pp. 307–326; C. W. Carter, Jr. & R. M. Sweet, Eds., Academic Press). **Absorption correction**: *SADABS Version 2.10.* (G. M. Sheldrick (2003)) Bruker AXS Inc., Madison, Wisconsin, USA. **Structure solution**: *SHELXS97* (G. M.

Sheldrick, Acta Cryst. (1990) A46 467–473). **Structure refinement**: *SHELXL97* (G. M. Sheldrick (1997), University of Göttingen, Germany). **Graphics**: *ORTEP3 for Windows* (L. J. Farrugia, J. Appl. Crystallogr. 1997, 30, 565).

Special details:

All hydrogen atoms were fixed.

It was not possible to accurately determine the absolute structure. The stereochemistry picked was based on the precursor molecule.

Table 2. Atomic coordinates [× 10^4], equivalent isotropic displacement parameters [$\text{Å}^2 \times 10^3$] and site occupancy factors. U_{eq} is defined as one third of the trace of the orthogonalized U^{ij} tensor.

Atom	x	y	z	U_{eq}	S.o.f.
C1	8751(2)	6074(2)	3731(1)	19(1)	1
C2	9122(2)	5900(2)	4668(1)	21(1)	1
C3	8299(3)	5119(2)	6044(1)	28(1)	1
C4	5712(2)	6638(2)	3565(1)	23(1)	1
C5	4375(2)	6107(2)	4126(1)	21(1)	1
C6	6761(3)	4549(2)	3131(1)	28(1)	1
C7	9261(2)	7440(2)	3394(1)	20(1)	1
C8	9424(2)	7436(2)	2445(1)	21(1)	1
C9	10653(2)	6693(2)	2061(1)	24(1)	1
C10	10831(3)	6677(2)	1195(1)	29(1)	1
C11	9771(3)	7417(2)	695(1)	31(1)	1
C12	8553(3)	8149(2)	1065(1)	31(1)	1
C13	8370(2)	8157(2)	1937(1)	25(1)	1
N1	7083(2)	5727(1)	3493(1)	19(1)	1
N2	7982(2)	5404(2)	5159(1)	23(1)	1
O1	10525(2)	6162(1)	4932(1)	25(1)	1
O2	2944(2)	6609(1)	3928(1)	28(1)	1
O3	4605(2)	5352(1)	4705(1)	28(1)	1
O4	5403(2)	4207(2)	2901(1)	38(1)	1

Table 3. Bond lengths [Å] and angles [°].

C1–N1	1.460(2)	C6–H6	0.9500
C1–C2	1.529(3)	C7–C8	1.514(2)
C1–C7	1.540(3)	C7–H7A	0.9900
C1–H1	1.0000	C7–H7B	0.9900
C2–O1	1.252(2)	C8–C13	1.389(3)
C2–N2	1.316(2)	C8–C9	1.397(3)
C3–N2	1.458(2)	C9–C10	1.384(3)
C3–H3A	0.9800	C9–H9	0.9500
C3–H3B	0.9800	C10–C11	1.394(3)
C3–H3C	0.9800	C10–H10	0.9500
C4–N1	1.457(2)	C11–C12	1.375(3)
C4–C5	1.511(3)	C11–H11	0.9500
C4–H4A	0.9900	C12–C13	1.393(3)
C4–H4B	0.9900	C12–H12	0.9500
C5–O3	1.210(2)	C13–H13	0.9500
C5–O2	1.315(2)	N2–H2	0.8800
C6–O4	1.221(3)	O2–H2A	0.8400
C6–N1	1.350(3)		

N1–C1–C2	114.23(15)	C5–C4–H4B	109.2
N1–C1–C7	112.29(15)	H4A–C4–H4B	107.9
C2–C1–C7	112.84(16)	O3–C5–O2	124.39(18)
N1–C1–H1	105.5	O3–C5–C4	124.09(17)
C2–C1–H1	105.5	O2–C5–C4	111.47(16)
C7–C1–H1	105.5	O4–C6–N1	123.7(2)
O1–C2–N2	122.19(18)	O4–C6–H6	118.1
O1–C2–C1	118.99(17)	N1–C6–H6	118.1
N2–C2–C1	118.69(16)	C8–C7–C1	111.60(15)
N2–C3–H3A	109.5	C8–C7–H7A	109.3
N2–C3–H3B	109.5	C1–C7–H7A	109.3
H3A–C3–H3B	109.5	C8–C7–H7B	109.3
N2–C3–H3C	109.5	C1–C7–H7B	109.3
H3A–C3–H3C	109.5	H7A–C7–H7B	108.0
H3B–C3–H3C	109.5	C13–C8–C9	118.44(17)
N1–C4–C5	112.27(15)	C13–C8–C7	121.51(17)
N1–C4–H4A	109.2	C9–C8–C7	120.05(17)
C5–C4–H4A	109.2	C10–C9–C8	121.13(19)
N1–C4–H4B	109.2	C10–C9–H9	119.4

C8–C9–H9	119.4	C8–C13–C12	120.5(2)
C9–C10–C11	119.7(2)	C8–C13–H13	119.7
C9–C10–H10	120.2	C12–C13–H13	119.7
C11–C10–H10	120.2	C6–N1–C4	116.25(16)
C12–C11–C10	119.78(19)	C6–N1–C1	120.33(16)
C12–C11–H11	120.1	C4–N1–C1	123.25(15)
C10–C11–H11	120.1	C2–N2–C3	121.40(16)
C11–C12–C13	120.5(2)	C2–N2–H2	119.3
C11–C12–H12	119.8	C3–N2–H2	119.3
C13–C12–H12	119.8	C5–O2–H2A	109.5

Symmetry transformations used to generate equivalent atoms:

Table 4. Anisotropic displacement parameters [$\text{Å}^2 \times 10^3$]. The anisotropic displacement factor exponent takes the form: $-2\pi^2[h^2a^{*2}U^{11} + \cdots + 2\,h\,k\,a^*\,b^*\,U^{12}]$.

Atom	U^{11}	U^{22}	U^{33}	U^{23}	U^{13}	U^{12}
C1	14(1)	22(1)	22(1)	0(1)	2(1)	0(1)
C2	17(1)	21(1)	24(1)	−2(1)	2(1)	1(1)
C3	26(1)	35(1)	22(1)	6(1)	−2(1)	−4(1)
C4	14(1)	28(1)	27(1)	4(1)	1(1)	3(1)
C5	16(1)	23(1)	22(1)	−3(1)	0(1)	−2(1)
C6	26(1)	30(1)	27(1)	−7(1)	7(1)	−3(1)
C7	17(1)	20(1)	24(1)	−1(1)	1(1)	−1(1)
C8	19(1)	18(1)	25(1)	2(1)	1(1)	−6(1)
C9	20(1)	25(1)	27(1)	3(1)	0(1)	−3(1)
C10	28(1)	28(1)	29(1)	−2(1)	6(1)	−4(1)
C11	41(1)	29(1)	23(1)	0(1)	1(1)	−10(1)
C12	35(1)	26(1)	31(1)	7(1)	−8(1)	−6(1)
C13	22(1)	20(1)	33(1)	2(1)	−3(1)	−4(1)
N1	15(1)	20(1)	21(1)	−1(1)	2(1)	1(1)
N2	17(1)	30(1)	22(1)	2(1)	−1(1)	−3(1)
O1	16(1)	35(1)	24(1)	−1(1)	0(1)	−2(1)
O2	14(1)	36(1)	33(1)	8(1)	5(1)	2(1)
O3	18(1)	37(1)	27(1)	7(1)	2(1)	1(1)
O4	29(1)	48(1)	38(1)	−17(1)	5(1)	−14(1)

288

Table 5. Hydrogen coordinates [× 10^4] and isotropic displacement parameters [$\text{Å}^2 \times 10^3$].

Atom	x	y	z	U_{eq}	S.o.f.
H1	9466	5424	3434	23	1
H3A	9207	4492	6089	42	1
H3B	7319	4734	6300	42	1
H3C	8582	5939	6337	42	1
H4A	5258	6809	2998	28	1
H4B	6106	7490	3795	28	1
H6	7643	3952	3051	33	1
H7A	8435	8105	3562	24	1
H7B	10318	7697	3648	24	1
H9	11379	6189	2399	29	1
H10	11671	6165	942	34	1
H11	9891	7415	100	37	1
H12	7831	8653	725	37	1
H13	7517	8659	2186	30	1
H2	7008	5241	4949	28	1
H2A	2246	6370	4284	41	1

Table 6. Hydrogen bonds [Å and °].

D–H$\cdots A$	$d(D$–H$)$	$d(H\cdots A)$	$d(D\cdots A)$	$\angle(DHA)$
N2–H2$\cdots$O3	0.88	2.01	2.858(2)	161.9
O2–H2A$\cdots$O1^{i}	0.84	1.76	2.5832(19)	167.1

Symmetry transformations used to generate equivalent atoms:

(i) x–1,y,z
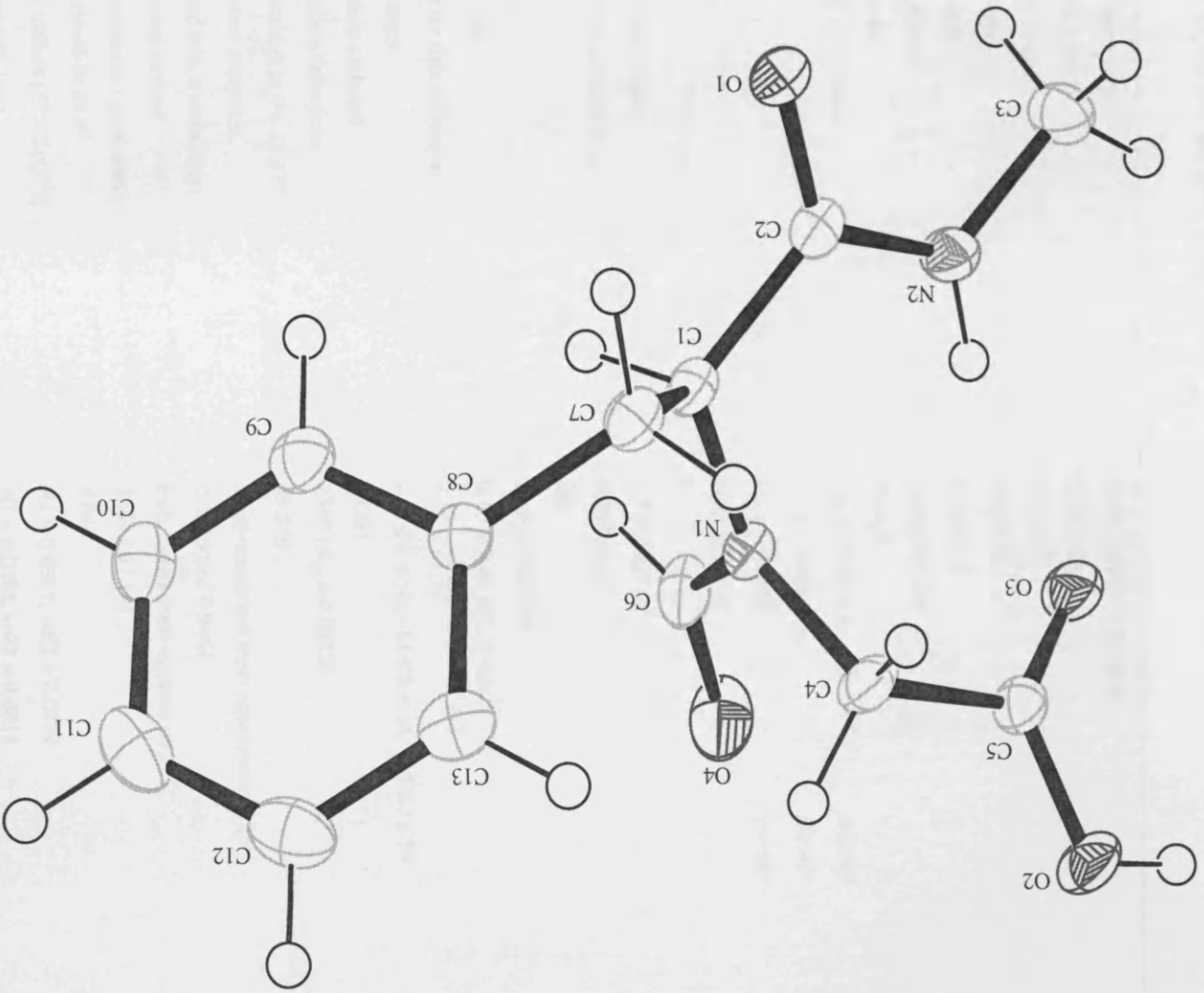
X-Ray structure of compound 259

Table 1. Crystal data and structure refinement.

Identification code	**2006src0919 (TG305)**
Empirical formula	$C_{11}H_{13}NO_3$
Formula weight	207.22
Temperature	120(2) K
Wavelength	0.71073 Å
Crystal system	Orthorhombic
Space group	$P2_12_12_1$
Unit cell dimensions	$a = 8.2328(2)$ Å $\quad \alpha = 90°$
	$b = 11.1850(2)$ Å $\quad \beta = 90°$
	$c = 11.3300(2)$ Å $\quad \gamma = 90°$
Volume	1043.31(4) Å^3
Z	4
Density (calculated)	1.319 Mg / m^3
Absorption coefficient	0.097 mm^{-1}
$F(000)$	440
Crystal	Slab; colourless
Crystal size	$0.60 \times 0.40 \times 0.12$ mm^3
θ range for data collection	$3.56 - 27.47°$
Index ranges	$-10 \leq h \leq 10, -14 \leq k \leq 14, -14 \leq l \leq 14$
Reflections collected	14281
Independent reflections	2380 [$R_{int} = 0.0312$]
Completeness to $\theta = 27.47°$	99.2 %
Absorption correction	Semi–empirical from equivalents
Max. and min. transmission	0.9885 and 0.9444
Refinement method	Full-matrix least-squares on F^2
Data / restraints / parameters	2380 / 0 / 141
Goodness-of-fit on F^2	1.044
Final R indices [$F^2 > 2\sigma(F^2)$]	$R1 = 0.0317, wR2 = 0.0779$
R indices (all data)	$R1 = 0.0384, wR2 = 0.0814$
Absolute structure parameter	0.0(9)
Largest diff. peak and hole	0.119 and -0.211 e Å^{-3}

Diffractometer: *Nonius KappaCCD* area detector (ϕ scans and ω scans to fill *asymmetric unit* sphere). **Cell determination:** DirAx (Duisenberg, A.J.M.(1992). J. Appl. Cryst. 25, 92-96.) **Data collection:** Collect (Collect: Data collection software, R. Hooft, Nonius B.V., 1998). **Data reduction and cell refinement:** *Denzo* (Z. Otwinowski & W. Minor, *Methods in Enzymology* (1997) Vol. 276: *Macromolecular Crystallography*, part A, pp. 307–326; C. W. Carter, Jr. & R. M. Sweet, Eds., Academic Press). **Absorption**

correction: *SORTAV* (R. H. Blessing, Acta Cryst. A51 (1995) 33–37; R. H. Blessing, J. Appl. Cryst. 30 (1997) 421–426). **Structure solution:** *SHELXS97* (G. M. Sheldrick, Acta Cryst. (1990) A46 467–473). **Structure refinement:** *SHELXL97* (G. M. Sheldrick (1997), University of Göttingen, Germany). **Graphics:** Cameron - A Molecular Graphics Package. (D. M. Watkin, L. Pearce and C. K. Prout, Chemical Crystallography Laboratory, University of Oxford, 1993).

Table 2. Atomic coordinates [$\times 10^4$], equivalent isotropic displacement parameters [$\text{Å}^2 \times 10^3$] and site occupancy factors. U_{eq} is defined as one third of the trace of the orthogonalized U^{ij} tensor.

Atom	x	y	z	U_{eq}	S.o.f.
C1	−19(2)	8792(1)	1960(1)	26(1)	1
C2	−1037(2)	8151(1)	1215(1)	32(1)	1
C3	−971(2)	8326(2)	−3(1)	43(1)	1
C4	96(2)	9129(2)	−486(1)	49(1)	1
C5	1110(2)	9779(2)	248(1)	47(1)	1
C6	1054(2)	9615(1)	1460(1)	35(1)	1
C7	−102(2)	8637(1)	3280(1)	27(1)	1
C8	−1183(2)	9591(1)	3837(1)	23(1)	1
C10	−1834(2)	8576(1)	5768(1)	23(1)	1
C11	−567(1)	7809(1)	6374(1)	21(1)	1
N1	−1134(1)	9567(1)	5127(1)	21(1)	1
C9	−480(2)	10445(1)	5744(1)	24(1)	1
O1	−438(1)	10461(1)	6840(1)	28(1)	1
O2	877(1)	7853(1)	6181(1)	28(1)	1
O3	−1273(1)	7079(1)	7130(1)	30(1)	1

Table 3. Bond lengths [Å] and angles [°].

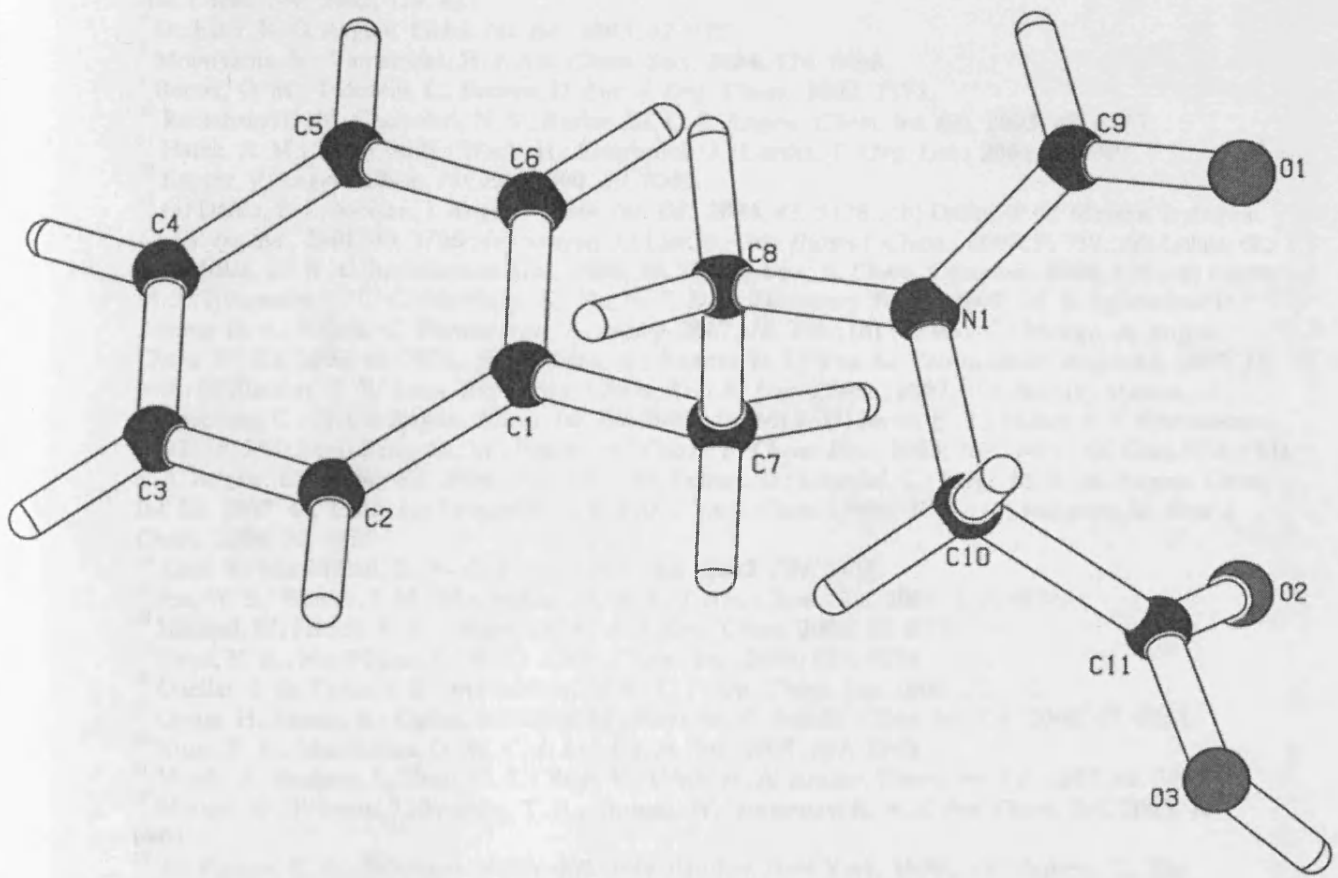|	
C1–C2	1.389(2)
C1–C6	1.396(2)
C1–C7	1.5074(16)
C2–C3	1.3946(19)
C3–C4	1.370(3)
C4–C5	1.385(3)
C5–C6	1.387(2)
C7–C8	1.5249(17)
C8–N1	1.4632(13)
C10–N1	1.4450(16)
C10–C11	1.5152(17)
C11–O2	1.2093(14)
C11–O3	1.3186(15)
N1–C9	1.3201(16)
C9–O1	1.2418(15)
C2–C1–C6	118.42(12)
C2–C1–C7	121.13(12)
C6–C1–C7	120.42(12)
C1–C2–C3	120.37(15)
C4–C3–C2	120.82(15)
C3–C4–C5	119.38(13)
C4–C5–C6	120.36(16)
C5–C6–C1	120.64(15)
C1–C7–C8	110.90(10)
N1–C8–C7	112.63(10)
N1–C10–C11	112.80(10)
O2–C11–O3	125.18(11)
O2–C11–C10	124.86(11)
O3–C11–C10	109.96(10)
C9–N1–C10	117.84(9)
C9–N1–C8	121.79(10)
C10–N1–C8	120.36(10)
O1–C9–N1	123.45(11)

Symmetry transformations used to generate equivalent atoms:

Table 4. Anisotropic displacement parameters [$\text{Å}^2 \times 10^3$]. The anisotropic displacement factor exponent takes the form: $-2\pi^2[h^2a^{*2}U^{11} + \cdots + 2\,h\,k\,a^*\,b^*\,U^{12}]$.

Atom	U^{11}	U^{22}	U^{33}	U^{23}	U^{13}	U^{12}
C1	28(1)	32(1)	20(1)	0(1)	0(1)	14(1)
C2	37(1)	33(1)	26(1)	−5(1)	−4(1)	15(1)
C3	57(1)	48(1)	24(1)	−11(1)	−12(1)	30(1)
C4	61(1)	66(1)	19(1)	5(1)	5(1)	40(1)
C5	44(1)	60(1)	36(1)	21(1)	14(1)	22(1)
C6	32(1)	44(1)	30(1)	6(1)	3(1)	10(1)
C7	31(1)	32(1)	18(1)	1(1)	0(1)	9(1)
C8	28(1)	26(1)	15(1)	1(1)	−1(1)	4(1)
C10	22(1)	26(1)	20(1)	−1(1)	0(1)	−1(1)
C11	27(1)	21(1)	15(1)	−2(1)	0(1)	−2(1)
N1	24(1)	23(1)	15(1)	0(1)	0(1)	1(1)
C9	28(1)	22(1)	22(1)	0(1)	−2(1)	2(1)
O1	36(1)	28(1)	20(1)	−5(1)	−4(1)	1(1)
O2	24(1)	32(1)	27(1)	3(1)	2(1)	4(1)
O3	28(1)	35(1)	27(1)	11(1)	−3(1)	−3(1)

C5
C6
C4
C8
C9
O1
N1
C1
C7
C3
C2
C10
O2
C11
O3

References

[1] Dalko, P. I.; Moisan, I. *Angew. Chem. Int. Ed.*, **2004**, *43*, 5138.

[2] (a) Eder, U.; Sauer, G.; Wiechert, R. *Angew. Chem. Int. Ed.*, **1971**, *10*, 496.; (b) Hajos, Z.; Parrish, D. R. *J. Org. Chem.*, **1974**, *39*, 1615.

[3] Seayad, J.; List, B. *Org. Biomol. Chem.*, **2005**, *3*, 719.

[4] Saito, S.; Yamamoto, H. *Acc. Chem. Res.*, **2004**, *37*, 570.

[5] Bui, T.; Barbas III, C. F. *Tetrahedron Lett.*, **2000**, *41*, 6951.

[6] (a) Córdova, A. *Acc. Chem. Res.*, **2004**, *37*, 102.; (b) List, B.; Pojarliev, P.; Biller, W. T.; Martin, H. J. *J. Am. Chem. Soc.* **2002**, *124*, 827.

[7] Duthaler, R. O. *Angew. Chem. Int. Ed.*, **2003**, *42*, 975.

[8] Momiyama, N.; Yamamoto, H. *J. Am. Chem. Soc.*, **2004**, *126*, 6498.

[9] Berner, O. M.; Tedeschi, L.; Enders, D. *Eur. J. Org. Chem.*, **2002**, 1877.

[10] Ramchary, D. B.; Chowdari, N. S.; Barbas III, C. S. *Angew. Chem. Int. Ed.*, **2003**, *42*, 4233.

[11] Hafez, A. M.; Taggi, A. E.; Wack, H.; Esterbrook, J.; Lectka, T. *Org. Lett.*, **2001**, *3*, 2049.

[12] Langer, P. *Angew. Chem. Int. Ed.*, **2000**, *39*, 3049.

[13] (a) Dalko, P. I.; Moisan, I. *Angew. Chem. Int. Ed.*, **2004**, *43*, 5138.; (b) Dalko, P. I.; Moisan, I. *Angew. Chem. Int. Ed.*, **2001**, *40*, 3726.; (c) Seayad, J.; List, B. *Org. Biomol. Chem.*, **2005**, *3*, 719.; (d) Lelais, G.; MacMillan, D. W. C. *Aldichimica Acta*, **2006**, *39*, 79.; (e) List, B. *Chem. Commun.*, **2006**, 819.; (f) Gaunt, M. J.; Johansson, C. C. C.; McNally, A.; Vo, N. T. *Drug Discovery Today*, **2007**, *12*, 8.; (g) Almasi D.; Alonso, D. A.; Nájera, C. *Tetrahedron: Asymmetry*, **2007**, *18*, 299.; (h) Palomo, C.; Meilgo, A. *Angew. Chem. Int. Ed.* **2006**, *45*, 7876.; (i) Guillena, G.; Ramón, D. J.; Yus, M. *Tetrahedron: Asymmetry*, **2007**, *18*, 693.; (j) Buckley, B. R. *Annu. Rep. Prog. Chem., Sect B: Org. Chem.*, **2007**, *103*, 90.; (k) Masson, G.; Housseman, C.; Zhu, J. *Angew. Chem. Int. Ed.* **2007**, *46*, 4614.; (l) Jarvo, E. R.; Miller, S. J. *Tetrahedron*, **2002**, *58*, 2481.; (m) Bengalia, M.; Puglisi, A.; Cozzi, F. *Chem. Rev.*, **2003**, *103*, 3401.; (n) Guo, H.-C.; Ma, J.-A. *Angew. Chem. Int. Ed.* **2006**, *465*, 354.; (o), Enders, D.; Grondal, C.; Hüttl, M. R. M. *Angew. Chem. Int. Ed.* **2007**, *46*, 1570.; (p) Tsogoeva, S. B. *Eur. J. Org. Chem.*, **2007**, 1701.; (q) Bengalia, M. *New J. Chem.*, **2006**, *30*, 1525.

[14] Alan, B.; MacMillan, D. W. C. *J. Am. Chem. Soc.* **2002**, *124*, 2458.

[15] Jen, W. S.; Wiener, J. M.; MacMillan, D. W. C. *J. Am. Chem. Soc.* **2000**, *122*, 9874.

[16] Halland, N.; Hazell, R. G.; Jørgensen, K. A. *J. Org. Chem.* **2002**, *67*, 8331.

[17] Paras, N. A.; MacMillan, D. W. C. *J. Am. Chem. Soc.* **2001**, *123*, 4370.

[18] Ouellet, S. G; Tuttle, J. B.; MacMillan, D. W. C. *J. Am. Chem. Soc.* **2005**, *127*, 32.

[19] Gotoh, H.; Masui, R.; Ogino, H.; Shoji, M.; Hayashi, Y. *Angew. Chem. Int. Ed.*, **2006**, *45*, 6853.

[20] Kunz, R. K.; MacMillan, D. W. C. *J. Am. Chem. Soc.* **2005**, *127*, 3240.

[21] Versly, J.; Ibrahem, I.; Zhao, G.-L.; Rios, R.; Córdova, A. *Angew. Chem. Int. Ed.*, **2007**, *46*, 778.

[22] Marigo, M.; Franzen, J.; Poulsen, T. B.; Zhuang, W.; Jørgensen K. A. *J. Am. Chem. Soc.* **2005**, *127*, 6964.

[23] (a) Popper, K. R., *The Logic of Scientific Investigation*, New York. **1959**.; (b) Hempel. C., *The Philosophy of Natural Science*, Prentice-Hall, Englewood Cliffs, N.J., **1973**.

[24] Carpenter, B. K. *Determination of Organic reaction Mechanisms*; John Wiley & Sons., **1984**.

[25] Billups, W. E.; Houk, K. N.; Stevens, R.V.; in Bernosconi, 1986, pt. 1, 633.

[26] (a) Walden, P. *Ber.*, **1893**, *26*, 210.; (b) Walden, P. *Ber.*, **1896**, *29*, 133.; (c) Walden, P. *Ber.*, **1899**, *32*, 1855.

[27] Tolbert, L. M.; Ali, B. *J. Am. Chem. Soc.*, **1981**, *103*, 2104.

[28] Skell, P. S.; Woodworth, R. C. *J. Am. Chem. Soc.*, **1956**, *78*, 4496.

[29] (a) Lwowski, W.; Woerner, F. P. *J. Am. Chem. Soc.*, **1965**, *87*, 5491.; (b) Watts, L.; Fitzpatrick, J. D.; Pettit, R. *J. Am. Chem. Soc.*, **1966**, *88*, 623.; (c) Yang, N. C.; Eisenhardt, W. *J. Am. Chem. Soc.*, **1971**, *93*, 1277.

[30] Collins, C. J. *Adv. Phys. Org. Chem.*, **1964**, *2*, 3.

[31] Polanyi, M.; Szabo, A. L., *Trans. Faraday Soc.*, **1934**, *30*, 508.

[32] Fliszar, S.; Carles, J. *J. Am. Chem. Soc.*, **1969**, *91*, 2637.

[33] Sheriden, R. S. *Org. Photochem.*, **1987**, *8*, 159.

[34] Heinrich, M. R.; Kirchstein, M. D. *Tetrahedron Lett.*, **2006**, *47*, 2115.

[35] Hoffman, R. W. *Dehydrobenzene and Cycloalkynes*; Academic press: New York, **1967**, p. 200.

[36] Chapman, O. L.; Mattes, K.; McIntosh, C. L.; Pacansky, J.; Calder, G. V.; Orr, G. J. *J. Am. Chem. Soc.*, **1973**, *95*, 6134.

[37] Coates, R. M.; Fretz, E. R. *J. Am. Chem. Soc.*, **1977**, *99*, 297.

[38] Forsén, S.; Hoffmann, R. A. *Acta Chem. Scand.*, **1963**, *17*, 1787.

[39] Davies, A. G. *Chem. Soc. Rev.*, **1993**, *22*, 199.

[40] (a) Canle-Lopez, M.; Santabella, J. A.; Steenken, S. *Chem. Eur. J.*, **1999**, *5*, 1192.; (b)Canle-Lopez. M.; Fernandez, M. I.; Rodriguez, S., Santaballa, J. A.; Steenken, S.; Vulliet, E. *ChemPhysChem*, **2005**, *6*, 2064.; (c) Bernhard, K.; Geimer, J.; Canle-Lopez, M.; Reynisson, J.; Beckert, D.; Gleiter, R.; Steenken, S. *Chem. Eur. J.*, **2001**, *7*, 4640.

[41] Strehlow, H. *Rapid Reactions in Solution*; VCH, New York. **1992**.

[42] Carpenter, B. K. *Determination of Organic reaction Mechanisms*; John Wiley & Sons., **1984**, pp 83-104

[43] (a)Topsom, R. D. *Prog. Phys. Org. Chem.*, **1876**, *12*, 1.;(b) Uger, S.H.; Hansch, C. *Prog. Phys. Org. Chem.*, **1976**, *12*, 91.; (c) Lewitt, L. S.; Widing, H. F. *Prog. Phys. Org. Chem.*, **1976**, *12*, 119.

[44] Benson, S. W. *Thermochemical Kinetics*, Wiley-Interscience, New York, **1976**.

[45] Maskill, H. *The investigation of Organic Reactions and their Mechanism*; Blackwell publishing. **2006**.

[46] Burkert, U.; Allinger, N. L. *Molecular Mechanics*. American Chemical Society, Washington, **1982**.

[47] Ohono, K.; Takahashi, R. *Chem. Phys Lett.*, **2002**, *356*, 409.

[48] Dewer, M. J. S. *The PMO Theory of Organic Chemistry*. Plenum, New York, **1975**.;

[49] Schleyer, P. v.-R.; Allinger, N. L.; Clark, T.; Gasteiger, J.; Kollman H. F.; Schaefer III, H. F.; Schreiner, P. R. *The Encyclopedia Computational Chemistry, vol 1*, Wiley, Chichester, **1998**.

[50] (a)Becke, A. D. *J. Chem. Phys.*, **1993**, *98*, 1372.; (b) Becke, A. D. *J. Chem. Phys.*, **1993**, *98*, 5648.; (c) Dickson, R. M.; Becke, A. D. *J. Chem. Phys.*, **1993**, *98*, 3898.

[51] (a) Ishihara, K.; Nakano, K. *J Am. Chem Soc.*, **2005**, *127*, 10504.; (b) Gryko, D. *Tetrahedron: Asymmetry*, **2005**, *16*, 1377.; (c) Sakakura, A.; Suzuki, K.; Ishihara, K. *Adv. Synth. Catal.*, **2006**, *348*, 2457.

[52] Ishihara, K.; Nakano, K. *J Am. Chem Soc.*, **2075**, *129*, 8930.

[53] Hong, B.-C.; Wu, M.-F.; Tseng, H.-C.; Liao, J.-H. *Org Lett.*, **2006**, *8*, 2217.

[54] (a) Chen, W.; Yuan, X.-H.; Li, R.; Du, W.; Wu, Y.; Ding, L.-Y.; Chen, Y.-C. *Adv. Synth. Catal.*, **2006**, *348*, 1818.; (b) Karlsson, S.; Högberg, H.-E. *Tetrahedron: Asymmetry*, **2002**, *13*, 923.

[55] Li, C.-F.; Liu, H.; Lioa, J.; Coa, Y.-J.; Liu, X.-P.; Xiao, W.-J. *Org Lett.*, **2007**, *9*, 1847.

[56] Yang, J. W.; Fonseca, M. T. H.; Vignola, N.; List, B. *Angew. Chem. Int. Ed.*, **2005**, *44*, 108.

[57] (a) Lattanzi, A. *Adv. Synth. Catal.*, **2006**, *348*, 339.; (b) Lattanzi, A. *Org Lett.*, **2005**, *7*, 2579.; (c) Sundén, H.; Ibrahem, I.; Córdova, A. *Tetrahedron Lett.*, **2006**, *47*, 99.

[58] Gotoh, H.; Masui, R.; Ogino, H.; Shoji, M.; Hayashi, Y. *Angew. Chem. Int. Ed.*, **2006**, *45*, 6853.

[59] (a) Chen, S.-H.; Hong, B.-C.; Su, C.-F.; Sarshar, S. *Tetrahedron Lett.*, **2005**, *46*, 8899.; (b) Shi, M.; Jiang, J.-K.; Li, C.-Q. *Tetrahedron Lett.*, **2002**, *43*, 127.; (c) Vasbinder, M. M.; Imbriglio, J. E.; Miller, S. J. *Tetrahedron*, **2006**, *62*, 11450.

[60] (a) Rios, R.; Sundén, H.; Ibrahem, I.; Zhoa, G.-L.; Eriksson, L.; Córdova, A. *Tetrahedron Lett.*, **2006**, *47*, 8547.; (b) Enders, D.; Hüttl, M. R. M.; Runsink, J.; Raabe, G.; Wendt, B. *Angew. Chem. Int. Ed.*, **2007**, *46*, 467.; (c) Brandau, S.; Mearten, E.; Jørgensen, K. A. *J Am. Chem Soc.*, **2006**, *128*, 14986.; (d) Zhoa, G.-L.; Córdova, A. *Tetrahedron Lett.*, **2006**, *47*, 7417.; (e) Xie, H.; Zu, L.; Li, H.; Wang, J.; Wang, W. *J Am. Chem Soc.*, **2007**, *129*, 10886.

[61] Hanessian, S.; Pham, V. *Org. Lett.*, **2000**, *2*, 2975.

[62] Girard, C.; Kagan, H.; *Angew. Chem. Int. Ed.*, **1998**, *37*, 2923.

[63] (a) Lemay, M.; Ogilvie, W. W. *Org. Lett.*, **2005**, *7*, 4141.; (b) Lemay, M.; Ogilvie, W. W. *J. Org. Chem.*, **2006**, *71*, 4663.

[64] Lemay, M.; Aumand, L.; Ogilvie, W. W. *Adv. Synth. Catal.*, **2007**, *349*, 441.

[65] Lee, S.; MacMillan, D. W. C. *Tetrahedron*, **2006**, *62*, 11413.

[66] Zhoa, G.-L.; Ibrahem, I.; Sundén, H.; Cordóva, A. *Adv. Synth. Catal.*, **2007**, *349*, 1210.

[67] Karlsson, S.; Högberg, H.-E. Eur. *J. Org. Chem.*, **2003**, 2782.

[68] (a) Allinger, N. L.; Yuh, Y. H.; Lii, J. H. *J. Am. Chem. Soc.*, **1989**, *111*, 8551.; (b) Allinger, N. L.; Lii, J. H. *J. Am. Chem. Soc.*, **1989**, *111*, 8566.; (c) Allinger, N. L.; Lii, J. H. *J. Am. Chem. Soc.*, **1989**, *111*, 8576.

[69] Ahrendt, K. A.; Borths, C. J.; MacMillan D. W. C. *J. Am. Chem. Soc.*, **2000**, *122*, 4243.

[70] Jen, W. S.; Wiener, J. M.; MacMillan, D. W. C. *J. Am. Chem. Soc.,* **2000**, *122*, 9874.

[71] Paras, N. A.; MacMillan, D. W. C. *J. Am. Chem. Soc.,* **2001**, *123*, 4370.

[72] Brown, S. P.; Goodwin, N. C.; MacMillan, D. W. C. *J. Am. Chem. Soc.,* **2003**, *125*, 1192.

[73] Austin, J. F.; MacMillan, D. W. C. *J. Am. Chem. Soc.,* **2002**, *124*, 1172.

[74] (a) Tuttle, J. B.; Ouellet, S. G.; MacMillan, D. W. C. *J. Am. Chem. Soc.,* **2006**, *128*, 12662.; (b) Tuttle, J. B.; Ouellet, S. G.; MacMillan, D. W. C. *J. Am. Chem. Soc.,* **2005**, *127*, 32.

[75] Northrup, A. B.; MacMillan, D. W. C. *J. Am. Chem. Soc.,* **2005**, *127*, 2458.

[76] Gordillo, R.; Houk, K. N. *J. Am. Chem. Soc.,* **2006**, *128*, 3543.

[77] King, H. D.; Meng, Z.; Denhart, D.; Mattson, R. M.; Kimura, R.; Wu, D.; Gao, Q.; Macor, J. E. *Org. Lett.,* **2005**, *7*, 3437.

[78] Halland, N.; Abruel, P. S.; Jørgensen, K. A. *Angew Chem. Int Ed.* **2003**, *42*, 661.

[79] Halland, N.; Hansen, T.; Jørgensen, K. A. *Angew. Chem. Int. Ed.,* **2003**, *42*, 4955.

[80] Chow, S. S.; Nevalainen, M.; Evans, C. A.; Johannes, C. W. *Tetrahedron Lett.,* **2006**, *48*, 277.

[81] Zora, M. *J. Mol. Struct. (TheoChem),* **2002**, *619*, 121.

[82] Gordillo, R.; Houk, K. N. *J. Am. Chem. Soc.,* **2006**, *128*, 3543.

[83] Allemann., C.; Gordillo, R.; Clemamte, F. R.; Cheong, P. H.-Y.; Houk, K. N. *Acc. Chem. Res.,* **2004**, *37*, 558.

[84] Gordillo, R.; Houk, K. N. *J. Am. Chem. Soc.,* **2006**, *128*, 3543.

[85] Gordillo, R.; Carter, J.; Houk, K. N. *Adv. Synth. Catal.,* **2004**, *346*, 1175.

[86] Bruvoll, M.; Hansen, T.; Uggerud, E. *J. Phys. Org. Chem.,* **2007**, *20*, 206.

[87] (a) Cavill, J. L.; Elliott, R. L.; Evans, G.; Jones, I. L.; Platts, J. A.; Ruda, A. M.; Tomkinson, N. C. O. *Tetrahedron,* **2006**, *62*, 410.; (b) Evans, G. J. S.; White, K.; Platts, J. A.; Tomkinson, N. C. O. *Org. Biomol. Chem.,* **2006**, *4*, 2616.

[88] Cavill, J. L.; Elliott, R. L.; Evans, G.; Jones, I. L.; Platts, J. A.; Ruda, A. M.; Tomkinson, N. C. O. *Tetrahedron,* **2006**, *62*, 410.

[89] Dinér, P.; Nielsen, M.; Marigo, M.; Jørgensen K. A. *Angew. Chem. Int. Ed.,* **2007**, *46*, 1983.

[90] Marigo, M.; Bertelsen, S.; Landa, A. Jørgensen K. A. *J. Am. Chem. Soc.,* **2006**, *128*, 5475.

[91] Ibrahem, I.; Rios, R.; Vesely, J.; Hammar, P.; Eriksson, L.; Himo, F.; Córdova, A. *Angew. Chem. Int. Ed.,* **2007**, *46*, 4507.

[92] Cavill, J. *Ph.D. Thesis, Cardiff University,* **2003**

[93] Ahrendt, K. A.; Borths, C. J.; MacMillan, D. W. C. *J. Am. Chem. Soc.* **2000**, *122*, 4243.

[94] Klopman, G.; Tsuda, K.; Louis, J. B.; Davis, R. E. *Tetrahedron,* **1970**, *26*, 4549.

[95] (a) Laloi-Diard, M.; Verchere, J.; Gosselin, P.; Terrier, F. *Tetrahedron Lett.* **1984**, *25*, 1267.; (b) Buncel, E.; Hoz, S. *Tetrahedron Lett.* **1983**, *24*, 4777.

[96] (a)Epstein, J.; Bauer, V.; Laxe, M.; Demek, M. *J. Am. Chem. Soc.* **1956**, *78*, 4068.; (b) Kice, J. L.; Legan E. *J. Am. Chem. Soc.* **1973**, *95*, 3912.; (c) Dixon, J. E.; Bruice, T. C. *J. Am. Chem. Soc.* **1971**, *93*, 6592.; (d) Buncel, E.; Wilson, H.; Chuaqui, C. *J. Am. Chem. Soc.* **1982**, *104*, 4896.

[97] Cavill, J. L.; Elliott, R. L.; Evans, G.; Jones, I. L.; Platts, J. A.; Ruda, A. M., Tomkinson, N. C. O. *Tetrahedron,* **2005**, *62*, 410.

[98] Jones, C. L. *Ph.D. Thesis, Cardiff University,* **2003**.

[99] Jones, I. L. *Ph.D. Thesis, Cardiff University,* **2006**.

[100] Cavill, J. L.; Peters, J.-U.; Tomkinson, N. C. O. *Chem. Commun.,* **2003**, 728.

[101] Battistuzzi, G.; Cacchi, S; Fabrizi, G. *Org. Lett.,* **2003**, *5*, 777.

[102] Krossing, I.; Raabe, I. *Angew. Chem. Int. Ed.,* **2004**, *43*, 2066.

[103] Ahrendt, K. A.; Borths, C. J.; MacMillan D. W. C. *J. Am. Chem. Soc.,* **2000**, *122*, 4243.

[104] Gordillo, R.; Houk, K. N. *J. Am. Chem. Soc.,* **2006**, *128*, 3543.

[105] Evans G. *Ph.D. Thesis, Cardiff University,* **2007**.

[106] Cavill, J. L. *Ph.D. Thesis, Cardiff University,* **2004**.

[107] Evans, G.; Gibbs. T. J. K.; Jenkins, R. L.; Coles, S. J.; Hursthouse, M. B.; Platts, J. A.; Tomkinson, N.C. O. *Angew. Chem. Int. Ed., in press,* **2008**.

[108] Huybrechts, G.; Rigaux, D.; Vankeerberghen J.; Van Mele, B. *Int. J. Chem. Kinet.* **1980**, *12*, 253.

[109] Fleming, I. *Frontier Orbitals and Organic Chemical Reactions.* Wiley, **1978**.

[110] Lelais, G.; MacMillan, D. W. C. *Aldichimica Acta,* **2006**, *39*, 79.

[111] Ahrendt, K. A.; Borths, C. J.; MacMillan, D. W. C. *J. Am. Chem. Soc.* **2000**, *122*, 4243.

[112] Pires, R.; Burger, K. Synthesis, **1996**, 281.

[113] Radics, G.; Koksch, B.; El-Kousy, S. M.; Spengler, J.; Burger, K. *Synlett*, **2003**, *12*, 1836.

[114] Hall, A.; Harris, L. D.; Jones, C. L.; Jenkins, R. L.; Tomkinson, N. C. O. *Tetrahedron Lett.* **2003**, *44*, 111.

[115] Cavill, J. L. *Ph.D. Thesis, Cardiff University*, **2004**.

[116] (a) Ahrendt, K. A.; Borths, C. J.; MacMillan, D. W. C. *J. Am. Chem. Soc.*, **2000**, *122*, 4243.; (b) Cavill, J. L.; Elliott, R. L.; Evans, G.; Jones, I. L.; Platts, J. A.; Ruda, A. M., Tomkinson, N. C. O. *Tetrahedron*, **2006**, *62*, 410.; (c) Lemay, M.; Ogilvie, W. W. *Org. Lett.*, **2005**, *7*, 4141.; (d) Lemay, M.; Ogilvie, W. W. *J. Org. Chem.*, **2006**, *71*, 4663.; (e)Benaglia, M.; Celentano, G.; Cinquini, M.; Puglisi, A.; Cozzi, F., *Adv. Synth. Catal.*, **2002**, *344*, 149.; (f) Park, J. K.; Sreekanth, P.; Kim, B. M., *Adv. Synth. Catal.*, **2004**, *346*, 49.

[117] Northrup, A. B.; MacMillan, D. W. C. *J. Am. Chem. Soc.*, **2002**, *124*, 2458.

[118] Mancilla, T.; Carrillo, L.; Zamudio-Rivera, L. S.; Beltran, H. I.; Farfan, N. *Org. Prep. Proc. Int.*, **2002**,*34*, 87.

[119] Cavill, J. L.; Elliott, R. L.; Evans, G.; Jones, I. L.; Platts, J. A.; Ruda, A. M., Tomkinson, N. C. O. *Tetrahedron*, **2006**, *62*, 410.

[120] Northrup, A. B.; MacMillan, D. W. C. *J. Am. Chem. Soc.*, **2002**, *124*, 2458.

[121] Ugi, I.; Hörl, W.; Hanusch-Kompa, C.; Schmid, T.; Herdtweck, E. *Heterocycles*, **1998**, *47*, 965.

[122] Mignani, G.; Morel, D.; Grass, F. *Tetrahedron Lett.*, **1987**, *28*, 5505.

[123] Ahrendt, K. A.; Borths, C. J.; MacMillan, D. W. C. *J. Am. Chem. Soc.*, **2000**, *122*, 4243.

[124] Smith, M. B.; March, J. *March's Advaned Organic Chemistry Wiley*: New York, **2001**, 1023.

[125] Harison, J. R.; O'Brien, P.; Porter, D. W.; Smith, N. M. *J. Chem. Soc., Perkin Trans. 1*, **1999**, 3623.

[126] Vazquez, E.; Galindo, A.; Gnecco, D.; Bernes, S.; Teran, J. L.; Enriquez, R. G. *Tetrahedron: Asymmetry* **2001**, *12*, 3209.

[127] Clarke, D. S.; Gabbutt, C. D.; Hepworth, J. D.; Heron, B. M. *Tetrahedron Lett.* **2005**, *46*, 5515.

[128] Georgiadis, M. P.; Couladouros, E. A.; Delithieos, A. K. *J. Pharm. Sci.* **1992**, *81*, 1126.

[129] Sloose, P.; Hootele, C. *Tetrahedron* **1981**, *37*, 4287.

[130] Pesti, J. A.; Yin, J.; Zhang, L.-H.; Anzalone, L. *J. A. Chem. Soc.*, **2001**, *123*, 11075.

[131] Lemay, M.; Ogilvie, W. W. *J. Org. Chem.*, **2006**, *71*, 4663.

[132] (a) Halland, N.; Hazell, R. G.; Jørgensen, K. A. *J. Org. Chem.* **2002**, *67*, 8331.; (b) Prieto, A.; Halland, N.; Jørgensen, K. A. *Org. Lett.* **2005**, *7*, 3897.

[133] Halland, N.; Abruel, P. S.; Jørgensen, K. A. *Angew Chem. Int Ed.* **2003**, *42*, 661.

[134] Halland, N.; Abruel, P. S.; Jørgensen, K. A. *Angew Chem. Int Ed.* **2004**, *43*, 1272.

[135] Pulkkinen, J.; Abruel, P. S.; Halland, N.; Jørgensen, K. A. *Adv. Synth. Catal.* **2004**, *346*, 1077.

[136] Ruda, A. M. *Ph.D. Thesis, Cardiff University*, **2007**.

[137] List, B.; Pojarliev, P.; Martin, H. *J. Org. Lett.* **2001**, *3*, 2423.

[138] Huang, Y.; Walji, A. M.; Larsen, C. H.; MacMillan, D. W. C. *J. Am. Chem. Soc.* **2005**, *127*, 15051.

[139] Lattanzi, A. *Org. Lett.*, **2005**, *7*, 2579.

[140] Ruda, A. M. *Ph.D. Thesis, Cardiff University*, **2007**.

[141] Gibbs, T. J. K.; Boomhoff, M.; Tomkinson N.C.O. Synlett, **2007**, 1573.

[142] Kihlberg, J.; Bergman, R.; Wickberg, B. *Acta Chem. Scand.*, **1983**, *37*, 911.

[143] Pettit, G. R.; Srirangam, J. K.; Herald, D. H.; Hamel, E. *J. Org. Chem.*, **1994**, *59*, 6127.

[144] Gibbs, T. J. K.; Tomkinson, N. C. O. *Org. Biomol. Chem,*. **2005**, 4043.

[145] Sunderg, R. J. *Indoles (Best Synthetic Methods)*, Academic Press, **1996**.

[146] Harrington, P. E.; Kerr, M. A. *Tetrahedron Lett.*, **1997**, *38*, 5949.

[147] Zeligs, M. A. *J. Med. Food*, **1998**, *1*, 67.

[148] Hong, C.; Firestone G. L.; Bjeldanes, L. F. *Biochem. Pharmacol.*, **2002**, *63*, 1085.

[149] Karthik, M.; Magesh C. J; Perumal, P. T.; Palanichamy, M.; Arabindoo, B.; Murugesan, V. *Applied Catalysis A: General*, **2005**, *286*, 137.

[150] Chakrabarty, M.; Ghosh, N.; Basak, R; Harigaya, Y. *Tetrahedron Lett.*, **2002**, *43*, 4075.

[151] Shi, M.; Cui, S.-C.; Li, Q.-J. *Tetrahedron*, **2004**, *60*, 6679.

[152] Wang, L.; Han, J.; Tian, H.; Sheng. J.; Fan, Z.; Tang, X. *Synlett*, **2005**, 337.

[153] Bartoli, G.; Bosco, M.; Foglia, G.; Giuliani, A.; Marcantoni, E.; Sambri, L. *Synthesis*, **2004**, 895.

[154] Ke, B.; Qin, Y.; Wang, Y.; Wang, F. *Synth. Commun.*, **2005**, *35*, 1209.

[155] Bandgar, B. P.; Shaikh, K. A. *Tetrahedron Lett.*, **2003**, *44*, 1959.

[156] Nagarajan, R.; Perumal, P. T. *Chem. Lett.*, **2004**, *33*, 288.

[157] Bifluco, G.; Bruno, I.; Ricco, R. *J. Nat. Prod.*, **1995**, *58*, 1254.

[158] Bell, R.; Carmeli, S. *J. Nat. Prod.*, **1994**, 57, 1587.

[159] Veluri, R.; Oka, I.; Wagner-Dobler, I.; Laastch, H. *J. Nat. Prod.*, **2003**, *66*, 1520.

[160] Perrin, D. D.; Armarego, W. L. F.; Perrin, D. R. In *Purification of Laboratory Chemicals*, 2nd Ed; Pergamon Press; Oxford. **1980**.

[161] Still, W. C.; Kahn, M.; Mitra, A. *J. Org. Chem.* **1978**, *43*, 2923.

[162] Ishihara, K.; Kurihara, H.; Matsumoto, M.; Yamamoto, H. *J.Am. Chem. Soc.* **1998**, *120*, 6920.

[163] Tita, T. T.;Kornet, M. J., *J. Heterocyclic Chem.*, **1987**, *24*, 409.

[164] Battistuzzi, G.; Cacchi, S; Fabrizi, G. *Org. Lett.,* **2003**, *5*, 777.

[165] Lemay, M.; Ogilvie, W. W. *Org. Lett.*, **2005**, *7*, 4141.

[166] Shendage, D. M.; Fröhlich, R.; Haufe, G. *Org. Lett.*, **2004**, *6*, 3675.

[167] Ahrendt, K. A.; Borths, C. J.; MacMillan, D. W. C. *J. Am. Chem. Soc.* **2000**, *122*, 4243.

[168] MacMillan, D. W. C.; Northrup, A. B. *J Am Chem Soc.* **2002**, *124*, 2458.

[169] Halland, N.; Hazell, R. G.; Jørgensen, K. A. *J. Org. Chem.* **2002**, *67*, 8331.

[170] List, B.; Pojarliev, P.; Martin, H. J. *Org. Lett.*, **2001**, *3* 2423.

[171] Nasreen, A.; Varala, R.; Adapa, S. R. *J. Heterocyclic Chem.*, **2007**, *44*, 983.

[172] Veluri, R.; Oka, I.; Wagner-Dobler, I.; Laatsch, H. *J. Nat. Prod.*, **2003**, *66*, 1520.